

**Environmental Security Technology Certification Program
(ESTCP)**

PHASE 1 DEMONSTRATION REPORT SUMMARY FOR:

**PELAN—A Transportable Neutron-Based UXO
Identification Probe**

ESTCP: 200106

February 13, 2004

Prepared by

Dr. Phillip C. Womble
Applied Physics Institute
Western Kentucky University



Report Documentation Page				Form Approved OMB No. 0704-0188	
Public reporting burden for the collection of information is estimated to average 1 hour per response, including the time for reviewing instructions, searching existing data sources, gathering and maintaining the data needed, and completing and reviewing the collection of information. Send comments regarding this burden estimate or any other aspect of this collection of information, including suggestions for reducing this burden, to Washington Headquarters Services, Directorate for Information Operations and Reports, 1215 Jefferson Davis Highway, Suite 1204, Arlington VA 22202-4302. Respondents should be aware that notwithstanding any other provision of law, no person shall be subject to a penalty for failing to comply with a collection of information if it does not display a currently valid OMB control number.					
1. REPORT DATE 13 FEB 2004		2. REPORT TYPE		3. DATES COVERED 00-00-2004 to 00-00-2004	
4. TITLE AND SUBTITLE Phase 1 Demonstration Report Summary for: PELAN - A Transportable Neutron-Based UXO Identification Probe				5a. CONTRACT NUMBER	
				5b. GRANT NUMBER	
				5c. PROGRAM ELEMENT NUMBER	
6. AUTHOR(S)				5d. PROJECT NUMBER	
				5e. TASK NUMBER	
				5f. WORK UNIT NUMBER	
7. PERFORMING ORGANIZATION NAME(S) AND ADDRESS(ES) Western Kentucky University, Applied Physics Institute, Bowling Green, KY, 42101				8. PERFORMING ORGANIZATION REPORT NUMBER	
9. SPONSORING/MONITORING AGENCY NAME(S) AND ADDRESS(ES)				10. SPONSOR/MONITOR'S ACRONYM(S)	
				11. SPONSOR/MONITOR'S REPORT NUMBER(S)	
12. DISTRIBUTION/AVAILABILITY STATEMENT Approved for public release; distribution unlimited					
13. SUPPLEMENTARY NOTES					
14. ABSTRACT					
15. SUBJECT TERMS					
16. SECURITY CLASSIFICATION OF:			17. LIMITATION OF ABSTRACT Same as Report (SAR)	18. NUMBER OF PAGES 159	19a. NAME OF RESPONSIBLE PERSON
a. REPORT unclassified	b. ABSTRACT unclassified	c. THIS PAGE unclassified			

EXECUTIVE SUMMARY

Purpose

During a two-week period in May 2002 (May 13-24), an extensive validation test of PELAN was conducted. Purpose of the test was a) to test PELAN's stability over a a long time period, different types of soil, etc. and b) to collect large amounts of data on different fills of shells (explosive and non-explosive fills) and other explosives not found in UXO (ANFO, SEMTEX etc.) Part b) was to broaden the library of explosives used in PELAN for the identification of different fills.

Materials used

The test was performed using the Pulsed ELemental Analysis with Neutrons (PELAN) system. The PELAN utilizes gamma-rays induced from neutron reactions. The PELAN consists of a pulsing neutron generator, a gamma-ray detector, data acquisition electronics, neutron generator control electronics, and computer with appropriate software to control these electronics and analyze the resulting data. In this demonstration, a laptop computer was employed to communicate with the PELAN. Over the two week period, there was only one PELAN failure due to the electronics of the neutron generator. The repair was accomplished on-site with a delay of less than 2 hours.

The demonstration was performed using:

- Five different types of PELAN placement: one on a table and four on different types of soil (gravel, sand, wet soil in 3'x3'x2' boxes and regular soil)
- Table 1 shows the items tested and explosives tested.

Table 1. Ordnance, Explosives, and Mine Targets

Explosive Items		
	<u>ITEM</u>	<u>EXPLOSIVE</u>
1	60 mm mortar	TNT
2	76 mm Projectile	RDX
3	76 mm projectile	TNT
4	81 mm mortar	Comp B
5	82 mm mortar	TNT
6	82 mm mortar	TNT
7	90 mm projectile	RDX/TNT (52/48)
8	90 mm projectile	RDX
9	90 mm rocket	TNT/RDX (60/40)
10	105 mm projectile	Comp B

Explosive Items		
	<u>ITEM</u>	<u>EXPLOSIVE</u>
11	120 mm mortar	TNT
12	122mm rocket	Comp B
13	155 mm projectile	TNT
14	ANFO (2 wt% fuel oil)	ANFO
15	ANFO (6 wt% fuel oil)	ANFO
16	ANFO (15 wt% fuel oil)	ANFO
17	Semtex-1A (samples)	Semtex
18	Shape Charge	PBX-108
19	Shape Charge	Octol
20	Sheet Explosive	PETN
21	Smokeless Powder	Smokeless Powder
22	FFV 028 (steel) mine	TNT or RDX/TNT
23	TMRP-6 (plastic) mine	TNT
24	Valmara 69 mine	Comp B
Inert Items		
1	60 mm mortar	Empty
2	60 mm mortar	Wax
3	60 mm mortar	Hard red wax
4	60 mm mortar	Plaster of Paris
5	90 mm projectile	Empty
6	90 mm projectile	Hard red wax
7	81 mm mortar	Empty
8	81 mm mortar	Wax
9	81 mm mortar	Sand
10	81 mm mortar	Plaster of Paris
11	105 mm mortar	Empty
12	105 mm mortar	Wax
13	105 mm mortar	Sand
14	155 mm projectile	Empty
15	155 mm projectile	Wax
16	155 mm projectile	Hard red wax

Data Collected

A total of 232 cases were examined. All the data were automatically analyzed at the end of each run and recorded in the PELAN computer and on a spreadsheet. Each run was 5 minute in duration. The data were used to establish:

- Stability of the background spectra. These measurements tested the long term stability of the PELAN measurements. If PELAN is to be used for extended periods at a site with a particular type of soil and a certain type of shells, a stable background means that the various background spectra can be measured and subsequently stored in a computer library. In addition to the data taken at the demonstration, a series of measurements was conducted at WKU to complement the demonstration. In the WKU measurements, the reproducibility of the backgrounds was tested.
- Repeatability of measurements. These measurements would establish the precision of the PELAN measurements. For 4 differently filled, different diameter shells, 10 measurements for each case were taken in a random order.

Analysis Performed:

- Linear independence of the background spectrum was examined. The independence of background coefficients was compared to the coefficients of the elemental responses.
- Validity of a decision tree built on the elemental content of the 232 cases examined.
- Receiver-operator characteristic curves were created for: 1) the elemental content, 2) elemental ratios, and 3) each decision point in the decision tree.

Results

Background

Stability of the background was measured by taking background spectra of the same shell and on the same soil at two different times. During the analysis of the data for this report, it was found that there was a paucity of data concerning the reproducibility/stability of the background utilized in the SPIDER measurements.

To offset this, we asked permission from the ESTCP Program Office to acquire more data at a especially prepared site at WKU. The inert or empty shells used during this test were the same shells used at Indian Head.

With this data, we can now begin to estimate the measurement uncertainty for various elements. The maximum value of the standard deviations is C=1.3 cps, N= 2 cps, O=2.4 cps, Cl=0.6 cps, Fe=0.5 cps, and H=5.5 cps. These values correspond to a statistical zero.

One key finding of this demonstration is that there is no unique value that statistically represents zero. Previous to this series of measurements, we considered +/-1.5 cps as essentially zero.

However, we determined that this depends upon the element. The final source of these variations between elements seems to be environmental.

Other conclusions:

1. The scalar products between various background spectrum indicate that there is a strong coupling between backgrounds i.e. that the backgrounds are very similar. Thus, performance should not change much from background to background.
2. The coefficient of the background is nearly orthogonal to the elemental responses multiplied by their respective coefficients. This indicates that there is very little inter-dependence between the various coefficients and that the spectrum is being properly fitted.
3. The environment plays a key role in the uncertainty in the measurement. For example, an environment with a high H content tends to have a high measurement uncertainty in the measurement of H. This is due to the effective subtraction which takes place in the SPIDER program. In other words: if one subtracts two large numbers with independent errors, the difference may be smaller than the propagated error.
4. For sand, gravel and the table, the backgrounds are relatively stable and may be taken once per day. It is even advisable to take only one background at a given location to minimize Si activation.
5. For the soil at Indian Head (which is presumed to be clay), we found that the soil holds moisture and releases it slowly. Thus, the thermal spectrum will change from day to day (particularly after precipitation). For ten-repeated runs at WKU, we did not see any changes in the soil. Due to its intrinsic high H content, the WKU soil and the Indian Head soil had higher uncertainties for the reasons stated above.

Measurement Stability

The repeatability of the PELAN measurements was validated by measuring certain shells ten times. The elemental content of each test was analyzed and the results returned to the operator immediately (less than 2 seconds) after the end of each measurement. The elements examined were hydrogen, carbon, nitrogen, oxygen, chlorine, and iron.

The standard deviations of repeated measurements were calculated and compared to the fitting errors returned by the SPIDER spectral analysis program.

The standard deviation increases for elements such as C and O as the shell size decreases. It also increases when there is very little or none of the element present. For example, the standard deviation of N in a wax-filled shell is very high since there is very little N wax. Hydrogen has higher standard deviation than C due to the fact that H is more prominent in the background spectra. As stated in the section of the report concerning background stability, the large standard deviation comes from the effective background subtraction process in SPIDER.

While the standard deviation is strongly affected by shell size, the error calculated by SPIDER (fitting error) drops only slightly with decreasing shell size. This is because the analysis program fits the entire spectrum at once and not individual gamma-ray peaks. The program SPIDER uses a least squares method of determining a linear combination of individual elemental responses for

the entire region fitted. Thus, the error calculated by the analysis program is affected strongly by the intensity and shape of the overall spectrum under analysis.

The standard deviations of the ratios of elements were compared to those calculated by error propagation. The standard deviations can be significantly higher than the propagated error. The standard deviations are especially high when there is very little (statistically zero) of a particular element (e.g. the C/N ratio for wax should be undefined since N should be zero).

The conclusion is that the fitting error calculated by SPIDER is strongly correlated to the background spectrum. The background spectrum, in turn, is caused mostly by the environment (soil or surface type). The uncertainties of ratios can become very high when there is very little of the element which comprises the denominator.

Decision Tree

Three decision trees were created and presented as part of the analysis of this data. In this executive summary, we will present the decision tree for the data taken with the shells. This decision tree was more thoroughly analyzed than its counterparts.

Figure 1 shows the decision tree used for the shell data. Decisions were made using elemental content of H (in cps), C (in cps), O (in cps), and N (in cps), and the elemental ratios C/H and C/N. Tables 2 and 3 show all the shell data in two segments: Table 2 includes all the data and the PELAN fill identification for shells between 155 mm and 76 mm inclusive. Table 3 has all the data and the PELAN fill identification for all 60 mm shells.

In both tables, some of the values have been manipulated to show their values in the decision tree process (e.g. all $H \leq 0$ have been set to $H=0.01$).

The highlighted rows mean:

- False positive PELAN identification
- False negative PELAN identification

In Table 2, using the highlighted blue line, we can divide the shells in two groups, namely the 155mm-90 mm shell group, and the 82 mm-76 mm shell group. The significance of this separation is due to the fact that prior to the Indian Head tests, the emphasis on the PELAN shell fill identification was concentrated to 105 mm and 90 mm shells. Therefore, the PELAN development was focused in that direction and not towards smaller shells. Based on the above grouping, Table 4 shows the percentage of false PELAN identification of the various fills.

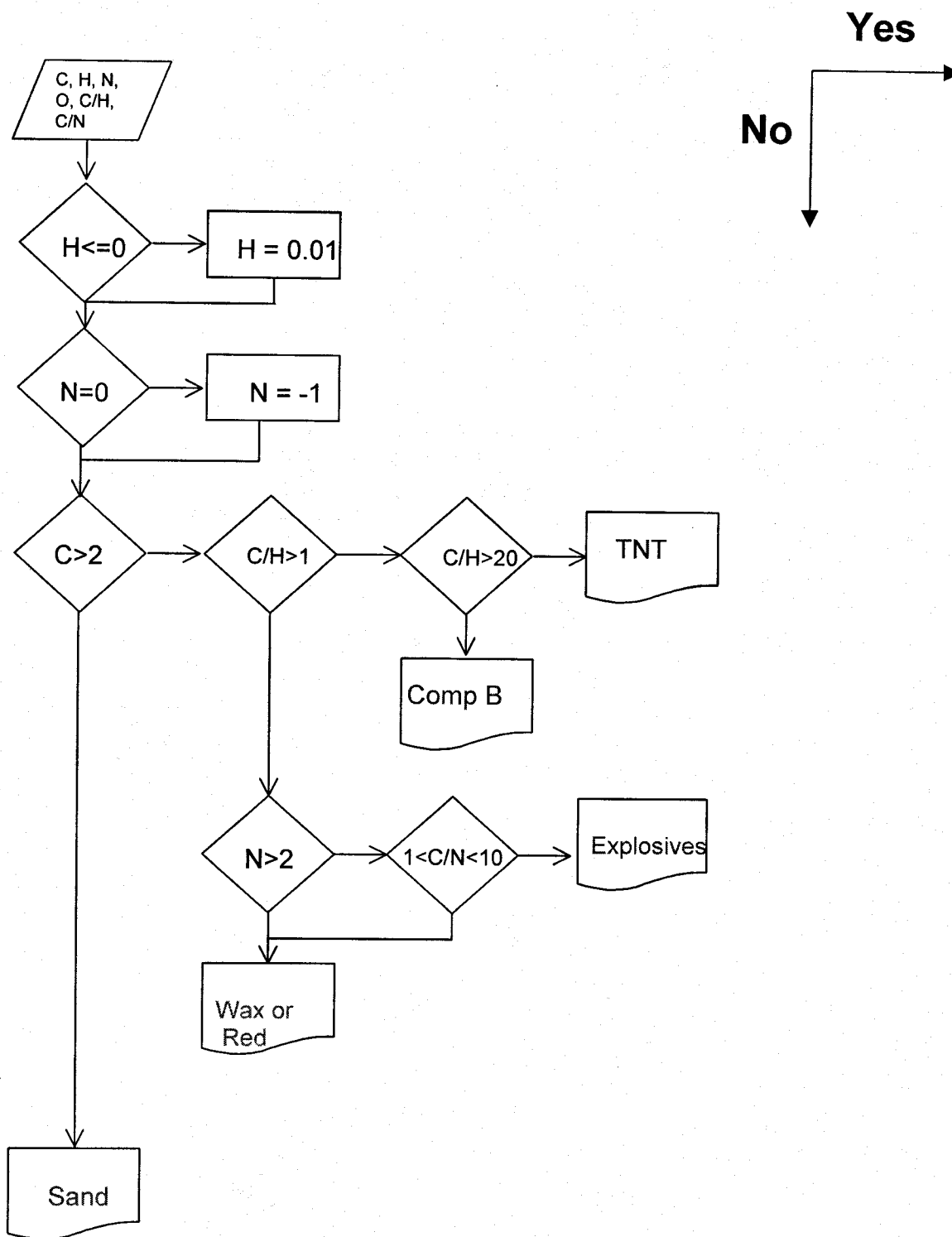


Figure 1. Decision tree for the shell data taken at NAVEODTECH.

Table 2. Data for all shells from 155 mm to 76mm inclusive. Column 3 shows the actual fill of the shell, and the the next-to-last column the PELAN identification. The last column indicates at which decision point the failure occurred.

Size (mm)	Amount of Fill	Fill	Surface	C (cps)	H (cps)	N (cps)	O (cps)	C/H	C/N	Decision Tree Result	Failure Mode
155	13.2 lbs	EMPTY	SOIL	-2.1	1.5	-2.1	-0.8	-1.40	0.98	Sand	
		RED	SOIL	7.5	33.5	1.7	5.0	0.22	4.49	Wax or Red	
		WAX	SOIL	8.3	59.9	1.6	1.9	0.14	5.20	Wax or Red	
		TNT	SOIL	18.8	5.4	4.9	5.5	3.51	3.86	CompB	
		TNT	TABLE	29.4	0.0	6.4	16.1	2941.00	4.62	TNT	
		TNT	GRAVEL	20.5	8.4	3.5	7.7	2.45	5.85	CompB	
		TNT	SAND	21.3	9.0	6.2	10.0	2.38	3.42	CompB	
		TNT	WETSOIL	19.2	0.0	7.9	5.2	1920.00	2.42	TNT	
		TNT	SAND	18.2	3.6	4.7	6.8	5.11	3.88	CompB	
		RED	SAND	14.7	55.1	-0.6	0.9	0.27	-24.05	Wax or Red	
		WAX	Gravel	14.1	102.9	1.0	-2.4	0.14	13.71	Wax or Red	
		RED	Soil	15.1	68.8	-0.7	2.5	0.22	-20.93	Wax or Red	
122	7.3 lbs	WAX	Wetsoil	10.1	26.5	3.7	-2.9	0.38	2.73	Explosives	W-2
		COMPB	SAND	15.3	8.1	6.2	11.0	1.89	2.47	CompB	
		COMPB	GRAVEL	11.9	6.7	4.5	10.8	1.78	2.64	CompB	
		COMPB	TABLE	13.5	5.8	6.5	14.5	2.33	2.08	CompB	
		COMPB	SOIL	11.1	11.0	3.3	4.8	1.01	3.36	CompB	
		COMPB	SOIL	13.8	20.4	6.8	8.4	0.68	2.03	Explosives	
		PROPEL.	WETSOIL	26.0	18.0	6.8	18.0	1.44	3.82	CompB	
120	2.7 lbs	COMPB	Table	11.2	6.3	5.4	10.8	1.77	2.05	CompB	
		TNT	SAND	11.3	0.7	2.3	4.1	16.14	4.91	CompB	
		TNT	GRAVEL	8.6	1.9	2.8	3.5	4.53	3.07	CompB	
		TNT	TABLE	13.7	1.4	4.5	8.5	9.79	3.04	CompB	
		TNT	SOIL	7.8	0.0	2.4	0.6	780.00	3.25	TNT	
105	2 lbs	TNT	Wetsoil	17.4	0.0	7.5	3.9	1735.00	2.30	TNT	
		WAX	SOIL	4.4	13.9	-1.8	-3.6	0.32	-2.45	Wax or Red	
		WAX	SOIL	5.3	11.6	0.1	-3.1	0.46	43.17	Wax or Red	
		WAX	SOIL	5.0	11.0	-1.0	-3.1	0.45	-4.83	Wax or Red	
		WAX	SOIL	5.7	9.5	-0.2	-2.6	0.60	-35.50	Wax or Red	
		WAX	SOIL	5.3	10.1	-1.5	-2.1	0.52	-3.47	Wax or Red	
		WAX	SOIL	5.5	13.3	-1.9	-4.0	0.42	-2.88	Wax or Red	
		WAX	SOIL	5.1	7.9	-0.5	-4.0	0.64	-9.79	Wax or Red	
		WAX	SOIL	5.5	8.2	-3.5	-4.8	0.67	-1.56	Wax or Red	

Size (mm)	Amount of Fill	Fill	Surface	C (cps)	H (cps)	N (cps)	O (cps)	C/H	C/N	Decision Tree Result	Failure Mode
		WAX	SOIL	4.8	5.3	-0.3	-4.6	0.89	-16.88	Wax or Red	
		WAX	SOIL	5.8	12.4	-1.2	-4.2	0.47	-4.83	Wax or Red	
		WAX	SOIL	4.7	8.0	-1.8	-3.4	0.59	-2.66	Wax or Red	
		SAND	SOIL	-1.6	0.0	-1.3	-2.7	-155.00	1.22	Sand	
		WAX	SAND	4.7	18.2	-1.1	-3.1	0.26	-4.27	Wax or Red	
		WAX	GRAVEL	8.2	23.0	-0.5	2.9	0.36	-16.40	Wax or Red	
		WAX	TABLE	-1.2	10.2	0.4	-1.3	-0.12	-3.00	Sand	
		WAX	SOIL	2.5	6.3	-2.6	-6.8	0.40	-0.96	Wax or Red	
		WAX	WETSOIL	5.5	7.3	7.3	-4.4	0.75	0.75	Wax or Red	
		WAX	TABLE	7.3	5.3	-0.2	2.4	1.37	-38.26	CompB	C/H>1
		SAND	SAND	0.9	0.0	0.6	-1.4	94.00	1.62	Sand	
		WAX	Soil	6.5	24.5	-1.8	-4.1	0.26	-3.66	Wax or Red	
		SAND	Soil	0.6	16.0	0.4	0.7	0.03	1.31	Sand	
		WAX	Wetsoil	10.3	4.5	-0.8	-3.5	2.31	-13.42	CompB	C/H>1
		RED	Wetsoil	9.9	2.6	2.2	-0.9	3.81	4.40	CompB	C/H>1
		EMPTY	Wetsoil	8.9	0.0	2.6	-4.4	892.00	3.40	TNT	C/H>1
		SAND	Table	-7.9	6.3	1.1	4.3	-1.27	-7.33	Sand	
90	1.6 lbs	TX50	SOIL	4.0	0.0	0.9	0.5	401.00	4.46	TNT	
		TX50	TABLE	6.1	2.4	1.4	4.7	2.50	4.24	CompB	
		TX50	GRAVEL	9.6	0.0	1.9	1.5	961.00	5.17	TNT	
		TX50	SAND	8.4	0.0	1.7	0.1	838.00	4.93	TNT	
		TNT/RDX	Wetsoil	21.5	4.8	4.9	5.7	4.51	4.40	CompB	
	1.1 lbs	rocket 1.1lb60/40	SOIL	12.9	7.3	3.4	4.0	1.77	3.84	CompB	
		rocket 1.1lb60/40	TABLE	12.1	3.5	2.6	9.2	3.48	4.74	CompB	
		rocket 1.1lb60/40	GRAVEL	18.0	2.6	3.7	4.2	6.91	4.93	CompB	
		rocket 1.1lb60/40	SAND	17.2	1.6	3.0	3.3	11.02	5.77	CompB	
		rocket 1.1lb60/40	WETSOIL	14.5	3.0	3.0	1.2	4.92	4.90	CompB	
		rocket 1.1lb60/40	Gravel	18.5	0.8	4.1	3.4	22.28	4.47	TNT	
		RED	SOIL	4.2	0.0	-2.4	-7.0	415.00	-1.71	TNT	C/H>1
		RED	SAND	6.2	0.0	-0.6	-3.1	621.00	-10.71	TNT	C/H>1
		RED	Wetsoil	8.8	0.0	0.9	-2.3	875.00	9.62	TNT	C/H>1
		Red	Table	-3.4	0.0	0.5	-2.1	-337.00	-6.74	Sand	
	1.8 lbs	RDX	SAND	3.0	1.7	0.6	1.5	1.76	5.00	CompB	
		RDX	GRAVEL	3.8	1.3	-0.2	-0.9	2.92	-19.00	CompB	
		RDX	TABLE	0.9	2.7	2.7	-5.0	-0.31	-0.31	Sand	
		RDX	SOIL	3.7	1.3	-0.2	-2.6	2.85	-18.50	CompB	
		RDX	WETSOIL	4.8	7.5	3.2	-1.5	0.64	1.50	Explosives	

Size (mm)	Amount of Fill	Fill	Surface	C (cps)	H (cps)	N (cps)	O (cps)	C/H	C/N	Decision Tree Result	Failure Mode
82		RDX	Wetsoil	9.4	1.5	4.1	-0.3	6.20	2.32	CompB	
		COMPB	WETSOIL	6.5	3.1	3.0	-4.1	2.10	2.17	CompB	
	1.4 lbs	COMPB	GRAVEL	6.4	4.7	-1.0	6.4	1.36	-6.40	CompB	
		TNT	GRAVEL	5.5	1.6	1.9	7.7	3.44	2.89	CompB	
		TNT	TABLE	2.9	0.0	0.2	1.7	288.00	16.94	TNT	
		TNT	SOIL	4.6	0.0	-0.2	-2.6	460.00	-23.00	TNT	
		TNT	WETSOIL	6.0	0.0	2.1	-1.7	600.00	2.86	TNT	
		TNT	SOIL	3.1	0.0	-0.3	-1.0	307.00	-9.90	TNT	
		TNT	TABLE	2.9	0.0	0.2	1.7	288.00	16.94	TNT	
		TNT	GRAVEL	8.6	1.2	-0.5	0.3	7.37	-17.96	CompB	
		TNT	SAND	6.0	0.0	0.7	-0.2	599.00	9.08	TNT	
		TNT	SAND	6.8	1.5	1.9	1.9	4.55	3.65	CompB	
		TNT	SOIL	5.1	0.0	0.6	-1.7	508.00	8.76	TNT	
81	2 lbs	PLASTER	SOIL	3.1	6.5	-1.8	2.3	0.48	-1.79	Wax or Red	
		PLASTER	SOIL	2.1	0.0	-2.0	1.1	207.00	-1.02	TNT	C/H>1
		PLASTER	SOIL	2.2	0.0	-1.9	-0.8	220.00	-1.14	TNT	C/H>1
		PLASTER	SOIL	2.4	0.0	-1.8	-0.6	243.00	-1.34	TNT	C/H>1
		PLASTER	SOIL	2.5	0.0	-1.0	-0.8	247.00	-2.38	TNT	C/H>1
		PLASTER	SOIL	0.9	0.0	-3.4	-0.2	85.80	-0.25	Sand	
		PLASTER	SOIL	1.0	0.0	-2.5	-0.2	104.00	-0.41	Sand	
		PLASTER	SOIL	1.5	0.0	-2.0	0.9	150.00	-0.75	Sand	
		PLASTER	SOIL	2.0	0.0	-1.3	0.3	196.00	-1.51	Sand	
		PLASTER	SOIL	2.0	0.0	-0.6	1.9	198.00	-3.54	Sand	
		SAND	SOIL	0.4	0.0	-3.0	-3.7	43.40	-0.15	Sand	
		WAX	SOIL	3.8	0.5	-3.7	-5.4	7.57	-1.03	CompB	
		EMPTY	SOIL	0.8	0.0	-3.2	-4.8	76.00	-0.24	Sand	
		EMPTY	SOIL	0.8	0.0	-3.2	-4.8	76.00	-0.24	Sand	
		PLASTER	SOIL	1.1	0.0	-5.3	-5.5	111.00	-0.21	Sand	
		PLASTER	SAND	2.1	8.2	-1.7	-0.3	0.26	-1.24	Wax or Red	
		COMPB	SAND	4.8	0.0	-0.1	0.0	480.00	-48.00	TNT	
		TNT	SAND	2.4	0.0	0.2	-0.4	240.00	12.00	TNT	
		PLASTER	GRAVEL	2.1	11.5	0.3	9.3	0.18	7.00	Wax or Red	
		PLASTER	TABLE	-4.1	4.3	-0.8	5.0	-0.95	5.13	Sand	
		COMPB	TABLE	1.6	0.0	-2.3	-2.5	180.00	-0.67	Sand	
		PLASTER	SOIL	-0.7	3.8	-0.2	-0.2	-0.18	3.50	Sand	
		POP	WETSOIL	2.8	3.8	-1.0	1.6	0.74	-2.80	Wax or Red	
		POP	WETSOIL	1.6	3.2	1.0	1.6	0.50	1.60	Sand	
		COMPB	WETSOIL	6.0	0.0	2.4	0.0	600.00	2.50	TNT	
		PLASTER	SAND	1.0	4.8	1.0	1.3	0.22	1.09	Sand	
		WAX	SAND	5.4	7.0	-0.8	-3.7	0.77	-6.81	Wax or Red	
		SAND	SAND	2.5	0.0	-0.6	-3.1	248.00	-4.13	TNT	C/H>1
		POP	SAND	1.5	7.0	-0.4	1.5	0.21	-3.74	Sand	

Size (mm)	Amount of Fill	Fill	Surface	C (cps)	H (cps)	N (cps)	O (cps)	C/H	C/N	Decision Tree Result	Failure Mode
76	1.7 lbs	Sand	SAND	1.0	0.0	0.3	-0.7	97.00	3.59	Sand	
		COMPB	Gravel	9.5	3.5	3.6	1.5	2.74	2.61	CompB	
		POP	Wetsoil	6.0	3.8	0.9	1.1	1.56	6.47	CompB	C/H>1
		Sand	Wetsoil	6.8	0.0	1.7	0.0	681.00	4.13	TNT	C/H>1
		SAND	Table	-2.4	0.0	-0.8	-0.3	-236.00	3.06	Sand	
		RDX	SOIL	4.0	0.0	-0.5	-1.3	403.00	-8.00	TNT	
		RDX	SOIL	4.1	0.0	0.0	-1.1	408.00	4080.00	TNT	
		RDX	SOIL	4.4	0.0	-0.7	-0.8	437.00	-6.48	TNT	
		RDX	SOIL	4.6	0.0	-0.6	0.0	456.00	-7.72	TNT	
		RDX	SOIL	4.6	0.0	-0.6	-1.7	456.00	-7.20	TNT	
		RDX	SOIL	4.8	0.0	-0.6	-2.0	475.00	-8.39	TNT	
		RDX	SOIL	4.9	0.0	-0.2	1.0	486.00	-23.82	TNT	
		RDX	SOIL	5.0	0.0	-0.4	-2.2	495.00	-12.38	TNT	
		RDX	SOIL	2.9	1.9	-1.1	-0.3	1.54	-2.60	CompB	
		RDX	SOIL	3.8	0.0	-0.6	-3.2	382.00	-6.35	TNT	
		RDX	SAND	2.7	0.0	1.0	0.3	270.00	2.70	TNT	
		TNT	SAND	4.0	0.0	-1.0	-2.9	400.00	-4.00	TNT	
		RDX	GRAVEL	5.0	5.0	2.5	4.9	1.00	2.00	Explosives	
		TNT	GRAVEL	5.6	0.8	-1.0	3.7	7.00	-5.60	CompB	
		RDX	TABLE	2.7	0.2	2.7	1.0	-13.50	1.00	Sand	C<2
		TNT	TABLE	3.9	0.0	0.6	-1.4	-390.00	-6.50	Sand	C<2
		RDX	SOIL	1.4	1.7	-1.4	-1.2	0.82	-1.00	Sand	C<2
		TNT	SOIL	1.2	0.0	3.1	5.8	120.00	0.39	Sand	C<2
		RDX	WETSOIL	5.4	0.0	4.8	1.3	540.00	1.13	TNT	
		TNT	WETSOIL	4.3	0.0	2.0	-2.7	430.00	2.15	TNT	
		RDX	SAND	6.0	1.9	1.3	1.8	3.08	4.54	CompB	
		TNT	Soil	3.4	0.0	-1.1	-1.6	340.00	-3.15	TNT	

Table 3 Data for all 60 mm shells. Column 3 shows the actual fill of the shell, and the next-to-last column the PELAN identification. The last column indicates at which decision point the failure occurred.

Size (mm)	Amount of Fill	Fill	Surface	C (cps)	H (cps)	N (cps)	O (cps)	C/H	C/N	Decision on Tree Result	Failure Mode
60	0.9 lbs	RED	SOIL	2.0	0.0	-1.7	-4.0	196	-1.15	Sand	
		EMPTY	SOIL	0.7	0.0	-5.2	-7.1	65.50	-0.13	Sand	
		EMPTY	SOIL	0.7	0.0	-5.2	-7.1	65.50	-0.13	Sand	
		PLASTER	SOIL	0.8	0.0	-5.1	-7.8	81.90	-0.16	Sand	
		WAX	SOIL	1.6	0.0	-3.8	-6.2	156	-0.41	Sand	
		SAND	SAND	0.8	0.0	-1.0	-2.1	80.00	-0.71	Sand	C<2
		TNT	SAND	1.9	0.0	-1.0	-2.1	190	-1.90	Sand	C<2
		TNT	GRAVEL							Wax or Red	N<2
				2.5	3.5	0.7	4.0	0.71	3.67	Red	
		BP	TABLE	-4.7	0.0	0.2	-0.4	-470	23.50	Sand	C<2
		TNT	TABLE	-1.6	4.3	1.1	-0.5	-0.37	-1.45	Sand	C<2

Size (mm)	Amount of Fill	Fill	Surface	C (cps)	H (cps)	N (cps)	O (cps)	C/H	C/N	Decisi on Tree Result	Failur e Mode
		TNT	SOIL	-0.8	0.0	-1.3	-1.6	-80.00	0.62	Sand	C<2
		TNT	WETSOIL	3.5	4.7	-1.0	-0.3	0.75	-3.50	Wax or Red	N<2
		POP	WETSOIL	1.5	2.8	0.7	0.7	0.52	2.09	Sand	
		WAX	WETSOIL	3.2	3.9	-1.0	0.0	0.82	-3.20	Wax or Red	
		WAX	WETSOIL	1.7	-0.3	0.3	0.0	-5.67	5.67	Sand	
		TNT	WETSOIL	2.4	1.1	0.7	-5.0	2.18	3.43	Comp B	
		WAX	SAND	2.1	0.5	-0.2	-0.5	4.40	-12.18	Comp B	C/H>1
		PLASTER	SAND	1.7	0.1	0.8	-2.1	18.56	2.06	Sand	
		RED	SAND	1.4	-1.5	1.9	-1.9	-0.94	0.75	Sand	
		TNT	Gravel	3.6	0.6	0.7	-1.0	5.58	5.10	Comp B	
		POP	Gravel	1.7	-0.4	0.6	-1.0	-4.49	2.81	Sand	
		TNT	Soil	2.3	-1.2	0.4	-3.1	-1.84	6.16	TNT	
		Pop	Table	-2.5	0.1	1.0	-0.6	-51	-2.57	Sand	

The false positive rate calculated in Table 4 utilizes the following formula:

$$\text{FalsePositiveRate} = \frac{\# \text{FalsePositives}}{\# \text{ofInertItemsEncountered}}$$

and the false negative rate:

$$\text{FalseNegativeRate} = \frac{\# \text{FalseNegatives}}{\# \text{ofExplosivesEncountered}}$$

Table 4. Collective results for decision tree in Figure 1.

Shell Size	Inert/Empty Shell Results			Explosive Shell Results		
	# Shells	# Incorrect Positive	% False Pos	# Shells	# Incorrect Negative	% False Neg
90-155	36	8	22	36	1	3
76-82	29	8	28	40	8	20
60	13	1	8	10	7	70
All	78	17	22	86	15	19

Analysis of Failures in Figure 1 Decision Tree

The primary failure mode for false negatives is the low C count rate. For 13 out of 15 of the false negatives, C<2. In the other two cases, C>2 but its relatively high H content force C/H<1. Since no or low N was measured, the second failure was in N<2.

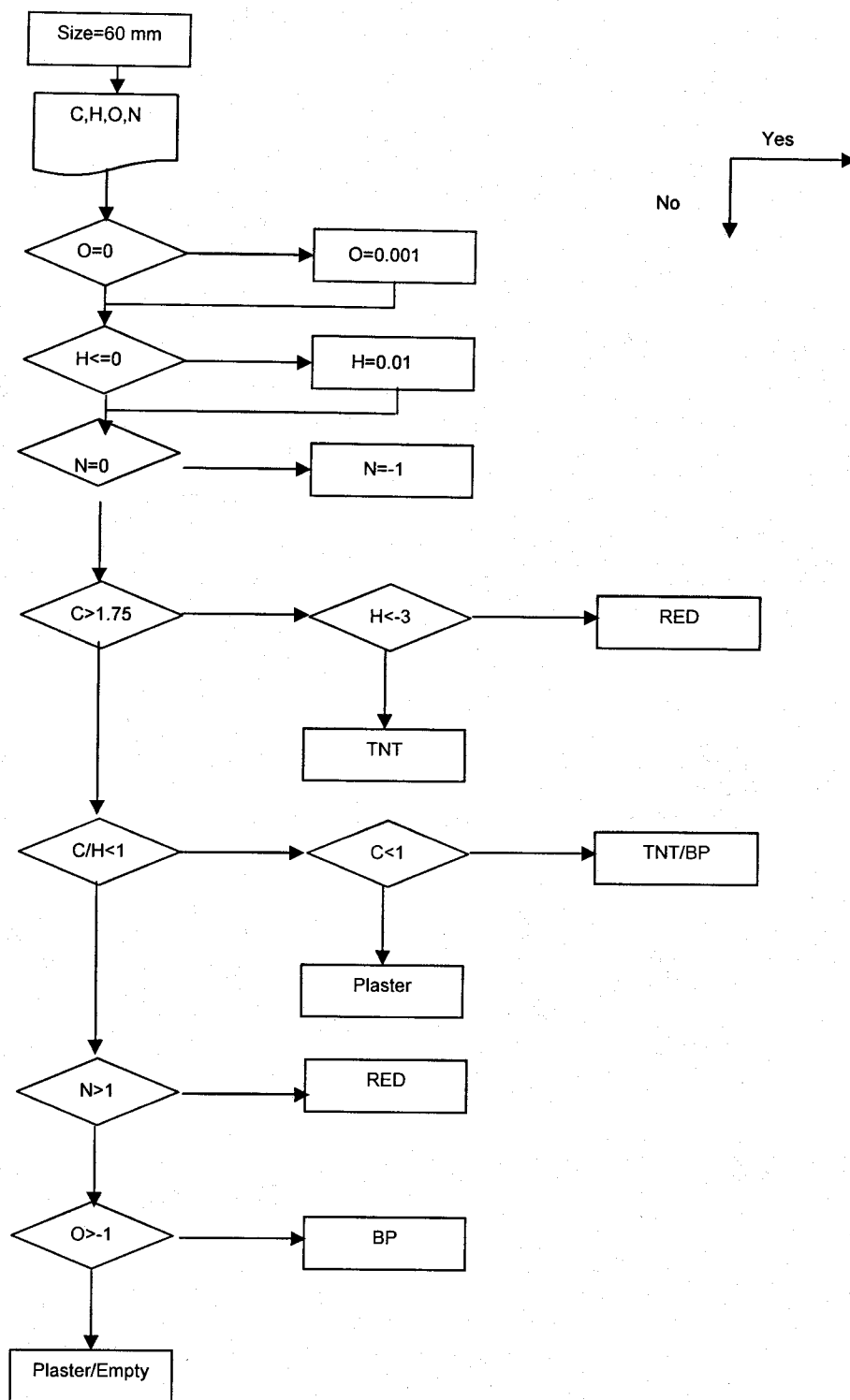


Figure 2. Decision tree for 60mm shells only.

The primary failure mode (17 out of 18) for false positives was a very low or negative H count-rate. Since H is arbitrarily set to 0.01 if $H < 0$, this forces high C/H ratios. Once $C/H > 1$, then the

only possible return value is an explosive. For completeness, a spurious N signal in a 155mm wax-filled shell forced a decision to "Explosives".

Making a more general statement about failures, we can say that they occur when the SPIDER analysis returns near-zero values. For example, the values returned in the four false negatives at 76mm are statistically zero or near-zero values.

When re-examining the data during the completion of this report, we realized that segregating the data by shell-size had advantages in the decision-making process. A separate, nearly autonomous, decision-tree for each shell size could be made. An example is given in Figure 2 for 60mm shells. When this decision tree is applied to the 60 mm shell data in Table 3, a 38% false positive rate and 0% false negative rate is achieved (falling dramatically from 70% false negative rate). Based on this, we expect that we could improve the performance of the decision-making process by incorporating the size of the shell in the decision tree.

Receiver Operator Characteristic Curves

Receiver-Operator Characteristic (ROC) curves were also generated as part of this report. Three curves are presented within the document: an ROC for each element, ROC of the ratios of certain elements, and the ROC of various decision tree points in the decision tree of Figure 1.

A significant result of the analysis is that, based on the ROC curves only, the ratio is no better than the data with which it is supplied. It is also important to note that the products of elemental content are very similar to the ratio.

Based on these ROC curves, the question arises whether ratios should be used in decision trees. While the ROC curves for ratios may not be as good as the ROC curves for the individual elements, the ratios eliminate the problems caused by different sized objects (e.g. 1 lb of TNT and 10 lb of TNT should have the same C/N ratio). However, this advantage may be offset due to the distribution of data. For example, if while measuring water, a small amount of carbon, 0.5 cps, would create a small C/H ratio. The 0.5 cps is well within the bounds of a statistical zero. Unfortunately, we cannot draw any conclusions about the appropriateness of using ratios from the ROC curves at this time and further investigation is required.

Conclusions from Decision Trees

1. The ROC curves of elemental ratios are no better than the ROC curves of the elemental contents which comprise them.
2. The decision tree used for the identification of the shell fill shows that PELAN has a 19% false negative rate overall and a 22% false positive rate. The false negative rate drops to 3% for shells 90 mm and above. These larger shells have a 22% false positive rate.
3. The decision tree can be improved by the addition of a condition based on size. In this manner, each size shell will have its own decision tree which would reduce its false negative and false positive rates. For example, the false negative rate for 60 mm shells decreases from 70% to 0% when a 60mm-shell-specific decision tree is applied.

One key question is how much data should be taken for a particular shell/environment. Unfortunately, there is no clear cut answer to this. The best answer is that sufficient data should be taken until a normal distribution can be fitted to the individual elemental content with a low chi-squared. For certain shells, such as the 60mm, the number of shells may be large to achieve a normal distribution due to the low mass of the explosive, the signal to noise ratio, etc. For the 155mm shell during the reproducibility tests, the normal distribution was reached after a few trials.

Another question is whether more data acquisition time would improve the measurement. In the table below, we show the results for two 60 mm shells with TNT on gravel. We have added these together and then fitted them with SPIDER.

Run	Fill	Size	Surface	C (cps)	O (cps)	N (cps)	H (cps)
1861	TNT	60	Gravel	3.6	-1	0.7	0.6
1361	TNT	60	Gravel	2.5	4	0.7	3.5
1861+1361	TNT	60	Gravel	3.81	1.24	0.29	1.8

In this case, there is no evidence that doubling the time of acquisition will increase the intensity of the measurement above background. When doubling the measurement time for the spectrum, the measurement time of the background must be doubled. Since the SNR is roughly constant, there seems to be no gain by increasing the acquisition time beyond what is necessary to have sufficient statistics for analysis.

We believe that the above data bears well towards the validation of PELAN as a potentially useful tool for the identification of explosives.

Lessons Learned

1. PELAN can be operated for 8 hour shifts.
2. Movement of shells from magazine to target to magazine takes approximately 10 minutes. In a demonstration such as this, one can only expect about 4 interrogations per hour rather than 7.
3. The moisture content of soils with high clay content can change rapidly. For clay soils in the future, the background must be examined every 4 hours.
4. Local weather and other projects can interfere with tight schedules. Plan for at least 1 lost day per every 10 working days.
5. The largest source of statistical uncertainty is the background measurement. Uncertainties for elements are greatest when there is a significant amount of that element in the background.
6. While ROC curves are useful in analyzing the total performance of a particular decision tree, they are difficult to use when building a decision tree.
7. Increasing the data collection times does not lead to greater accuracy.
8. Greater use of shell size segregation should be made. For example, the false negative rate for 60 mm shells decreases from 70% to 0% when a 60mm-shell-specific decision tree is applied.

9. A specific elemental content for a given shell/environment should be repeated until the data approximates a normal distribution function. For larger shells, this may be a few times. However, it may be require a very large data set to achieve this distribution with the smaller shells.

Environmental Security Technology Certification Program (ESTCP)

PHASE 1 DEMONSTRATION REPORT FOR: PELAN—A Transportable Neutron-Based UXO Identification Probe

ESTCP: 200106

February 13, 2004

Prepared by

Dr. Phillip C. Womble
Applied Physics Institute
Western Kentucky University



TABLE OF CONTENTS

TABLE OF CONTENTS.....	ii
TABLE OF FIGURES.....	iv
TABLE OF TABLES.....	vi
COMMONLY USED ACRONYMS.....	vii
1.0 INTRODUCTION.....	1
1.1. BACKGROUND.....	1
1.2. OFFICIAL DOD REQUIREMENT STATEMENTS.....	1
1.3. OBJECTIVES OF THE DEMONSTRATION.....	1
1.4. REGULATORY DRIVER.....	1
1.5. PREVIOUS TESTING OF TECHNOLOGY.....	2
2.0 TECHNOLOGY DESCRIPTION.....	3
2.1. TECHNOLOGY DEVELOPMENT AND APPLICATION.....	3
2.1.1. DESCRIPTION OF PELAN.....	3
2.1.1.1. BLOCK DIAGRAM.....	3
2.1.2. DESCRIPTION OF PELAN COMPONENTS.....	7
2.1.2.1. BGO DETECTOR.....	8
2.1.2.2. POWER AND DATA MODULE.....	8
2.1.3. PRINCIPLE OF OPERATION.....	9
2.1.4. THE PFTNA PRINCIPLE.....	11
2.1.5. METHODOLOGY.....	12
2.1.6. PREVIOUS MEASUREMENTS TO VALIDATE THE SOFTWARE.....	14
2.1.7. DATA COLLECTION.....	14
2.1.8. CORRECTING FOR SHIELDING EFFECTS DUE TO LARGE MASSES OF FE.....	16
2.1.9. INTRODUCTION TO DECISION TREES.....	19
2.1.9.1. ALGORITHMS FOR PELAN DECISION TREES.....	20
2.1.9.2. DESIGNING A DECISION TREE.....	20
2.2. ADVANTAGES AND LIMITATIONS OF THE TECHNOLOGY.....	24
2.3. FACTORS AFFECTING COST AND PERFORMANCE.....	25
3.0 SITE / FACILITY DESCRIPTION.....	25
3.1. BACKGROUND.....	25
3.2. SITE / FACILITY CHARACTERISTICS.....	25
4.0 DEMONSTRATION APPROACH.....	27
4.1. PERFORMANCE OBJECTIVES.....	27
4.2. PHYSICAL SETUP AND OPERATION.....	29
4.3. SAMPLING PROCEDURES.....	30
4.4. ANALYTICAL PROCEDURES.....	32
5.0 PERFORMANCE ASSESSMENT.....	33
5.1. PERFORMANCE DATA.....	33
5.1.1. BACKGROUND STABILITY.....	43
5.1.2. MEASUREMENT STABILITY.....	59
5.1.3. TEMPERATURE / HUMIDITY EFFECTS.....	85
5.1.4. LINEAR INDEPENDENCE OF SPECTRA.....	91
5.1.5. COMPLETED DATA.....	98
5.1.6. RECEIVER OPERATOR CHARACTERISTIC CURVES.....	106
5.1.7. DECISION TREE.....	108
5.1.7.1. BUILDING THE FIRST DECISION TREE.....	109
5.1.7.2. ANALYSIS OF FAILURES IN THE FIRST DECISION TREE.....	117
5.1.7.3. BUILDING THE SECOND DECISION TREE.....	120
5.2. DATA ASSESSMENT.....	128
5.3. TECHNOLOGY COMPARISON.....	129
6.0 COST ASSESSMENT.....	130
6.1. COST REPORTING.....	130
6.2. COST ANALYSIS.....	131
7.0 REGULATORY ISSUES.....	132
7.1. ENVIRONMENTAL CHECKLIST.....	132

7.2.	OTHER REGULATORY ISSUES.....	132
7.3.	END-USER ISSUES.....	132
8.0	TECHNOLOGY IMPLEMENTATION.....	132
8.1.	DOD NEED.....	132
8.2.	TRANSITION.....	132
9.0	LESSONS LEARNED.....	132
10.0	REFERENCES.....	133
APPENDIX A—POINTS OF CONTACT.....		A-1
APPENDIX B—DATA ARCHIVING AND DEMONSTRATION PLAN.....		A-2

TABLE OF FIGURES

FIGURE 1.	PELAN III.....	2
FIGURE 2.	PELAN BLOCK DIAGRAM.....	3
FIGURE 3.	PALMTOP / LAPTOP PELAN OPERATOR SCREEN 1.....	4
FIGURE 4.	PALMTOP / LAPTOP PELAN OPERATOR SCREEN 2.....	5
FIGURE 5.	PALMTOP COMPUTER SCREEN.....	6
FIGURE 6.	NEUTRON TUBE SCHEMATIC DIAGRAM.....	7
FIGURE 7.	BLOCK DIAGRAM OF POWER AND DATA MODULE.....	8
FIGURE 8.	NUCLEAR CAPTURE REACTIONS AND FAST NEUTRON (INELASTIC SCATTERING).....	10
FIGURE 9.	PULSED NEUTRON GENERATOR TIME SEQUENCE.....	11
FIGURE 10.	ASTM GRAPHS.....	15
FIGURE 11.	SPECTRUM ABOVE SOIL AND ON SOIL.....	16
FIGURE 12A.	TYPICAL PELAN SPECTRUM.....	17
FIGURE 12B.	EFFECTS OF IRON ON SPECTRUM.....	18
FIGURE 12C.	90MM FAST SPECTRUM.....	18
FIGURE 13.	AMMONIUM NITRATE / FUEL OIL BOMB DECISION TREE.....	19
FIGURE 14.	LAYOUT AREA FOR PELAN DEMO.....	26
FIGURE 15.	PELAN AT NAVEODTECH AREA.....	29
FIGURE 16.	FIELD OPERATION OF PELAN.....	30
FIGURE 17.	EXAMPLE OF DIFFERENT SOILS USED WITH PELAN.....	32
FIGURE 18.	EMPTY 60 MM ON ALL SOIL TYPES.....	35
FIGURE 19.	FIVE DIFFERENT -SIZED SHELLS ON SAND.....	36
FIGURE 20.	FIVE DIFFERENT -SIZED SHELLS ON SOIL.....	37
FIGURE 21.	155 MM AND 60 MM EMPTY SHELL ON SAND.....	38
FIGURE 22.	155 MM AND 60 MM EMPTY SHELL ON GRAVEL.....	39
FIGURE 23.	155 MM AND 60 MM EMPTY SHELL ON SOIL.....	40
FIGURE 24.	155 MM AND 60 MM EMPTY SHELL ON WETSOIL.....	41
FIGURE 25.	155 MM AND 60 MM EMPTY SHELL ON TABLE.....	42
FIGURE 26.	WKU FIELD TESTS OF PELAN III.....	43
FIGURE 27.	TWO EMPTY 81 MM ON SAND.....	49
FIGURE 28.	TWO EMPTY 60 MM ON SAND.....	50
FIGURE 29.	TWO EMPTY 155 MM ON GRAVEL.....	51
FIGURE 30.	TWO EMPTY 90 MM ON GRAVEL.....	52
FIGURE 31.	TWO EMPTY 105 MM ON SOIL.....	53
FIGURE 32.	TWO EMPTY 90 MM ON SOIL.....	54
FIGURE 33.	TWO EMPTY 155 MM ON WETSOIL.....	55
FIGURE 34.	TWO EMPTY 105 MM ON WETSOIL.....	56
FIGURE 35.	TWO EMPTY 105 MM ON TABLE.....	57
FIGURE 36.	TWO EMPTY 81 MM ON TABLE.....	58
FIGURE 37.	TEN MEASUREMENTS OF 76 MM SHELL WITH RDX.....	66
FIGURE 38.	TEN MEASUREMENTS OF 155 MM SHELL WITH TNT.....	67
FIGURE 39.	TEN MEASUREMENTS OF 105 MM SHELL WITH WAX.....	68
FIGURE 40.	SPECTRA OF 60 MM SHELL (WAX, PLASTER OF PARIS, AND RED WAX).....	70
FIGURE 41.	SPECTRA OF 81 MM SHELL (WAX, PLASTER OF PARIS, AND SAND).....	71
FIGURE 42.	FOUR DIFFERENT-SIZE SHELLS WITH WAX.....	72
FIGURE 43.	60 MM AND 81 MM WITH PLASTER OF PARIS.....	73
FIGURE 44.	SPECTRA OF 76 MM SHELL (RDX AND TNT).....	74
FIGURE 45.	SPECTRA OF 82 MM SHELL WITH TNT.....	75
FIGURE 46.	SPECTRA OF 90 MM SHELL (RDX AND COMPB).....	76
FIGURE 47.	2%, 6%, & 15% ANFO ON SOIL.....	77
FIGURE 48.	SPECTRA OF STEEL AND PLASTIC AT MINES.....	78
FIGURE 49.	ROCKET SPECTRA (90 MM AND 122 MM).....	79
FIGURE 50.	60 MM, 81MM, 155 MM SHELLS ON SOIL.....	80
FIGURE 51.	OCTOL TARGET ON FOUR MEDIA.....	81
FIGURE 52.	60MM TARGET ON ALL MEDIA.....	82
FIGURE 53.	76MM TARGET ON ALL MEDIA.....	83

FIGURE 54.	SMOKELESS POWDER TARGET ON ALL MEDIA.....	84
FIGURE 55A.	GAMMA PEAK VARIATION AS A FUNCTION OF TEMPERATURE FOR A BGO DETECTOR.....	85
FIGURE 55B.	DEMONSTRATION GRAPHS OF TEMPERATURE, HUMIDITY, AND CHANGE OF ENERGY POSITION.....	86
FIGURE 56.	76MM SHELL WITH RDX ON SAND (DIFFERENT TEMPERATURES AND HUMIDITY).....	88
FIGURE 57.	SEMTEX ON SOIL DIFFERENT TEMPERATURES AND HUMIDITY).....	89
FIGURE 58.	81MM ON GRAVEL (SAME TEMPERATURES, DIFFERENT HUMIDITY).....	90
FIGURE 59A.	SPECTRA RESIDUALS FOR R1307 FITTED WITH B1308.....	93
FIGURE 59B.	SPECTRA RESIDUALS FOR R1307 FITTED WITH B1308 COMPARED TO ELEMENTAL RESPONSES..	94
FIGURE 60.	81MM POP AND TNT 81MM ON SAND.....	95
FIGURE 61.	81MM POP AND TNT 81MM ON GRAVEL.....	96
FIGURE 62.	81MM POP AND TNT 81MM ON WET SOIL.....	97
FIGURE 63.	ROC CURVE FOR ELEMENTS H, C, O, AND N.....	106
FIGURE 63B.	ATOMIC DENSITIES FOR EXPLOSIVES, DRUGS AND INNOCUOUS MATERIALS.....	107
FIGURE 63C.	ROC CURVES FOR C ELEMENTAL CONTENT, O ELEMENTAL CONTENT, AND THEIR RATIO.....	108
FIGURE 64.	DECISION TREE FOR SHELL DATA AT NAVEODTECH.....	112
FIGURE 65.	ROC CURVES FOR VARIOUS DECISION TREE POINTS.....	118
FIGURE 66.	DECISION TREE FOR 60MM SHELLS ONLY.....	119
FIGURE 67.	DECISION TREE FOR ALL DATA TAKEN AT NAVEODTECH.....	121

TABLE OF TABLES

TABLE 1.	ELEMENTAL DENSITIES AND RATIOS OF THREE CLASSES OF SUBSTANCES.....	11
TABLE 2.	ORDNANCE, EXPLOSIVES AND MINE TARGETS.....	27
TABLE 3.	ELEMENTAL COMPOSITIONS AND RATIOS FOR THE EXPLOSIVES EMPLOYED IN THE DEMONSTRATIONS	31
TABLE 3A.	LABORATORY MEASUREMENTS OF THE MOISTURE WITHIN THE "WET SOIL" DURING THE DEMONSTRATION	31
TABLE 4A.	REPRODUCIBILITY DATA FOR VARIOUS BACKGROUNDS ON SOIL	45
TABLE 4B.	REPRODUCIBILITY DATA FOR VARIOUS BACKGROUNDS ON SAND	46
TABLE 4C.	REPRODUCIBILITY DATA FOR VARIOUS BACKGROUNDS ON GRAVEL	47
TABLE 4D.	BACKGROUND REPRODUCIBILITY DATA FOR RANDOMLY CHOSEN POSITION ON THE SOIL	48
TABLE 5.	REPRODUCIBILITY RESULTS FOR 155 MM SHELL WITH TNT	60
TABLE 6.	REPRODUCIBILITY RESULTS FOR 105 MM SHELL WITH WAX	60
TABLE 7.	REPRODUCIBILITY RESULTS FOR 81 MM SHELL WITH COMPB.....	61
TABLE 8.	REPRODUCIBILITY RESULTS FOR 81 MM SHELL WITH PLASTER OF PARIS.....	61
TABLE 9.	REPRODUCIBILITY RESULTS FOR 76 MM SHELL WITH RDX.....	62
TABLE 10A.	THE STANDARD DEVIATION OF THE PELAN MEASUREMENTS FOR VARIOUS ELEMENTS	62
TABLE 10B.	THE STANDARD DEVIATIONS OF RATIOS BASED ON REPRODUCIBILITY MEASUREMENTS.....	62
TABLE 11.	A SELECTION OF DATA FROM TABLE 17 SHOWING THE ERROR DETERMINED BY THE ANALYSIS PROGRAM SPIDER AS A FUNCTION OF ENVIRONMENT.....	63
TABLE 12.	SUMMARY OF AVERAGE FITTING ERRORS CALCULATED BY THE PROGRAM SPIDER FOR TYPE OF ENVIRONMENT	65
TABLE 13.	THE SCALAR PRODUCT OF VARIOUS SPECTRA	91
TABLE 14.	SCALAR PRODUCTS OF THE BACKGROUND WITH THE ELEMENTAL RESPONSES	92
TABLE 15.	SCALAR PRODUCT OF THE RESIDUALS WITH THE ELEMENTAL RESPONSES.....	93
TABLE 16.	ELEMENTAL COMPOSITION USED IN THE DECISION TREE FOR ALL THE SHELLS	98
TABLE 17A.	THE AVERAGE, STANDARD DEVIATION, MAXIMUM AND MINIMUM FOR C AND H CONTENT FOR THE REPEATED SPECTRA	109
TABLE 17B.	THE AVERAGE, STANDARD DEVIATION, MAXIMUM AND MINIMUM FOR N AND O CONTENT FOR THE REPEATED SPECTRA	110
TABLE 18.	DATA FOR ALL SHELLS FROM 155 MM TO 60 MM INCLUSIVE.....	113
TABLE 19.	DATA FOR THE 60 MM SHELL.....	116
TABLE 20.	COLLECTIVE RESULTS FOR DECISION TREE.....	117
TABLE 21.	DATA FOR ALL EXPLOSIVES AND INERTS EXAMINED WITH PELAN.....	122
TABLE 22.	COST FOR INSPECTION OF UXO SPECIFIC TO PELAN TECHNOLOGY.....	130

COMMONLY USED ACRONYMS OR UNITS

ANFO	Ammonium Nitrate- Fuel Oil mixture
API	Applied Physics Institute
ASTM	American Standards of Testing and Materials
AT	Anti-tank
BGO	Bismuth germanate $\text{Bi}_3\text{Ge}_4\text{O}_{12}$
COMP B	A mixture of TNT and RDX
cps	counts per second
CW	Chemical Warfare agent
DoD	Department of Defense
DOE	Department of Energy
ESTCP	Environmental Security Technology Certification Program
GSO	Gadolinium ortho-silicate
HE	High explosive
HEAT	High Explosive Anti-Tank
IEDs	Improvised explosive devices
MCNP	Monte Carlo N-Particle code
NAVEODTECH	Navy Explosive Ordnance Disposal Technology division
NG	Neutron generator
NRC	Nuclear Regulatory Commission
PELAN	Pulsed ELemental Analysis with Neutrons
PFTNA	Pulsed Fast/Thermal Neutron Analysis
PINS	Portable Isotopic Neutron System
PoP	Plaster of Paris
RDD	Radioactive dispersive devices
RDX	A military explosive
ROC	Receiver operator characteristic
SNR	Signal to noise ratio
SPIDER	SPectrum Interpolation and DEconvolution Routine
TNA	Thermal neutron analysis
TNT	Tri-nitro toluene
uCi	micro Curies (37,000 decays/second)
UXO	Unexploded Ordnance
WKU	Western Kentucky University

1. Introduction

1.1 Background

At a recent conference [1], the following facts about the Kaho'olawe, HI remediation effort were presented. Of the 8,700 magnetic anomalies detected by mine-detectors: 4,500 were metal debris, 3,850 were magnetic rocks, and only 350 were UXO (about 4%). Furthermore, it was suggested [1] that using confirmation sensors instead of visually inspecting each detected anomaly would save millions of dollars in remediation costs.

PELAN (Pulsed ELemental Analysis with Neutrons) is a man-portable system for the detection of explosives and chemical warfare agents, weighing less than 45 kg. It is based on the principle that explosives and other contraband contain various chemical elements such as H, C, N, O, etc. in quantities and ratios that differentiate them from innocuous substances. The pulsed neutrons are produced with a pulsed 14 MeV (d-T) neutron generator. Separate gamma-ray spectra from fast neutron, thermal neutron and activation reactions are accumulated and analyzed to determine elemental content. Data analysis is performed in an automated manner and a final result of whether or not a threat is present is returned to the operator.

PELAN is a powerful tool for explosives detection because it relies on all the major and minor chemical elements to make a decision. Multiple elements are utilized to reach a final decision. The ability to simultaneously measure multiple elements reduces the possibility of false alarms and increases operator safety by reducing the amount of time required for analysis.

1.2 Official DoD Requirement Statements

None.

1.3 Objectives of the Demonstration

The Phase I Demonstration had the following objectives:

- To obtain a library of elemental signatures of a variety of shells as found in ranges and proving grounds
- To check the reliability of the decision trees produced through elemental ratios.
- To determine the range of validity of the decision trees
- To ascertain the repeatability of the measurements, false positive and false-negative rates.

The PELAN was demonstrated against the following UXO:

- UXO sizes from 60 mm to 122 mm
- Inert fills including: plaster of Paris, wax, and sand.

The demonstration was performed at Indian Head, Maryland, May 13-24, 2002.

1.4 Regulatory Driver

None.

1.5 Previous Testing of Technology

PELAN has undergone several field demonstrations for its ability to detect contraband materials. It has undergone two field trials on its ability to detect improvised explosive devices. It has undergone two field trials on its ability to detect chemical warfare agents. Finally, it has been tested on its ability to detect narcotics within a ship's bulkhead.

The chemical warfare agent demonstrations are described in the following reports:

- PELAN System Evaluation at Aberdeen Proving Ground, Edgewood Area, Prepared by TVA for PMCD, September 2001.
 - Evaluates PELAN's ability to characterize chemical warfare agents.
- Test and Evaluation of PELAN as an Identifier of Chemical Warfare Agents, Poellkappelle, Belgium, October 2001.
 - Evaluates PELAN's ability to characterize chemical warfare agents and HE.

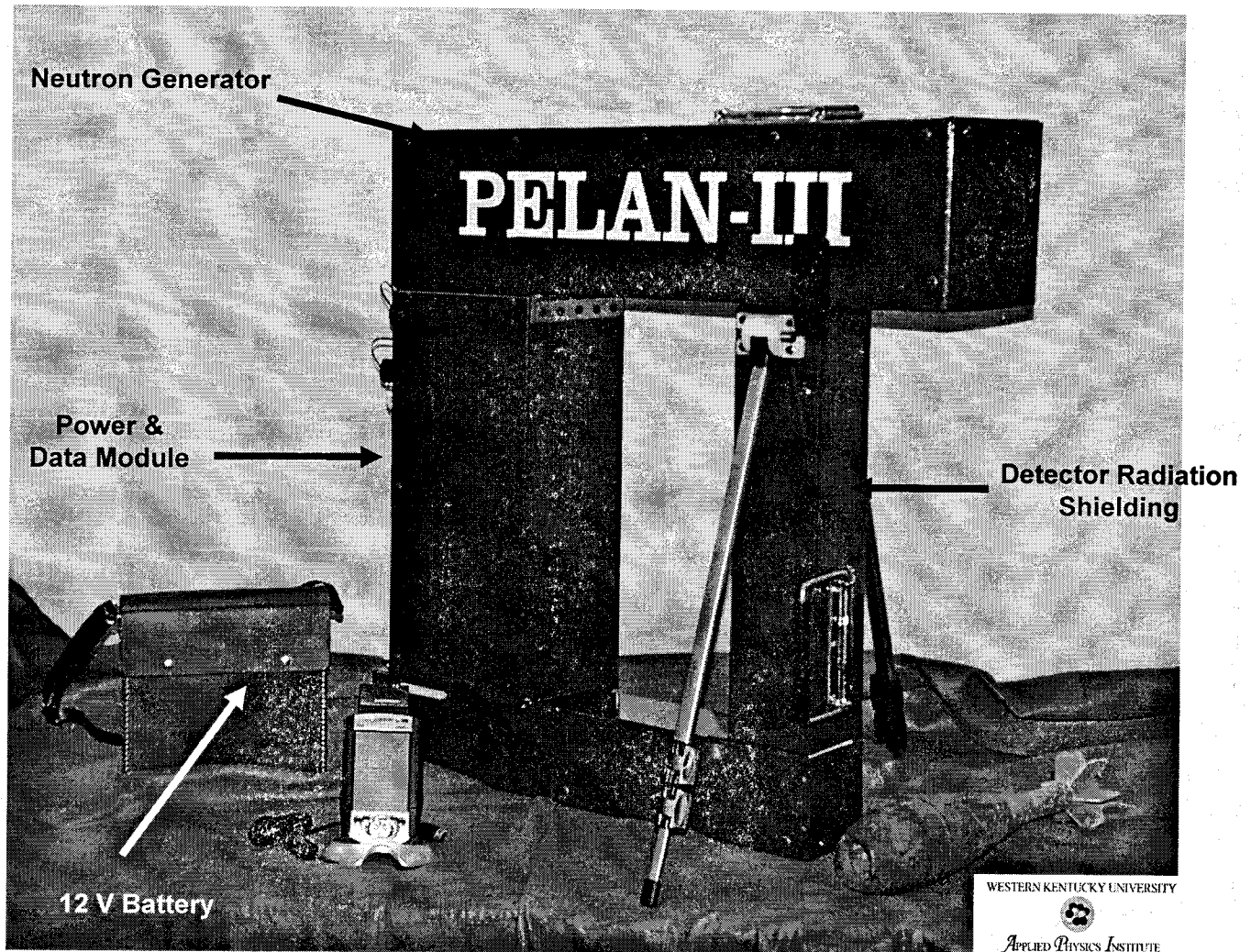


Figure 1. PELAN III with an identification of its components.

On improvised explosive devices:

- Development of PELAN, Final Report, December 1999.
 - Evaluates PELAN's ability to detect improvised explosive devices.

Reports on the other demonstrations (which occurred in early 2002) are still being prepared.

2. Technology Description

2.1 Technology Development and Application

2.1.1 DESCRIPTION OF PELAN

2.1.1.1 BLOCK DIAGRAM

PFTNA is the method is used to identify all the major and some of the minor chemical elements within an object. PELAN is the device (US patent #5,982,838 (Nov. 1999)) that was developed for the automatic acquisition of γ ray spectra, and their subsequent analysis using a software program called SPIDER. Algorithms in PELAN based on elemental ratios similar to those in Table 1 (see section **Principle of Operation**), as well as the presence or absence of other chemical elements, provide the operator of PELAN with information concerning the object. PELAN is programmed to present the decision on a palmtop computer as "THREAT!!" or "NO THREAT", or in any other way that the operator would like to have the results presented.

Figure 2 shows the block diagram of PELAN. Its main components are:

- A neutron generator which provides the interrogating particles.
- A γ -ray detector that detects the electromagnetic radiation (fingerprints) emitted from the chemical elements within the object.
- A power and data module that provides the electrical power to the neutron generator and the γ -ray detector, controls the operation of the neutron generator, collects, analyzes and stores the signals from the detector, and finally presents to the PELAN operator the results of the analysis.
- Radiation shielding (thick line around the γ -ray detector) between the neutron generator and

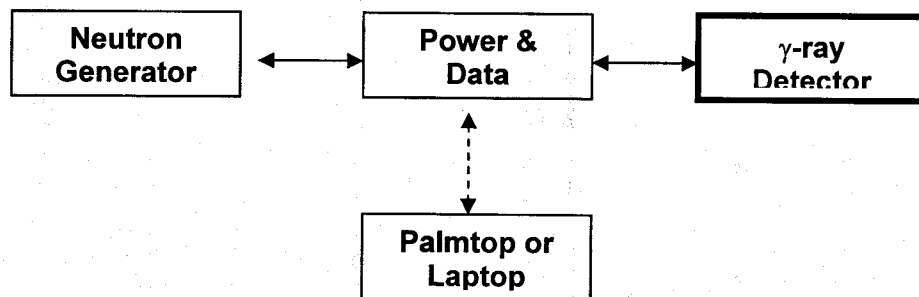


Figure 2. PELAN block diagram

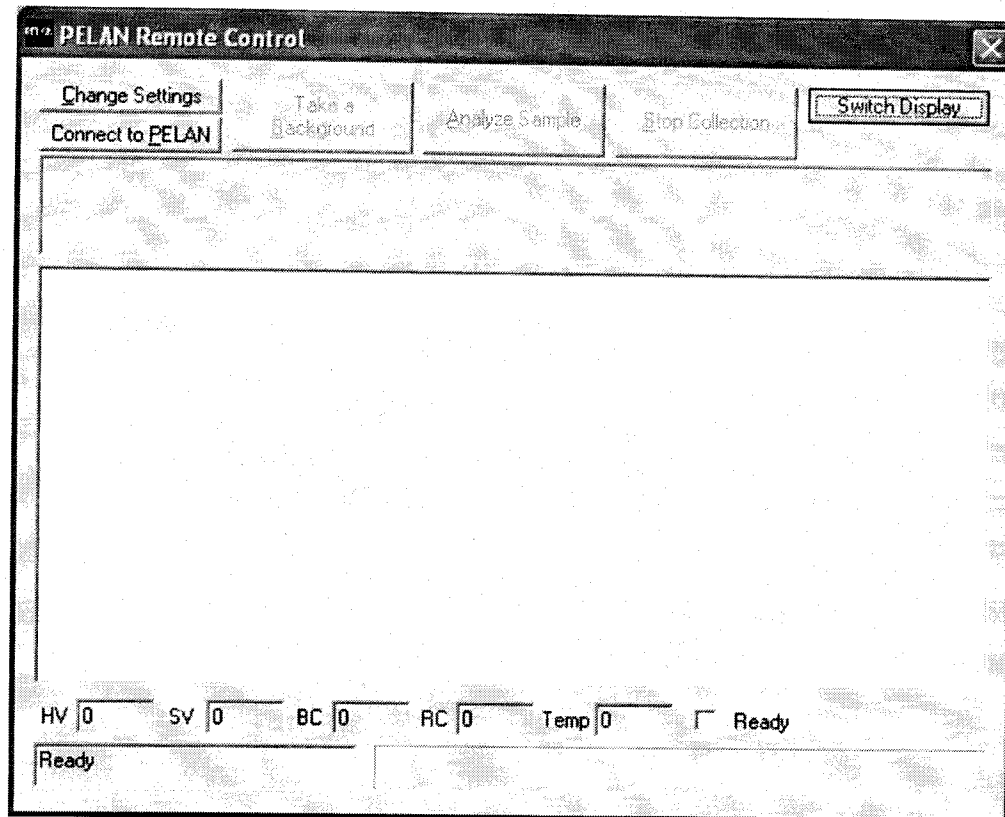


Figure 3. Palmtop/laptop PELAN operational screen I.

the detector.

- A palmtop or a laptop computer is used by the operator to start the interrogation of an object, and to display the results of the interrogation. The connection between the palmtop/laptop and the power and data module can be either wireless or hard-wired (indicated by the dashed connecting line).

Each PELAN contains the above components, although they can be configured differently depending on the function for which the PELAN has been designed. Figure 1 shows model PELAN III. The upper horizontal rectangular object is the neutron generator, the lower horizontal rectangular is the γ -ray detector, and the small vertical rectangular is the shielding between the detector and the neutron generator. The larger vertical rectangular is the Power and Data Module. The palmtop has a wireless connection with the Power and Data Module. PELAN III can be operated either from a 12 V DC source (battery pack in Figure 1) or with AC voltage.

PELAN is operated remotely with either the laptop or the palmtop. A typical, automatic PELAN operational cycle is as follows:

1. When PELAN is energized from the laptop or palmtop, the neutron generator ramps to the appropriate high voltage and filament current, and the neutron production starts within a few seconds.

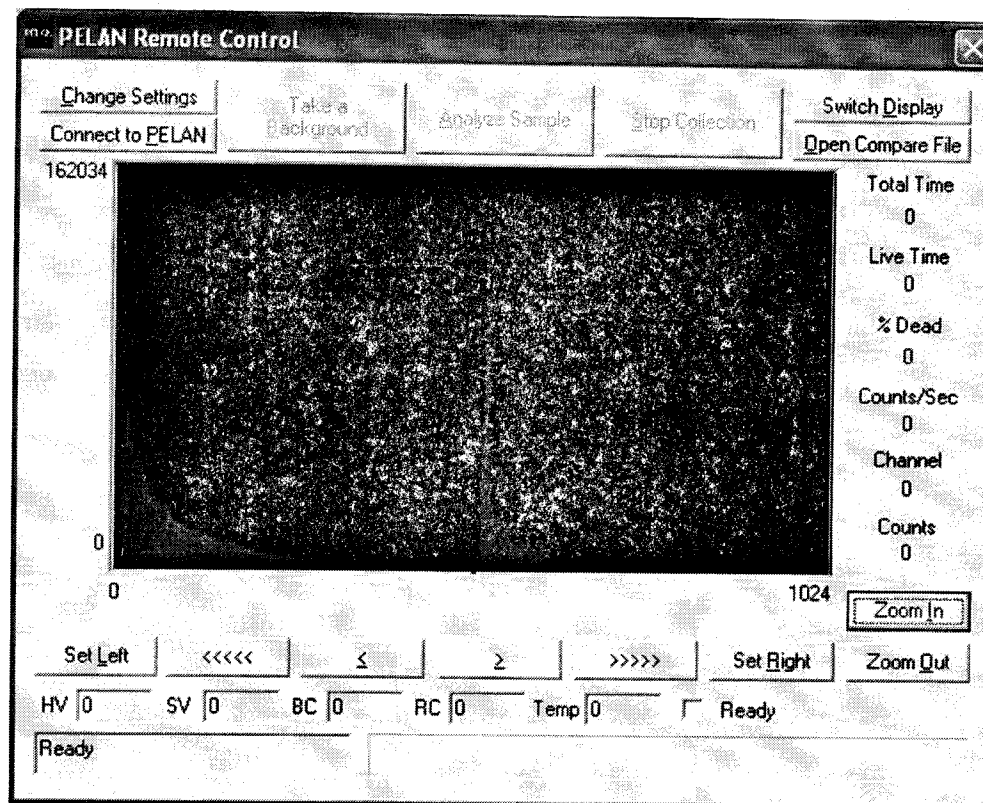


Figure 4. Palmtop/laptop PELAN operational screen II.

2. After the generator is stabilized, gamma ray spectra are acquired for five minutes.
3. At the end of the data acquisition, the high voltage of the neutron generator is switched off, stopping the neutron production in just a few seconds.
4. The data is transferred (in approximately 20 s) from the data acquisition card to the on board computer, where it is analyzed.
5. Based on a predetermined decision tree, the identification of the object is made, and the words "THREAT" or "NO THREAT" appear on the laptop/palmtop computer screen.

On the laptop/palmtop, the three on-screen buttons that control the operation of PELAN are:

Take a background: By depressing it, an automatic 5 minute data acquisition cycle starts. This cycle is used for taking a background spectrum, away from the exact location of the object to be interrogated (see also the section on SPIDER). The neutron generator is automatically turned off at the end of the data acquisition cycle.

START: By depressing it, an automatic 5 minute data acquisition cycle starts. This cycle is used for taking a gamma-ray spectrum of the interrogated object. The neutron generator is automatically turned off at the end of the data acquisition cycle.

STOP: By depressing it, the neutron generator is turned off instantaneously. This button can function either as an **EMERGENCY OFF** switch, or for stopping the acquisition of a spectrum.

The other icons on the top of Screen I (Figure 3) of the laptop are:

Switch display: Changes the display from Screen I to Screen II (see Figure 4).

Change settings: Should a different laptop be used, this button allows the user to change the RF network settings.

The buttons at the bottom of Screen I and on the palmtop are for information and diagnostics. If there is a problem starting PELAN, the values or check marks next to each button can help pinpoint the trouble:

HV: Neutron generator (NG) high voltage (nominal display value 85 kV)

SV: NG source voltage (nominal display value 1.5)

BC: NG beam current (nominal display value 1.5)

RC: Reservoir current (nominal display value 1.5)

Ilock: Interlock. When checked, interlock on the Power and Control Module is closed

NG Ready: When checked, PELAN is ready for operation.

Below these buttons, there is a bar graph that displays the time left to complete the data acquisition cycle.

The icons in Screen II (Figure 4) have the same name as those in Screen I and perform the same function. Screen II allows the operator to observe in real time the acquisition of the gamma-ray spectra. There are two gamma-ray spectra displayed during acquisition. The one on the left is a

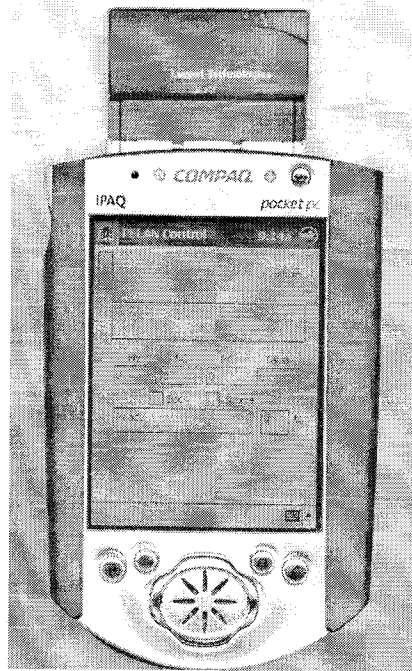
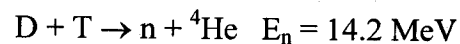


Figure 5. Palmtop computer screen.

spectrum from fast neutron induced nuclear reactions. The one on the right is a spectrum from thermal neutron induced nuclear reactions. The vertical scale displays the numbers of accumulated gamma rays. The horizontal scale is calibrated to display the energy of the gamma rays. The icons below the spectra allow the operator to select and expand or contract a portion of the displayed spectrum. On the right side of the screen there is information on the acquisition time, the acquisition rate, and, while using the cursor, the position (in channels) and number of counts for the particular channel selected with the cursor. The **Open Compare File** allows the operator to display and compare, along with the acquiring spectrum, a previously acquired gamma-ray spectrum.

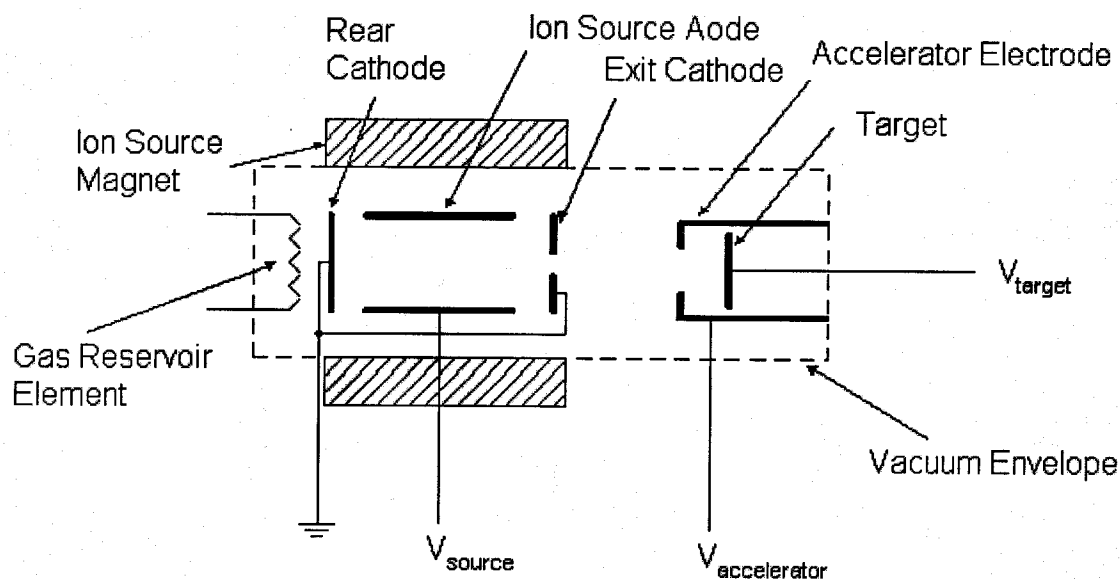
2.1.2 DESCRIPTION OF THE PELAN COMPONENTS

The neutron generator in PELAN produces neutrons using the (D-T) reaction. Neutrons are produced by creating deuterium ions and accelerating these ions onto a tritium target.



Neutrons produced from the D-T reaction are emitted isotropically (uniformly in all directions) from the target along with a He nucleus (α particle) emitted in the exact opposite direction of the neutron.

The neutron generator in PELAN is a sealed tube neutron generator (see Fig. 6). The ion source, ion optics, the accelerator electrode and target are enclosed within a vacuum envelope. Either glass or ceramic insulators provide high voltage insulation between the ion optical elements of



NEUTRON TUBE SCHEMATIC

Figure 6. Schematic diagram of a neutron tube (courtesy of ThermoMFPhysics).

the tube. The neutron tube is, in turn, enclosed in a metal housing, the accelerator head, which is filled with a dielectric medium [SF_6 gas at 100 psi (6.5 atm) pressure] to insulate the high voltage elements of the tube from its surroundings. The basic features of a sealed neutron tube are illustrated in Figure 6. Ions are generated using a low gas pressure, cold cathode ion source which utilizes crossed electric and magnetic fields. The gas pressure of the ion source is regulated, by heating or cooling the gas reservoir element. The ion source anode is at a positive potential, either dc or pulsed, with respect to the source cathodes. The ion source voltage V_{source} is normally between 2 and 7 kilovolts. Plasma is formed along the axis of the anode trapping electrons, which in turn ionize the gas in the source. The ions are extracted through the exit cathode and are accelerated by the potential difference between the exit cathode and the accelerator electrode. The accelerator voltage $V_{\text{accelerator}}$ is normally between 70 and 120 kilovolts. Varying the accelerator voltage controls neutron output. The accelerated ions impinge onto the tritium target, producing 14.2 MeV neutrons.

2.1.2.1 BGO DETECTOR

The gamma ray detector used in PELAN is a bismuth germanate (BGO) crystal. BGO detectors are utilized because of their high efficiency for measuring gamma rays over the range of energies of interest (from 170 keV to 9 MeV) and for their high resistance to activation by radiation. The energy resolution of BGO detectors is sufficient to identify and quantify all chemical elements of interest.

2.1.2.2 POWER AND DATA MODULE

Figure 7 shows a block diagram of the power and data module. Its main components are:

- The interface card that sends to the neutron generator controller the appropriate values of voltage and current for its operation. Through this card, commands are also transmitted to

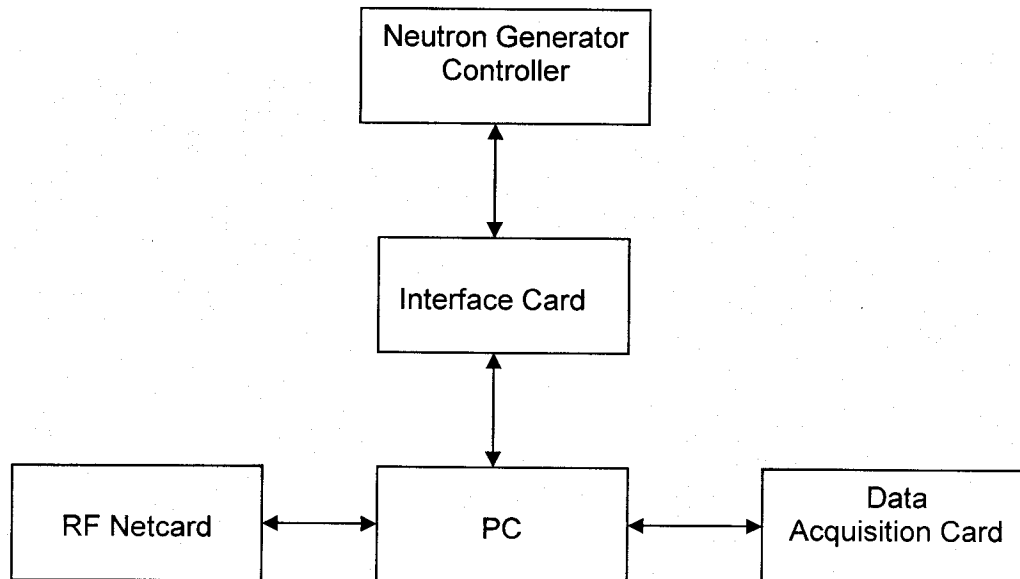


Figure 7. Block diagram of the Power and Data Module.

the other components of the module.

- The neutron generator controller that sets the appropriate voltage and current values to the neutron generator. The controller also monitors the various diagnostic signals (e.g. SF₆ pressure) to and from the neutron generator.
- The data acquisition card receives the analog signals from the detector and digitizes them. The acquired spectra are stored in the PC where they are reduced and analyzed.
- The RF network card transmits and receives information from the laptop and the palmtop.

2.1.3 Principle of operation

High explosives (TNT, RDX, C-4, etc.) are composed primarily of the chemical elements hydrogen, carbon, nitrogen, and oxygen. Many innocuous materials are also primarily composed of these same elements. These elements, however, are found in each material with very different ratios and concentrations. It is thus possible to identify and differentiate e.g. TNT from paraffin. For narcotics, the C/O ratio is at least a factor of two larger than innocuous materials. Table 1 shows the atomic density of elements for various materials along with the atomic ratios. Explosives have been shown [2] to be differentiated by the utilization of both C/O ratio and N/O ratios. The problem of identifying explosives is thus reduced to the problem of elemental identification.

Nuclear techniques show a number of advantages for non-destructive elemental characterization. These include the ability to examine bulk quantities with speed, high elemental specificity, and no memory effects from the previously measured object. These qualities are important for an effective detection system for explosives and drugs.

In particular, neutrons have been utilized for several decades to measure the above mentioned elements. In oil exploration, the carbon/oxygen ratio (C/O) is a measure of oil saturation [3]. In the coal industry, elements such as sulfur and chlorine are routinely measured with neutron interrogation [4,5]. In the airline industry, the inspection of checked luggage for high explosives has been proposed through the use of neutrons for the identification of the nitrogen content within a piece of luggage [6]. Neutron-based systems have also been proposed for detection of narcotics and other contraband [7,8] by the measurement of C/O.

The physical principles that all these methods are based upon have been established for a number of years, and have been extensively used by nuclear physicists and chemists for the investigation of nuclear structure.

In principle, a neutron impinging on an object can initiate one of several nuclear reactions with the chemical elements of which the object is composed (Figure 8). In most of these cases, as a result of these reactions, γ rays are emitted with characteristic and distinct energies. These γ rays are like the "fingerprints" of the elements contained in the object. By counting the number of γ rays emitted with a specific energy (e.g. the γ rays of sulfur), one can deduce the amount of the element contained within the object. In the case of an object that is hidden among other innocuous materials, the identification takes place through the correlation of various chemical elements observed, coupled to the information about the innocuous material itself.

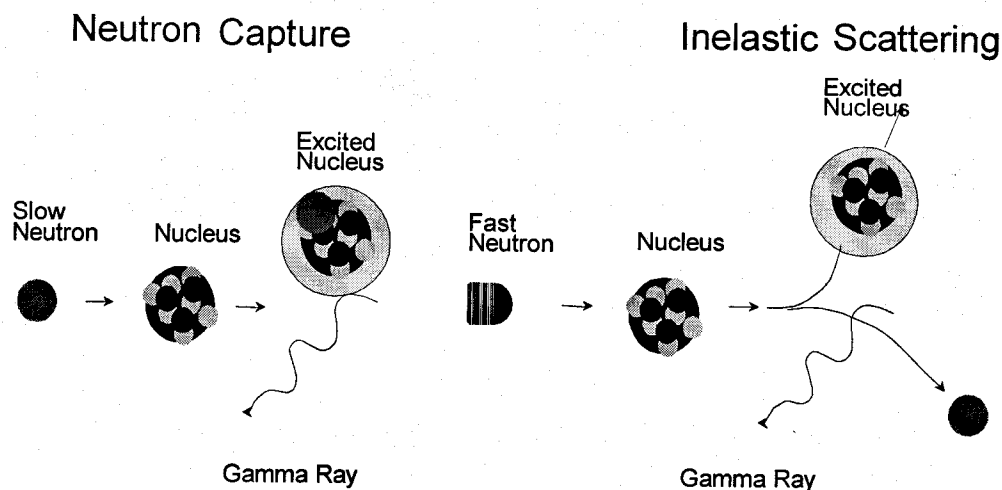


Figure 8. Nuclear reactions initiated by thermal neutrons (capture reactions) and fast neutrons (inelastic scattering).

Neutrons are highly penetrating particles. Their intensity is not diminished by the thickness of common containers. To a lesser extent, the outgoing γ rays are also very penetrating, easily exiting the interrogated volume to be detected by an appropriate set of detectors placed outside the object. Thus, the method is non-intrusive (the interrogation can take place from a distance of several centimeters) and non-destructive because of the very small amount of radiation absorbed by the interrogated object.

Depending on the chemical elements to be measured, one might have to use neutrons of several energies. In many of the neutron-based applications currently in use, radioisotopic sources (Am-Be, ^{252}Cf) are utilized for neutron production. These sources can excite a host of chemical elements (H, C, S, Fe, etc.) through neutron capture reactions. However, there are other elements such as C and O which need neutron energies several MeV higher than those available from the radioactive sources. To satisfy this, a neutron source is required that can produce the high energy neutrons for measurement of elements such as C and O, and low energy (0.025 eV) for elements such as H and Cl. It has been shown [9, 10] that such a task can be accomplished with the utilization of a pulsed neutron generator. This technique is called Pulsed Fast/Thermal Neutron Analysis (PFTNA).

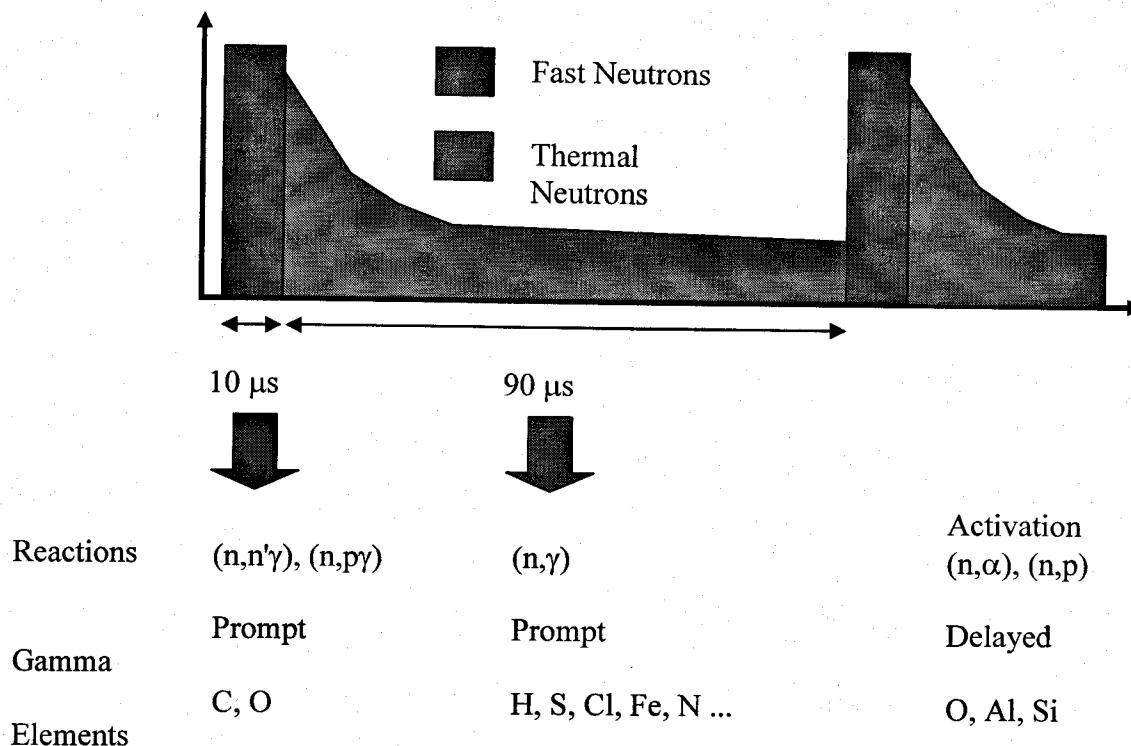


Figure 9. Pulsed neutron generator time sequence.

2.1.4 The PFTNA Principle

The basis of PFTNA is a pulsed neutron generator utilizing the deuterium-tritium (d-T) reaction. The pulsed d-T neutron generator provides 14 MeV neutrons which in turn initiate several types of nuclear reactions ($(n,n'\gamma)$, $(n,p\gamma)$, (n,γ) etc.) on the object under scrutiny. The γ rays from these reactions are detected by a suitable set of detectors (usually bismuth germanate (BGO) scintillators). During the neutron pulse, the γ -ray spectrum is primarily composed of γ rays from the $(n,n'\gamma)$ and $(n,p\gamma)$ reactions on elements such as C and O, and is stored at a particular memory location within the data acquisition system. These reactions have gamma-ray emission times on the order of a few femtoseconds or less. Since the time of flight of 14 MeV neutrons is

Table 1. Elemental densities and ratios of three classes of substances.

Density or Ratio	H	C	N	O	Cl	C/O	C/N	Cl/O
Narcotics	High	High	Low	Low	Medium	High, >3	High	Very High
Explosives	Low-Medium	Med	High	Very High	Medium to None	Low, <1	Low, <1	Low to Medium
Plastics	Medium-High	High	High to Low	Medium	Medium to None	Medium	Very High	-

approximately 5 centimeters per nanosecond, these reactions happen immediately. The speed of the neutrons means that they do not linger in the vicinity of the object but quickly move out into space. Thus, once the neutron generator has turned off, the inelastic reactions are eliminated.

Between pulses, some of the fast neutrons that are still within the object lose energy by collisions with low atomic number elements composing the object. When the neutrons have an energy less than 1 eV, they are captured by such elements as H, N, and Fe through (n,γ) reactions. The γ rays from this set of reactions are detected by the same set of detectors but stored at a different memory address within the data acquisition system. It takes several collisions before the neutron is moderated from 14 MeV (velocity $\sim 20\%$ of the speed of light) to thermal kinetic (0.025 eV) energies (velocity ~ 2.2 km/s). The actual time for this moderating process is difficult to estimate but believed to take on the order of a microsecond. Only about 10-20% of the total neutrons emitted are moderated in this manner and thus, the justification of the statement that the fast spectrum is composed *primarily* of inelastic reactions. After the neutron generator has turned off, these thermal neutrons drift throughout the object and around the PELAN. It takes many microseconds (sometimes even milliseconds) before the thermal neutrons have diffused from the area. The time of diffusion depends on the geometry of the area e.g. a PELAN enclosed in a small confined space with high-hydrogen content (10 wt% or greater) will have a longer diffusion time.

This procedure is repeated with a frequency of approximately 10 kHz. This pulsing is NOT to maximize the 14 MeV neutron flux but to maximize the thermal neutron flux. We have found, based on years of experience, the optimum quiescent period is between 50 μ s to 150 μ s. The switching power supplies in the neutron generator systems have optimum duty factors around 10%. Thus, we arrive at the neutron pulse duration of 10 μ s with a frequency of 10 kHz.

After a predetermined number of pulses, there is a longer pause that allows the detection of γ rays emitted from elements such as Si and P that have been activated. Therefore, by utilizing fast neutron reactions, neutron capture reactions, and activation analysis, a large number of elements contained in an object can be identified in a continuous mode without sampling. Figure 9 shows the time sequence of the nuclear reactions taking place.

There is only one "pure" spectrum of a particular type of reaction: the activation spectrum. The spectrum taken during the neutron pulse is composed of inelastic reactions, thermal capture reactions, and activation reactions. The reaction rate of the inelastic reactions is at least an order of magnitude above the other types of reactions. The spectrum between pulses is dominated by thermal capture reactions but activation reactions (such as O and Si) can easily be seen and must be taken into account. There is a pause of a few seconds before an activation reaction is begun and is more than enough time to eliminate short-lived isotopes and completely dispel any thermal neutrons.

2.1.5 Methodology

PFTNA uses low resolution, high Z detectors such as bismuth germanate (BGO) or gadolinium ortho-silicate (GSO). Data analysis of the resulting γ -ray spectra is performed with the computer

software called SPIDER, a spectrum deconvolution code developed for the Windows 95/98/NT platforms[11].

To use SPIDER, one must first measure the response of the detector in question to γ rays from pure elements. For example, a block of pure graphite is used to determine the detector's response to the C γ rays. To determine the detector's response to elemental H, a response is measured from a water sample.

In the absence of any sample placed in front of the detector, the detector records γ rays emanating from the materials surrounding the detector, as well as from the materials inside and around the neutron generator. This spectrum is called the background spectrum. When a sample is placed in front of the detector and a gamma ray spectrum is acquired, the counts in the i th channel of the spectrum of a sample, S , can be represented by the equation:

$$S_i = k * B_i + \sum_{j=1}^n c_j * E_{i,j} \quad (1)$$

where B_i is the background spectrum at the i th channel and k is its coefficient, $E_{i,j}$ is the response of the j th element at the i th channel and c_j is its coefficient, and n is the total number of elements utilized to fit the spectrum. SPIDER employs a least-squares algorithm to fit Equation (1).

Another way to understand the process is through the use of linear algebra. Consider any spectrum, S , to be a $1 \times N$ column vector where N is the number of channels. Consider the spectra given by pure elements to be row vectors with dimension $N \times 1$. The background can be considered as a row vector as well. Let R be an operator with dimension $M \times N$ where $M = \text{number of elements} + 1$. The elemental spectra are the rows of R along with the background. Thus the elements and the background form an orthonormal basis for this vector space.

In terms of linear algebra:

$$S = RC \quad (2)$$

where C is a column vector of coefficients. Thus the problem becomes to invert R and have it operate on S . The least squares part of the process is to then shift the elements of S from -2 to $+2$ i.e. that $S_i(1) = S_i$ where (1) designates a shifted spectrum from the origin spectrum, S . This shifting process is to reduce errors caused by shifts in the energy calibration of the spectrum.

When examining the deconvolution process in this manner, then one realizes that the background spectrum is not subtracted. It is manipulated by changing its amplitude to give the lowest chi-square. Also, the background cannot be subtracted "incorrectly" since no true subtraction is being performed.

The elemental responses are the response of the detector to a pure element. For example, a block of graphite is used to measure the elemental response of carbon. A spectrum of this carbon is taken using the PFTNA method and stored. In the case of carbon, the $2^+ \rightarrow 0^+$ transition (4.430 MeV) is the most prominent. A measurement of the geometry in the absence of carbon is also taken. The background spectrum is used to "strip" (subtracted channel by channel) the carbon spectrum. At the end of this process only the 4.430 MeV gamma (and its escape peaks) remain in the spectrum. This reduced spectrum becomes the elemental response of carbon.

In this manner, the elemental response contains the following information: 1) the cross-section of the reaction, 2) branching ratios of the various gamma rays, 3) the detector efficiency, and 4) the geometry of the detector. Mathematically, $cps = \varepsilon(E) * \phi * \sigma(E) * N$ where $\varepsilon(E)$ = efficiency of the detector at gamma ray energy, E , ϕ = neutron flux in $n/cm^2/s$, $\sigma(E)$ = the cross-section (or probability) of gamma-ray energy, E , and N is the number of atoms of a particular element. The thermal neutron flux, ϕ_{th} , is a function of the fast neutron flux, ϕ , related by $\phi_{th} = k * \phi * N_H$ where k is some constant based on the geometry of the moderating material and N_H is the number of H atoms in the moderating material.

The coefficients that are returned from the SPIDER program are dimensionless quantities and must be scaled to some physical units. In our work, we have found it convenient to multiply the coefficients by the area of the most prominent peak in the stored elemental response. The area of the peak is in units of counts per second (cps) and thus, answers returned by SPIDER to the users are in cps as well. This system of units is somewhat arbitrary and confusion can arise when one tries to determine the correct chemical ratios of elements.

2.1.6 Previous Measurements to Validate the Software

We have performed numerous measurements to ensure that the SPIDER software produces accurate quantitative results. We acquired several coal samples which contained various quantities of carbon, hydrogen, oxygen, sulfur, sodium, and chlorine. These elements are measured through fast neutron reactions (C, O, Na) and thermal neutron capture (H, S, Cl).

Using appropriate ASTM sampling techniques, samples were prepared and sent to an ASTM-approved laboratory. The samples were also measured using a PFTNA-based system with the SPIDER software. Figure 10 shows very good agreement between ASTM methods and the results of SPIDER.

This shows that the PELAN method of data analysis produces quantitatively accurate results.

In response to a specific suggestion to compare background measurements 1 m above the soil and on the soil, we have prepared Figure 11. We examine the ratios of these spectra between peaks. The ratio during the neutron burst changes by a factor of 2 in the fast spectrum and the ratio between neutron bursts changes by a factor 4 in the thermal spectrum. This indicates that more neutrons are being moderated and that a simple $1/r^2$ model is not appropriate for the spectrum taken between bursts.

For the spectrum taken during the neutron burst, we are unsure exactly what is the more important distance: the distance from detector to soil or the distance from neutron generator to soil. The spectrum shown below seems to be some linear combination of the effects of these distances.

2.1.7 Data Collection

In Figure 12 A, the fast spectrum is the figure to the left side of the page and the thermal spectrum is to the right side of the page. These spectra have energy between 100 keV and ~12

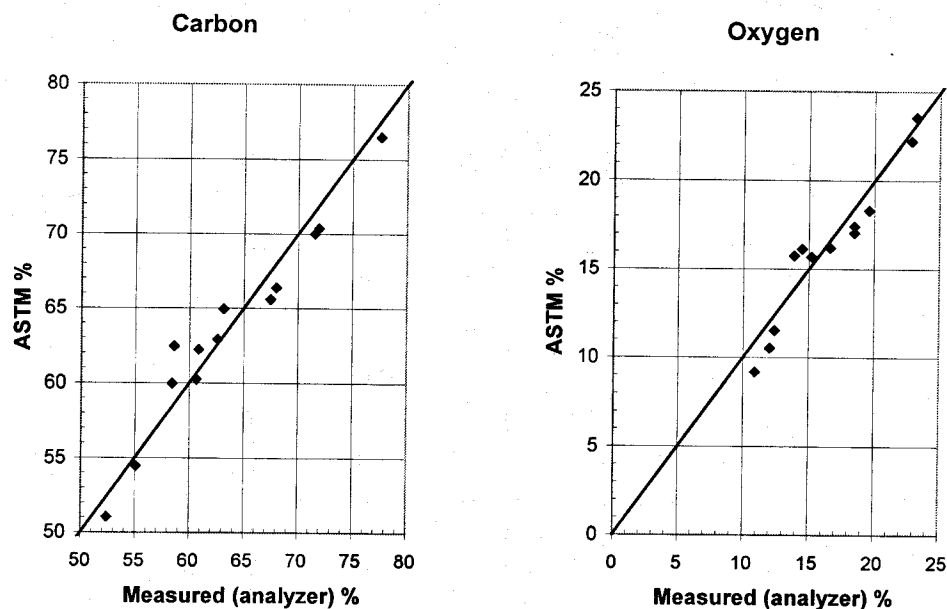


Figure 10. Graphs of ASTM measured values of carbon and oxygen in coal samples versus those determined by a PELAN-like measurement.

MeV. Each channel represents 25 keV in the 512 channel spectrum. For each interrogation, both spectra are recorded in a user-defined folder on the hard-drive within the PELAN.

Each interrogation (including data collection and data reduction and analysis) is performed in five minutes.

A measurement procedure for a specific target proceeds as follows:

1. For shells to be interrogated on the ground, PELAN is placed at some distance from the shell of interest, and a spectrum with an empty shell is taken. The empty shell is the same size (diameter) as the shell of interest. This is called the "background" spectrum.
2. PELAN is placed within 6 inches of the shell interest.
3. A spectrum is taken of the shell of interest and automatically stored on the hard-drive.
4. The SPIDER program loads both the shell of interest and the background spectrum. Each spectrum (fast,thermal) is deconvoluted separately.
5. The results (in counts per second) are returned to the user. These results are recorded.
6. The goodness of fit is determined by 1) a chi-square of nearly unity and 2) each data point in the fitting region within 3 standard deviations. The fit and its residuals are recorded in a comma-separated value file which can be analyzed by programs such as Excel, SigmaPlot, SAS, etc.
7. Depending on the shell fill, all major chemical elements (such as carbon, hydrogen, oxygen, nitrogen, silicon, calcium) will be recorded in counts per second.
8. These results are recorded on a spreadsheet. Typically, many elemental ratios are calculated. We will look for elemental ratios or contents which tend to segregate types of munitions.

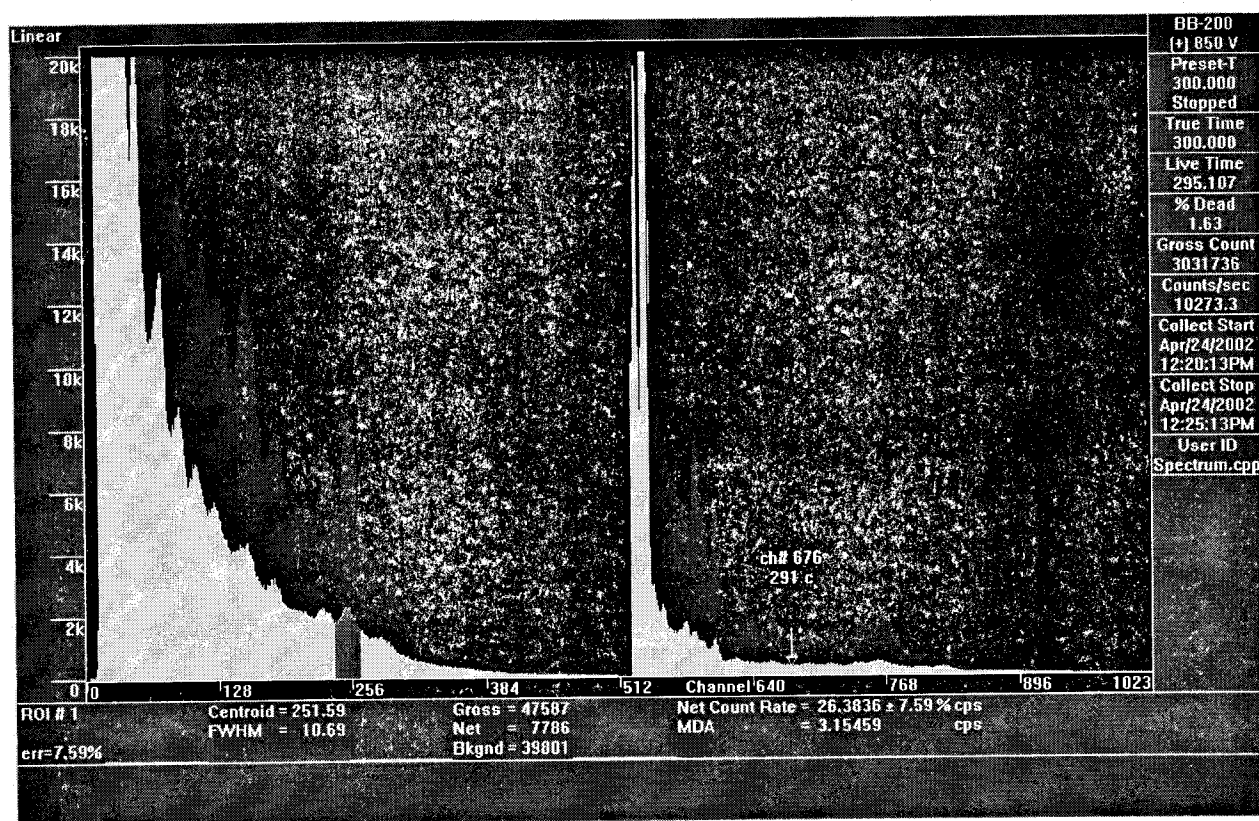


Figure 11. The yellow spectrum is taken 1 m above the soil and the blue spectrum is taken on the soil. This data was taken prior to the demonstration at WKU's Applied Physics Institute.

9. The limits for the thresholds are based on these plots. Typically, one tends to err on the side of safety and be more inclusive with possible threats.

2.1.8 Correcting For Shielding Effects Due to Large Masses of Fe

Iron is an excellent shielding material for neutrons. Thus an empty shell can effectively shield the underlying soil from neutrons. This shown in Figure 12B where an empty 105mm shell spectrum is compared to a soil background with no shell. In the region of the O gamma ray at 6.130 MeV, the shielding effect is particularly noticeable.

If one tries to analyze the Fe shell spectrum with the empty background, the oxygen count rate may be negative. Also, in the thermal spectrum, the strong iron signal may also camouflage the chlorine gamma rays (which are near in energy).

The best way to solve this problem is to use a shell that is the same size and type of shell of the ordnance under scrutiny e.g. if one wants to measure 105mm shell with TNT, then an empty 105mm shell spectrum is used as a background. In the field, carrying an assortment of shells is not desirable or feasible.

In order to circumvent this problem, we have devised the following algorithm.

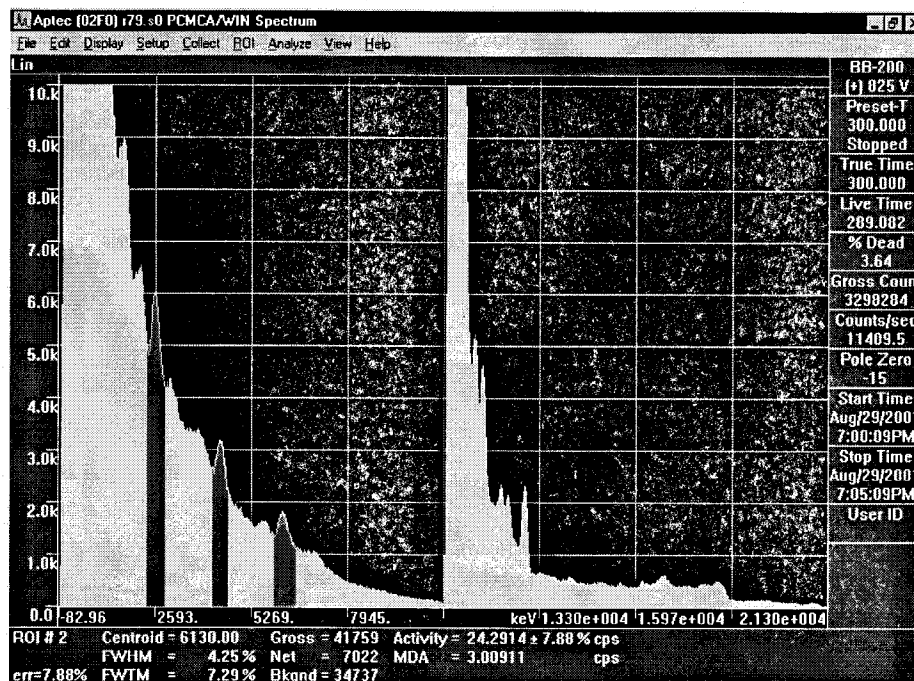


Figure 12A. The spectrum on the left is the fast spectrum. The spectrum on the right is the thermal spectrum.

1. Measure two spectrum: an empty spectrum ("empty") and a spectrum with a massive Fe object ("Fe").
2. Fe has an inelastic gamma ray at 846 keV (see Figure 12B). We will first compute the area of this peak for the empty spectrum and the Fe spectrum. These values are stored in memory.
3. For an unknown shell, the area around this peak is also computed.
4. Let $R = \frac{S_{Fe,unknown} - S_{Fe,1}}{S_{Fe,2} - S_{Fe,unknown}}$ where $S_{Fe,1}$ =area of 846 keV for the empty spectrum, $S_{Fe,2}$ = area of 846 keV for the Fe spectrum, and $S_{Fe,unknown}$ =area of 846 keV for unknown shell
5. Then we modify the empty spectrum by the following formula:

$$C_{NewBackground}(\#ch) = \frac{C_1(\#ch) + R \cdot C_2(\#ch)}{1 + R}$$

where $C_{NewBackground}$ = the new interpolated background spectrum being generated, #ch= channel number, C_1 is the empty spectrum, and C_2 is the Fe spectrum.

Figure 12C shows a comparison between a 90mm shell and a spectrum interpolated by the above described procedure using a 105mm shell as the Fe shell. The thermal spectrum is in good agreement, especially in the region of the H gamma ray. However, the procedure under-corrects in the fast spectrum. This under-correction will provide a bias towards lowering the value of O for the fill material of this shell when the interpolated spectrum is used in the SPIDER program (essentially an over-subtraction). While not as accurate as using shells of the same size, this

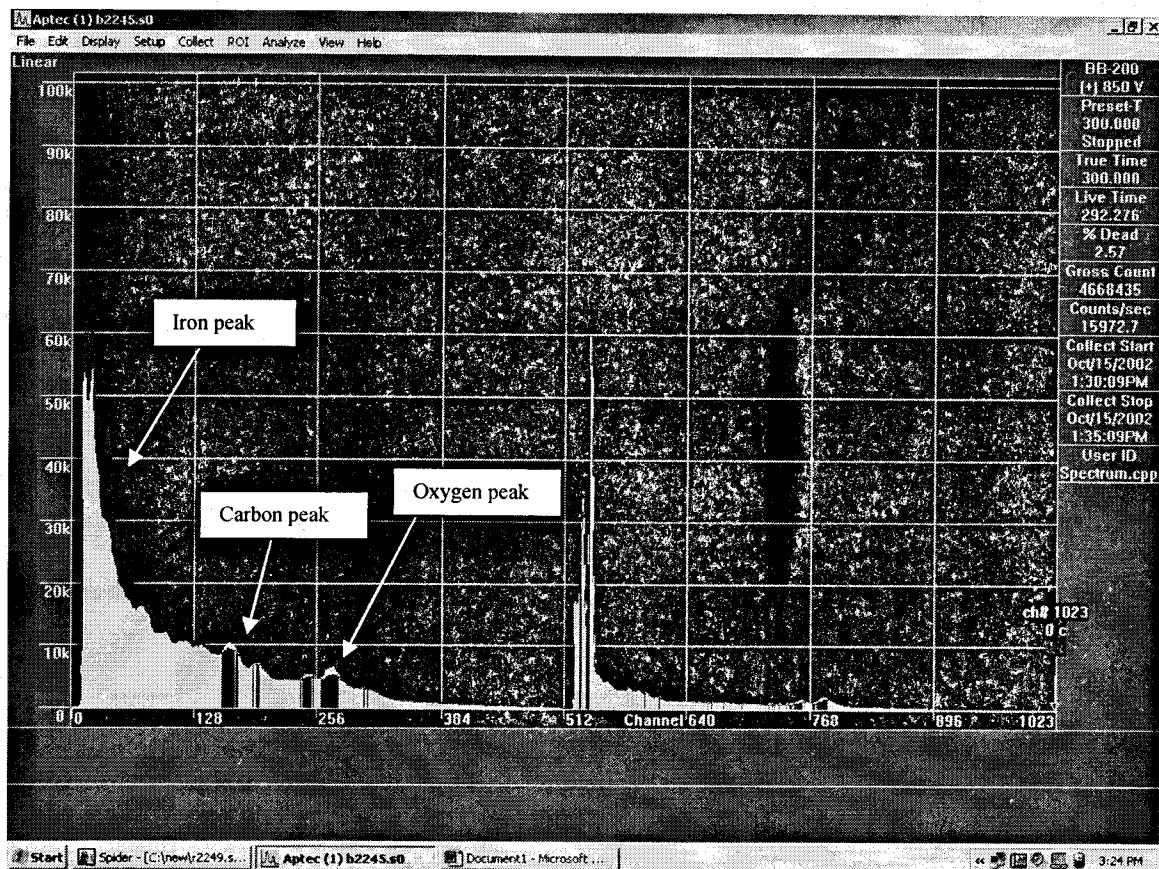


Figure 12B. Two spectra with and without presence of Fe on soil. Yellow spectrum is an empty background. Blue spectrum is a 105mm shell.

method does a remarkable job in determining the proper correction. The interpolation and the analysis are performed in an automatic manner without any user intervention.

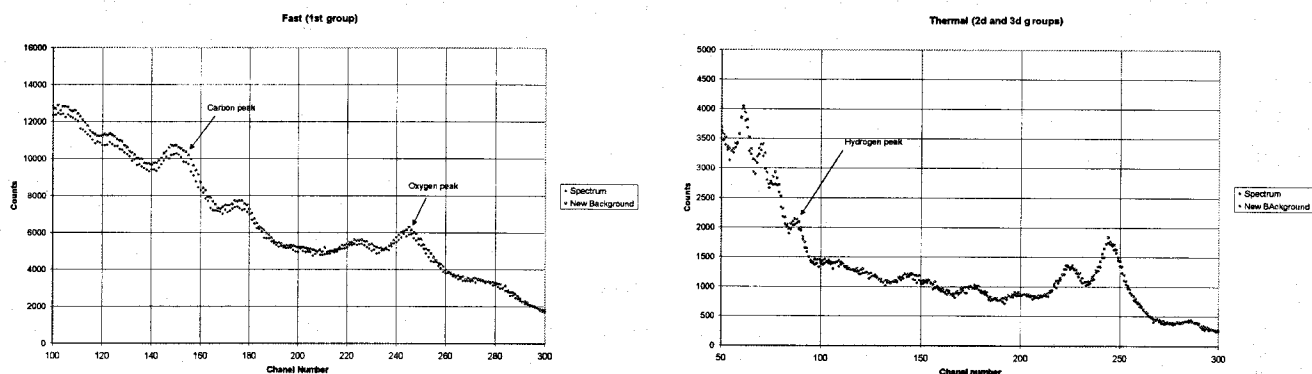


Figure 12C. The figure on the left is the fast spectrum for a 90mm (blue) and interpolated background (purple). The figure on the right is the thermal spectrum. See text for details

2.1.9 Introduction to Decision Trees

For PELAN, the following distinction is made:

- Calibration --Refers to the energy calibration of the PELAN gamma-ray spectrum. This is performed automatically each time the PELAN is turned on, using a small radioactive source permanently attached near the detector. No user intervention is required.
- PELAN Library---Refers to the identification of an object. In order for PELAN to identify a substance or an object, it must be trained to do so. This training is performed by analyzing a variety of objects that PELAN will encounter in a specific situation. For each object, all major elements and important minor elements are identified and quantified. It is these data which form the basis of the decision tree.

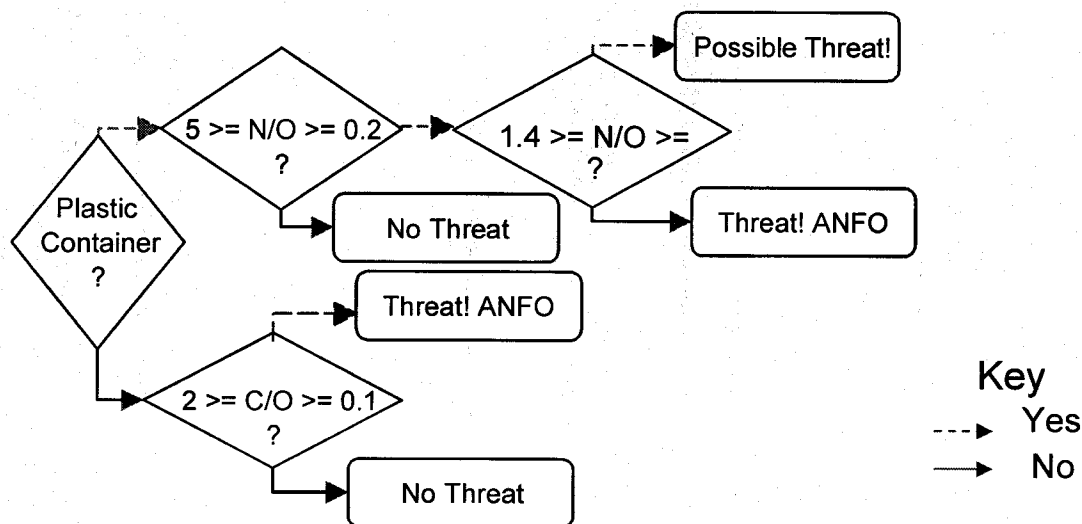


Figure 13. Example of a decision-tree for ammonium nitrate –fuel oil (ANFO) bomb.

For PELAN, to automatically identify an object through its elemental composition, a library of the substances that it will be asked to identify must reside in its computer. PELAN, based on a decision tree previously prepared by the operator and residing in the computer can then make a decision. This section shows how can the operator change the decision tree in order to conform to the identification of the objects, for the particular set of conditions that PELAN will be operating on.

The PELAN software code is written in MSVisual C++ and containing a tree of decision making algorithms composed of a series of **if/then** and **and/or** program steps. These statements set **greater than** and **less than** limits on elemental counting rates and their ratios that relate to characteristics of known substances. The decision tree uses deductive reasoning to identify one substance from others conclusively. Using MSVisual C++, one can modify the decision tree by changing the numbers limiting the coefficients and ratios. The output statements, such as **"THREAT EXPLOSIVES!"** can be chosen from a list at the appropriate command line.

2.1.9.1 Algorithms for PELAN Decision Trees

Successful characterization by elemental analysis using PELAN depends on developing pattern recognition through experimental investigation using known substances. Explosives, chemical warfare agents and contraband drugs are chemical substances with distinct elemental signatures. After interrogating several substances of the above as well as a variety of innocuous substances, characteristic differences will be evident and can be noted for use in determining an unknown substance. Based on the experimental results, elemental ratios as well as the presence or absence of specific chemical elements can be used in making a decision whether an unknown substance belongs to a group of "dangerous" substances, or is an innocuous one.

To create a decision tree for any certain application, the pre-existing decision tree for a previous application can be modified. The code sets limits for elemental responses and for characteristic elemental ratios. They progress logically to deduce a result such as "Explosive Threat!," "TNT!" or "Drugs!"

The responses can be dependent on the material of the container and its physical properties and they can be affected by other objects in the container. Attention should be given to the background and the container, particularly if the amount of substance to be analyzed is small.



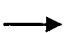
Conducting experimental tests for contraband and dangerous substances may be restricted and test materials are difficult to obtain. It is possible to substitute the above materials with a combination of chemicals that, when mixed, have the same chemical elemental composition as the materials to be identified. These are referred to as simulants.

2.1.9.2 DESIGNING A DECISION TREE

A decision tree is a graphic representation that illustrates the sequence of operations to be performed to get the solution of a problem.

Guidelines for drawing a decision tree:

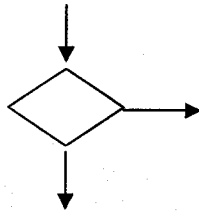
Decision trees are usually drawn using some standard symbols (see example in Figure 13).

Name	Symbol	Use in decision tree
Diamond		denotes a decision to be made. The program should continue along one of two routes (e.g., IF/ ELSE).
Rectangle		denotes the Terminal condition.
Flow Line		denotes the direction of logic flow in the program.

The following are some guidelines in making a decision tree:

- In drawing a proper decision tree, all necessary requirements should be listed in a logical order.
- The decision tree should be clear, neat and easy to follow. There should not be any room for ambiguity in understanding the decision tree.
- The usual direction of the flow is from left to right or top to bottom.

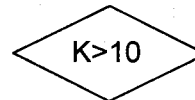
- d. Only one flow line should enter a decision symbol, but two or three flow lines, one for each possible answer, should leave the decision symbol.



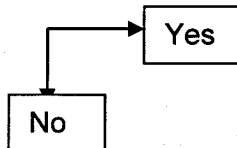
- e. Only one flow line is used in conjunction with the terminal symbol.



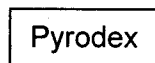
- f. Write the test condition inside the diamond symbol.



- g. The flow line pointing to right indicates a YES and the flow line pointing down indicates NO



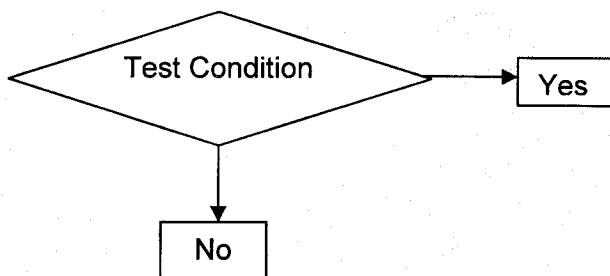
- h. Write the terminal condition in the rectangular symbol



- i. Ensure that the decision tree has a logical start and finish.

2.1.9.3 Guidelines for converting a decision tree into a C programming language code

- The following shows how to convert a decision block into a simple *if else* statement in C.



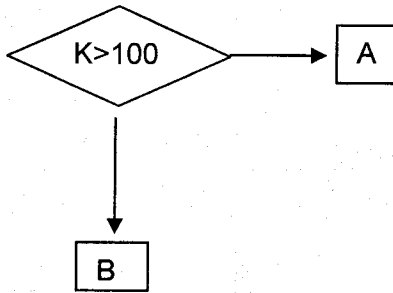
A Decision Block

```

if(test condition)
{
  statement for YES
}
else
{
  statement for NO
}
  
```

The C code

- The decision block ends in either another decision block or a terminal condition.



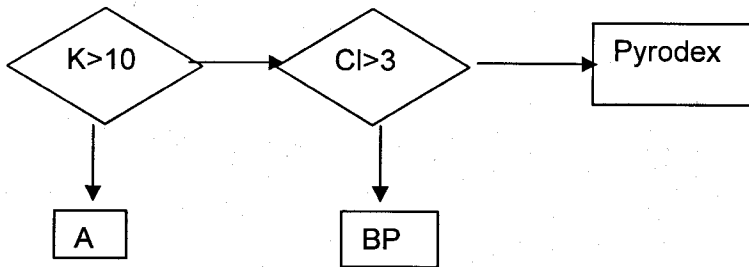
Decision block ending in terminals

```

If(K>100)
{
  statement A
}
else
{
  statement B
}
  
```

The C code

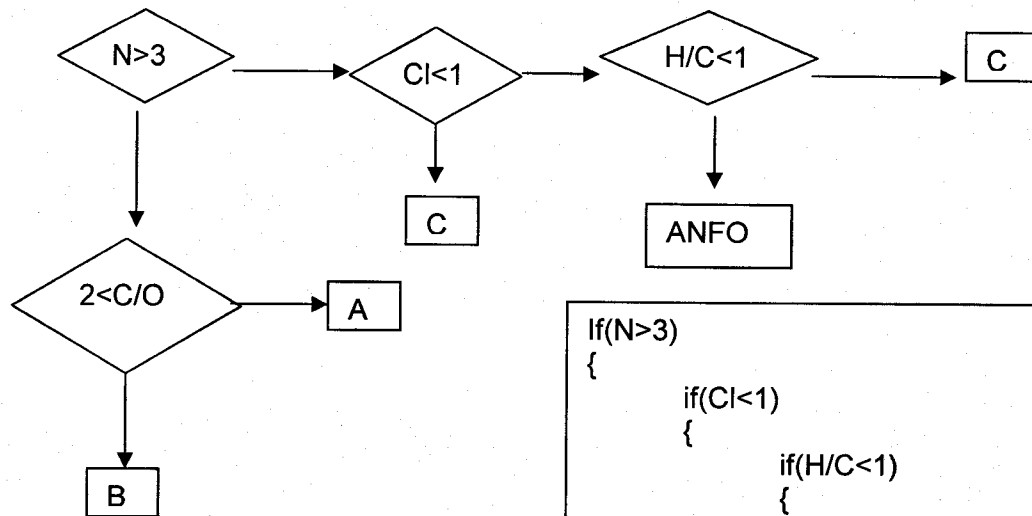
If a decision block ends in another decision block, we have a corresponding nested **if else** code in C. Each else has a matching if. A is the corresponding else statement for the condition $K > 10$ and BP is the corresponding else statement for $CI > 3$.



```

If(K>10)
{
    if(CI>3)
    {
        Pyrodex
    }
    else
    {
        BP
    }
}
else
{
    A
}
  
```

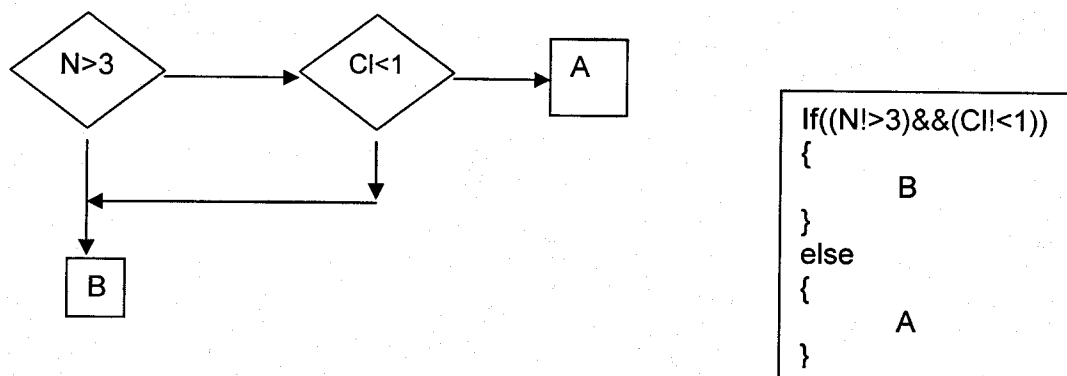
One more level of nested if else code is illustrated here.



```

If(N>3)
{
    if(CI<1)
    {
        if(H/C<1)
        {
            C4
        }
        else
        {
            ANFO
        }
    }
    else
    {
        C
    }
}
else
{
    if(2<C/O)
    {
        A
    }
    else
    {
        B
    }
}
  
```

Sometimes two decision blocks share a common Yes or NO edge. In C code the sharing edges then also share a common if or else statement.



2.2 Advantages and Limitations of the Technology

Prominent alternative technologies can be divided into two groups: a) shape recognition techniques, and b) content recognition techniques. Shape recognition techniques include GPR, and x-ray backscattering. Other than PELAN, content recognition techniques include TNA, NQR, vapor detection, and neutron backscattering. From the nuclear techniques, TNA is methodologically closest to PELAN. TNA is primarily used to detect one element, nitrogen. PELAN bases its UXO identification on several chemical elements, not just on nitrogen. Assuming that TNA and PELAN have comparable detection probability for detecting N, therefore PELAN is expected to have a lower false negative rate due to its multi-element approach. Why?

Let's consider two conditions: the first condition is for N, and the second condition is for C. Furthermore, let us say that the probability of false negatives is 10% for the first condition and for the second condition, 20% (i.e. N is a better parameter to determine a threat than C). Using only the condition for N gives a probability of false negatives 10% but in the case of a Boolean "and" between the two conditions, the total probability of false negative is 10%*20% or 2%.

Furthermore, in the case of sandy soils and in particular in desert terrain, PELAN is totally unaffected by the presence of silicon which masks nearly completely the nitrogen signal. It should be pointed out that currently there is no single method that is capable identifying the fill of a shell under any terrain conditions, amount of explosive, etc.

The signal to noise ratio (SNR) is primarily affected from all the substances that surround the object under interrogation (e.g. soil). A spectrum of all gamma rays from the substances around the interrogated object is the background spectrum (or noise). Since soil contains some of the same elements that are inside a shell (hydrogen, oxygen, calcium etc.) the signal to noise ratio is affected primarily by the background.

PELAN Capabilities	PELAN Limitations
Identifies contents of shell	Cannot image an object
Unaffected by the thickness of a shell	Does not perform wide area survey
Can differentiate types of HE or combinations of HE & chemical agents	Affected by clutter
Can be transported easily, requires low power, poses minimum radiation danger	Needs computer libraries for proper identification
Can interrogate an object without touching it	SNR depends on surrounding materials

2.3 Factors Affecting Cost and Performance

- Neutron generator is the most expensive item. Current prices range between \$55,000 and \$70,000 for a neutron generator. We are currently working in reducing appreciably this price. The other three sections of the PELAN (computer/data module, shielding, and detector) have a cost less than \$5K each.
- Performance is primarily affected by "clutter", i.e. substances around the object under interrogation that contain appreciable amounts of H, C, N, and O.
- Amount of explosive.

3. Site/Facility Description

3.1 Background

The test site chosen was at the Naval Explosive Ordnance Technology Center (NAVEODTECH) at Indian Head, Maryland. This site was chosen because of the availability of ordnance and also because NAVEODTECH was sponsoring a demonstration of PELAN to evaluate features developed under a separate contract. Since this Phase I demonstration was not a demonstration of the device but more a validation of the methodology, the site of this demonstration was not a critical parameter. NAVEODTECH has access to a wide variety of shell-sizes, types, and explosives. This was critical to the success of the test.

3.2 Site/Facility Characteristics

Four different soil environments were tested: gravel, sand, local soil, and wet local soil. Targets were placed on the surface of these soil environments. For the gravel, sand, and wet soil, specially constructed 3' x 3' wooden boxes were constructed. Each of these boxes were filled with the appropriate soil to a depth of 1'.

Targets were also interrogated on a wooden table-approximately 3' above the local soil.

During the tests, the ambient temperature varied from 53° F to 93° F. Relative humidity varied between 22% to 63%.

A small canopy was raised and the system was operated from inside this area. Standard 115V AC power was provided by extension cords connected to a nearby building. Figure 16 shows a picture of this control area. The PELAN itself was located approximately 80' from the control area. Figure 14 shows a rough drawing of area in location to the magazine and the nearby warehouse/office.

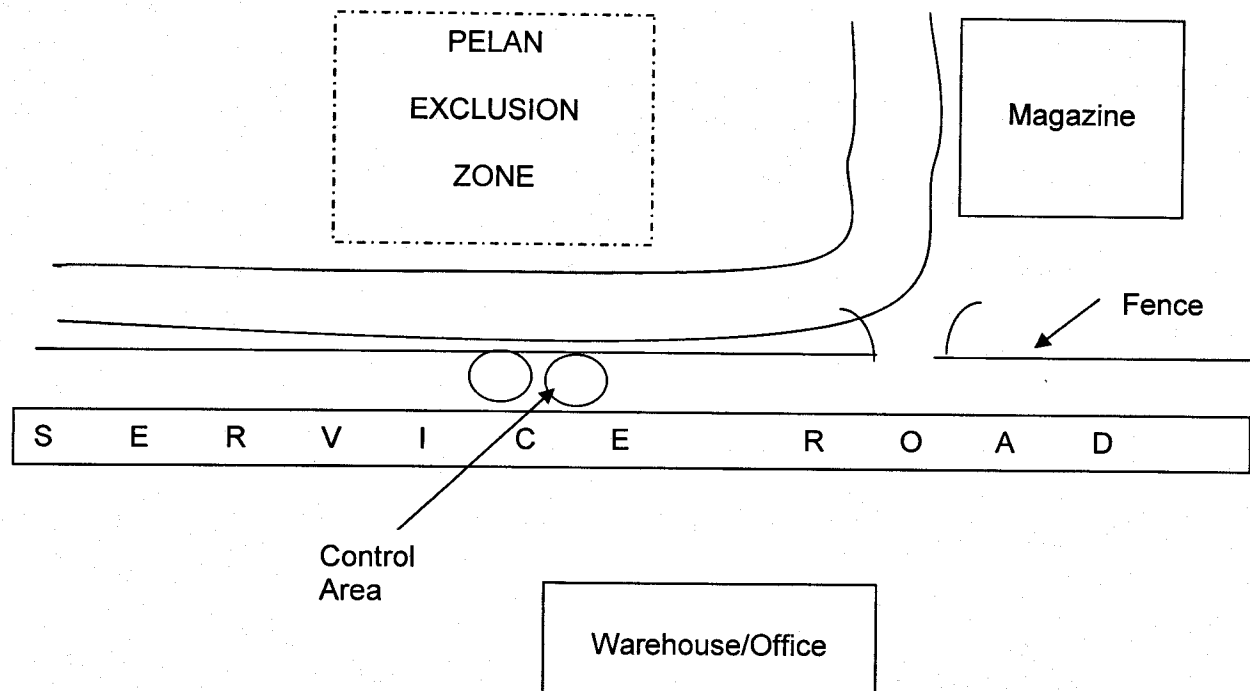


Figure 14. Layout of Area for PELAN Demonstration.

4. Demonstration Approach

4.1 Performance Objectives

The Phase I Demonstration had the following objectives:

- To obtain a library of elemental signatures of a variety of shells as found in ranges and proving grounds
- To check the reliability of the decision trees produced through elemental ratios
- To determine the range of validity of the decision trees
- To ascertain the repeatability of the measurements, false positive and false-negative rates.

The PELAN was demonstrated against the following UXO:

- UXO sizes from 60 mm to 155 mm filled with TNT, CompB, or RDX
- Various other explosives such as SEMTEX, a PETN sheet explosive, Smokeless Powder, etc.
- Inert fills including: plaster of Paris, wax, and sand
- A complete listing is shown in Table 2

Table 2. Ordnance, Explosives, and Mine Targets

Explosive Items		
	<u>TYPE</u>	<u>EXPLOSIVE</u>
1	60 mm mortar	TNT
2	76 mm Projectile	RDX
3	76 mm projectile	TNT
4	81 mm mortar	Comp B
5	82 mm mortar	TNT
6	82 mm mortar	TNT
7	90 mm projectile	RDX/TNT (52/48)
8	90 mm projectile	RDX
9	90 mm rocket	TNT/RDX (60/40)
10	105 mm projectile	Comp B
11	120 mm mortar	TNT
12	122mm rocket	Comp B
13	155 mm projectile	TNT
14	ANFO 2%	ANFO
15	ANFO 6%	ANFO

Explosive Items		
	<u>TYPE</u>	<u>EXPLOSIVE</u>
16	ANFO 15%	ANFO
17	Semtex-1A (samples)	Semtex
18	Shape Charge	PBX-108
19	Shape Charge	Octol
20	Sheet Explosive	PETN
21	Smokeless Powder	Smokeless Powder
22	FFV 028 (steel) mine	TNT or RDX/TNT
23	TMRP-6 (plastic) mine	TNT
24	Valmara 69 mine	Comp B
Inert Items		
1	60 mm mortar	Empty
2	60 mm mortar	Wax
3	60 mm mortar	Hard red wax
4	60 mm mortar	Plaster of Paris
5	90 mm projectile	Empty
6	90 mm projectile	Hard red wax
7	81 mm mortar	Empty
8	81 mm mortar	Wax
9	81 mm mortar	Sand
10	81 mm mortar	Plaster of Paris
11	105 mm mortar	Empty
12	105 mm mortar	Wax
13	105 mm mortar	Sand
14	155 mm projectile	Empty
15	155 mm projectile	Wax
16	155 mm projectile	Hard red wax

The length of the scheduled demonstration was two weeks. The data to be taken were divided in the following topics:

- Gamma ray spectra of empty shells were placed on different types of soil. These spectra are identified as background spectra. The subsequent analysis of a shell uses one of this background spectra as a reference in quantifying the major chemical elements of the shell's contents.
- Stability of the background spectra. These measurements were testing the long term stability of the PELAN measurements. If PELAN is to be used for extended periods at a site with a particular type of soil and a certain type of shells, a stable

background means that the various background spectra can be measured and subsequently stored in a computer library.

- Repeatability of measurements. These measurements were to establish the precision of the PELAN measurements. Measurements were taken in a random order for this task along with 4 differently filled, different diameter shells. Measurements were continued until there are 10 measurements per shell.

The spectra were analyzed using the gamma ray analysis program, SPIDER, and the elemental content along with several elemental ratios are computed. These were statistically analyzed by comparing the standard deviation in the measurements with the error calculated by SPIDER.

Standard deviations for the elemental measurements and the various ratios were calculated using the STDEV in EXCEL™. STDEV assumes that its arguments are a sample of the population. The standard deviation was calculated using the "nonbiased"

or "n-1" method. The formula used is: $STDEV = \sqrt{\frac{n \sum x^2 - (\sum x)^2}{n(n-1)}}$ where n is the number of points and x is the data.

The error calculated by SPIDER was determined from the stability tests given in Tables 5 – 9 and from a selection of the data presented in Table 13. The details and results of this analysis will be discussed in section 5.1 Performance Data.

For a variety of shells, soil types, fills, 5-minute PELAN measurements are taken. Using 35 of these spectra, a decision tree was established. The decision tree was used for the automatic identification of the contents of the other shells.

4.2 Physical Setup and Operation

Figures 15 & 16 show the physical setup of PELAN at NAVEODTECH/Indian Head MD.



Figure 15. Location of PELAN at NAVEODTECH area.

Figure 15 shows the physical location of PELAN during the test phase at NAVEODTECH. At a distance of 45 ft around PELAN, the area was marked and posted with radiation signs. This was the distance from PELAN where the radiation dose rate was measured to be the allowed dose rate for the general public (0.05 mRem/hr, not to exceed 2 mRem at any hour). To the right of the picture, across from the paved road are the magazines where shells are kept.

PELAN was operated from a laptop, physically located at an area outside the fenced area where PELAN was. Figure 16 shows the location for the operation of PELAN. There were two cable connections between PELAN and the canopied area: one cable carried the 110V AC power to PELAN, and the other was a hard-wired communication cable between the laptop and PELAN. Although PELAN can also be operated through an RF wireless control, NAVEODTECH requested that for safety reasons PELAN should be operated with a hard-wired connection.



Figure 16. Canopied area from where PELAN was operated.

4.3 Sampling Procedures

A list of available shells ranging between 155 mm and 60 mm was prepared by NAVEODTECH. The shell were filled either with high explosive (e.g. TNT, RDX), or with one of the inert fills used for ballistic tests (Plaster of Paris, sand). Several tables were prepared by ESTCP and NAVEODTECH, indicating the specific shells that would be used for each of the tests. Following a predetermined procedure based on the

performance objectives, EOD technicians placed different types of shells in front of PELAN. Table 3 shows the elemental compositions of the explosives used in this demonstration.

Table 3. Elemental compositions and ratios for the explosives employed in the demonstrations.

Explosive	Elemental Composition (e.g water H=2, O=1)						Ratios		
	C	H	N	O	S	K	C/H	C/N	C/O
TNT	7	5	3	6			1.4	2.3	1.2
RDX	3	6	6	6			0.50	0.50	0.50
Comp B, Grade A	2.0	2.6	2.2	2.7			0.77	0.93	0.76
Comp B-3C	2.0	2.5	2.2	2.7			0.82	0.95	0.77
PETN	5	8	4	12			0.63	1.3	0.42
Octol 75/25	1.8	2.6	2.4	2.7			0.69	0.75	0.66
PBX 108							-	-	-
Semtex 1A (approx)	1.8	3.5	2.5	2.5			0.51	0.74	0.73
Smokeless Powder (Black Powder) 75% KNO ₃ , 10% S, 15% Charcoal	1.7	0	1	3	0.42	1	-	1.7	0.56
TX-50 (50% TNT/ 50% RDX)	5	5.5	4.5	6			0.90	1.1	0.83

To evaluate the performance of PELAN on different type soils, three wooden boxes 3'x3'x1' deep were prepared and filled with sand, gravel, and typical soil from the area. The sand boxes are shown in Figure 17.

The soil box had different amounts of water poured in, to simulate different ground moisture levels. The box with the area soil was the more problematic box. Because of its small size, the moisture level could be appreciably different in a 3-hour interval. This was manifested several times, and different background measurements had to be taken at time intervals much smaller than anticipated. Table 3A shows the variation of the moisture within the "wet" soil during the demonstration.

Table 3A. Laboratory measurements of the moisture within the "wet soil" during the demonstration.

	20-May	22-May	24-May
	(grams)	(grams)	(grams)
Amount of Moisture	7.84	20.17	13.46
Percent Moisture	21%	20%	18%



Figure 17. Boxes with different types of soil used in the measurements with PELAN.

4.4 Analytical Procedures

PELAN spectra of shells and explosives were taken based on a sampling procedure discussed in 4.3. A detailed description of the data analysis is addressed in 2.1.5 Methodology (p. 12).

Below is a summary:

1. Gamma ray spectra (one during the neutron pulse and one between pulses) are collected for a five minute period.
2. These spectra are automatically analyzed by the SPIDER data analysis program.
3. The results are tallied in a spreadsheet and data notebook.
4. For reproducibility, the average and standard deviation of the repeated measurements is calculated. These data are examined versus shell size, soil type, etc. to establish any correlations.
5. For the decision tree, elemental content and elemental ratios are calculated. These data are examined to determine if there is a pattern in the elemental composition. The patterns can sometimes be discerned by plotting ratios and trying determine if there is any segregation of types of materials.
6. Once a pattern has been discerned, rules or conditions for the decision-tree can be made.
7. The decision is programmed into the computer and more data is taken to verify the decision tree.

5. Performance Assessment

5.1 Performance Data

During the two-week period May 13-24, 2002, PELAN data were taken at Indian Head. The data were taken following the schedule outlined in 4.1.

Background measurements were taken with empty 155mm, 105mm, 90mm, 81mm, and 60mm shells on four different types of soil (sand, gravel, soil, and wet soil) and on a table. Figures 18 through 25 present some of the background spectra. For each background measurement, two different gamma-ray spectra were accumulated, one from fast neutron induced reactions (indicated as "fast" spectrum) and another from thermal neutron capture reactions (indicated as "thermal" spectrum). More details on the PELAN principle and the method of analysis can be found in the 2.1.5 Methodology section (p. 12).

Figure 18, shows the background spectra of a 60 mm empty shell placed on five different types of support. The spectra taken during the neutron pulse which we henceforth refer to as the "fast spectrum or spectra", show that all four types of soil have approximately the same gamma-ray yield over the complete spectrum. The gamma ray spectrum, however taken on the table shows that the background spectrum on the table is lower by at least a factor of two. This is the same behavior that we had seen previously, as shown in Figure 11 (p. 16).

The spectra taken between neutron pulses which we will henceforth refer to as the "thermal spectrum or spectra", show larger variations in the Si and H content, depending on the type of soils. The letters C, O, Si, H indicate the significant gamma-ray energies of the corresponding chemical elements.

Figure 18 is typical of the gamma ray spectra presented in this report. For the fast spectrum, the primary region of interest for C, N, and O lies between 3 MeV and 8 MeV and this is region shown in all subsequent fast spectra presented in this report. In this region in Figure 18, we can see from the right: a complex of O gamma rays with the primary one at 6.13 MeV (labeled "O" at channel 245) and then the C gamma ray at 4.43 MeV (labeled "C" at channel 180). The "hump" shaped peak to the right of the 6.13 MeV is another O gamma ray at approximately 6.8 MeV (between channels 264 and 314). To the immediate left of the 6.13 MeV peak is the first escape peak of the 6.13 MeV and is due to the loss of a pair-production photon of 0.511 MeV energy. Between C (4.43 MeV) and the first escape of O is the region (between channels 190 and 214) where N may be found (5.11 MeV). Unfortunately the cross-section for the production of the N gamma ray is 26.1 mb (compared to 185 mb for C (4.430 MeV) and 82.5 mb for O (6.13 MeV). To the immediate left (channels 130 to 164) of the 4.430 MeV C gamma ray is a complex of gamma rays composed of the first escape peak of the 4.430 MeV gamma ray and other gamma ray of O (~3.6 MeV).

The major fitting region for the thermal spectra is area around the gamma ray of H (2.22 MeV or between channels 590 and 615) between 1 MeV and 3 MeV. We will, again, show this region for all subsequent thermal spectra presented in this report. Two gamma rays dominate the

spectrum Si at 1.78 MeV (labeled "Si", between channels 575 and 590) and H at 2.22 MeV (labeled "H"). To the left of the Si (1.78 MeV) is the gamma ray from K at 1.46 MeV (between channels 561 and 581). This intensity of this gamma ray diminishes with distance from the soil as can be seen by contrasting the data taken on the table with the soil data.

The intensity of Si gamma ray at 1.78 MeV fluctuates considerably during a series of measurements. The $^{28}\text{Si}(n,p)$ reaction produces ^{28}Al which has a 2.24 minute half-life. During a series of consecutive measurements with no delays (<1 minute) between measurement, the intensity of this gamma ray builds to a maximum. If the delay between measurements is approximately 5 minutes (or over 2 half-lives) then the intensity will be considerably diminished (5% of its original value). The data from Si, then, is of limited value due to these wild fluctuations.

Also in Figure 18, we see a difference of a factor of 2 in the background between data taken on the ground and the data taken on the table. This is in good agreement with the spectra in Figure 11 which was taken prior to demonstration at WKU. Using a point source model, both the neutron flux and the photon flux should vary as $1/r^2$ and then the number of photons detected should vary as the product of these fluxes i.e. $1/r^4$. The inverse square law while valid for point-like objects may not be valid under these conditions. It is true that the neutron generator beam spot may be point-like, the ground which nearly surrounds the detector is NOT point-like. A Monte Carlo code such as MCNP is an appropriate method to understand this difference but no such calculation was performed.

Figure 19 shows the background spectra of 5 shells on sand. A spectrum taken without a shell in front of PELAN is also included. The shielding effect of the ground can be seen in the fast spectrum. The spectrum without any shell shows an increased oxygen yield, indicative of the shielding absence.

Figure 20 is similar to Figure 19 on soil. Figures 21 through 25 show two shells (155m and 60mm) on all five media.

In Figures 21 and 22, the O gamma ray in the fast spectrum is obviously reduced to this shielding effect. In Figure 25, another effect, neutron scattering from the shell, can be seen along with the shielding effect. The neutron scattering is characterized by the overall raised continuum. Figures 23 and 24 also show this raised continuum effect whereas Figures 21 and 22 do not. This is due to high H content of the soils relative to the gravel and sand. On the table (Fig. 25) with the lower background the neutron scattering from the shell is noticeable whereas it is completely hidden by the larger backgrounds on the ground.

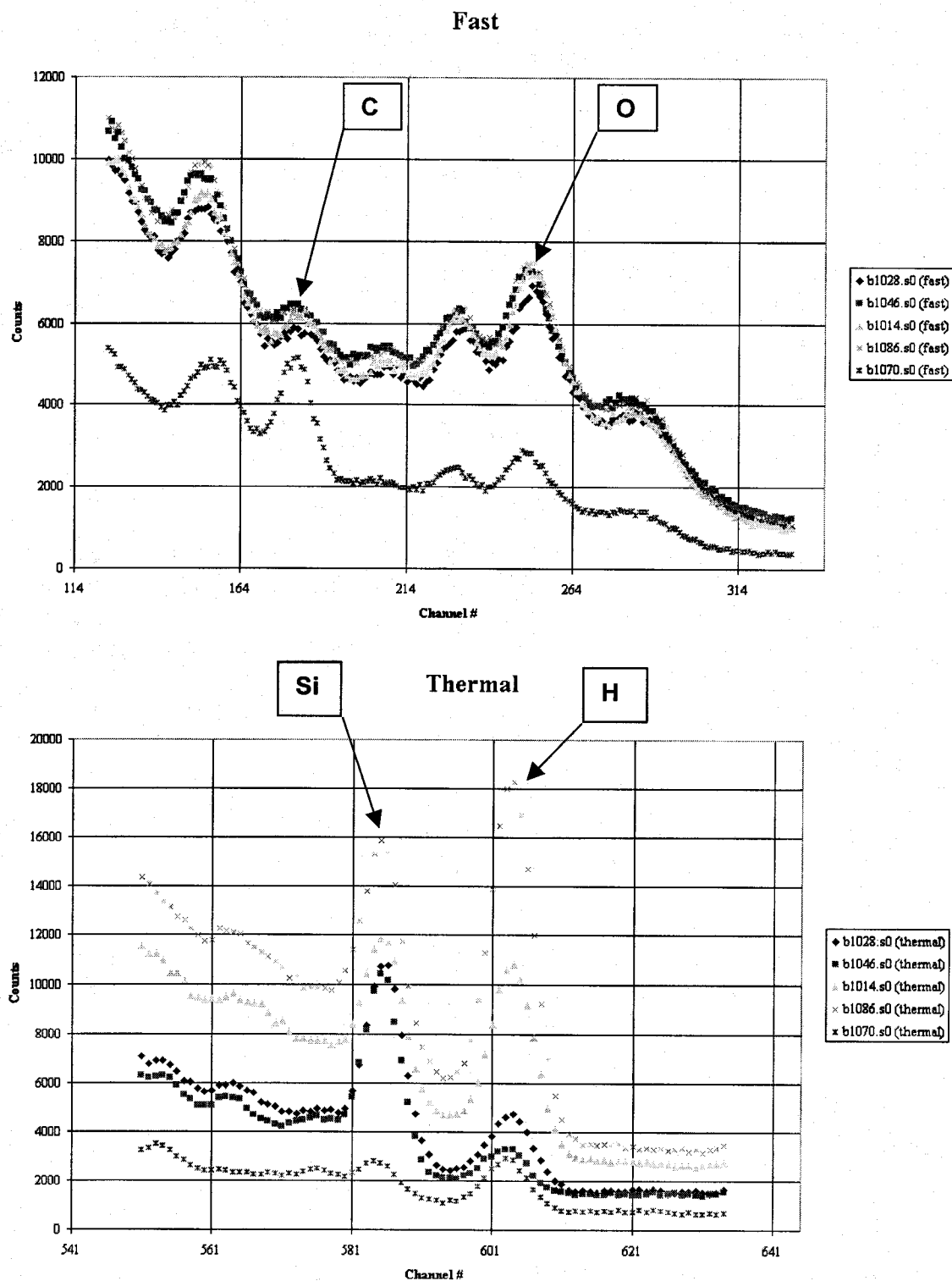


Figure 18. Empty 60mm shell on sand (B1028), Gravel (B1046), Soil (B1014), Wet soil (B1086), and Table (B1070). Top spectrum is the “fast” spectrum and bottom is the “thermal” spectrum. See text for additional discussion of the features.

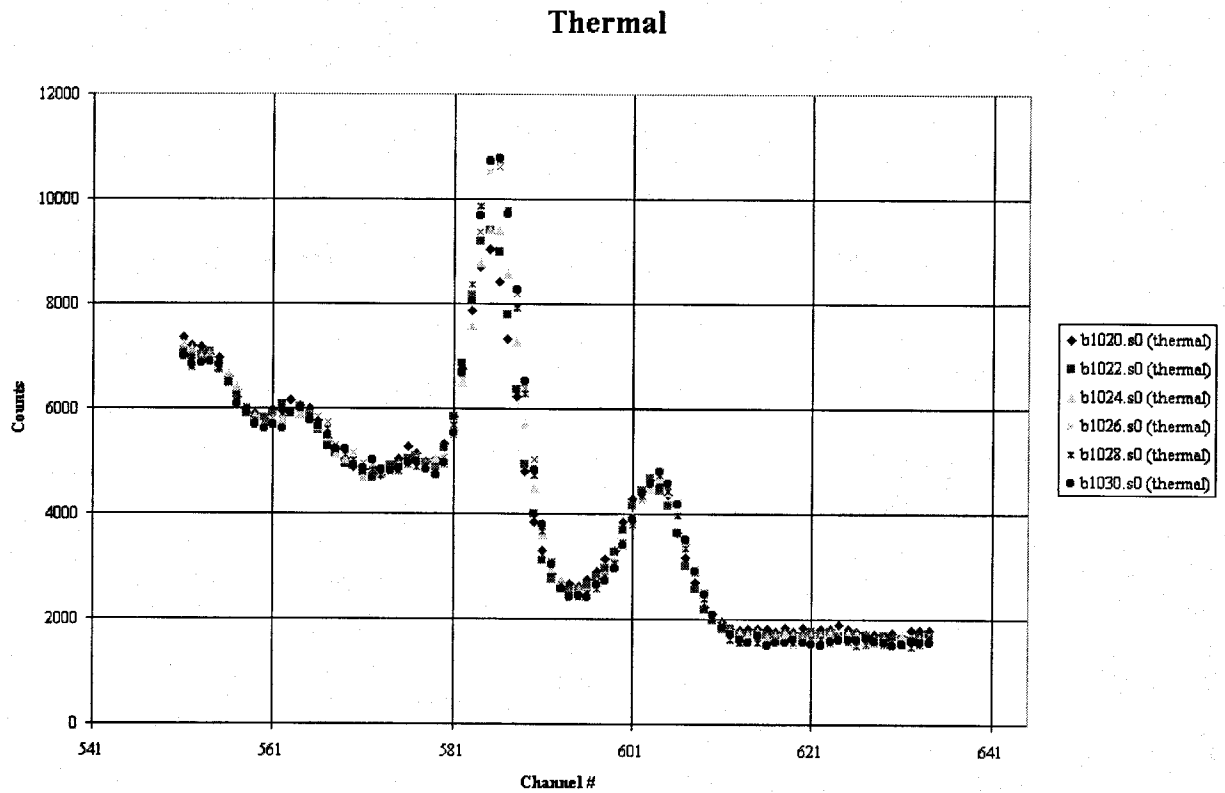
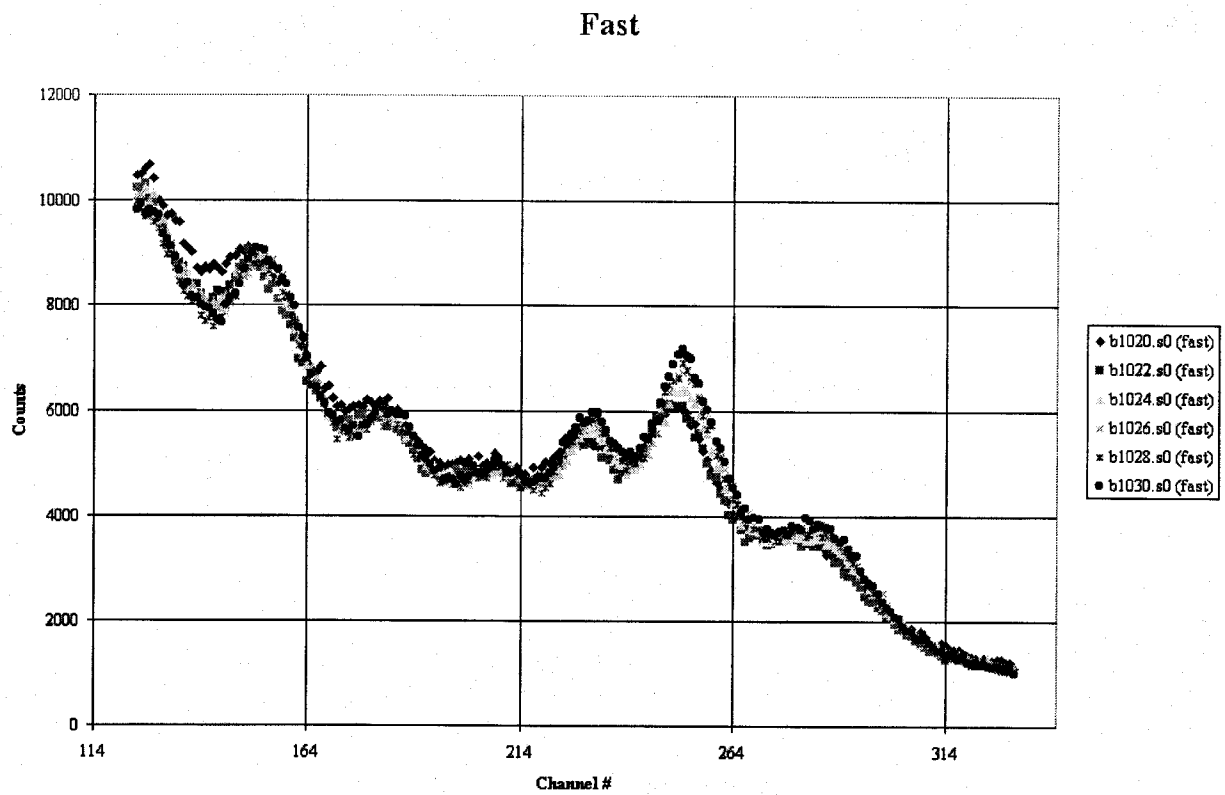
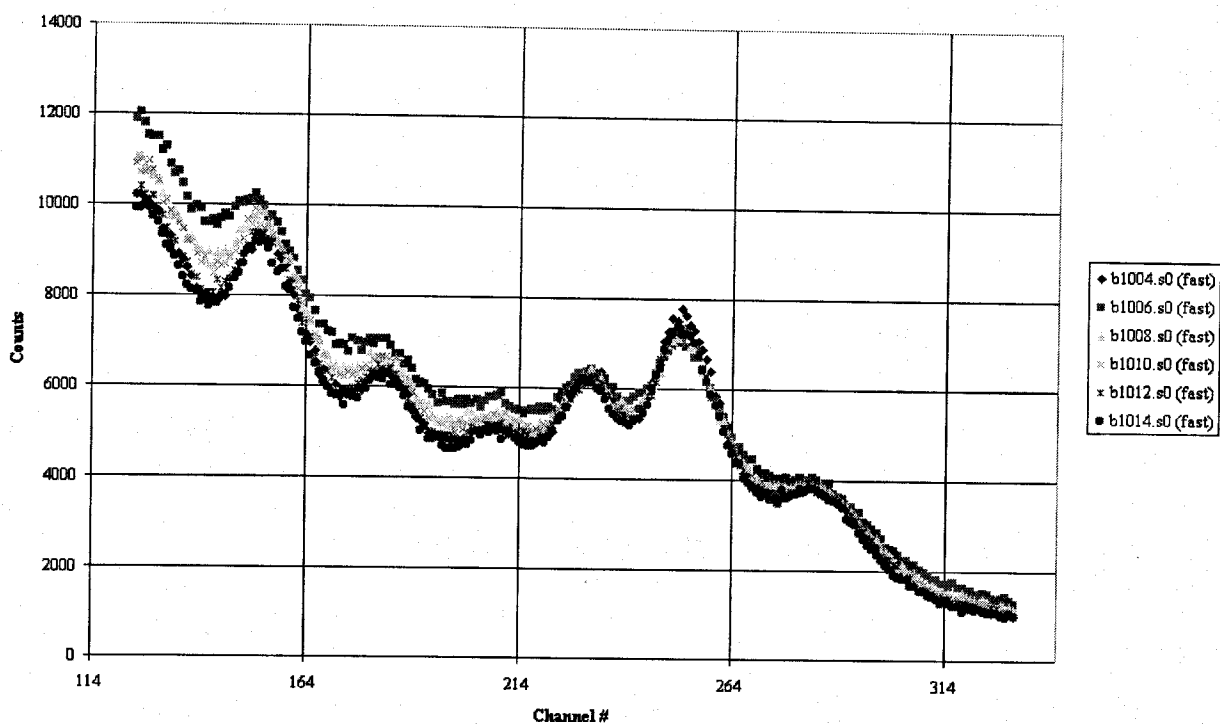


Figure 19. Background spectra of five shells on sand, and a spectrum without a shell. B1020=155mm, B1022=105mm, B1024= 90mm, B1026= 81mm, B1028=60mm, B1030= no shell.

Fast



Thermal

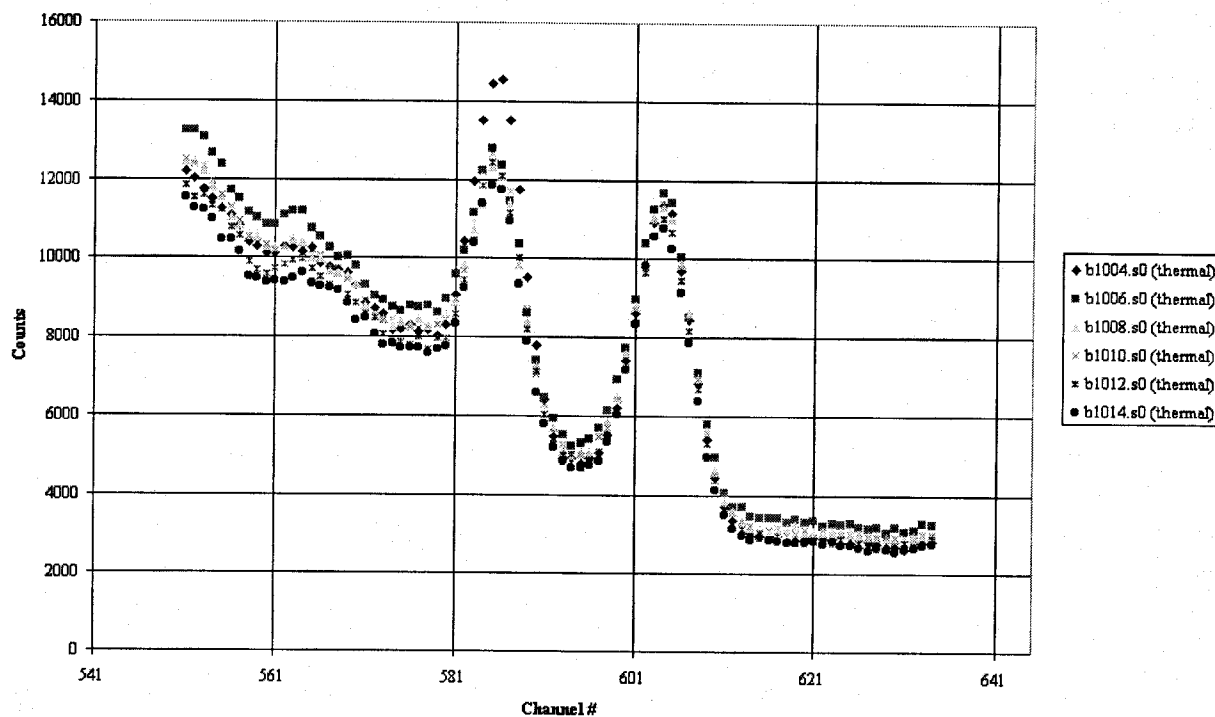


Figure 20. Background spectra of five shells on soil, and a spectrum without a shell. B1006=155mm, B1008 =105mm, B1010= 90mm, B1012= 81mm, B1014=60mm, B1004= no shell.

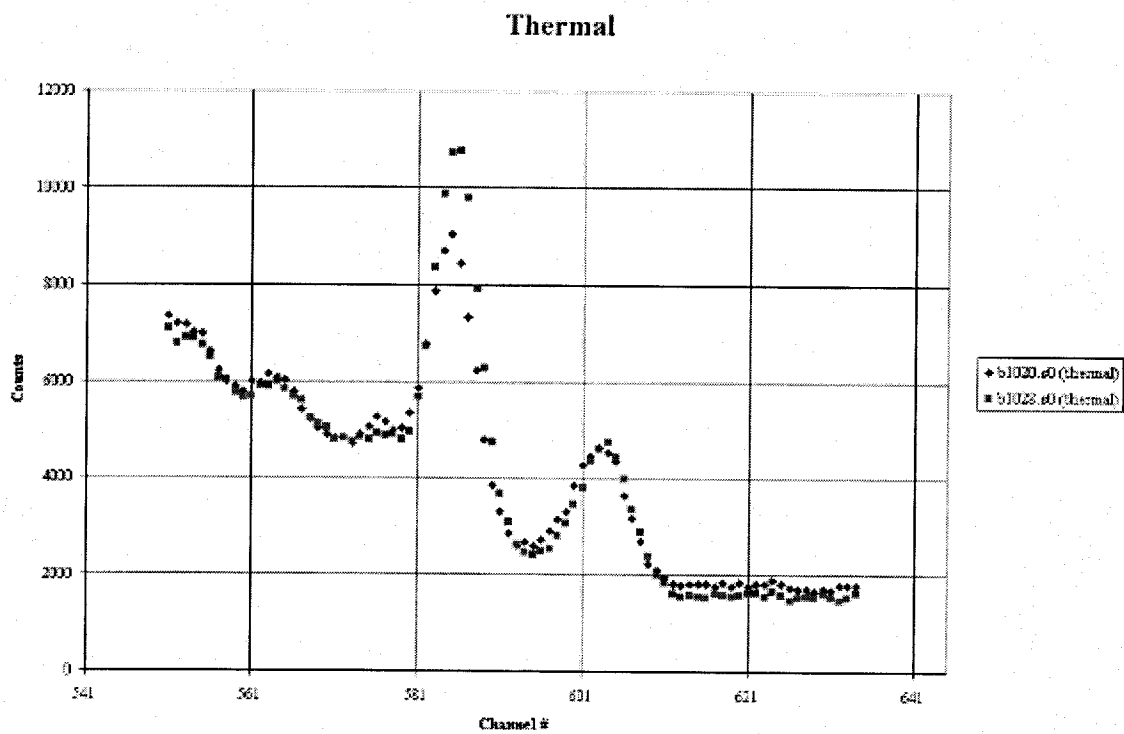
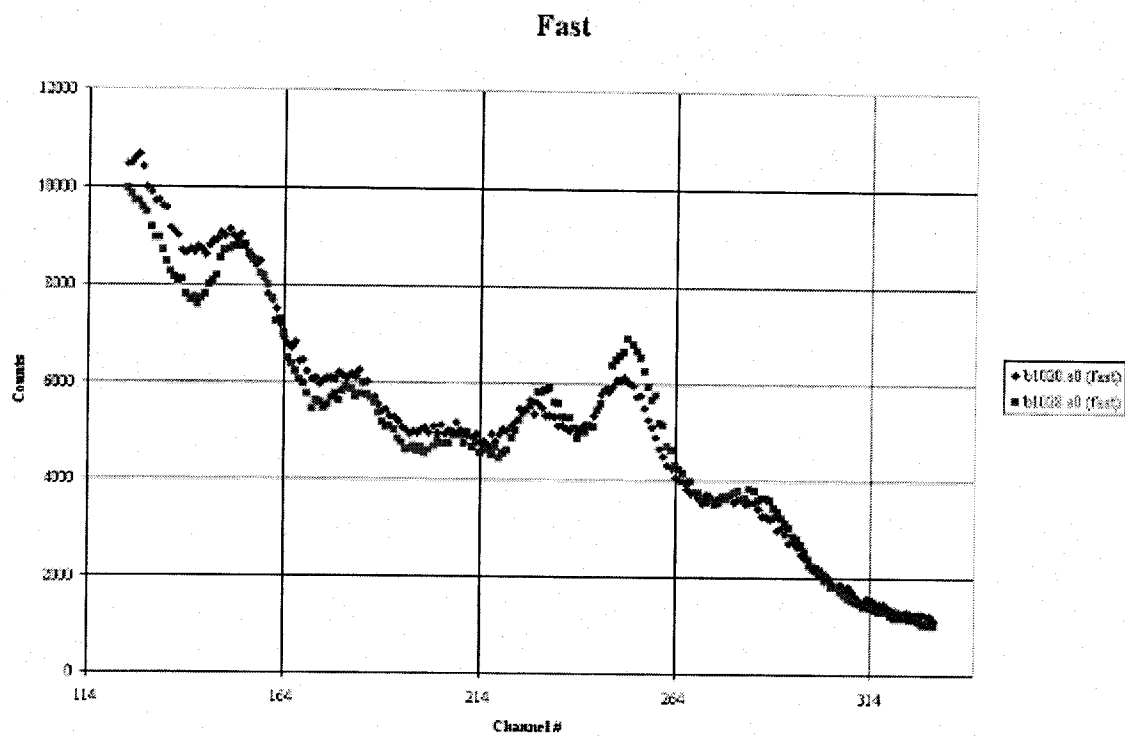


Figure 21. Two empty shells (B1020=155mm, B1028=60mm) on sand.

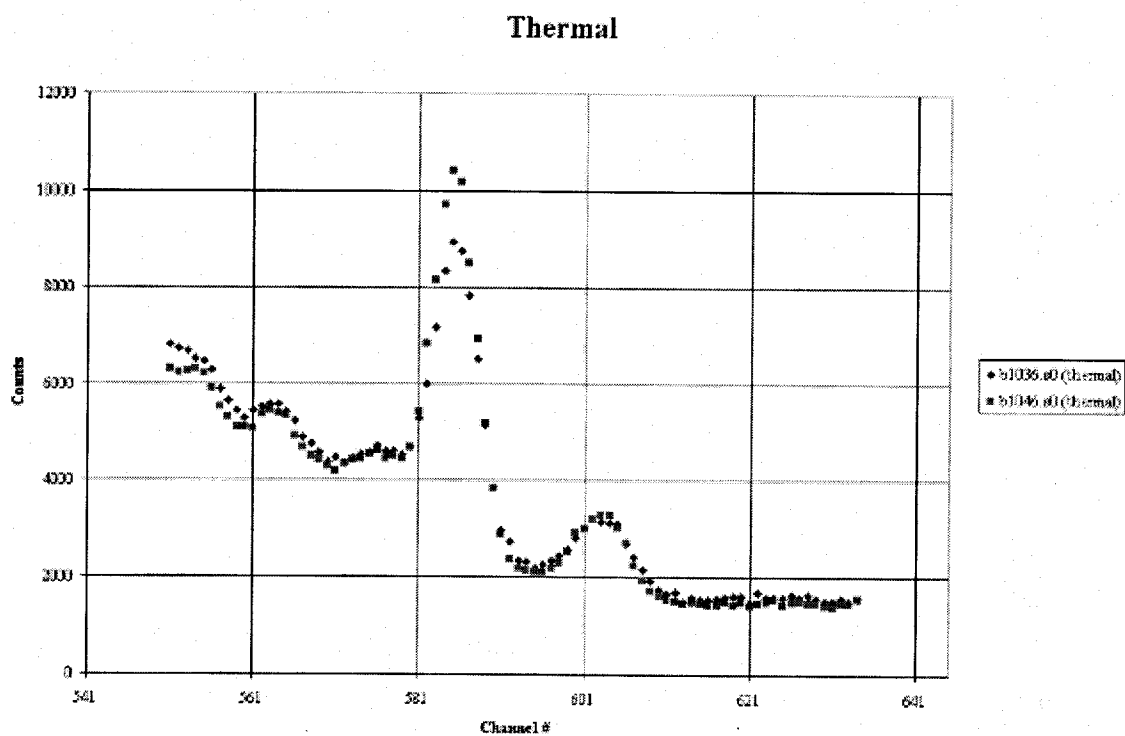
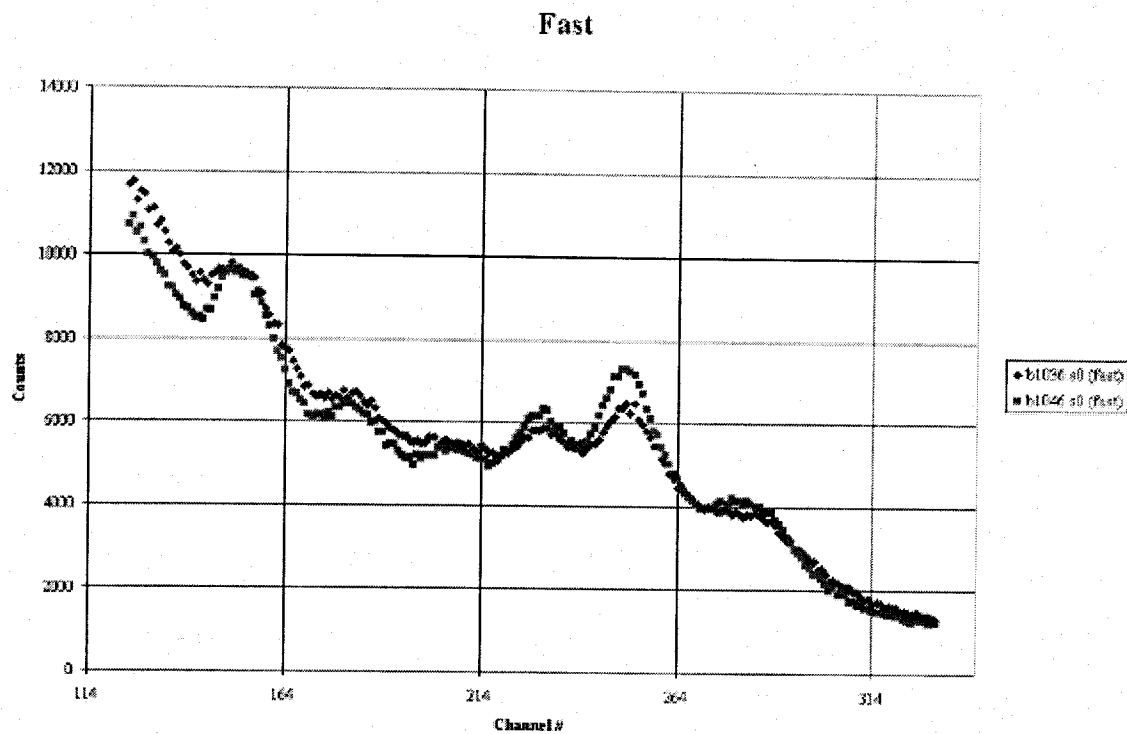


Figure 22. Two empty shells (B1036=155mm, B1046=60mm) on gravel.

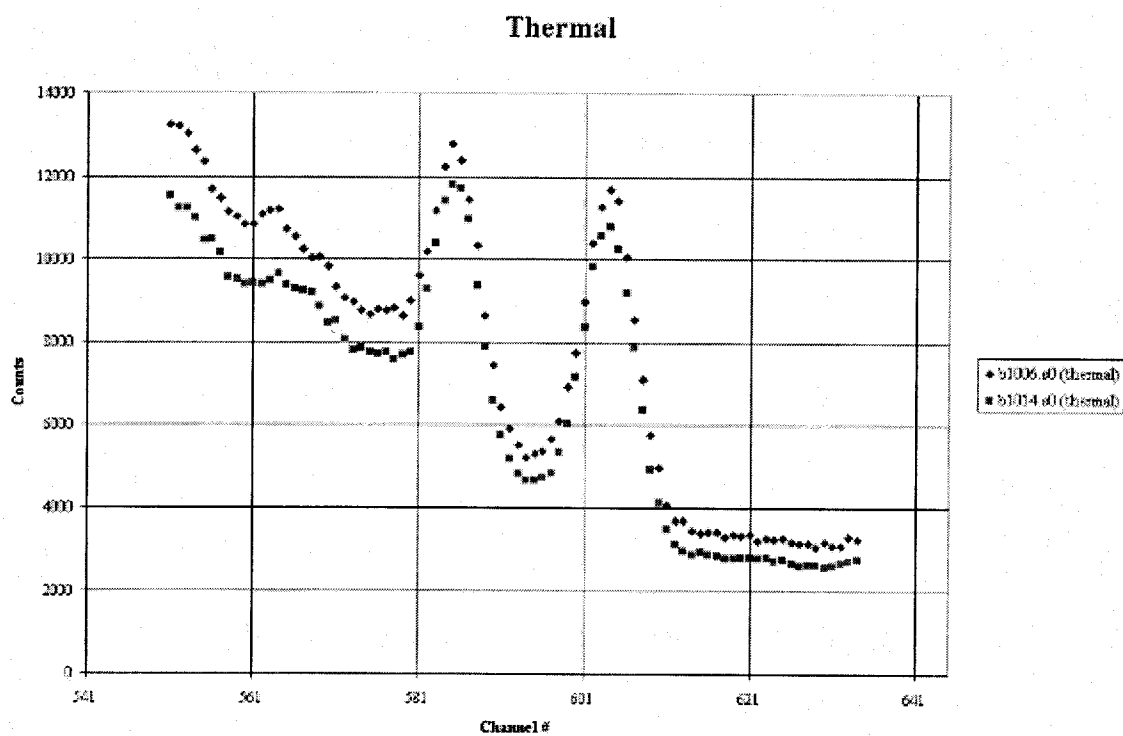
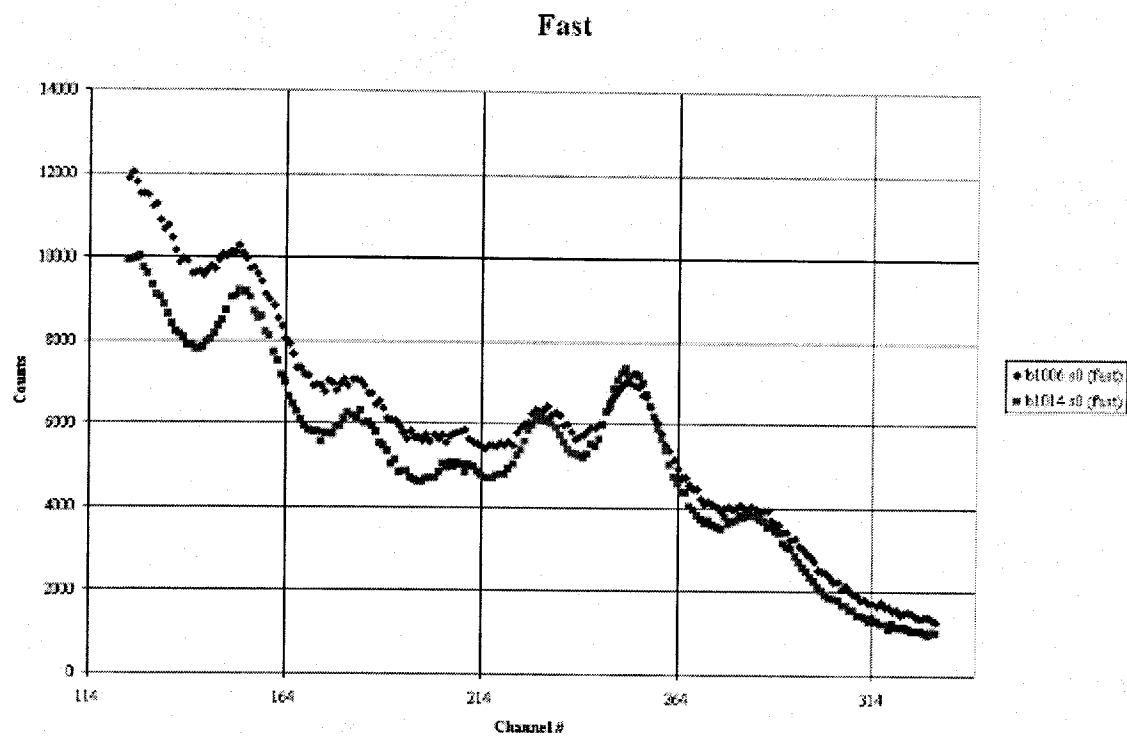


Figure 23. Two empty shells (B1006=155mm, B1014=60mm) on soil.

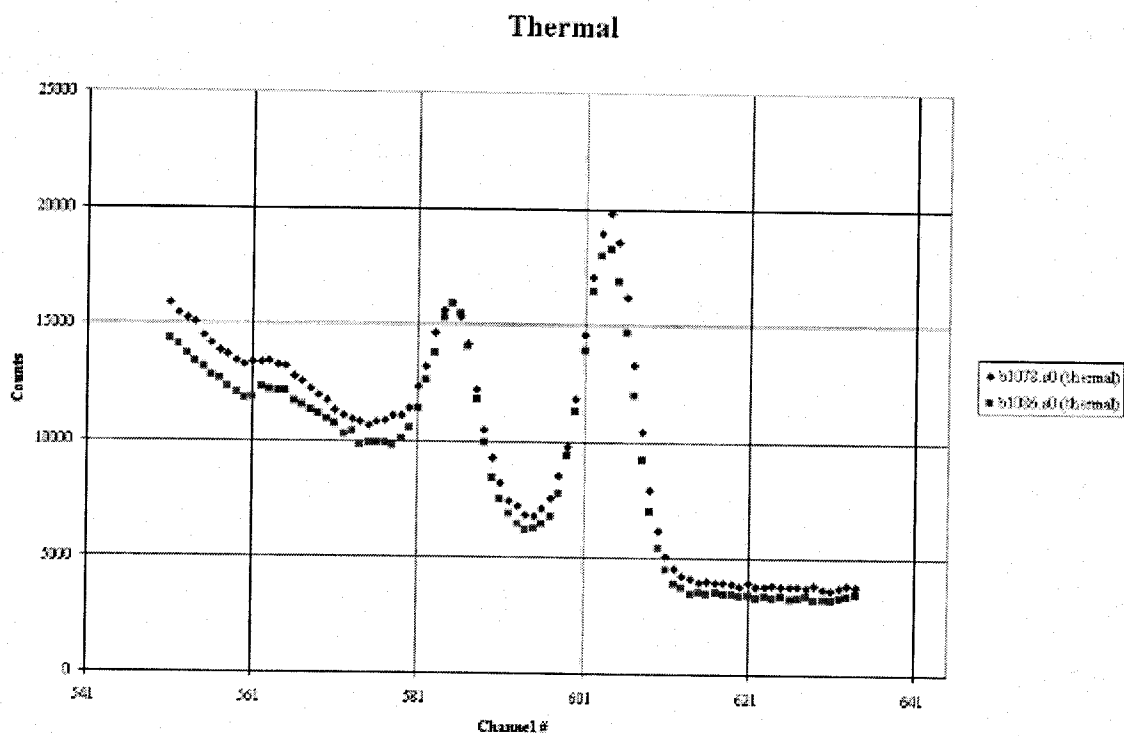
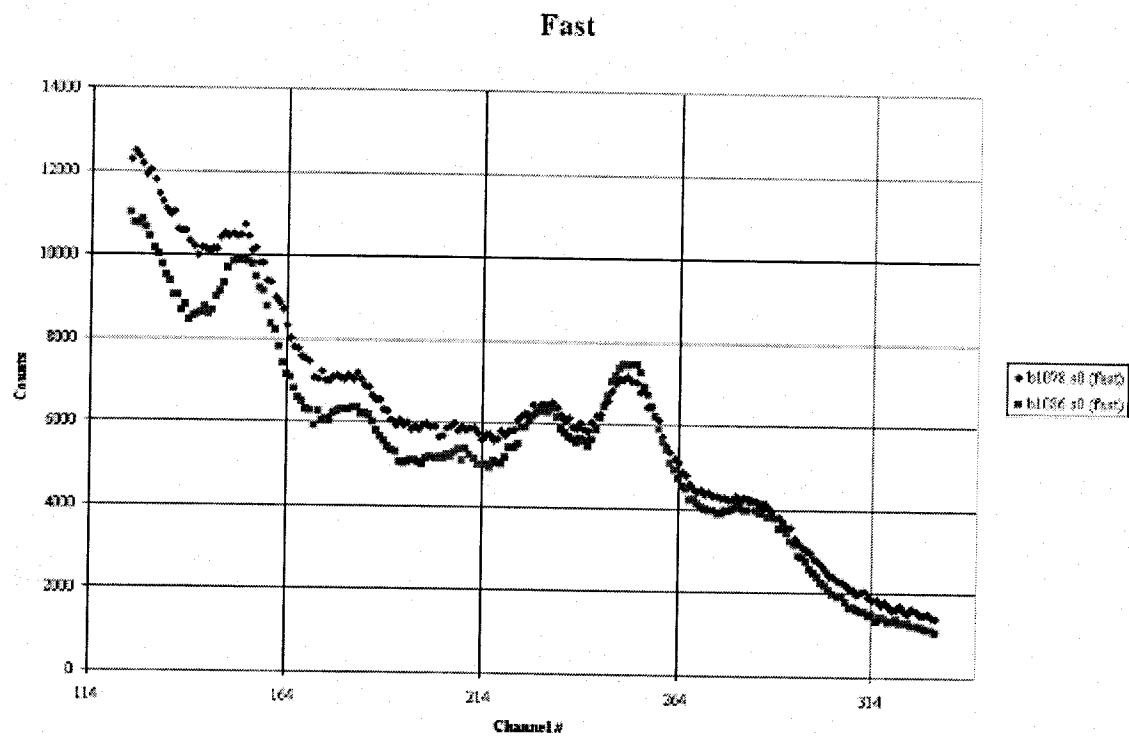


Figure 24. Two empty shells (B1078=155mm, B1086=60mm) on wet soil.

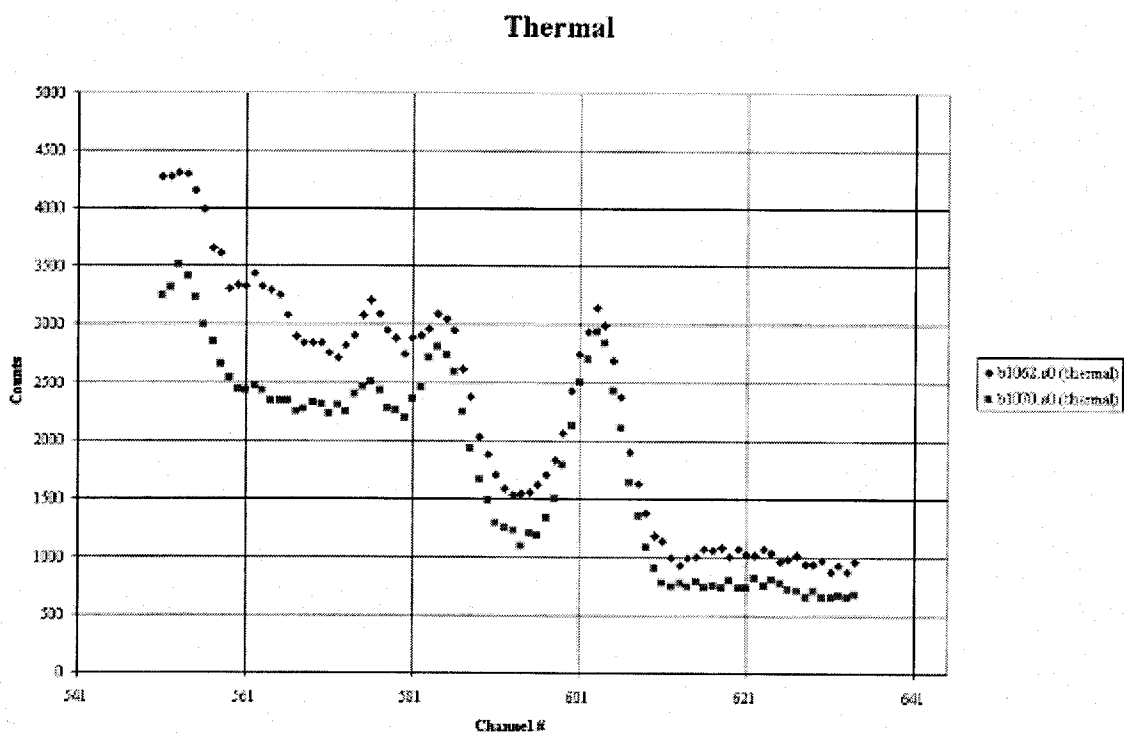
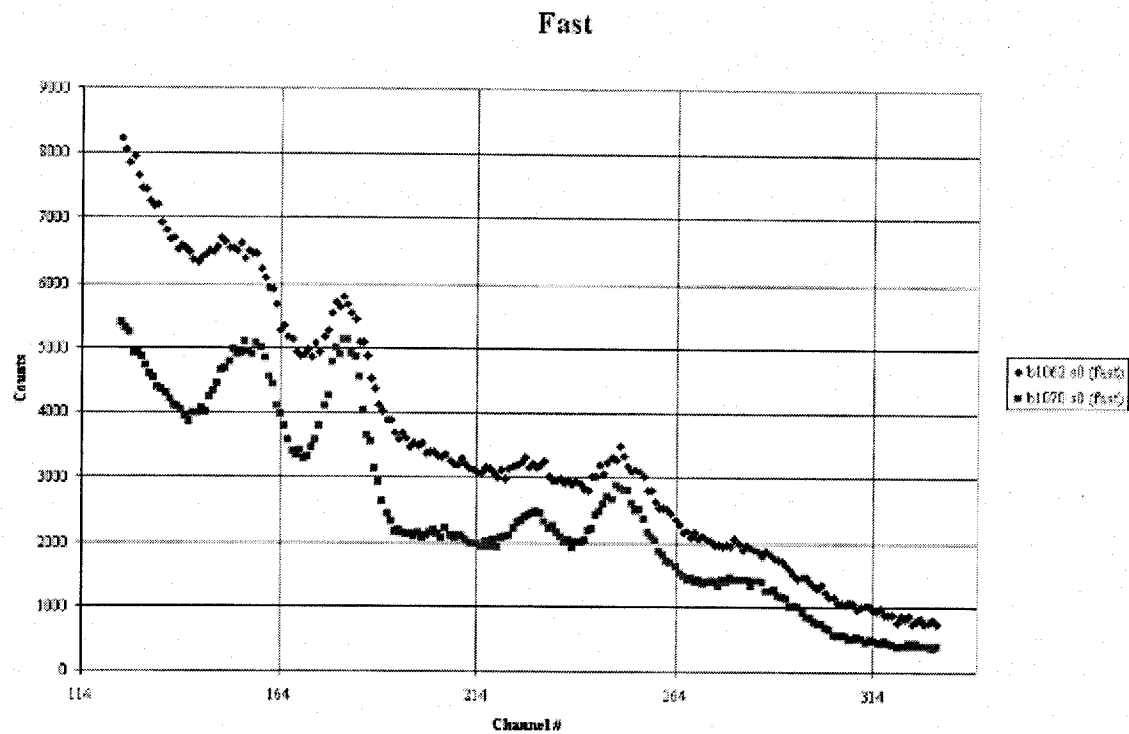


Figure 25. Two empty shells (B1062=155mm, B1070=60mm) on a table.

5.1.1 Background Stability

Stability of the background was measured by taking background spectra of the same shell and on the same soil at two different times. In some cases, the two spectra were taken at different dates. Figures 26-35 show a comparison of the fast and thermal spectra of the same background taken at different times.

During the analysis of the data for this report, it was found that there was a paucity of data concerning the reproducibility/stability of the background utilized in the SPIDER measurements.

To offset this, we asked permission from the ESTCP Program Office to acquire more data at a especially prepared site at WKU. The inert or empty shells used during this test were the same shells used at Indian Head.

In Tables 4A, 4B, and 4C, we see the stability of the background with respect to shell size and soil type. Due to Si activation, it became difficult to measure the H content accurately. In order to correct this problem, a background was fitted with the preceding background to minimize differences in the Si activation.

In Table 4D, we have chosen random spots on the soil approximately 1 m apart and analyzed these spectra using another randomly chosen spot.

With this data, we can now begin to estimate the measurement uncertainty for various elements. The maximum value of the standard deviations for the data below is C=1.3 cps, N= 2 cps, O=2.4 cps, Cl=0.6 cps, Fe=0.5 cps, and H=5.5 cps. By choosing the maximum standard deviation, we are taking the "worst case scenario". Since our averages for these measurements are near zero, we can say that any measurement below these standard deviation maxima can be construed as zero.

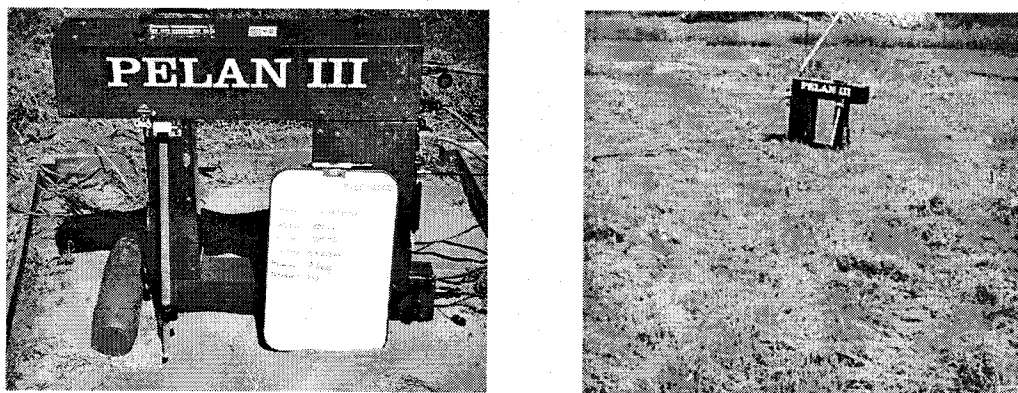


Figure 26. Pictures taken during supplemental data collection at WKU (September 2002). Picture on left is PELAN measuring 105 mm shell on sand. Picture on right is PELAN measuring backgrounds at randomly chosen points (orange flags).

One key result of this demonstration is that we have determined that there is no unique value that statistically represents zero. Previous to this series of measurements, we considered +/-1.5 cps as essentially zero. But as we can see, this depends upon the element. The final source of these variations between elements seems to be environmental. If one examines the standard deviations of H in the sand and the gravel, they are nearly equal to one. However, for soil measurements, the standard deviations of H are quite large. This may be explained by the fact that the intensity of H in the soil is very high. Recall for Poisson statistics for two numbers, G and B, that if $N=G-B$ then uncertainty in $N = \sqrt{G+B}$ which may be larger than N if G and B are nearly equal.

A large quantity of H (region between channels 590-615) can be seen in the soil spectra (Figures 31 and 32) and wet soil spectra (Figs. 33 and 34). The spectra taken on the table (Figs. 35 and 36), the gravel spectra (Figs. 29 and 30), and the sand spectra (Figs. 27 and 28) have nearly the same H content. This trend was also reproduced in the spectra taken at WKU (not shown) where the H content was much higher for soil than gravel or sand. This is a strong indication that the soil is holding a large amount of hydrogen. We can see some evidence of hydrogen retention (probably due to local rain) in the sand (Figs. 27 and 28) when compared to the table (Figs. 35 and 36) and to the gravel (Figs. 29 and 30).

Also to note, there is a large carbon peak in all of the table data shown (Figs. 25, 35 and 36). Soil, wet-soil, sand, and gravel have nearly equal amounts of C (channel 180) in their backgrounds.

Figures 27-36 show that no matter what the shell size nor the background, the spectra are nearly identical. The standard deviations discussed above are an indication of this. The large H standard deviation is because of the statistical argument stated above i.e. that if two large numbers are subtracted from one another; the difference may be smaller than propagated uncertainty.

Table 4A. Reproducibility data for various backgrounds on soil. Taken at WKU.

105mm data analysis							
Spectrum	Background	C (cps)	N (cps)	O (cps)	Cl (cps)	Fe (cps)	H (cps)
b2126	b2128	-0.307	-1.54	-0.407	0.337	0.675	-4.01
b2128	b2130	-0.122	1.29	0.32	0.933	-0.669	9.37
b2130	b2132	0.585	0.05	0.845	0.551	0.774	-2.74
b2132	b2134	0.455	-0.18	-0.992	-0.087	-0.023	-3.07
b2134	b2136	-0.544	-1.08	1.23	1.47	-0.351	4.02
b2136	b2138	1.39	0.73	-0.06	0.713	-0.095	-0.45
b2138	b2140	-1.33	-0.47	0.931	-0.209	-0.327	0.0514
	Average	0.0	-0.2	0.3	0.5	0.0	0
	STD.DEV.	0.9	1	0.8	0.6	0.5	5
90 mm data analysis							
Spectrum	Background	C (cps)	N (cps)	O (cps)	Cl (cps)	Fe (cps)	H (cps)
b2142	b2144	1.23	-0.09	0.156	0.09	-0.168	1.21
b2144	b2146	-0.321	-0.78	-1.37	0.151	0.477	1.82
b2146	b2148	1.25	-0.16	2.86	-0.128	-0.157	1.37
b2148	b2150	-0.048	1.06	-0.826	1.62	0.45	0.975
b2150	b2152	-1.34	1	0.56	-0.06	0.26	2.76
b2152	b2154	1.54	-0.05	0.744	0.443	0.397	-0.779
b2154	b2156	-0.8	-0.01	-0.349	0.18	-0.117	-2.54
b2156	b2158	1.41	-0.064	-0.334	-0.047	0.299	-0.904
	Average	0.4	0.1	0.2	0.3	0.2	0.5
	STD. DEV	1	0.6	1	0.6	0.3	2
60 mm data analysis							
Spectrum	Background	C (cps)	N (cps)	O (cps)	Cl (cps)	Fe (cps)	H (cps)
b2162	b2164	0.367	0.24	0.335	0.865	0.292	7.53
b2164	b2166	-0.523	-1.48	0.163	0.436	-0.226	-1.67
b2166	b2168	0.48	1.08	0.266	0.47	0.094	-1.56
b2168	b2170	-0.812	-2.59	-0.943	0.11	0.07	-2.96
b2170	b2172	0.877	0.02	0.057	1.35	0.164	1.95
b2172	b2174	-0.812	0.27	0.71	0.254	0.04	1.17
b2174	b2176	-0.047	2.96	0.472	-0.02	-0.06	-0.196
	Average	-0.1	0.0	0.2	0.5	0.05	0
	STD. DEV	0.7	2	0.5	0.5	0.2	4

Table 4B. Reproducibility data for various backgrounds on sand. Taken at WKU.

105 mm data analysis							
Spectrum	Background	C (cps)	N (cps)	O (cps)	Cl (cps)	Fe (cps)	H (cps)
b2063	b2065	2.31	0.25	1.19	1.04	-0.102	1.03
b2065	b2067	0.461	0.1	2.25	0.121	0.085	-0.017
b2067	b2069	-0.841	1.14	-1.49	1.08	-0.194	0.124
b2069	b2071	-0.228	-2.22	-1.65	0.236	-0.25	-1.49
b2071	b2073	-0.288	0.57	-0.136	0.827	0.118	-1.11
b2073	b2075	0.029	-0.85	1.56	0.235	0.05	0.8
b2075	b2077	0.841	1.19	0.094	1.29	0.079	0.736
b2077	b2079	-0.719	1.35	0.314	0.597	-0.132	-1.03
	Average	0.2	0.2	0.2665	0.67825	-0.04325	-0.1
	STD. DEV.	1	1	1	0.4	0.1	1
90 mm data analysis							
Spectrum	Background	C (cps)	N (cps)	O (cps)	Cl (cps)	Fe (cps)	H (cps)
b2081	b2083	0.304	-0.81	1	0.675	0.086	-0.349
b2083	b2085	0.845	1.58	-0.493	0.375	-0.322	-1.09
b2085	b2088	-0.553	-0.85	-0.77	0.757	0.271	-0.654
b2088	b2090	0.076	0.5	1.79	0.741	0.227	0.493
b2090	b2092	-0.29	-0.1	0.018	0.346	-0.019	0.965
b2092	b2094	0.166	0.77	0.649	0.743	-0.061	1.54
b2094	b2096	0.308	-2.36	0.904	0.757	-0.142	-4
b2096	b2098	0.509	-0.52	-1.78	0.517	-0.045	1.13
b2098	b2100	0.328	3.68	3.28	0.567	0.018	1.05
	Average	0.2	0.2	0.5	0.6	0.0	-0.1
	STD. DEV.	0.4	2	2	0.2	0.2	2
60 mm data analysis							
Spectrum	Background	C (cps)	N (cps)	O (cps)	Cl (cps)	Fe (cps)	H (cps)
b2102	b2104	-0.131	1.13	0.684	0.189	-0.107	-1.31
b2104	b2106	0.119	-1.66	0.136	0.59	0.114	-0.156
b2106	b2109	0.845	1.6	-0.461	1.19	-0.227	0.044
b2109	b2111	-0.05	-1.13	0.242	0.449	0.065	0.357
b2111	b2113	-0.264	0.94	1.04	0.49	-0.008	-1.35
b2113	b2115	0.818	-0.7	-0.211	0.626	-0.02	1.37
b2115	b2117	-0.982	-0.54	0.906	0.484	0.09	-0.57
b2117	b2119	0.222	0.5	-0.246	0.47	-0.401	-0.281
b2119	b2121	0.811	1.14	0.628	0.285	-0.109	0.05
	Average	0.2	0.1	0.3	0.5	-0.1	-0.2
	STD. DEV.	0.6	1	0.5	0.3	0.2	0.8

Table 4C. Reproducibility data for various backgrounds on gravel. Taken at WKU

105 mm data analysis							
Spectrum	Background	C (cps)	N (cps)	O (cps)	Cl (cps)	Fe (cps)	H (cps)
2001	2003	-0.98	-0.65	-3.16	0.62	0.26	-0.9
2003	2005	-1.84	-1.13	-2.9	0.39	-0.33	0.28
2005	2007	2.02	2.67	2.35	1.09	-0.15	-0.12
2007	2009	-1.69	-0.86	-0.97	0.33	0.05	-0.79
2009	2011	0.69	0.61	1.03	0.36	-0.17	-0.24
2011	2013	0.8	1.07	1.5	1.35	0.1	0.23
2013	2015	-0.27	-0.11	0.18	0.39	-0.32	-1.79
2015	2017	0.62	-0.04	-0.59	0.51	-0.04	-0.5
2017	2019	-0.1	0.97	3.3	0.23	-0.05	-0.83
	Average	-0.1	0.3	0.1	0.6	-0.1	-0.5
	STD. DEV.	1	1	2	0.4	0.2	0.6
90 mm data analysis							
Spectrum	Background	C (cps)	N (cps)	O (cps)	Cl (cps)	Fe (cps)	H (cps)
2021	2023	0.32	-1.53	-0.37	0.34	-0.1	0.21
2023	2025	-0.89	-0.07	0.33	0.54	-0.03	0.87
2025	2027	2.39	1.57	2.99	0.51	-0.11	-0.3
2027	2029	-0.71	-0.71	-0.25	0.66	-0.04	-0.21
2029	2031	-0.33	0.67	-0.67	0.38	-0.07	-1.38
2031	2033	-0.7	-0.8	-0.07	0.37	-0.01	-0.13
2033	2035	0.42	0.6	-0.47	0.24	-0.1	-0.41
2035	2037	-0.51	-1.05	-2.11	0.84	-0.12	-1.87
2037	2039	2.57	2.58	6.06	0.38	-0.29	-0.4
	Average	0.3	0.1	0.6	0.5	-0.10	-0.4
	STD. DEV.	1	1	2	0.2	0.08	0.8
60 mm data analysis							
Spectrum	Background	C (cps)	N (cps)	O (cps)	Cl (cps)	Fe (cps)	H (cps)
2041	2043	-0.51	-0.24	-0.2	0.82	-0.04	0.36
2043	2045	1.33	-0.9	0.39	0.54	-0.27	-1.23
2045	2047	0.8	0.71	2.28	0.1	-0.08	0.3
2047	2049	-1.67	-0.27	-1.09	0.51	0.12	0.18
2049	2051	1.19	0.93	-0.69	0.25	-0.21	-1.38
2051	2053	-0.4	-1.65	1.46	0.37	-0.15	0.72
2053	2055	-0.29	1.53	-0.16	0.3	-0.07	0.16
2055	2057	0.56	-0.22	-1.06	0.19	0.03	-2.04
2057	2059	0.87	-1.06	1.42	0.45	-0.29	1.74
	Average	0.2	-0.1	0.3	0.4	-0.1	-0.1
	STD. DEV.	1	1	1	0.2	0.1	1

**Table 4D. Background reproducibility data for randomly chosen positions on the soil.
Taken at WKU.**

Spectrum	Background	C (cps)	N (cps)	O (cps)	Cl (cps)	Fe (cps)	H (cps)
2207	2231	-0.91	0.48	-0.69	-0.04	-0.06	0.01
2213	2231	-0.19	0.79	-1.68	0.6	-0.08	-13.51
2217	2231	-1.37	0.81	0.51	0.28	0.29	2.4
2219	2231	-1.07	0.27	-0.5	0.63	-0.03	-1.1
2221	2231	-0.25	1.72	-0.44	0.42	0.04	-0.74
2223	2231	1.26	0.88	2.1	0.7	0.21	5.22
2225	2231	-1.02	1.43	0.69	0.56	-0.2	-4.5
2227	2231	-0.62	0.1	0.9	0.2	-0.08	-0.06
2229	2231	-1.14	0.54	0.91	1.09	0.28	3.13
	Average	-0.6	0.8	0.2	0.5	0.04	-1
	STD. DEV.	0.8	0.5	1	0.3	0.2	5

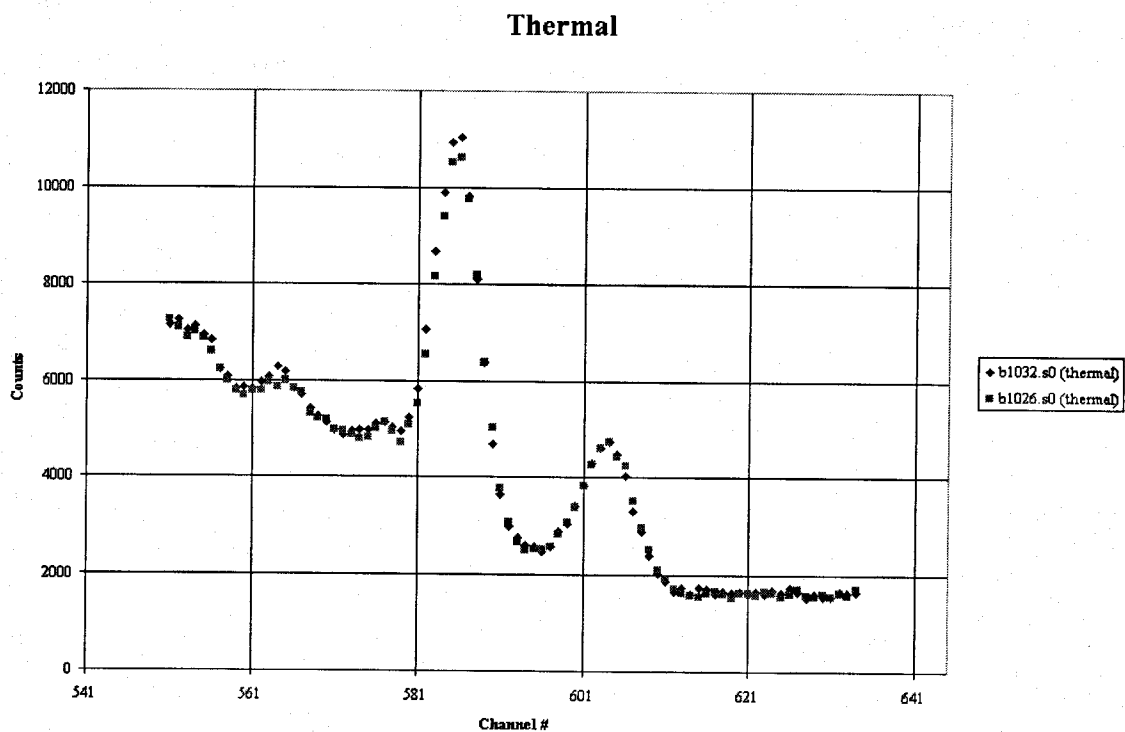
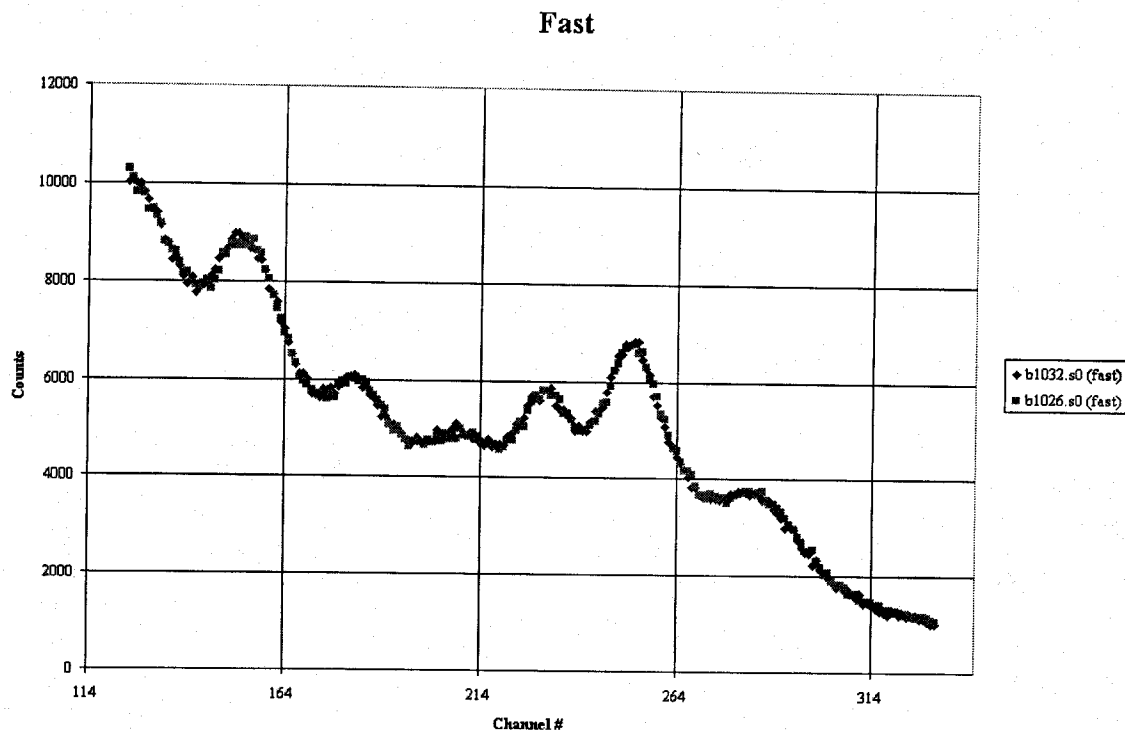


Figure 27. Comparison of two background spectra of the same shell (81mm) on the same soil (sand).

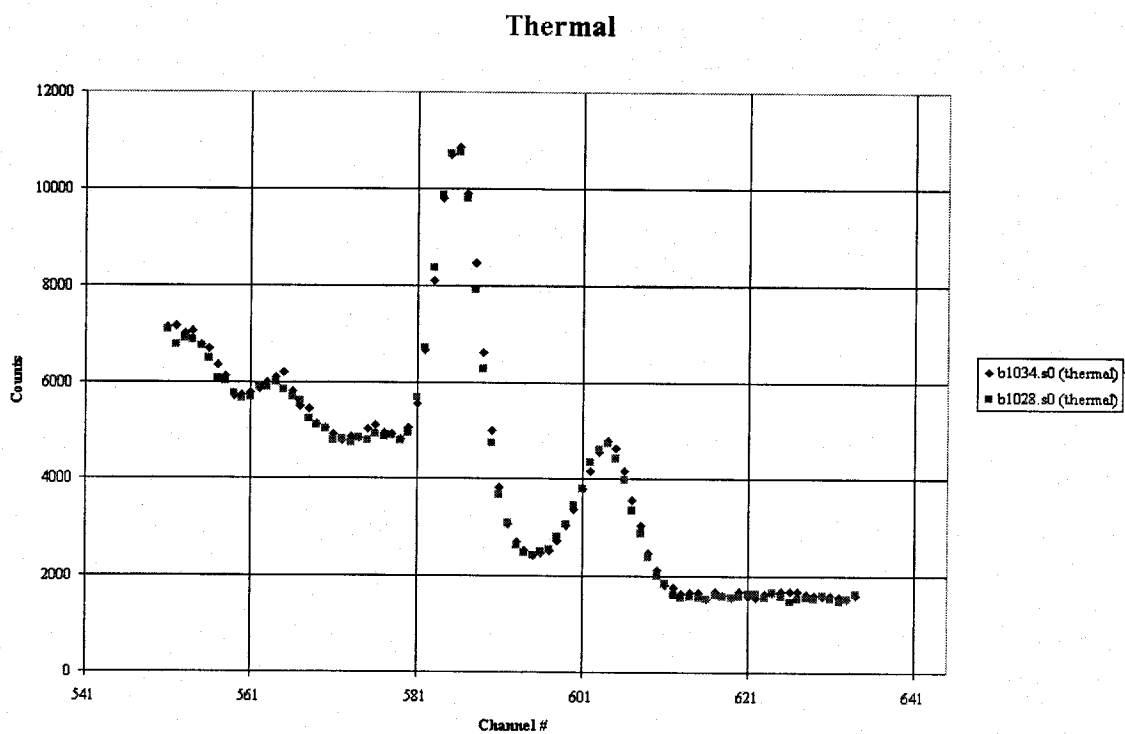
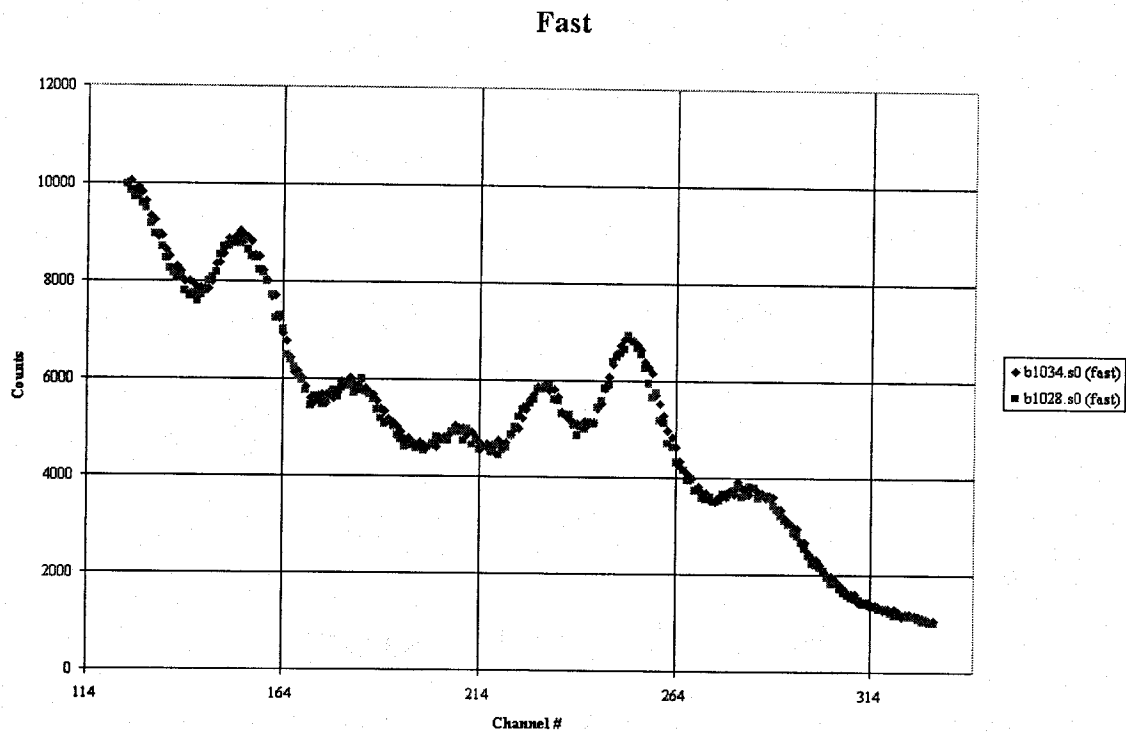


Figure 28. Comparison of two background spectra of the same shell (60mm) on the same soil (sand).

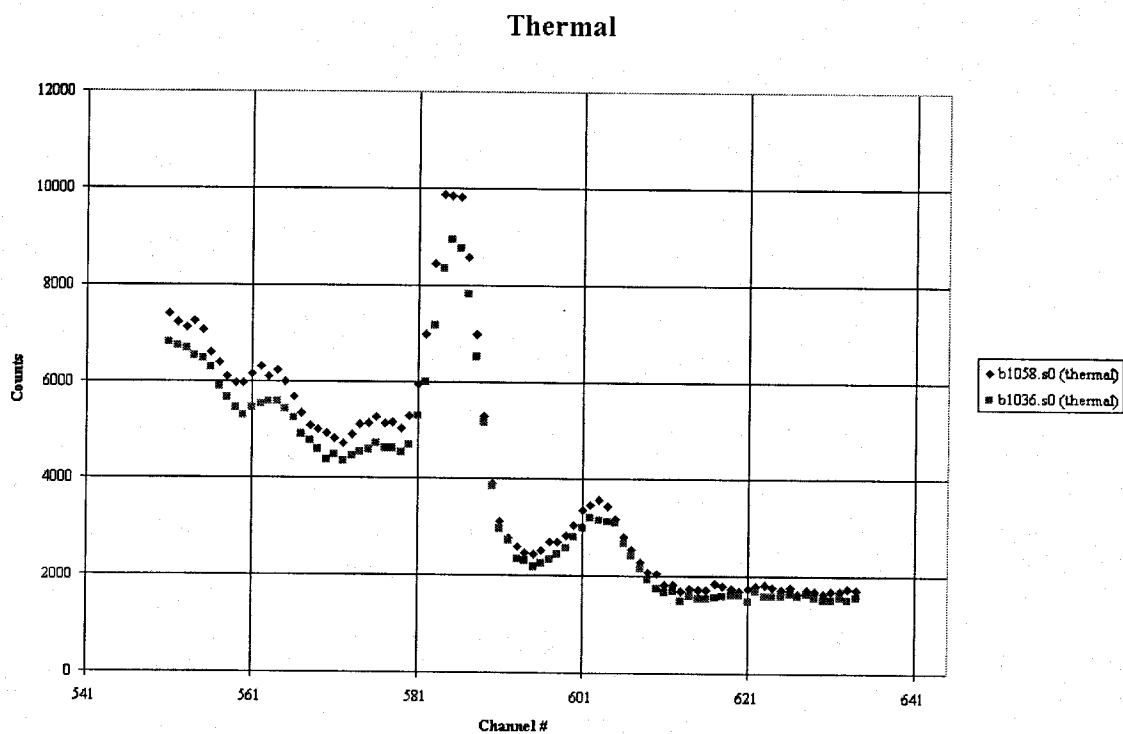
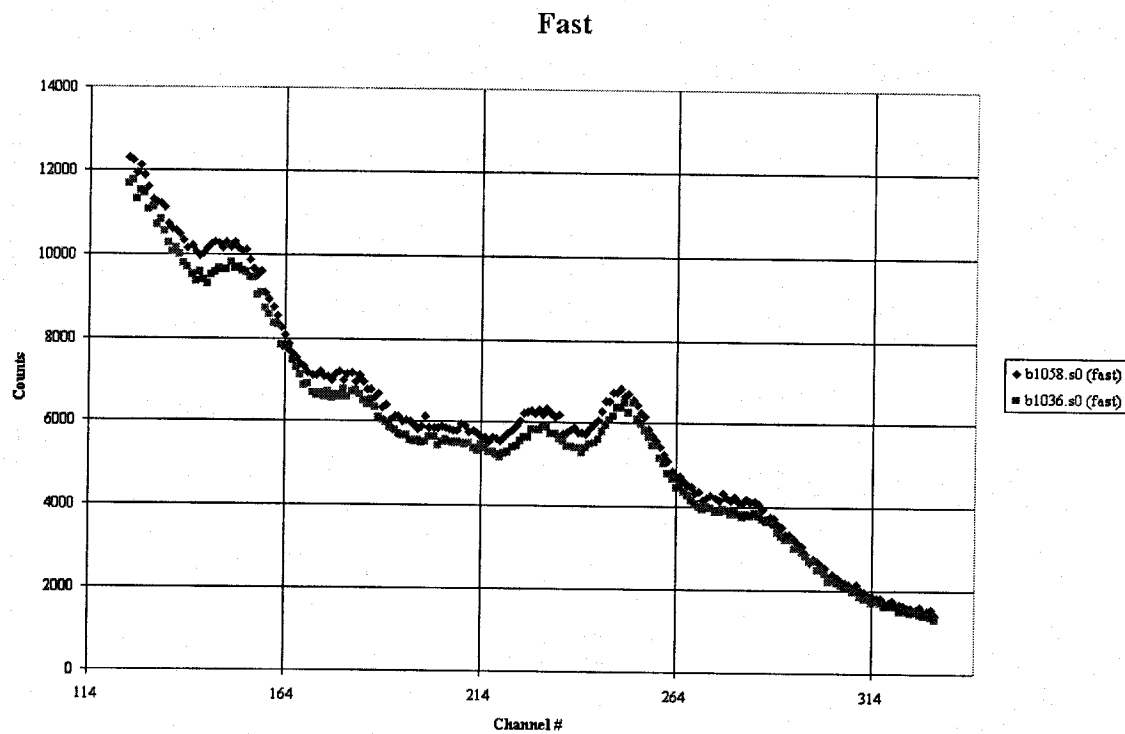


Figure 29. Comparison of two background spectra of the same shell (155mm) on the same soil (gravel).

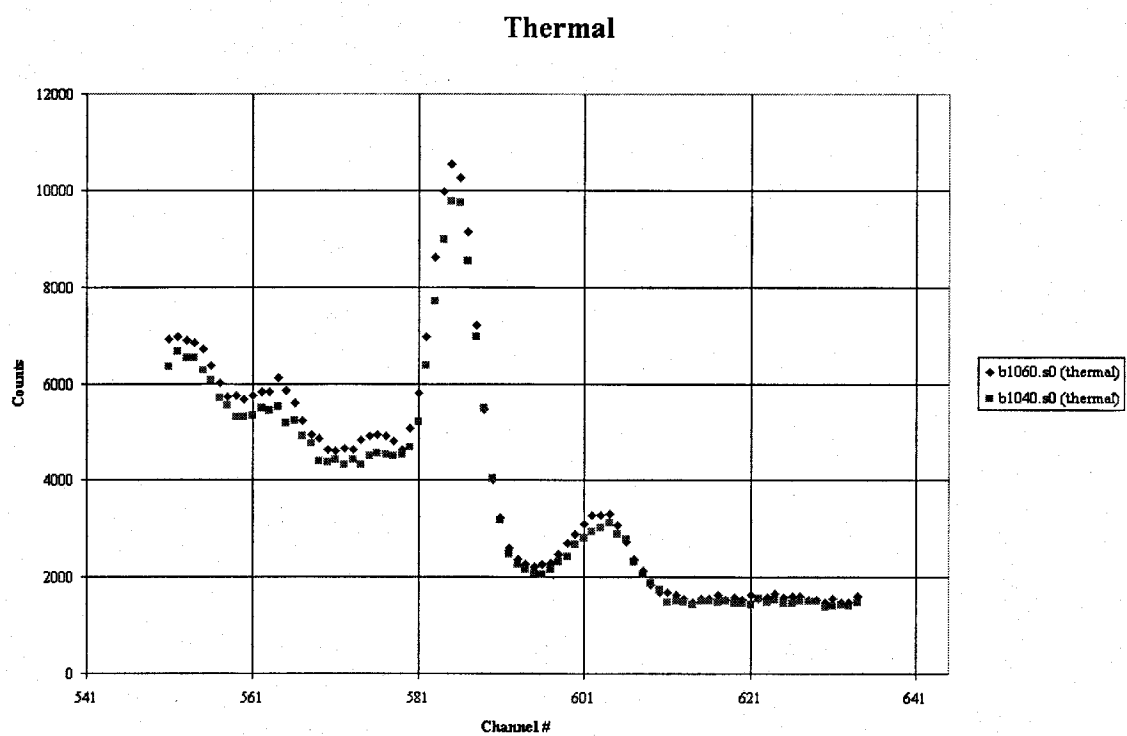
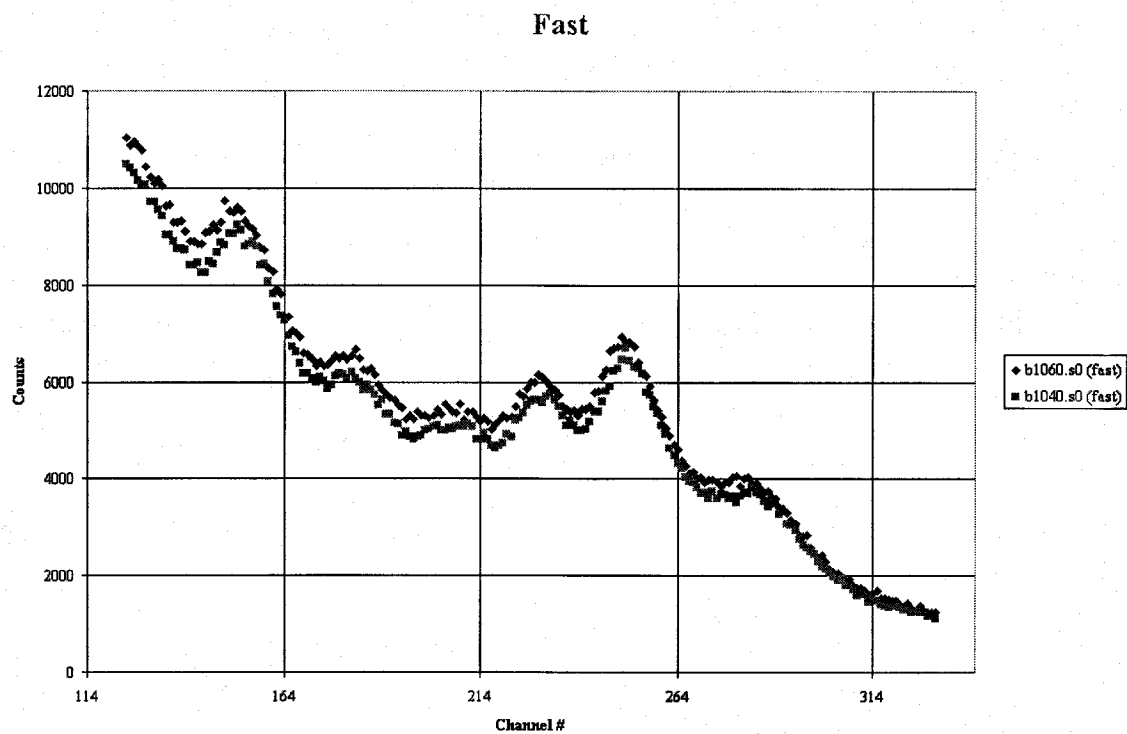


Figure 30. Comparison of two background spectra of the same shell (90mm) on the same soil (gravel).

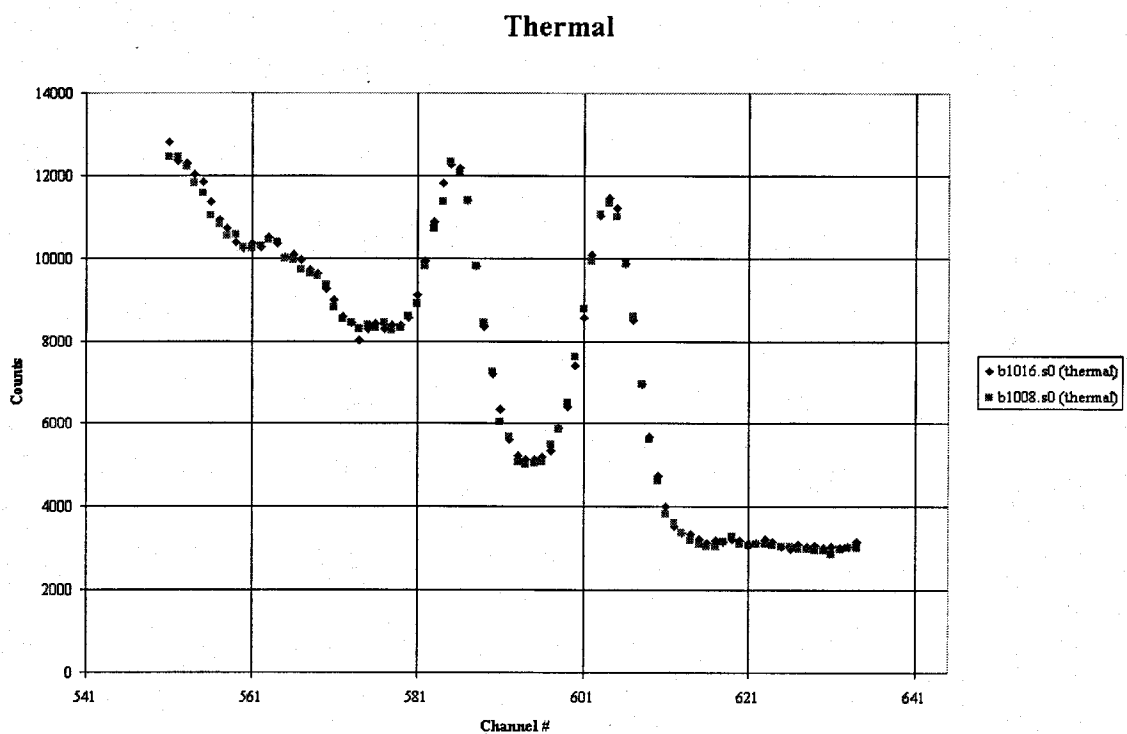
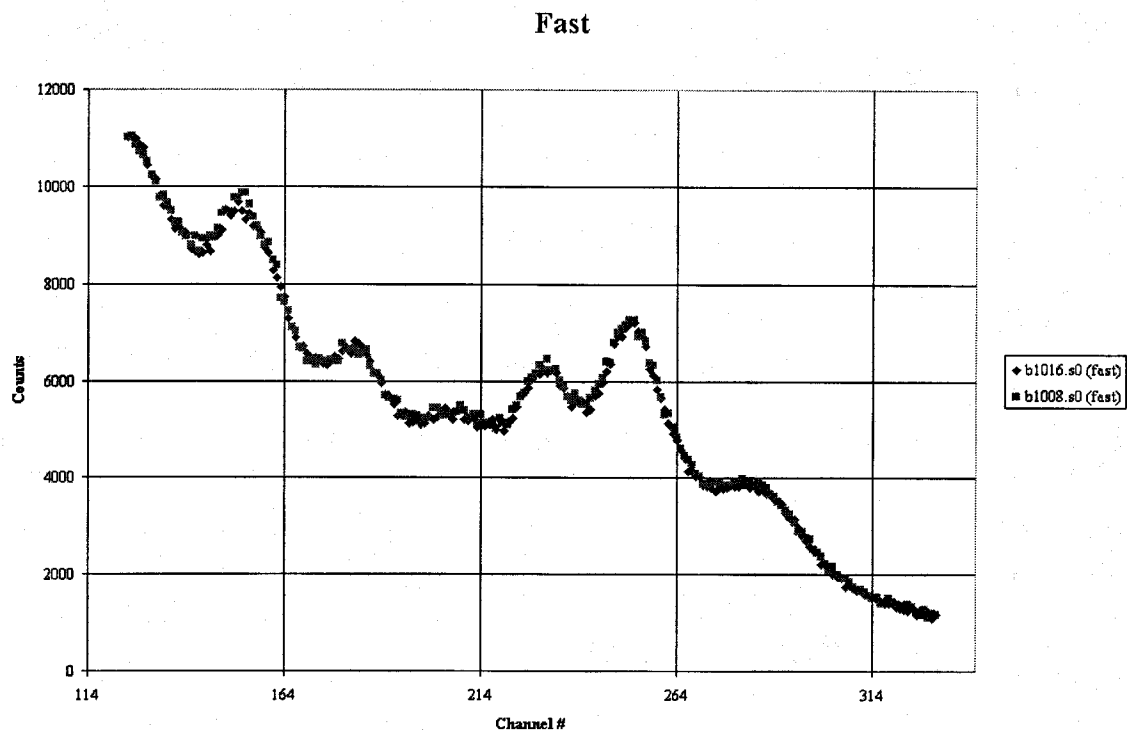


Figure 31. Comparison of two background spectra of the same shell (105mm) on the same soil (soil).

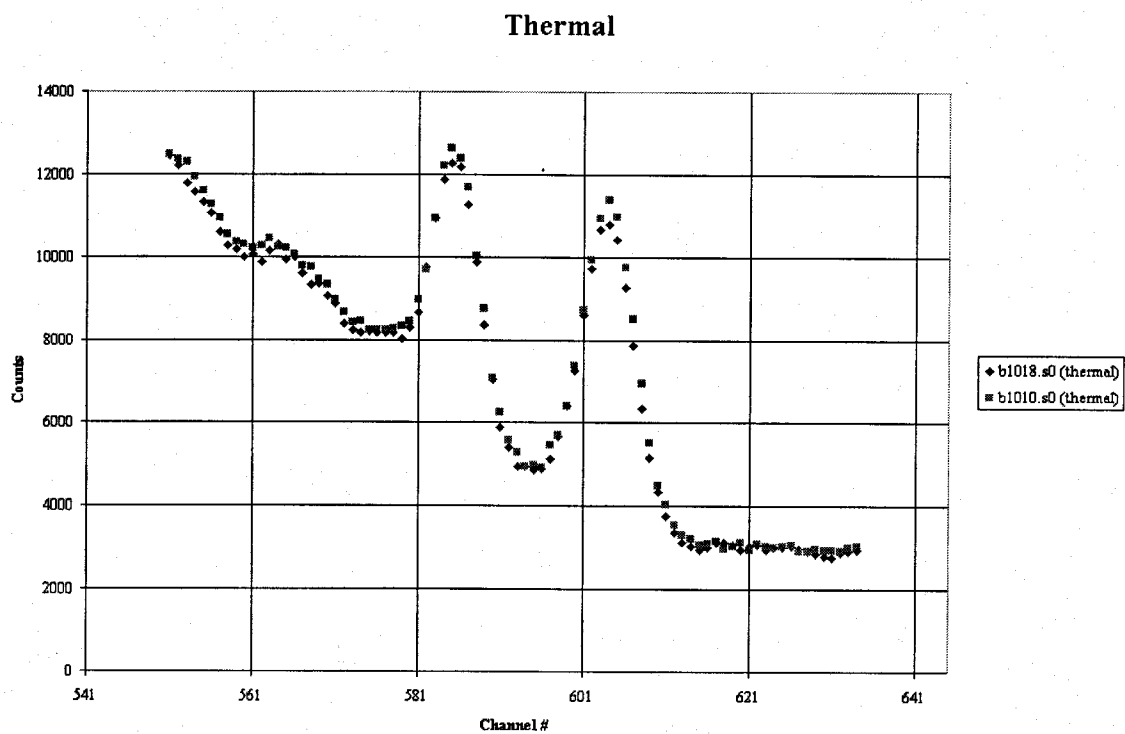
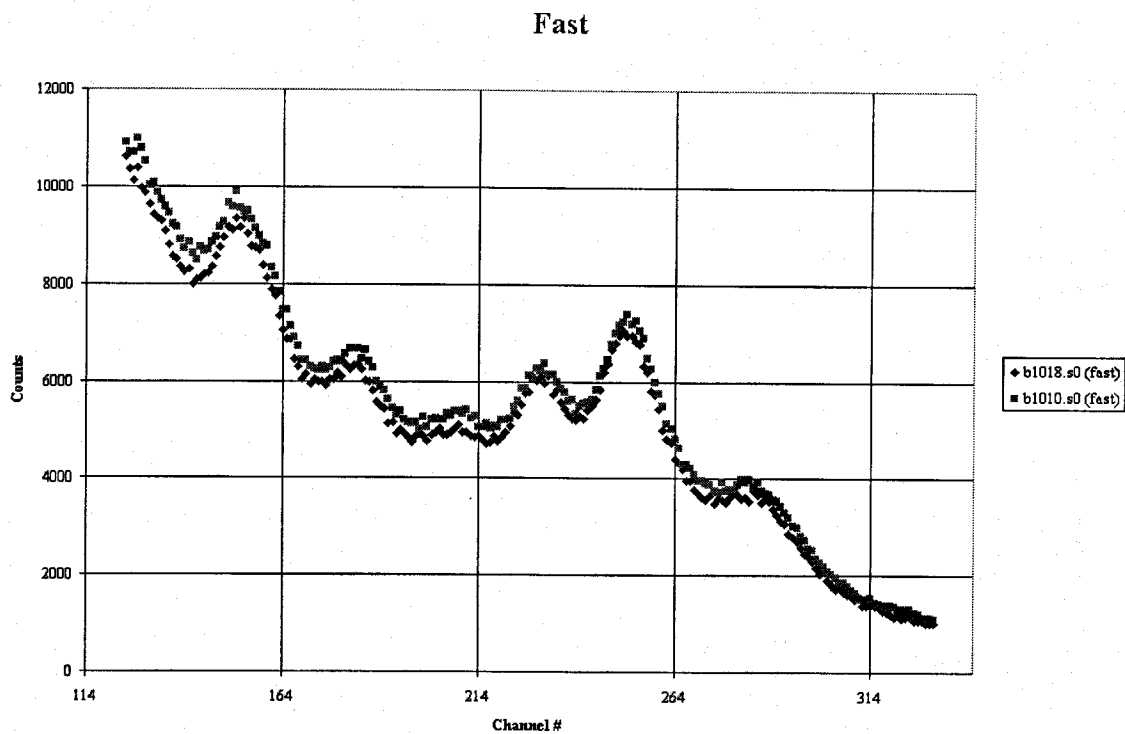


Figure 32. Comparison of two background spectra of the same shell (90mm) on the same soil (soil).

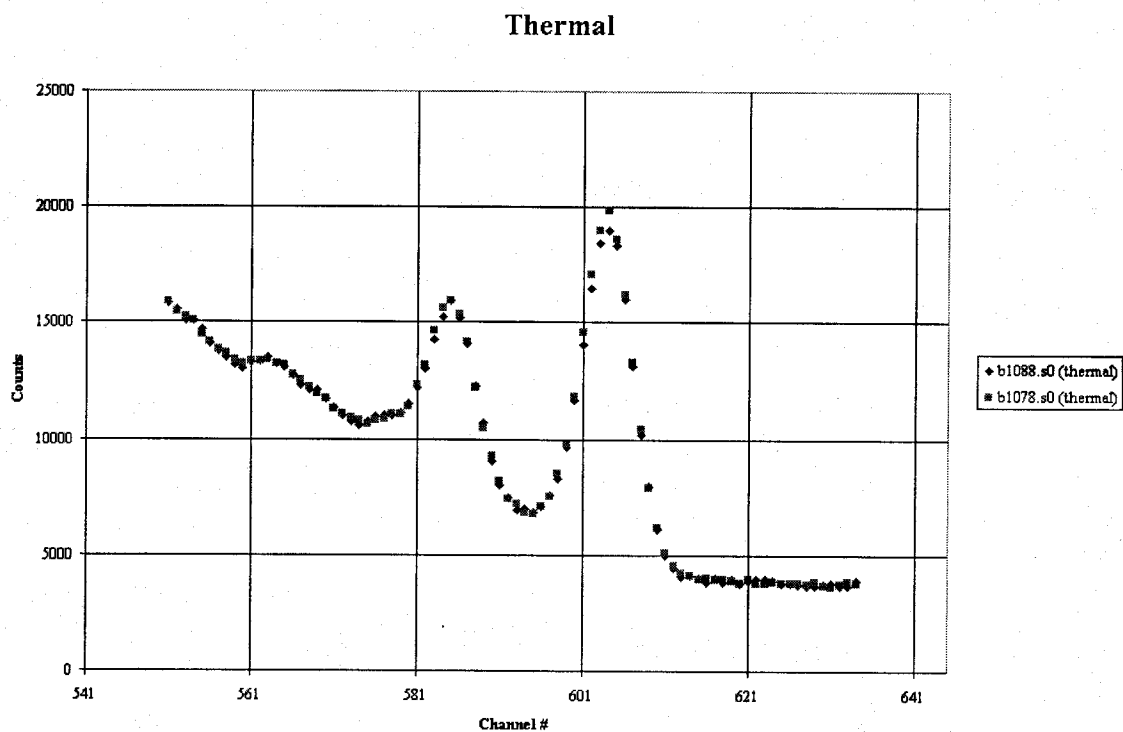
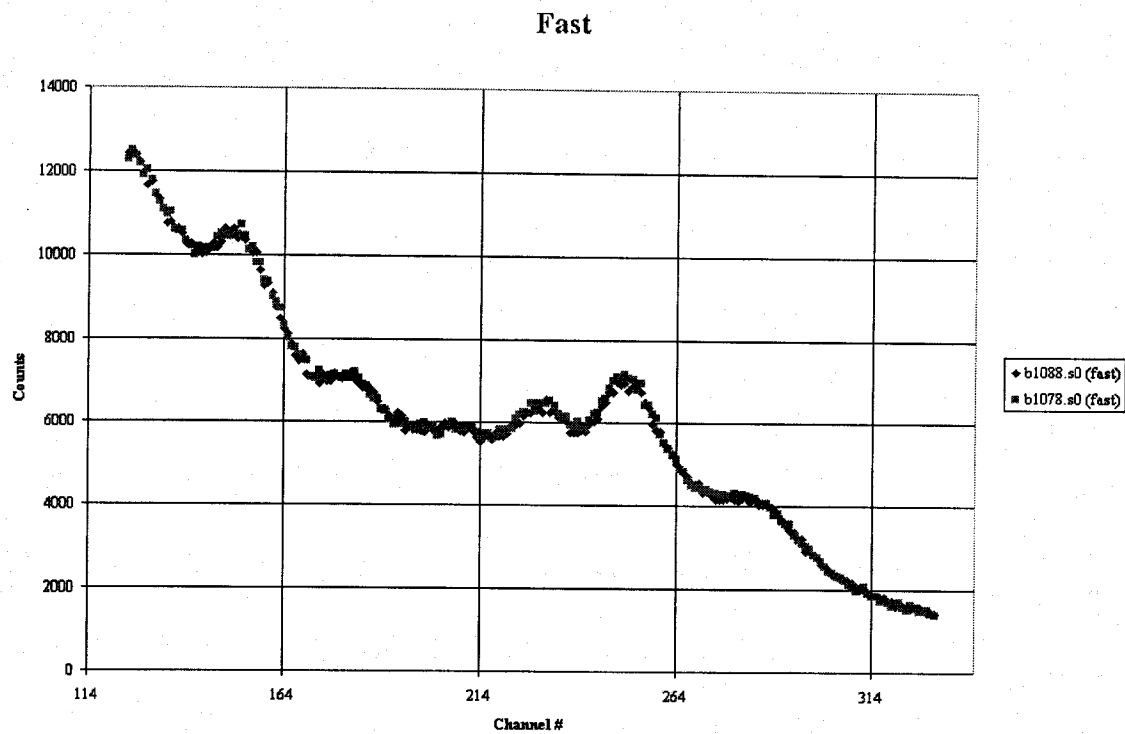


Figure 33. Comparison of two background spectra of the same shell (155mm) on the same soil (wet soil).

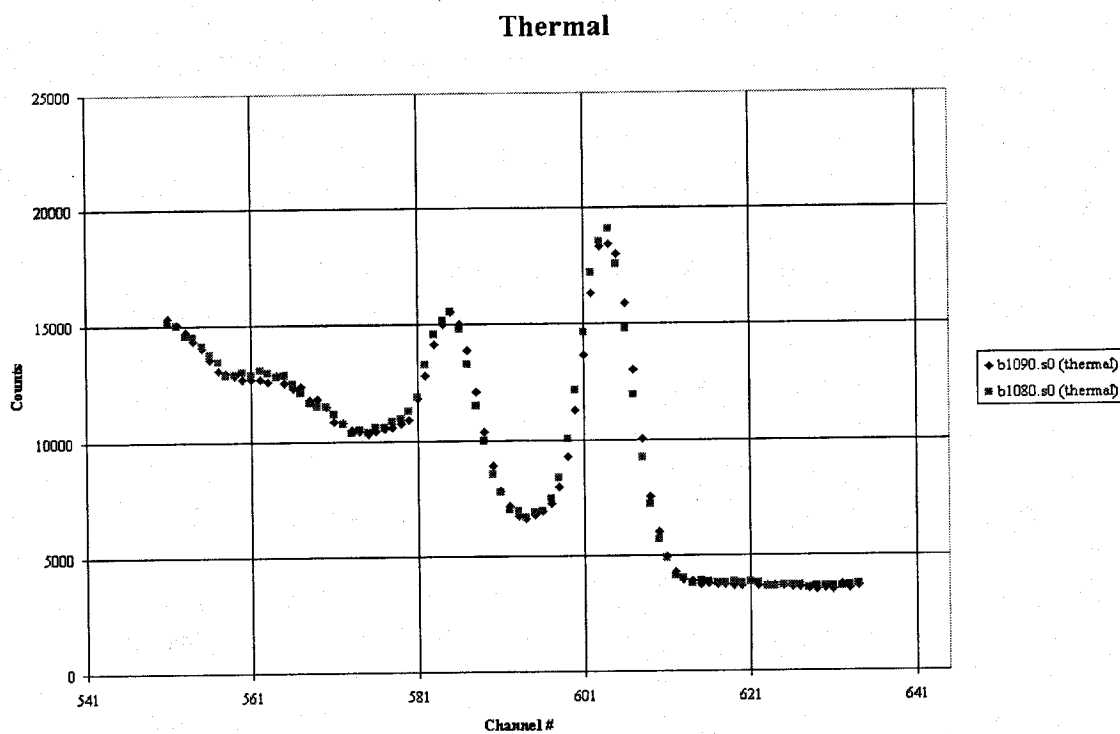
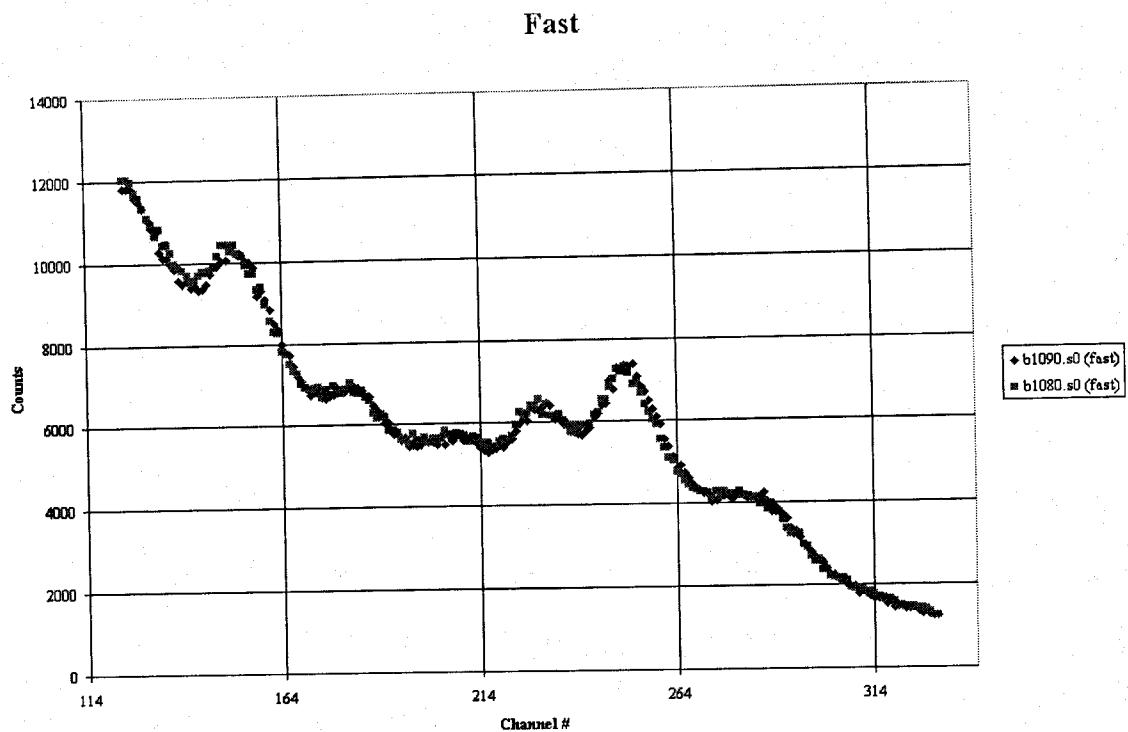


Figure 34. Comparison of two background spectra of the same shell (105mm) on the same soil (wet soil).

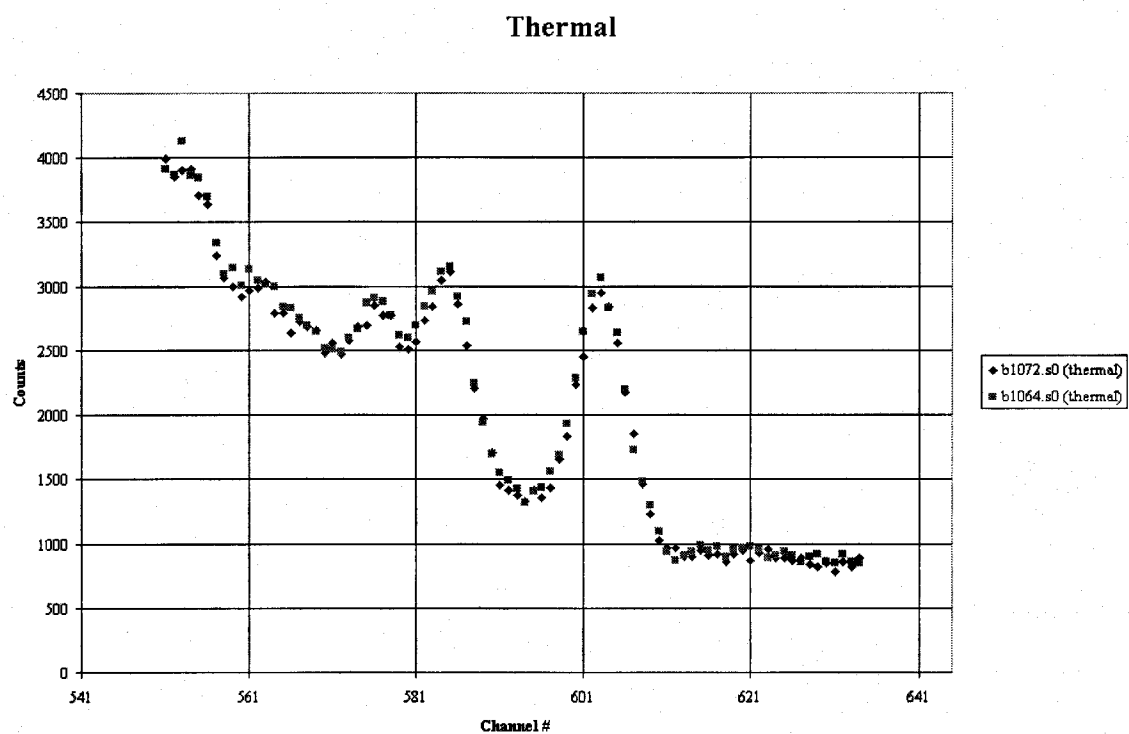
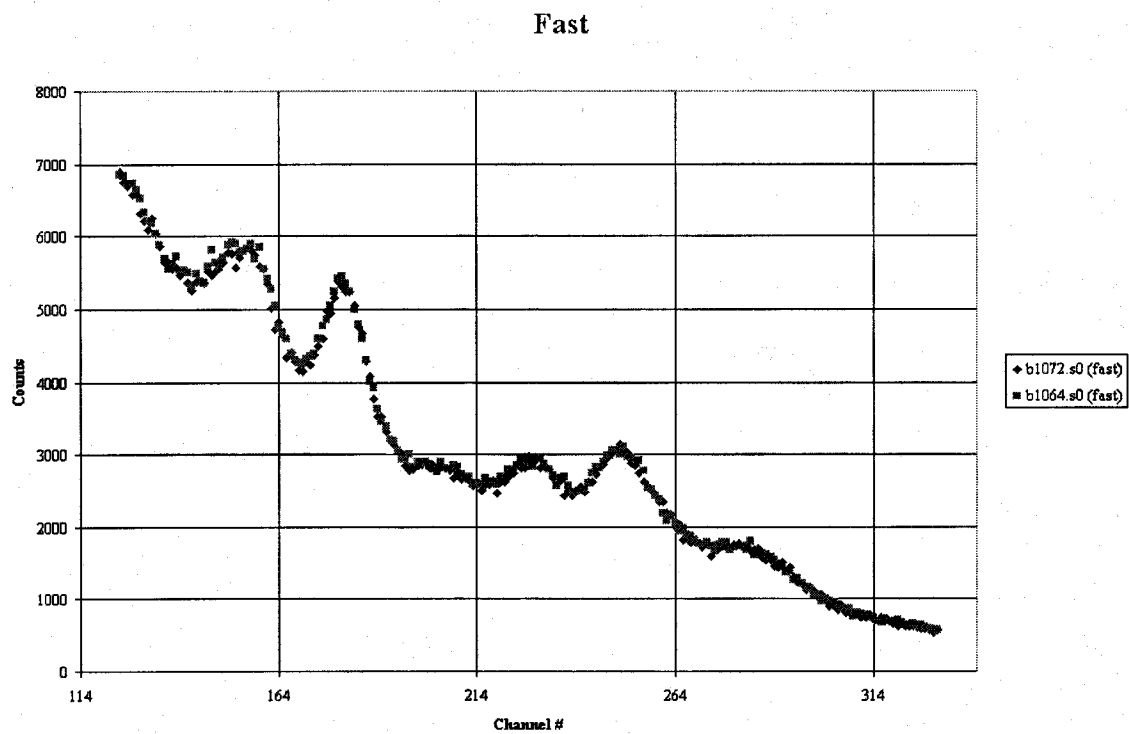


Figure 35. Comparison of two background spectra of the same shell (105mm) on the same support (table).

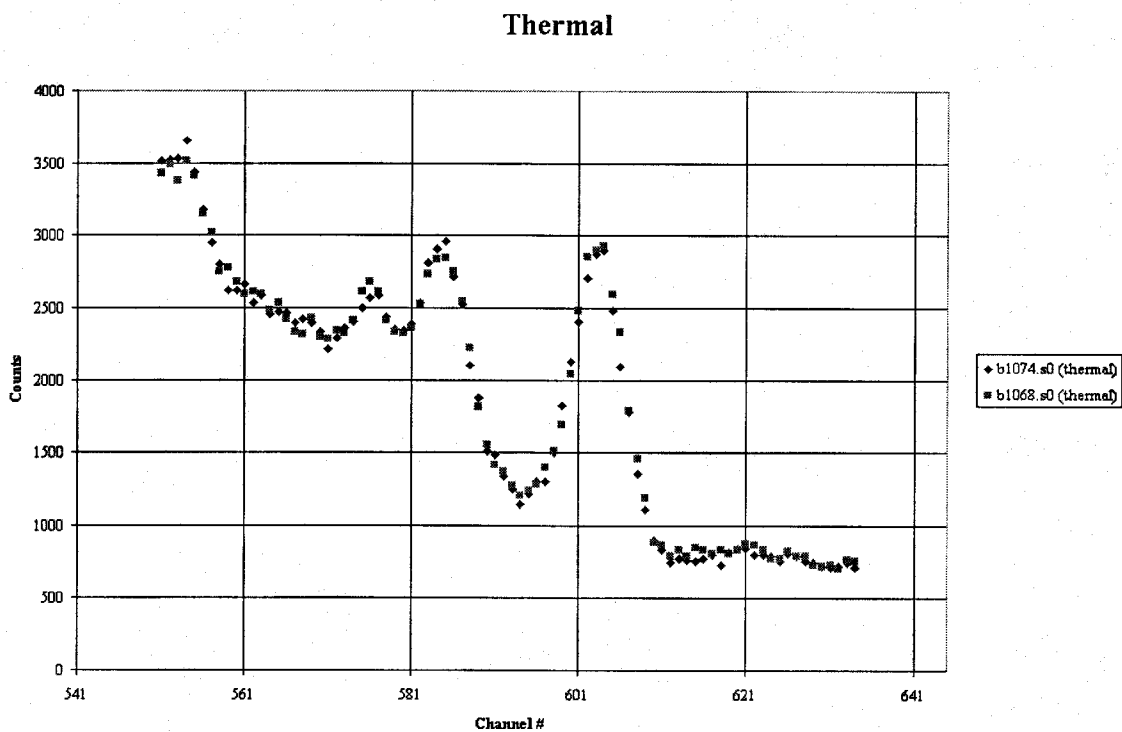
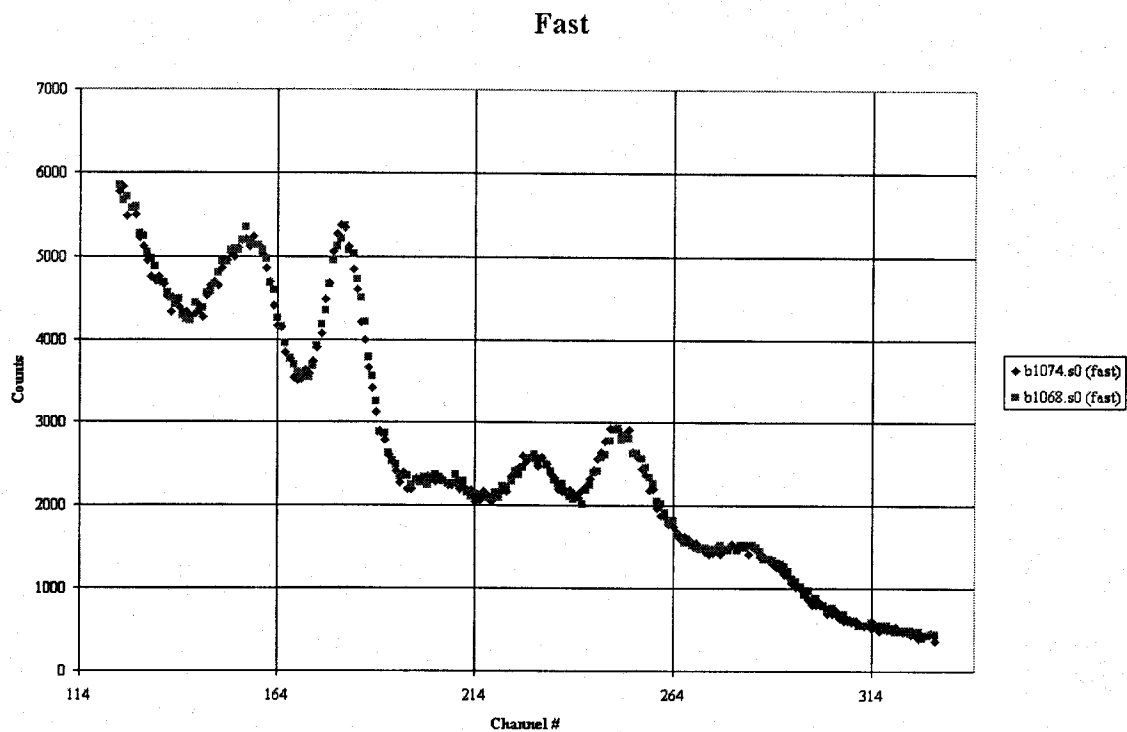


Figure 36. Comparison of two background spectra of the same shell (81mm) on the same support (table).

5.1.2 Measurement Stability

The repeatability of the PELAN measurements was validated by measuring certain shells ten times. The elemental content of each test was analyzed and the results returned to the operator immediately (less than 2 seconds) after the end of each measurement. The elements examined were hydrogen, carbon, nitrogen, oxygen, chlorine, and iron.

Standard deviations were calculated from ten measurements for particular shell content and shell size using the EXCEL™ program. All these measurement were done in the soil (none in wet soil) environment indicated in Table 16 (column labeled "surface"). The results of each series of measurements are shown in Tables 5 through 9. The errors given in parentheses are those fitting errors computed by the analysis program SPIDER. The standard deviations given at the bottom of Tables 5 – 9 do not take the error determined by SPIDER into account.

Table 10A shows the collective results of these measurements. The standard deviation increases for elements such as C and O as the shell size decreases. It also increases when there is very little or none of the element present. For example, the standard deviation of N in wax-filled shell is very high since there is very little N in the wax compound. Hydrogen has higher standard deviation than C due to the fact that H is more prominent in the background spectra. As stated in the section of the report concerning background stability, the large standard deviation comes from the effective background subtraction process in SPIDER.

The standard deviations of the ratio of elements of Table 10B are NOT calculated by error propagation but rather, by the EXCEL™ STDEV function. We see, then, that the uncertainties in the ratios can be higher than those derived by error propagation techniques (i.e. if $q = \frac{x}{y}$ then

$$\sigma_q = \left(\frac{x}{y}\right) * \sqrt{\left(\frac{\sigma_x}{x}\right)^2 + \left(\frac{\sigma_y}{y}\right)^2}. \text{ The standard deviations are especially high when there is very}$$

little (statistically zero) of a particular element (e.g. the C/N ratio for wax should be undefined since N should be zero).

In Tables 5 – 9 notice that while the standard deviation is strongly affected by shell size, the error calculated by SPIDER (fitting error) drops only slightly with decreasing shell size. This is because the analysis program fits the entire spectrum at once and not individual gamma-ray peaks. The program SPIDER uses a least squares method of determining a linear combination of individual elemental responses for the entire region fitted. Thus, the error calculated by the analysis program is affected strongly by the intensity and shape of the overall spectrum analyzed. The intensity of the respective fast and thermal spectra for the repeatability tests (shown below in Figures 37 – 39) decreases only slightly with decreasing shell size in the same environment (in soil, for example), because the signal from the environment constitutes the majority of the total signal.

A selection (runs 1589 – 1798) of the data from Table 16 along with the error calculated by the SPIDER is shown in Table 11. Columns labeled "±" indicate the error given by SPIDER for elemental measurements (in cps). Note that the error given by SPIDER correlates distinctly

according to each background type (the column labeled "surface": table, gravel, sand, or wet soil). The average fitting error is calculated for each environment. We now also calculate the standard deviation in the fitting errors for each environment and define a quantity "variation" as two standard deviations of the fitting errors for that environment.

The groupings according to environment type indicate a strong correlation between the environment and the fitting error given by SPIDER. Because the repeatability tests were done in a soil environment as defined in Table 16, the average SPIDER error for this data (Tables 5 – 9) will be considered as representative of this type environment.

These average SPIDER errors are summarized in Table 12. We have used an extra significant figure to demonstrate the very small variation in average error. Note that the average fitting error is statistically different in one or more elements for any two environments. In Table 12 sand and gravel are the most similar.

Thus, conclusion of Table 12 is that the fitting error calculated by SPIDER seems to be strongly correlated to the background spectrum. The background spectrum, in turn, is caused mostly by the environment (soil or surface type).

Table 5. Reproducibility results for 155 mm shell with TNT. Fitting error (in cps) is shown in parenthesis.

Type of shell: 155 TNT, Weight of fill: 13.2 lbs							
Foreground	Background	C (cps)	O (cps)	N (cps)	Fe (cps)	Cl (cps)	H(cps)
1127	1189	16.9 (1.0)	15.0 (0.6)	6.9 (1.3)	1.8 (0.3)	3.0 (0.5)	36.2 (2.8)
1130	1189	16.3 (1.0)	14.7 (0.6)	5.0 (1.3)	1.5 (0.3)	2.3 (0.5)	26.6 (2.9)
1133	1189	17.5 (1.0)	14.8 (0.6)	5.3 (1.3)	1.3 (0.3)	2.9 (0.5)	31.8 (2.8)
1136	1189	17.4 (1.0)	14.9 (0.6)	6.8 (1.3)	2.3 (0.3)	2.9 (0.5)	24.4 (2.9)
1139	1189	16.3 (0.9)	14.8 (0.6)	3.9 (1.3)	1.5 (0.3)	2.2 (0.5)	26.2 (2.9)
1142	1189	16.5 (1.0)	16.0 (0.6)	5.7 (1.3)	1.6 (0.3)	2.5 (0.5)	25.3 (2.9)
1145	1189	16.4 (1.0)	15.2 (0.6)	7.0 (1.3)	2.1 (0.3)	2.8 (0.5)	30.2 (2.8)
1148	1189	16.1 (0.9)	13.6 (0.6)	4.6 (1.3)	2.3 (0.3)	2.0 (0.5)	24.8 (2.8)
1151	1189	17.0 (0.9)	15.5 (0.6)	6.0 (1.3)	2.8 (0.3)	2.6 (0.5)	25.0 (2.8)
1154	1189	17.3 (1.0)	15.3 (0.6)	4.9 (1.3)	2.3 (0.3)	2.3 (0.5)	24.8 (2.8)
Average		16.8	15.0	5.6	1.9	2.5	27.5
Stdev		0.5	0.6	1.1	0.5	0.3	3.9
%Stdev		3%	4%	19%	24%	14%	14%

Table 6. Reproducibility results for 105 mm shell with wax. Fitting error (in cps) is shown in parenthesis.

Type of shell: 105 Wax, Weight of fill: 2 lbs							
Foreground	Background	C (cps)	O(cps)	N(cps)	Fe(cps)	Cl(cps)	H(cps)
1159	1223	3.6 (0.9)	4.0 (0.6)	0.9 (1.3)	4.8 (0.3)	0.9 (0.5)	24.9 (2.8)
1162	1223	4.5 (0.9)	4.2 (0.6)	2.3 (1.3)	4.8 (0.3)	1.3 (0.5)	22.6 (2.8)
1165	1223	4.1 (0.9)	3.9 (0.6)	1.6 (1.3)	4.0 (0.3)	1.7 (0.5)	21.7 (2.8)
1168	1223	4.8 (0.9)	4.5 (0.6)	2.5 (1.3)	5.0 (0.3)	1.9 (0.5)	20.2 (2.8)
1171	1223	4.4 (0.9)	4.6 (0.6)	1.0 (1.3)	3.9 (0.3)	1.6 (0.5)	20.5 (2.8)
1174	1223	4.7 (0.9)	3.1 (0.6)	0.7 (1.3)	4.8 (0.3)	1.7 (0.5)	23.9 (2.8)
1177	1223	4.3 (0.9)	3.3 (0.6)	2.1 (1.3)	4.3 (0.2)	1.3 (0.5)	18.6 (2.8)
1180	1223	4.6 (0.9)	2.5 (0.6)	-0.8 (1.3)	3.4 (0.3)	2.0 (0.5)	18.8 (2.8)

1183	1223	3.9 (0.9)	2.6 (0.6)	2.3 (1.3)	4.1 (0.3)	1.8 (0.5)	16.0 (2.8)
1186	1223	4.9 (0.9)	2.7 (0.6)	1.4 (1.3)	4.3 (0.3)	2.0 (0.5)	22.0 (2.8)
Average		4.4	3.5	1.4	4.3	1.6	20.9
Stdev		0.4	0.8	1.0	0.5	0.3	2.7
%Stdev		10%	23%	73%	12%	21%	13%

Table 7. Reproducibility results for 81 mm shell with CompB. Fitting error (in cps) is shown in parenthesis.

Type of shell: 81 CompB, Weight of fill: 2 lbs							
Foreground	Background	C(cps)	O(cps)	N(cps)	Fe(cps)	Cl(cps)	H(cps)
1098	1288	2.6 (0.9)	7.3 (0.6)	4.0 (1.3)	1.2 (0.2)	0.5 (0.5)	35.6 (2.6)
1100	1288	4.2 (0.9)	5.7 (0.6)	2.2 (1.3)	1.0 (0.2)	1.3 (0.4)	27.4 (2.7)
1103	1288	3.7 (0.9)	6.2 (0.6)	2.8 (1.3)	1.2 (0.2)	0.2 (0.5)	24.9 (2.7)
1106	1288	3.4 (0.9)	5.8 (0.6)	2.7 (1.3)	1.5 (0.2)	0.7 (0.5)	25.9 (2.7)
1109	1288	2.9 (0.9)	5.2 (0.6)	3.4 (1.3)	1.5 (0.2)	0.8 (0.4)	26.2 (2.7)
1112	1288	2.7 (0.9)	5.6 (0.6)	1.5 (1.3)	1.1 (0.2)	0.9 (0.5)	27.3 (2.6)
1115	1288	2.5 (0.9)	4.5 (0.6)	3.9 (1.3)	1.5 (0.2)	0.4 (0.5)	25.6 (2.8)
1118	1288	3.4 (0.9)	4.6 (0.6)	2.3 (1.3)	0.8 (0.2)	0.7 (0.5)	29.3 (2.7)
1121	1288	3.7 (0.9)	5.6 (0.6)	2.0 (1.3)	0.6 (0.2)	0.5 (0.5)	26.6 (2.8)
1124	1288	2.2 (0.9)	5.9 (0.6)	3.8 (1.3)	0.6 (0.2)	0.7 (0.5)	22.3 (2.8)
Average		3.1	5.6	2.9	1.1	0.7	27.1
Stdev		0.6	0.8	0.9	0.3	0.3	3.5
%Stdev		20%	14%	31%	30%	45%	13%

Table 8. Reproducibility results for 81 mm shell with plaster of Paris (PoP). Fitting error (in cps) is shown in parenthesis.

Type of shell: 81 PoP, Weight of fill: 2 lbs							
Foreground	Background	C(cps)	O(cps)	N(cps)	Fe(cps)	Cl(cps)	H(cps)
1191	1288	2.0 (0.9)	7.3 (0.6)	1.5 (1.3)	0.5 (0.2)	1.8 (0.5)	21.8 (2.6)
1194	1288	1.0 (0.9)	6.8 (0.6)	1.5 (1.3)	0.7 (0.2)	1.2 (0.5)	13.2 (2.6)
1197	1288	0.8 (0.9)	7.2 (0.6)	2.8 (1.3)	1.0 (0.2)	1.4 (0.5)	14.2 (2.6)
1200	1288	0.3 (0.9)	5.8 (0.6)	1.3 (1.3)	0.8 (0.2)	1.3 (0.4)	11.6 (2.6)
1203	1288	0.8 (0.9)	5.5 (0.6)	2.1 (1.3)	0.7 (0.2)	1.7 (0.4)	12.5 (2.6)
1206	1288	1.3 (0.9)	5.0 (0.6)	1.6 (1.3)	0.7 (0.2)	1.5 (0.5)	11.2 (2.6)
1209	1288	0.8 (0.9)	5.8 (0.6)	1.0 (1.3)	0.4 (0.2)	1.4 (0.4)	11.0 (2.6)
1212	1288	-0.2 (0.9)	6.0 (0.6)	0.1 (1.3)	0.5 (0.2)	1.1 (0.4)	11.1 (2.6)
1215	1288	1.4 (0.9)	5.4 (0.6)	2.5 (1.3)	0.8 (0.2)	1.3 (0.4)	12.3 (2.6)
1218	1288	1.2 (0.9)	5.1 (0.6)	1.6 (1.3)	0.3 (0.2)	1.9 (0.4)	12.5 (2.6)
Average		0.9	6.0	1.6	0.6	1.5	13.1
Stdev		0.6	0.8	0.8	0.2	0.3	3.2
%Stdev		64%	14%	47%	33%	18%	24%

Table 9. Reproducibility results for 76 mm shell with RDX. Fitting error (in cps) is shown in parenthesis.

Type of shell: 76 RDX, Weight of fill: 1.7 lbs							
Foreground	Background	C(cps)	O(cps)	N(cps)	Fe(cps)	Cl(cps)	H(cps)
1225	1291	3.3 (0.9)	-8.6 (0.6)	1.3 (1.3)	3.1 (0.2)	2.9 (0.4)	8.3 (2.5)
1228	1291	4.1 (0.9)	-9.3 (0.6)	1.3 (1.3)	3.1 (0.2)	2.1 (0.4)	5.1 (2.5)
1231	1291	3.7 (0.9)	-8.3 (0.6)	1.1 (1.3)	2.9 (0.2)	2.3 (0.4)	0.2 (2.6)
1234	1291	3.4 (0.9)	-8.3 (0.6)	1.9 (1.3)	3.3 (0.2)	2.6 (0.4)	1.9 (2.6)
1237	1291	2.2 (0.9)	-7.8 (0.6)	0.7 (1.3)	2.3 (0.2)	2.6 (0.4)	11.9 (2.5)
1240	1291	4.1 (0.9)	-7.4 (0.6)	1.4 (1.3)	2.1 (0.2)	2.9 (0.4)	3.5 (2.6)
1243	1291	4.2 (0.9)	-9.0 (0.6)	1.6 (1.3)	1.8 (0.2)	2.4 (0.4)	5.1 (2.5)
1246	1291	3.7 (0.9)	-8.4 (0.6)	1.1 (1.3)	2.6 (0.2)	2.3 (0.4)	4.6 (2.5)
1249	1291	3.7 (0.9)	-9.3 (0.6)	1.2 (1.3)	2.4 (0.2)	2.2 (0.4)	-0.8 (2.5)
1252	1291	3.0 (0.9)	-9.6 (0.6)	1.5 (1.3)	2.5 (0.2)	2.2 (0.4)	3.0 (2.5)
Average		3.5	-8.6	1.3	2.6	2.4	4.3
Stdev		0.6	0.7	0.3	0.5	0.3	3.7
%Stdev		17%	-8%	24%	19%	12%	87%

Table 10A. The standard deviations (in percent) of the PELAN measurements for various elements.

Shell Size (mm)	Shell Content	C (%)	O (%)	N (%)	Fe (%)	Cl (%)	H (%)
155	TNT	3	4	19	24	14	14
105	Wax	10	23	73	12	21	13
81	CompB	20	14	31	30	45	13
81	Plaster of Paris	64	14	47	33	18	24
76	RDX	17	8	24	19	12	87

Table 10B. Standard deviations (in percent) of ratios based on reproducibility measurements.

	C/H	C/N	C/O
155 TNT	12	19	4
105 Wax	15	136	27
81 CompB	22	42	23
81 PoP	58	170	63
76 RDX	297	19	18

Table 11. A selection of data from Table 17 showing the error determined by the analysis program SPIDER as a function of environment. Columns labeled "±" indicate the fitting error given by SPIDER for elemental measurements. See text for more details.

Run	Size	Fill	Surface	C (cps)	± (cps)	H (cps)	± (cps)	N (cps)	± (cps)	O (cps)	± (cps)
1589	82	TNT	TABLE	2.9	0.7	-2.6	1.3	0.2	0.8	1.7	0.3
1592	90	TX50	TABLE	6.1	0.7	2.4	1.4	1.4	0.8	4.7	0.3
1595	4.5	semte x-1a	TABLE	15.0	0.7	5.1	1.4	1.8	0.8	9.6	0.3
1598	1	Smok e less	TABLE	10.7	0.7	0.5	1.4	0.2	0.8	5.3	0.3
1601	155	TNT	TABLE	29.4	0.8	-4.0	1.6	6.4	1.0	16.1	0.4
1604		ANFO (2 wt%)	TABLE	5.1	0.7	9.4	1.4	2.8	0.8	13.0	0.3
1607		ANFO (6 wt%)	TABLE	4.6	0.7	12.5	1.4	3.4	0.8	13.4	0.3
1610	105	WAX	TABLE	7.3	0.8	5.3	1.7	-0.2	0.9	2.4	0.3
1613		ANFO (15 wt%)	TABLE	8.3	0.7	17.9	1.4	3.5	0.8	12.8	0.3
1616	shp chrg	6.1lbs pxb- 108	TABLE	24.3	0.8	-4.6	1.8	6.9	0.9	14.6	0.4
1619	shp chrg	0.9lbs Octol	TABLE	8.3	0.7	1.8	1.3	1.9	0.8	5.0	0.3
1622	Sheet explo	21lb PETN	TABLE	33.4	0.8	14.5	1.7	3.8	0.9	24.6	0.4
1625	TMRP-6	11.2lb TNT	TABLE	39.9	0.8	10.4	1.5	3.2	0.8	12.5	0.3
1628	Val69 Mine	6lb Comp B	TABLE	10.5	0.7	1.8	1.4	2.1	0.8	4.0	0.3
1631	90	rocket 1.1lb 60/40	TABLE	12.1	0.8	3.5	1.4	2.6	0.9	9.2	0.4
1634	FFV028 stl mine	12.35 TNT	TABLE	14.9	0.8	6.3	1.4	7.1	0.9	12.9	0.4
Average (TABLE)					0.8		1.5		0.8		0.3
Two standard deviations in Average					0.1		0.3		0.1		0.0
1643	82	TNT	GRAVEL	8.6	0.9	1.2	1.4	-0.5	1.2	0.3	0.5
1646	90	TX50	GRAVEL	9.6	0.9	-1.0	1.4	1.9	1.2	1.5	0.5
1649	155	TNT	GRAVEL	20.5	0.9	8.4	1.5	3.5	1.3	7.7	0.5
1652	90	rocket 1.1lb 60/40	GRAVEL	18.0	0.9	2.6	1.4	3.7	1.3	4.2	0.6
1655	FFV028 stl mine	12.35 TNT	GRAVEL	20.0	0.9	7.8	1.5	6.8	1.3	7.7	0.6
1666	2 wt%	ANFO	GRAVEL	3.2	0.9	13.8	1.6	6.2	1.3	10.8	0.6

Run	Size	Fill	Surface	C (cps)	± (cps)	H (cps)	± (cps)	N (cps)	± (cps)	O (cps)	± (cps)
1669	6 wt%	ANFO	GRAVEL	5.6	0.9	15.4	1.5	3.6	1.3	9.7	0.6
1672	15 wt%	ANFO	GRAVEL	9.0	0.9	26.9	1.6	4.7	1.3	11.9	0.6
1675	shp chrg	6.1lbs pxb- 108	GRAVEL	29.2	0.9	17.4	1.7	8.3	1.3	10.5	0.6
1678	shp chrg	0.9lbs Octol	GRAVEL	4.9	0.9	-1.6	1.5	2.9	1.3	4.7	0.6
1681	Sheetex pl	21lbP ETN	GRAVEL	36.3	0.9	39.8	1.6	5.4	1.3	19.4	0.6
1684	TMRP-6	11.2lb TNT	GRAVEL	38.7	0.9	13.4	1.6	6.1	1.3	9.3	0.6
1687	Val69 Mine	6lb Comp B	GRAVEL	9.7	0.9	0.1	1.5	1.1	1.3	3.6	0.5
Average (GRAVEL)					0.9		1.5		1.3		0.5
Two standard deviations in Average					0.1		0.2		0.1		0.0
1699	82	TNT	SAND	6.0	0.9	-2.3	1.8	0.7	1.2	-0.2	0.5
1702	90	TX50	SAND	8.4	0.9	-1.1	1.8	1.7	1.2	0.1	0.6
1705	4.5	semte x-1a	SAND	10.5	0.9	5.5	1.8	3.9	1.3	5.2	0.6
1708	1.8	semte x-1a	SAND	5.7	0.9	3.3	1.8	2.1	1.2	4.5	0.6
1711	1	smokl ess	SAND	6.2	0.9	6.1	1.8	2.8	1.3	4.1	0.6
1714	155	TNT	SAND	21.3	0.9	9.0	1.8	6.2	1.3	10.0	0.5
1717	0.02	ANFO	SAND	4.3	0.9	19.6	1.8	6.3	1.3	9.1	0.6
1720	0.06	ANFO	SAND	6.6	0.9	23.3	1.9	5.1	1.2	8.3	0.6
1723	0.15	ANFO	SAND	8.5	0.9	36.6	1.9	5.4	1.2	8.8	0.5
1726	shp chrg	6.1lbs pxb- 108	SAND	26.8	0.9	15.6	2.0	8.7	1.3	7.7	0.6
1729	shp chrg	0.9lbs Octol	SAND	5.4	0.9	4.5	1.8	1.6	1.3	4.6	0.6
1732	Sheetex pl	21lbP ETN	SAND	34.3	0.9	46.6	1.9	6.7	1.3	18.9	0.6
1735	TMRP-6	11.2lb TNT	SAND	39.4	0.9	17.8	1.9	6.2	1.2	7.5	0.6
1738	Val69 Mine	6lb Comp B	SAND	8.0	0.9	2.1	1.8	1.2	1.2	2.5	0.5
1741	90	rocket 1.1lb6 0/40	SAND	17.2	0.9	1.6	1.8	3.0	1.3	3.3	0.6
1744	FFV028 stl mine	12.35 TNT	SAND	21.0	0.9	10.7	1.8	6.8	1.3	7.3	0.6
1747	60	WAX	SAND	2.1	0.9	0.5	1.8	-0.2	1.2	-0.5	0.6
1750	81	PLAS TER	SAND	1.0	0.9	4.8	1.8	1.0	1.2	1.3	0.5
1753	81	WAX	SAND	5.4	0.9	7.0	1.8	-0.8	1.2	-3.7	0.5

Run	Size	Fill	Surface	C (cps)	± (cps)	H (cps)	± (cps)	N (cps)	± (cps)	O (cps)	± (cps)
Average (SAND)					0.9		1.8		1.3		0.6
Two standard deviation in Average					0.1		0.1		0.1		0.0
1762	155	TNT	WETSOI L	19.2	1.0	-4.8	4.7	7.9	1.4	5.2	0.6
1765	0.02	ANFO	WETSOI L	3.3	0.9	21.4	4.8	3.9	1.3	11.3	0.6
1768	0.06	ANFO	WETSOI L	4.0	0.9	22.3	4.8	4.6	1.3	11.1	0.6
1771	0.15	ANFO	WETSOI L	6.3	0.9	36.9	4.9	5.8	1.3	8.6	0.6
1774	shp chrg	6.1lbs pxb- 108	WETSOI L	21.5	1.0	-32.7	5.1	8.9	1.3	9.8	0.6
1783	shp chrg	0.9lbs Octol	WETSOI L	4.8	0.9	0.9	4.5	3.5	1.3	3.0	0.6
1786	Sheetex pl	21lbP ETN	WETSOI L	30.7	0.9	52.0	4.8	6.5	1.3	14.8	0.6
1789	TMRP-6	11.2lb TNT	WETSOI L	34.0	1.0	33.0	4.7	5.8	1.3	5.2	0.6
1792	Val69 Mine	6lb Comp B	WETSOI L	7.1	0.9	-1.8	4.5	2.3	1.3	-0.2	0.6
1795	90	rocket 1.1lb6 0/40	WETSOI L	14.5	0.9	3.0	4.5	3.0	1.3	1.2	0.6
1798	FFV028 stl mine	12.35 TNT	WETSOI L	18.2	0.9	-3.2	4.7	4.3	1.3	4.1	0.6
Average (WET SOIL)					0.9		4.7		1.3		0.6
Two standard deviation in Average					0.0		0.4		0.1		0.0

Table 12.Summary of average fitting errors calculated by the program SPIDER for type of environment ("Surface" column).

Surface	C		H		N		O	
	averag e error (cps)	variatio n (2 σ) (cps)	averag e error (cps)	variatio n (2 σ) (cps)	averag e error (cps)	variatio n (2 σ) (cps)	averag e error (cps)	variatio n (2 σ) (cps)
SOIL	0.91	0.04	2.70	0.11	1.30	0.00	0.58	0.02
TABLE	0.75	0.07	1.47	0.30	0.85	0.10	0.34	0.03
GRAVEL	0.89	0.05	1.52	0.19	1.28	0.08	0.55	0.02
SAND	0.88	0.05	1.83	0.12	1.25	0.10	0.55	0.02
WET SOIL	0.93	0.04	4.73	0.37	1.31	0.06	0.60	0.02

Figures 36,37, and 38 show the collective 10 measurements for each of three targets out of the 5 that were measured. For a given munition/environment, the spectra seem statistically equivalent.

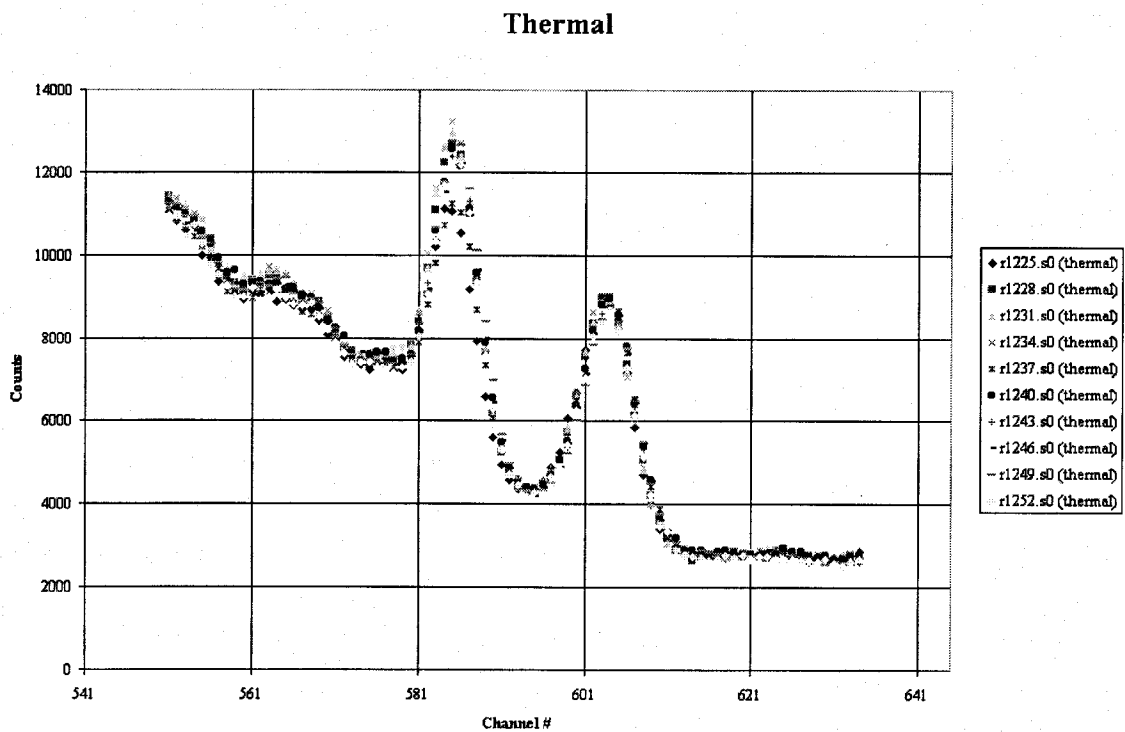
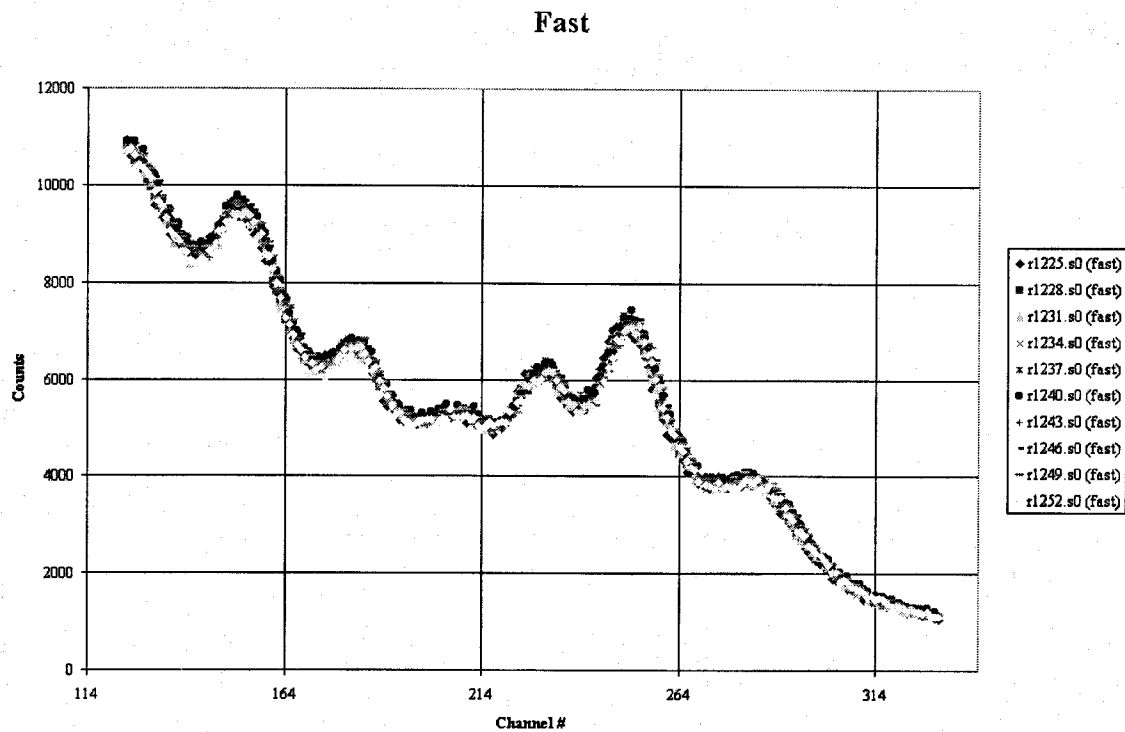


Figure 37. Ten measurements of a 76 mm shell with RDX.

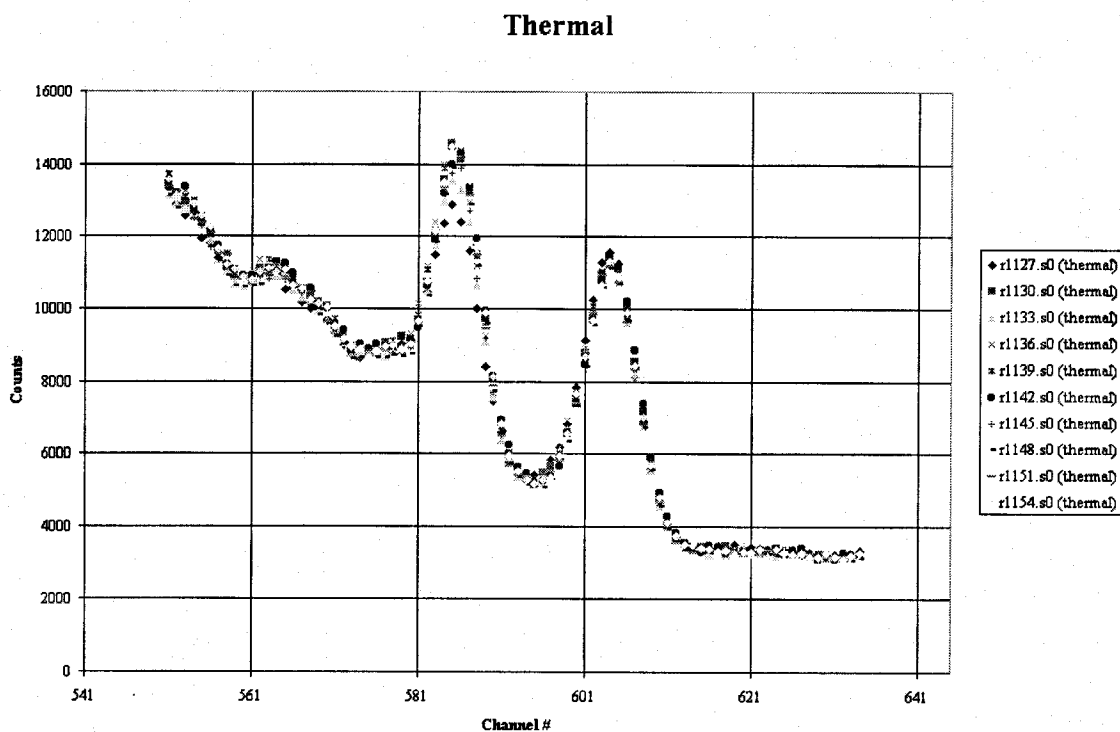
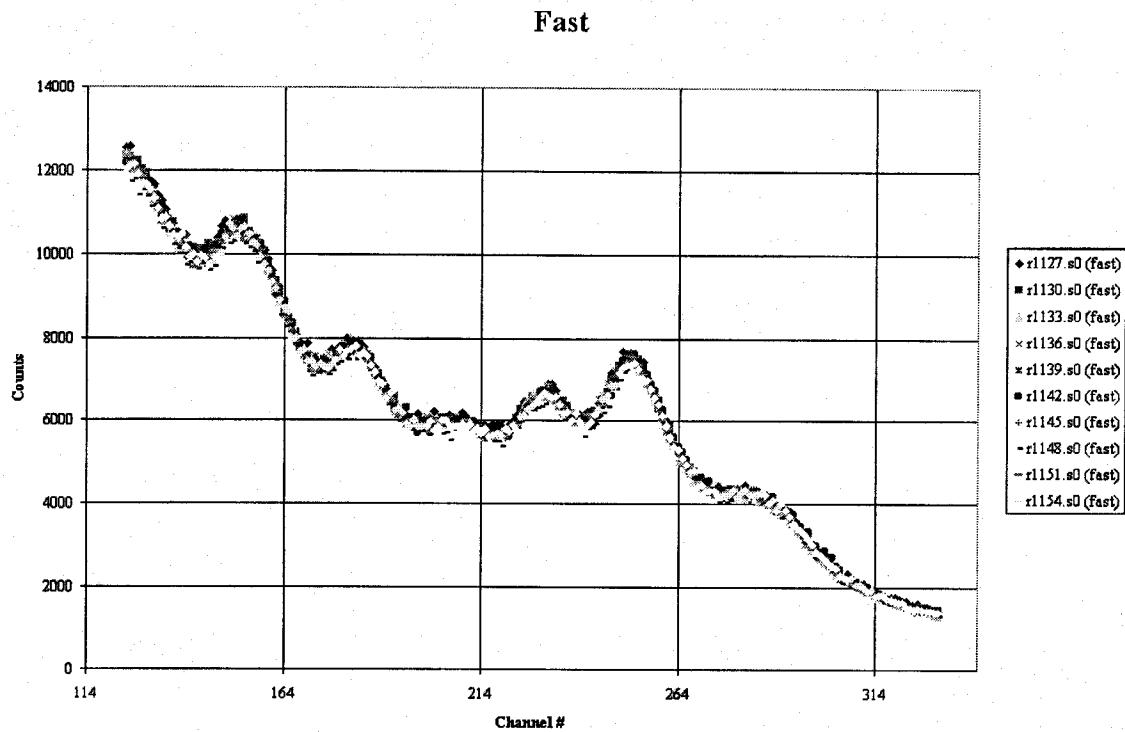


Figure 38. Ten measurements of a 155 mm shell with TNT.

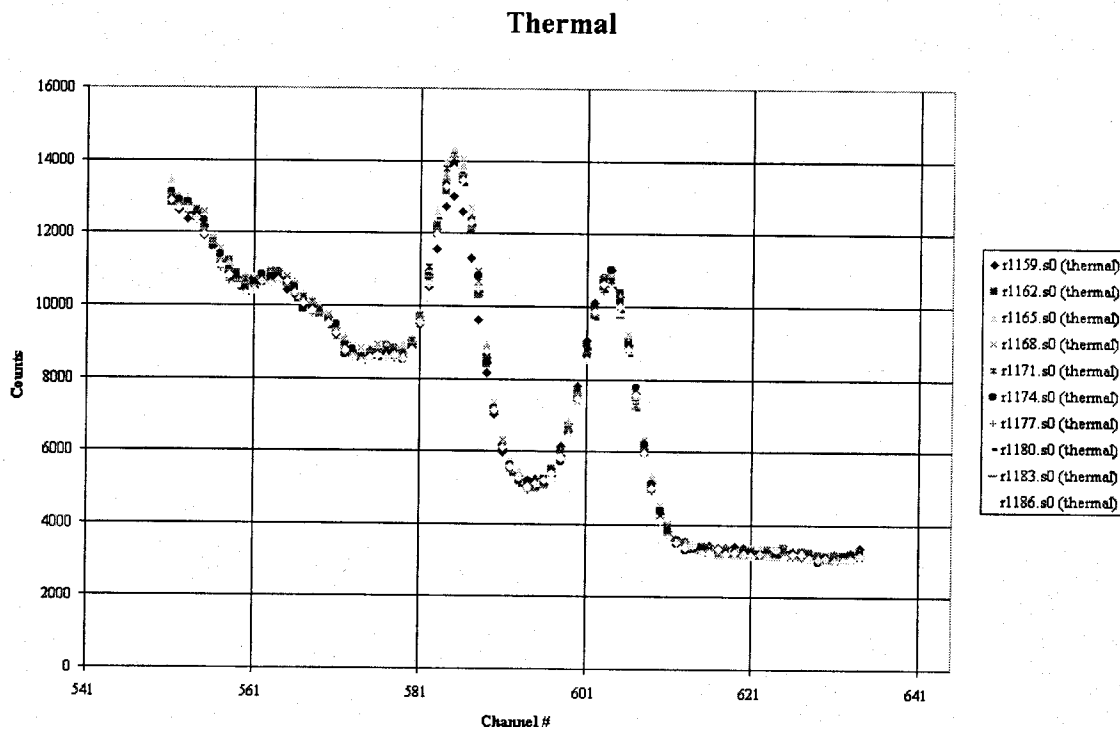
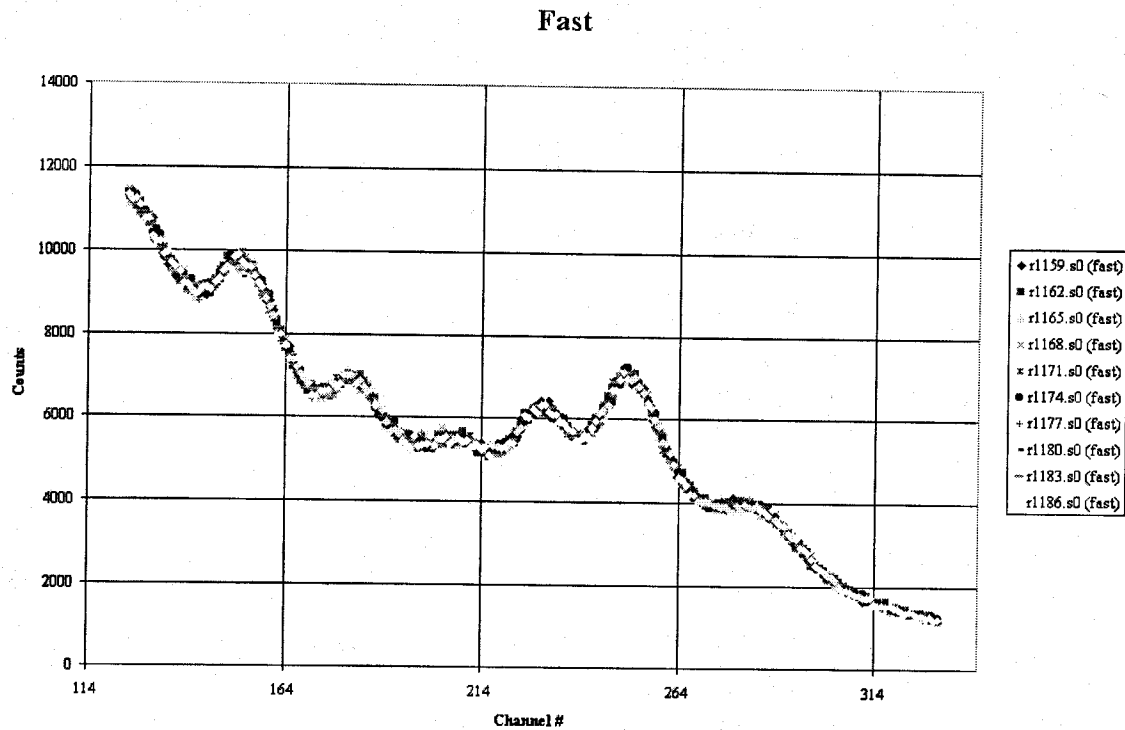


Figure 39. Ten measurements of a 105 mm shell with Wax.

The following figures contain spectra of selected measurements for shells with inert fills and for several shells that were used for the construction of PELAN library.

Figure 40 shows the three inert fillers (wax, plaster of Paris, and red wax) in a 60 mm. There seems to be no visible difference in the spectra.

Figure 41 shows the same inert fillers for an 81 mm shell and again, there is no visible differences in the spectra.

Figure 42 shows the wax-filled inert shells of various sizes. The H content of the 155mm and 105mm munitions is clearly above the smaller shells. This leads to a conclusion that we have surpassed a threshold with these larger shells.

Figure 43 shows the plaster-of-Paris-filled shells. There is a small variation in the H gamma ray but otherwise, there are no visible differences.

Figure 44 shows two 76mm shells on soil with RDX and TNT. There seems to be slightly more H in the RDX shell.

Figure 45 shows two 82mm TNT-filled shells on the soil. There are no visible differences.

Figure 46 shows two 90mm projectiles on soil with one filled with RDX and the other, Comp B. The Comp B has higher H, C, O, and N contents visible.

Figure 47 shows 2% fuel oil, 6% fuel oil, and 15% fuel oil mixtures of ANFO. The N peak, which is difficult to see in most spectra, is clearly illustrated in these spectra. Otherwise, there are no visible differences between the spectra.

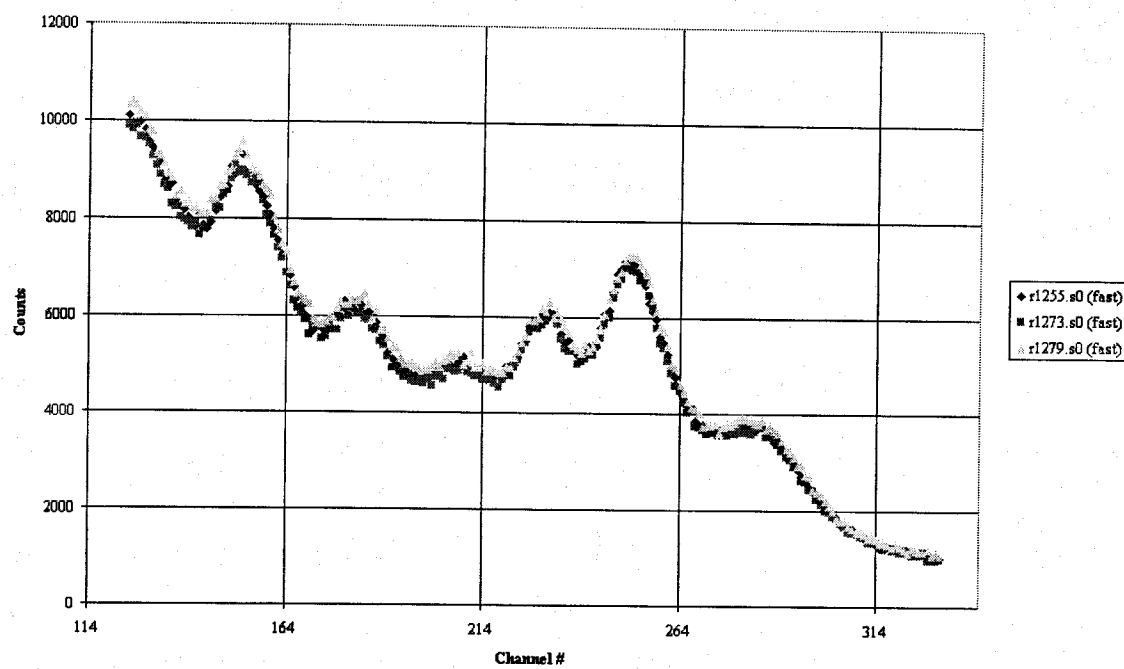
Figure 48 shows a comparison of the steel mine and the plastic anti-tank mine. The AT mine definitely shows a higher H content.

Figure 49 shows a comparison of a 90 mm filled with 60% TNT and 40% RDX and 120 mm rocket filled with CompB. The apparent higher O content in the 90 mm shell must be from environmental effects. The O count-rates in Table 16 are similar for both ordnance.

Figure 50 shows a 60mm TNT shell, an 81mm CompB shell, and a 155mm TNT shell. The differences in the spectra are mainly from the shielding effect discussed in the Background Stability section.

The next series of figures show an item placed on all five media. It is interesting to note that the H content for Figures 51-54 varies with the environment. It seems to have no relation to shell contents. One can rank the H content in the following manner with 1 being largest: 1) wet soil, 2) soil, 3) sand, 4) gravel, and 5) table. This, again, indicates that the signals of the contents of the shells "ride" upon a very high background. Thus the uncertainty in the measurement comes primarily from the environment.

Fast



Thermal

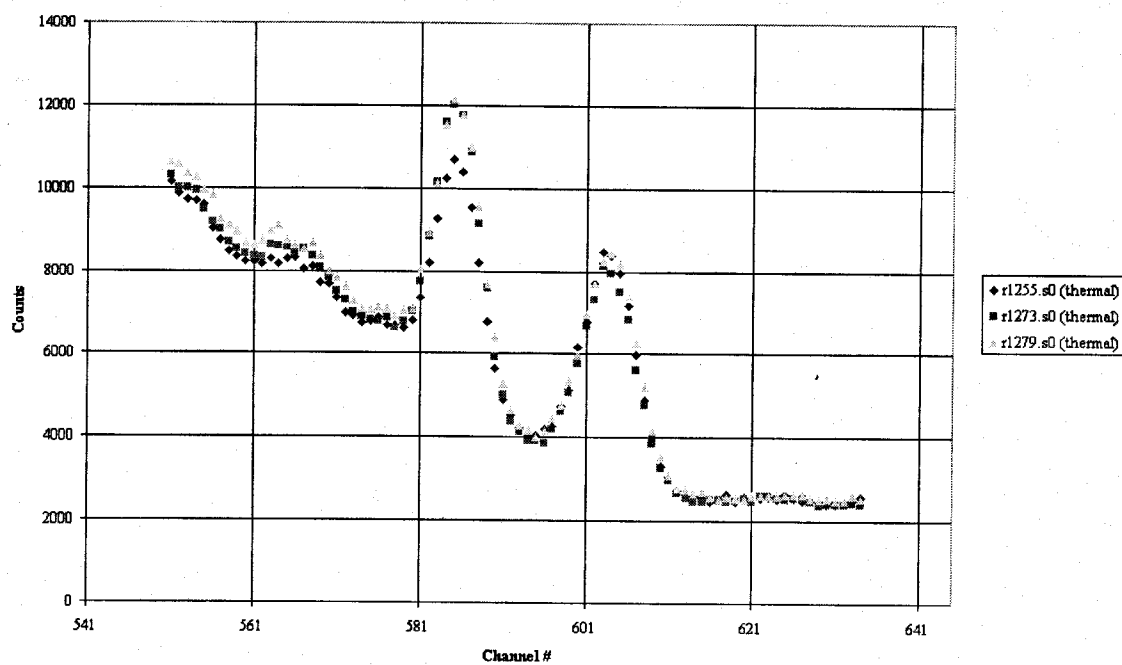


Figure 40. Spectra of a 60 mm shell filled with wax (R1255), plaster of Paris(R1273) and red wax (R1279).

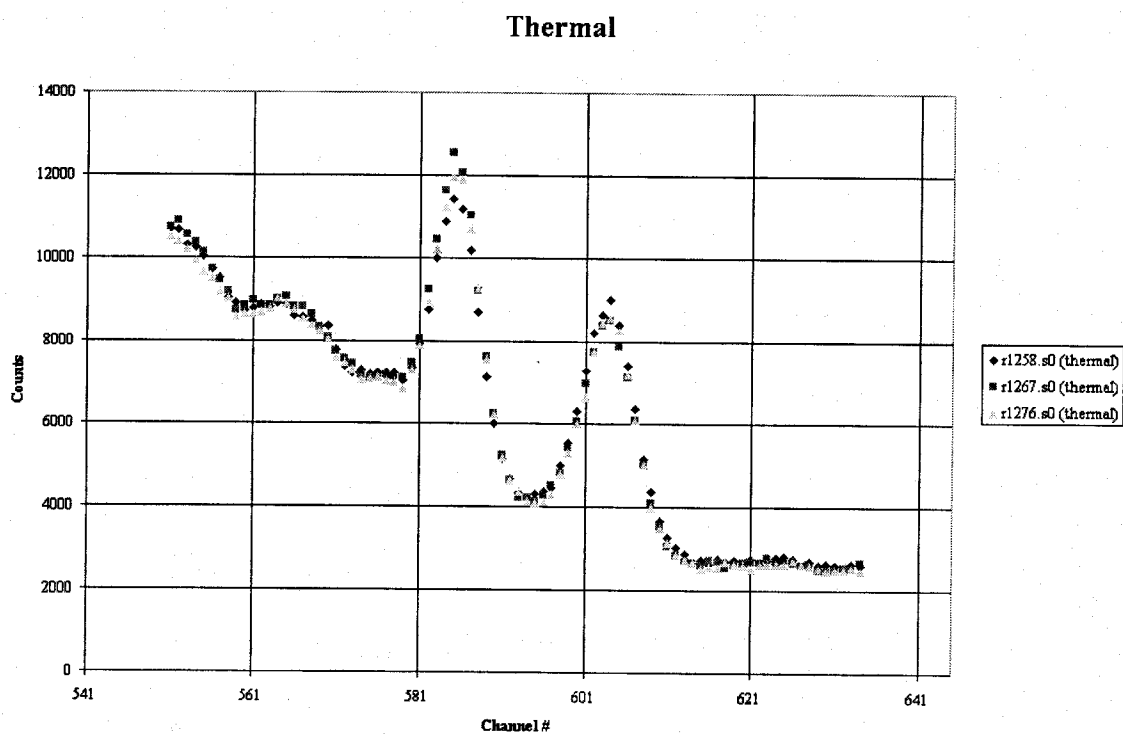
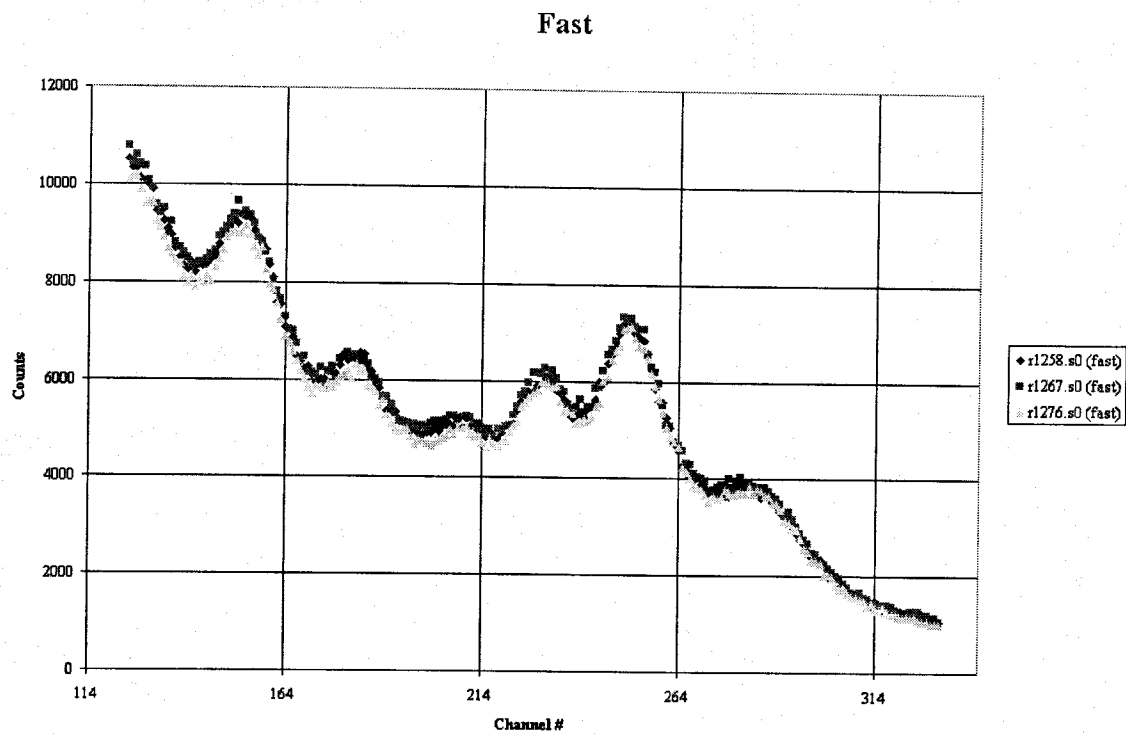
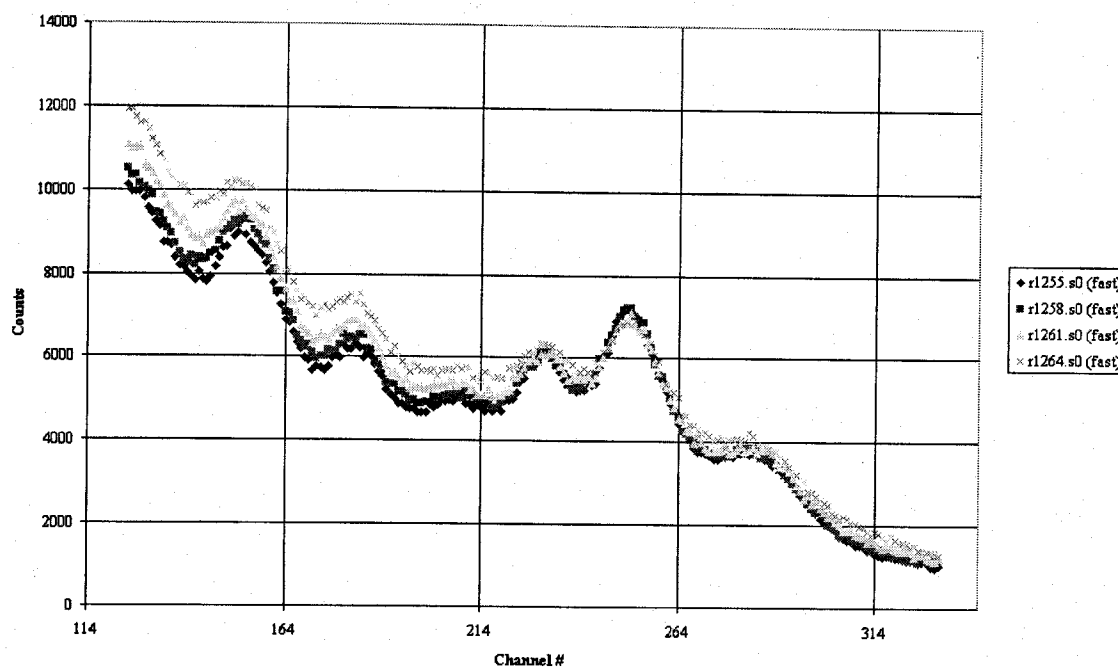


Figure 41. Spectra of a 81 mm shell filled with wax (R1258), sand(R1267) and plaster of Paris (R1276).

Fast



Thermal

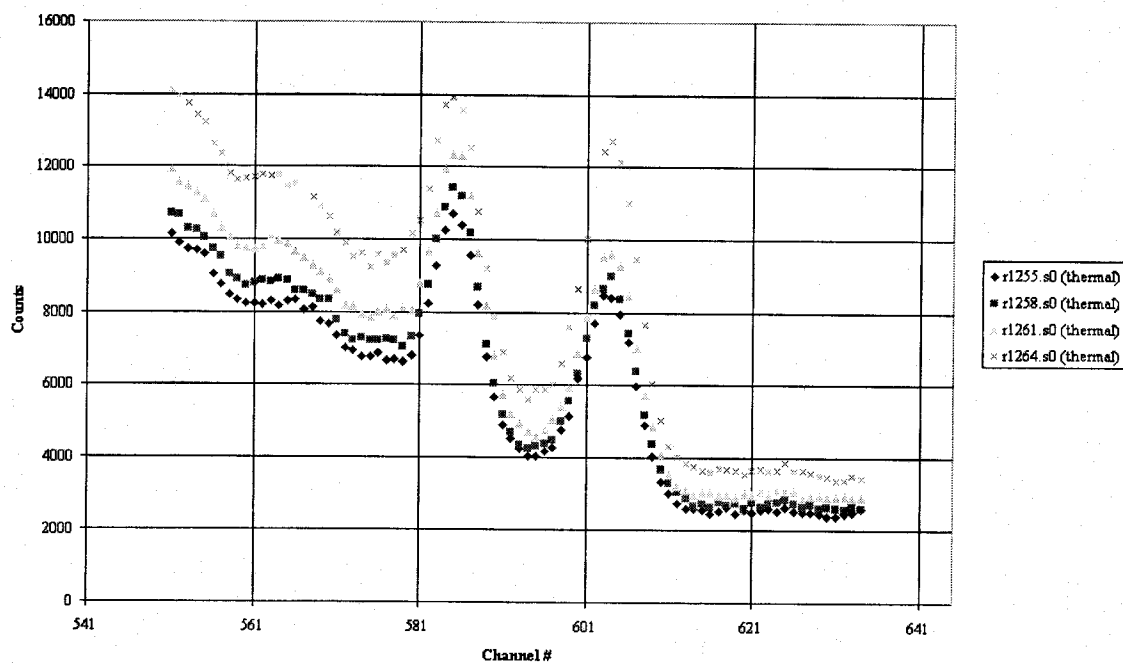


Figure 42. Spectra of a 60 mm shell (R1255), 81mm shell(R1258) 105mm shell(R1261) and 155mm shell (R1264) filled with wax .

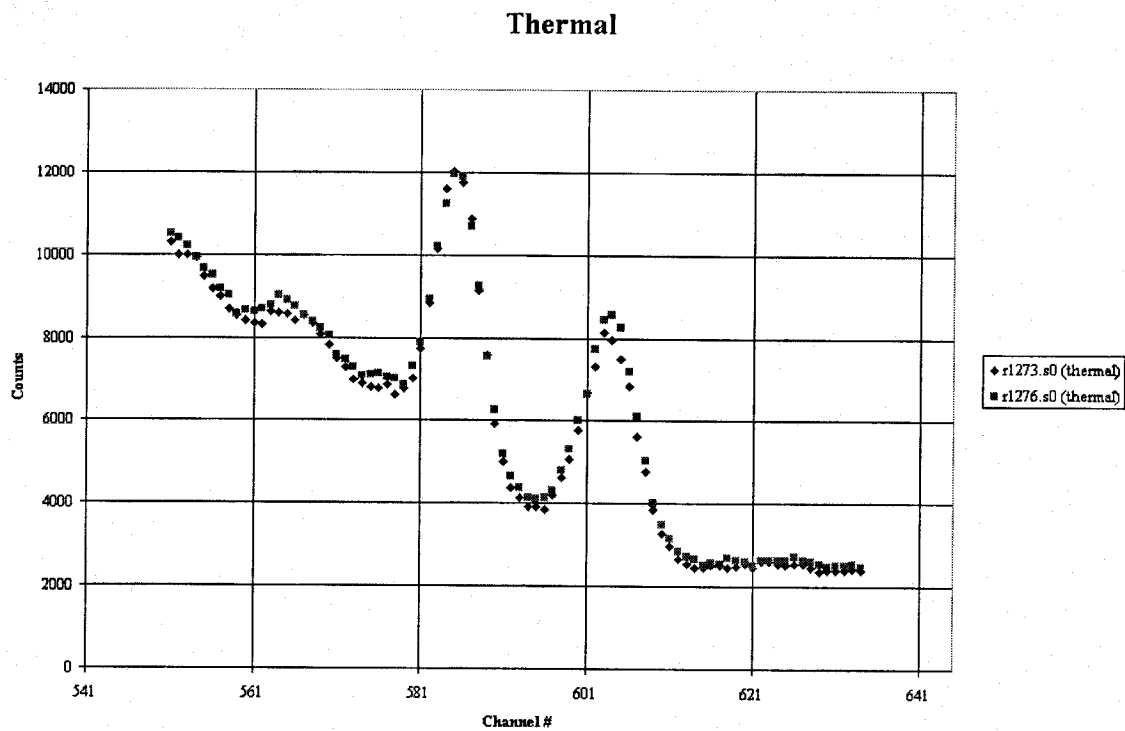
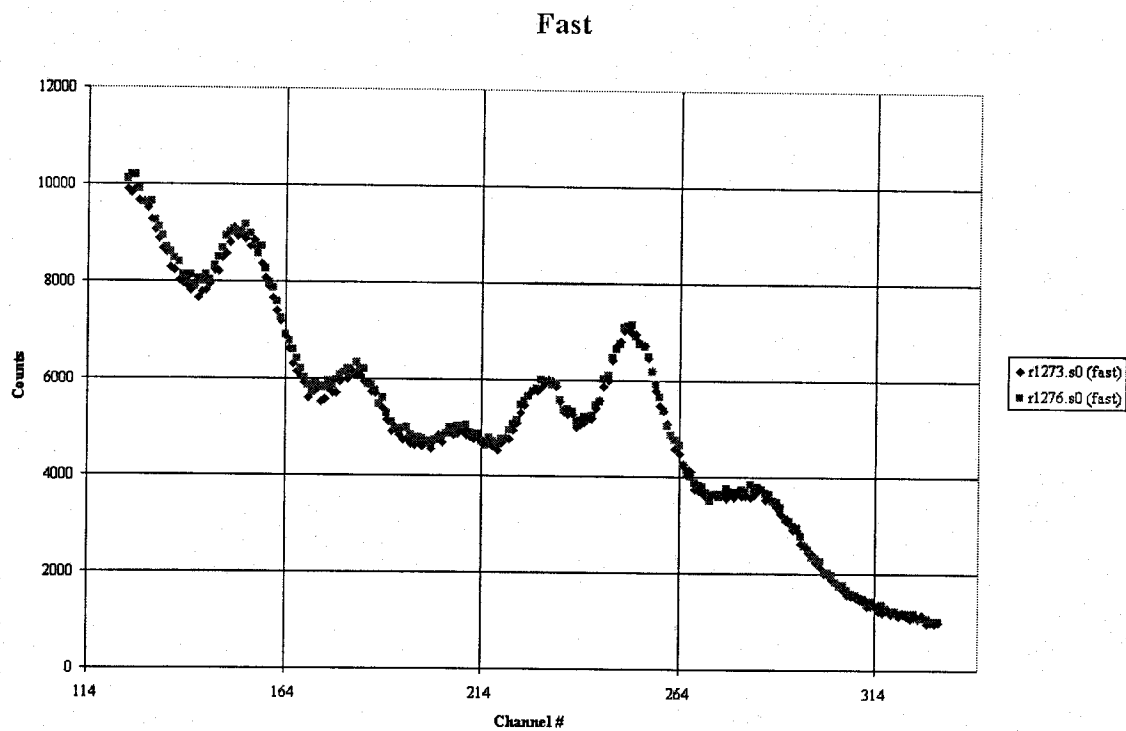
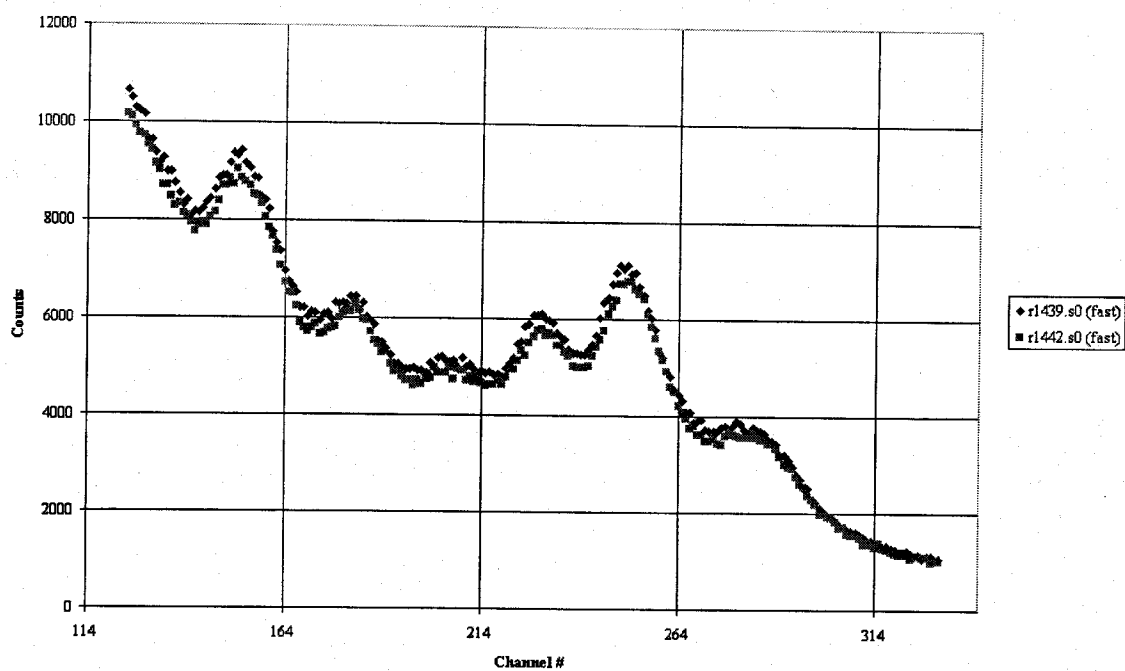


Figure 43. Spectra of a 60 mm shell (R1273) and 81 mm shell (R1276) with plaster of Paris.

Fast



Thermal

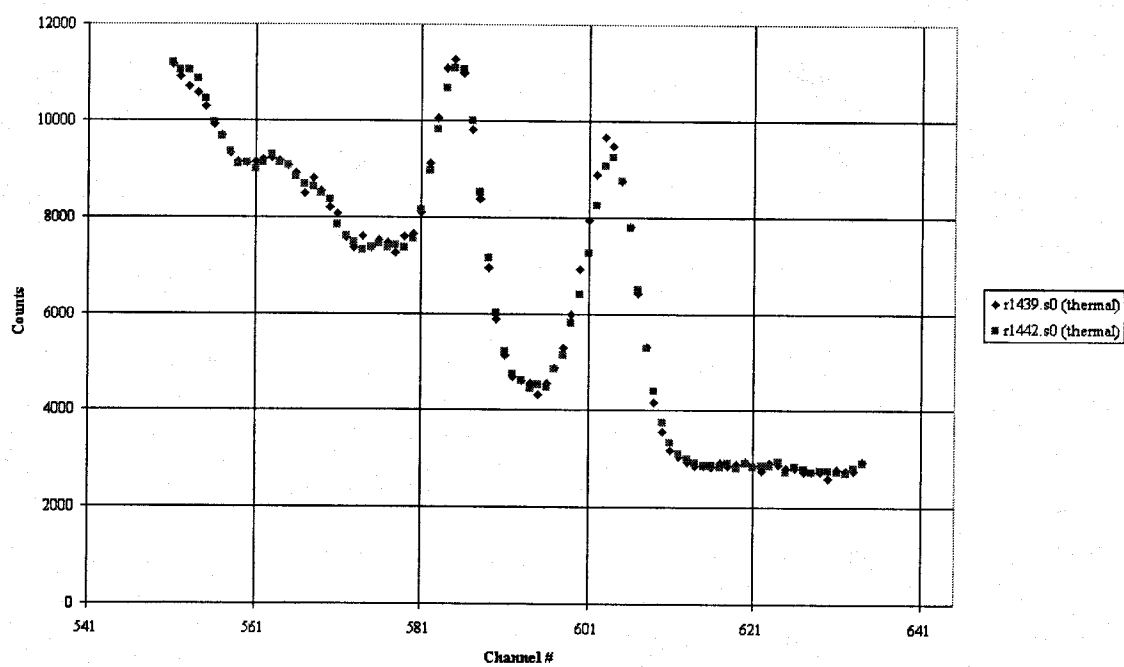


Figure 44. Spectra of a 76 mm shell filled with RDX (R1439) and TNT (R1442).

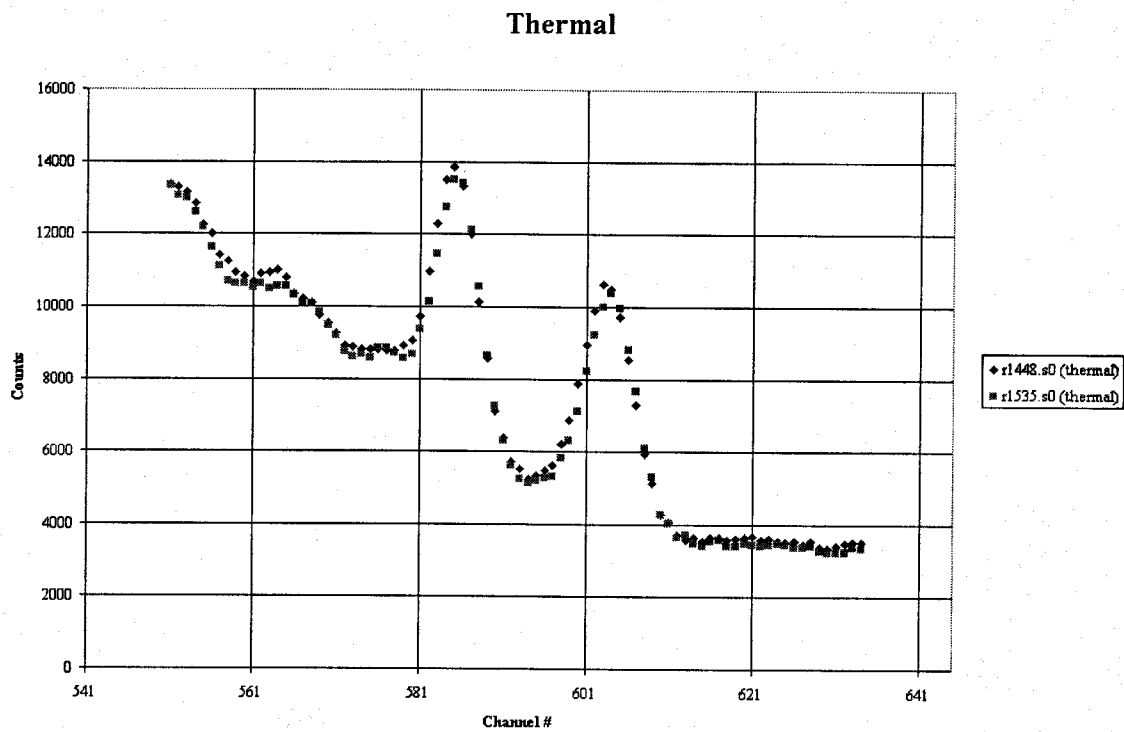
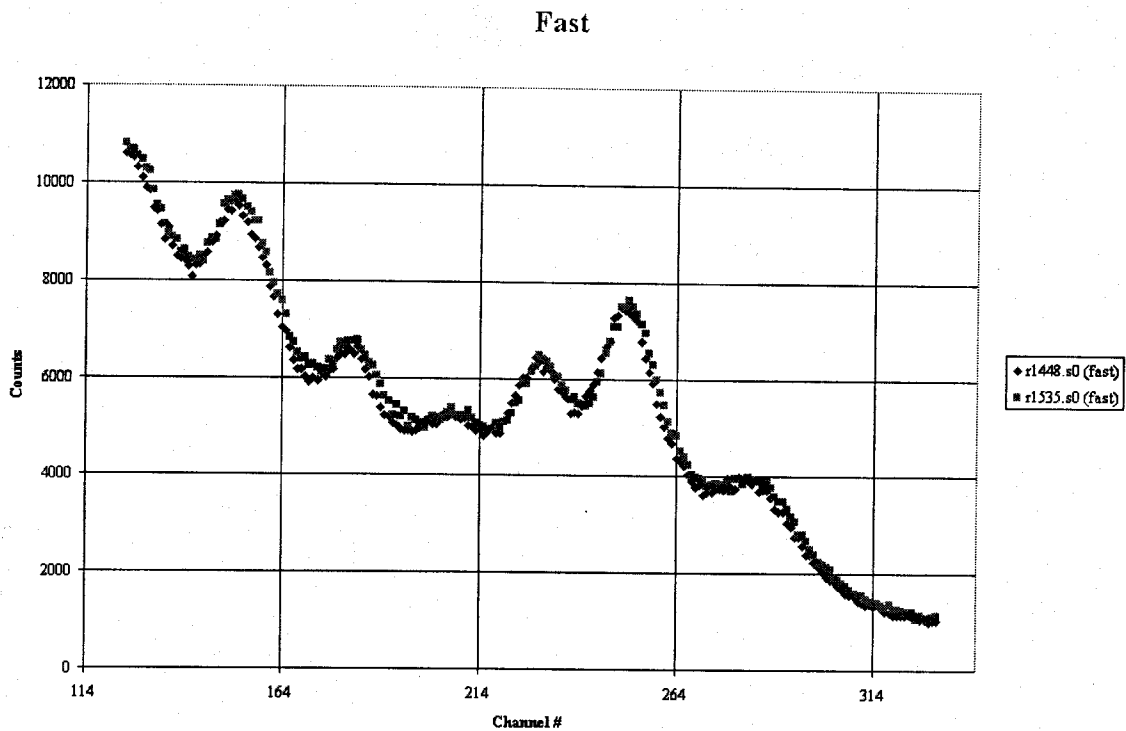


Figure 45. Spectra of a 82 mm shell filled with TNT(R1448, R1535).

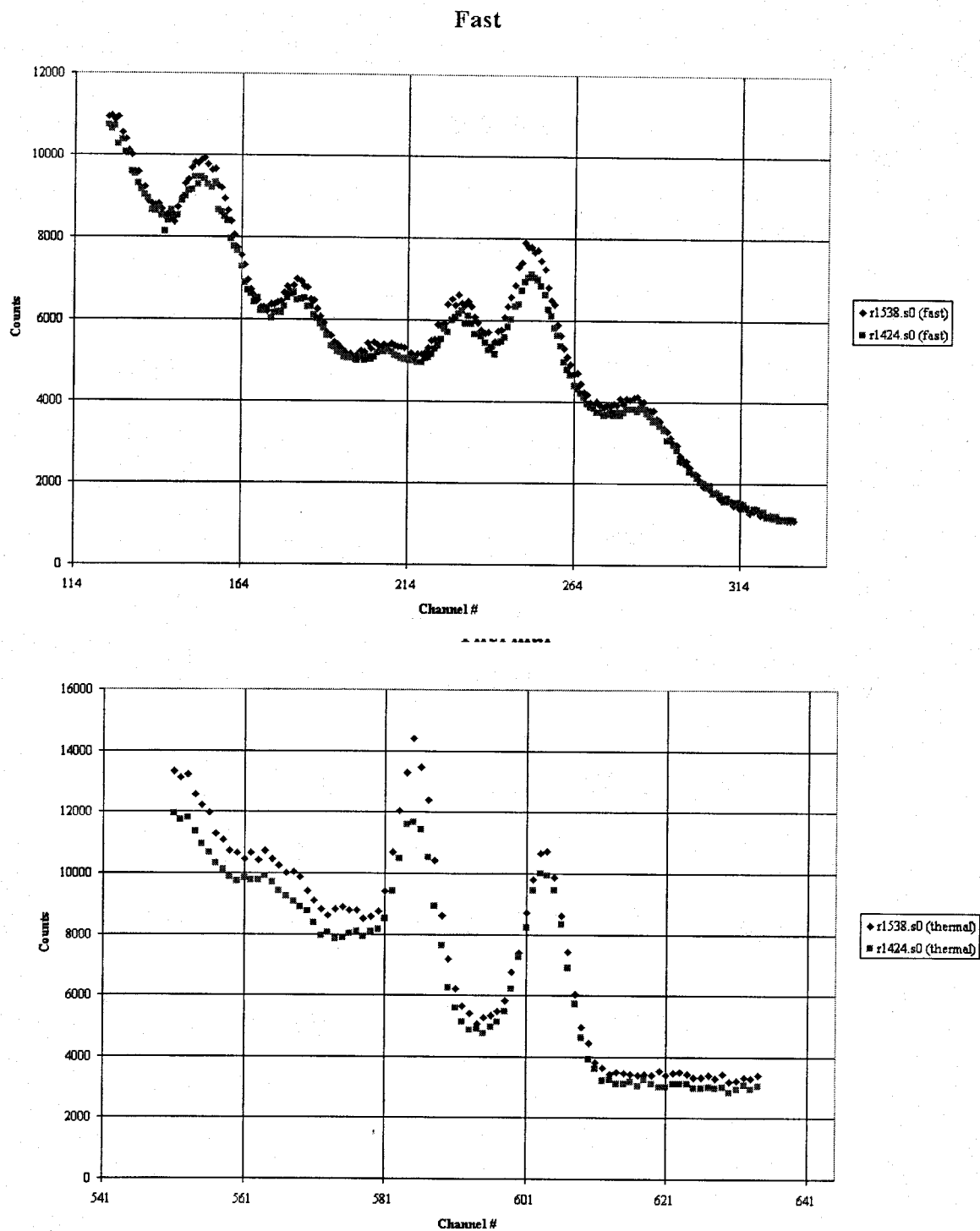
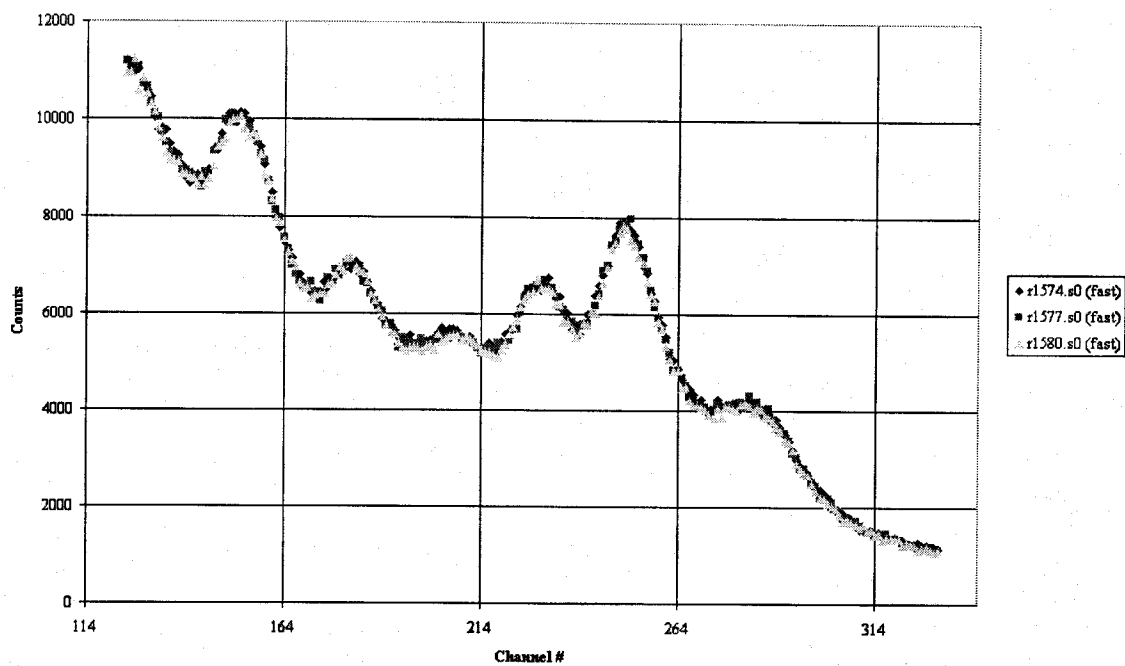


Figure 46. Spectra of a 90mm shell filled with RDX (R1424) and CompB (R1538).

Fast



Thermal

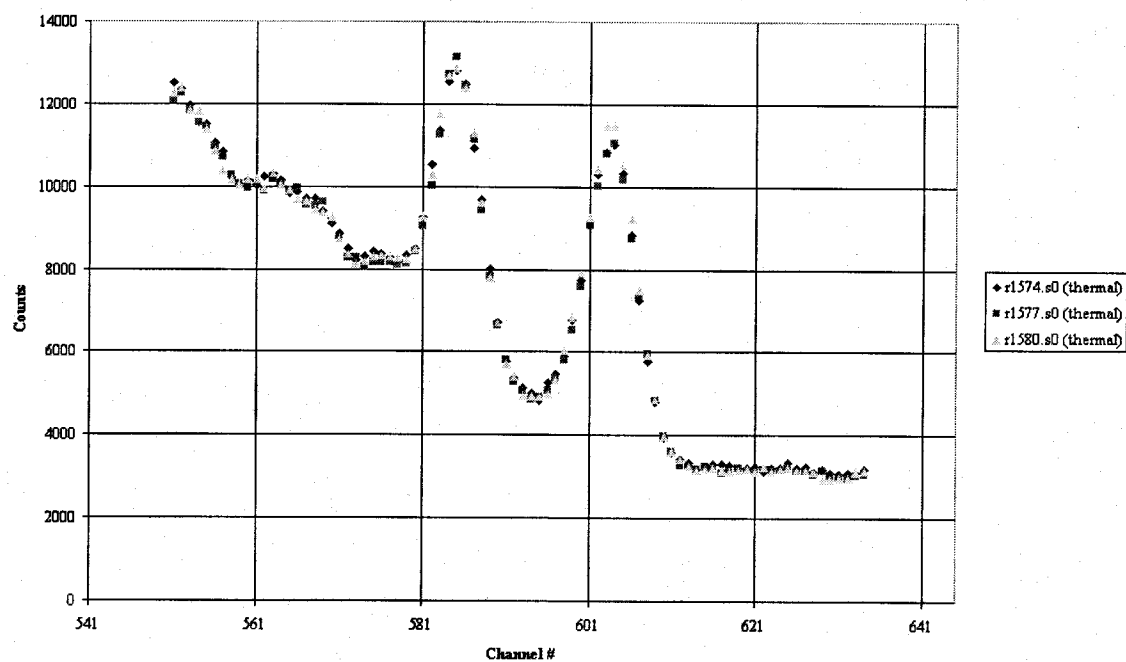
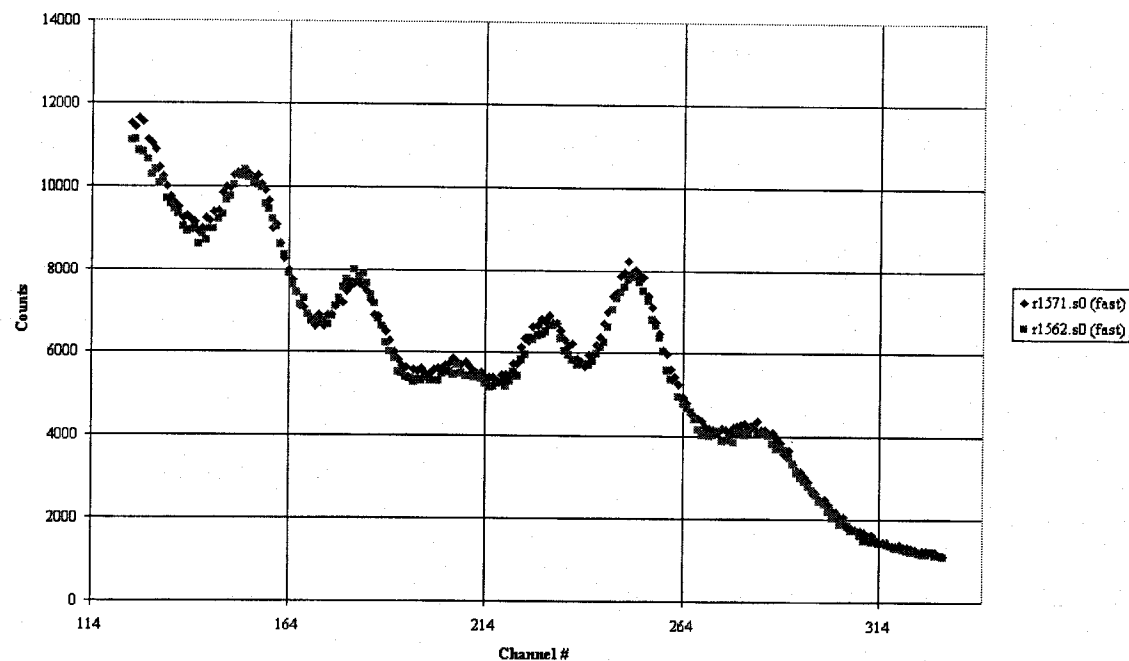


Figure 47. 2%, 6% and 15% ANFO on soil.

Fast



Thermal

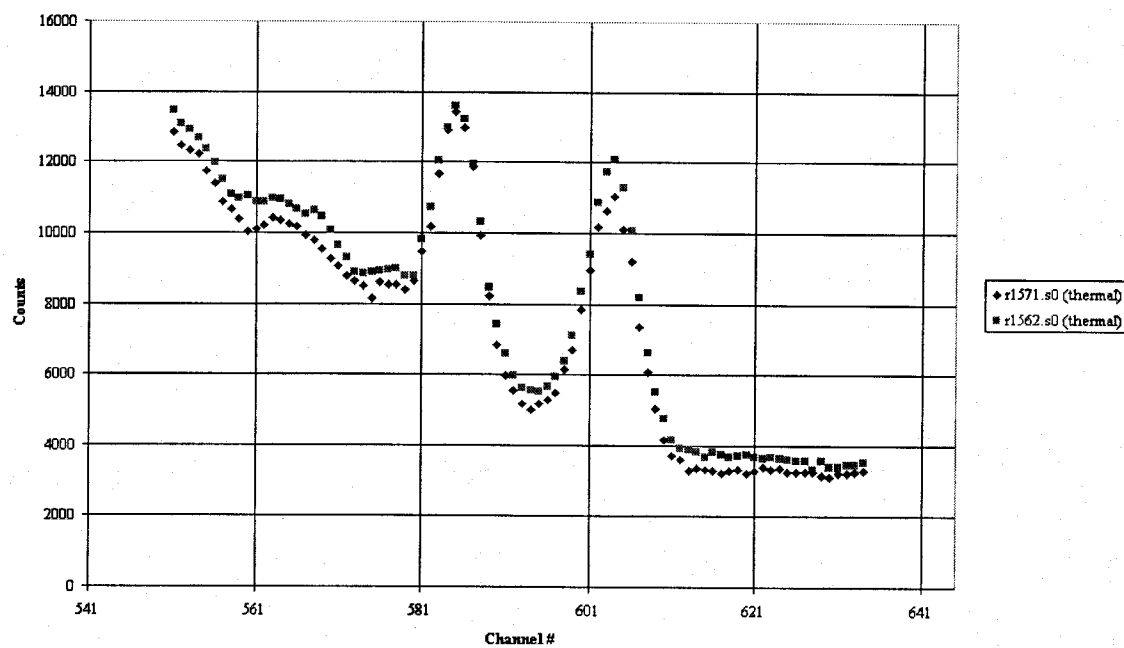
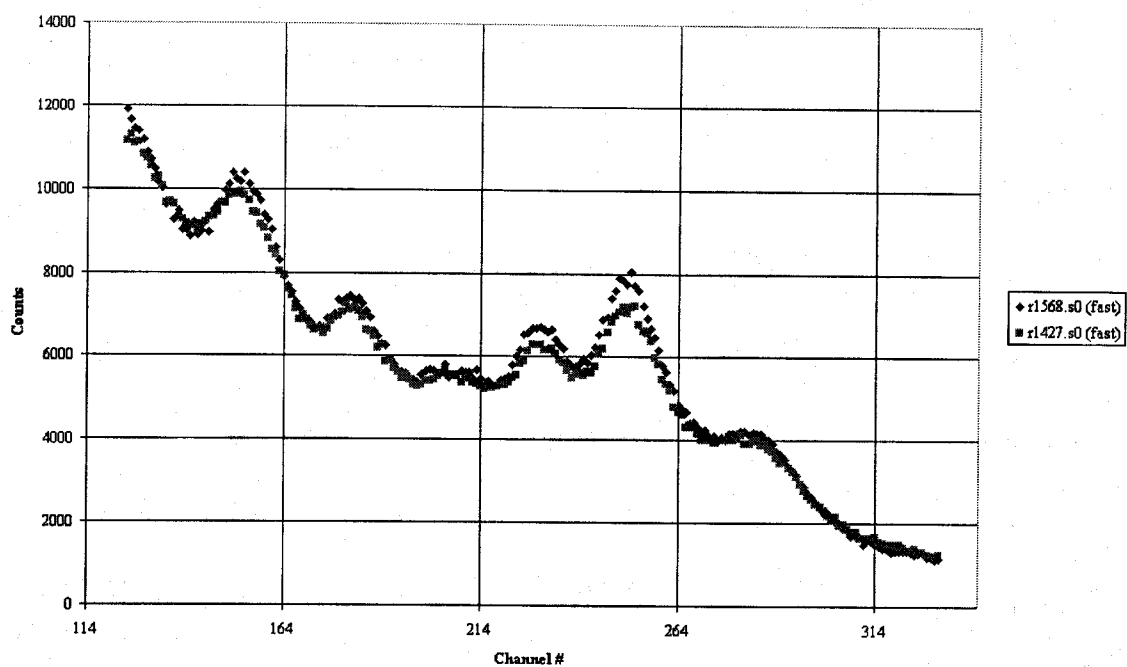


Figure 48. Spectra of a steel (R1571) and plastic (R1562) AT mines.

Fast



Thermal

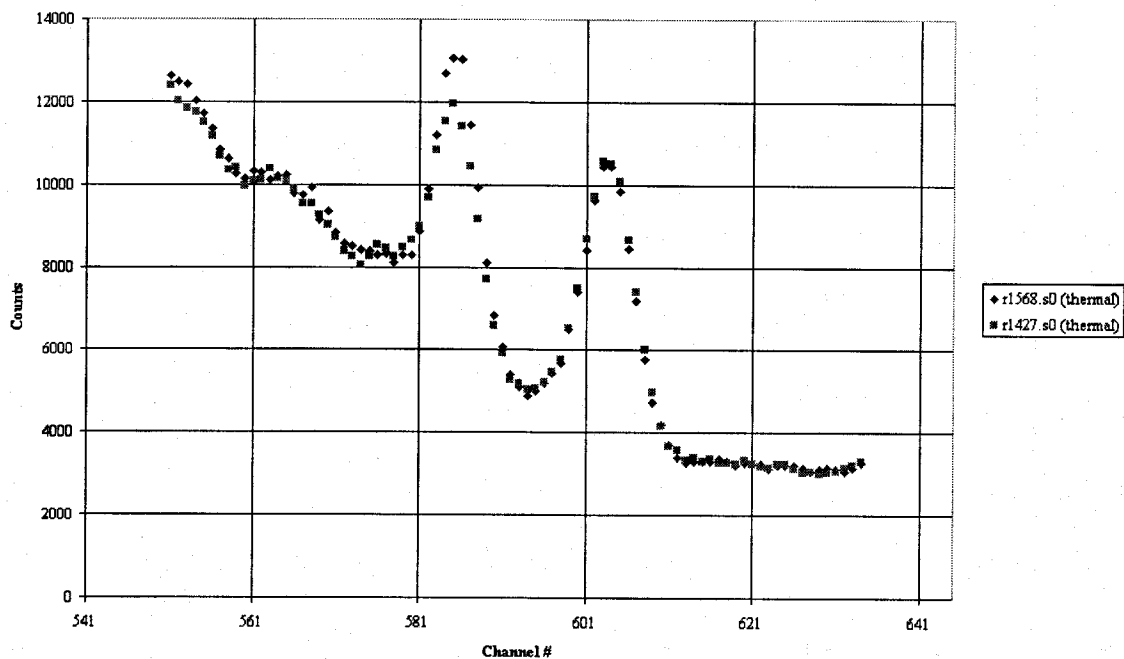
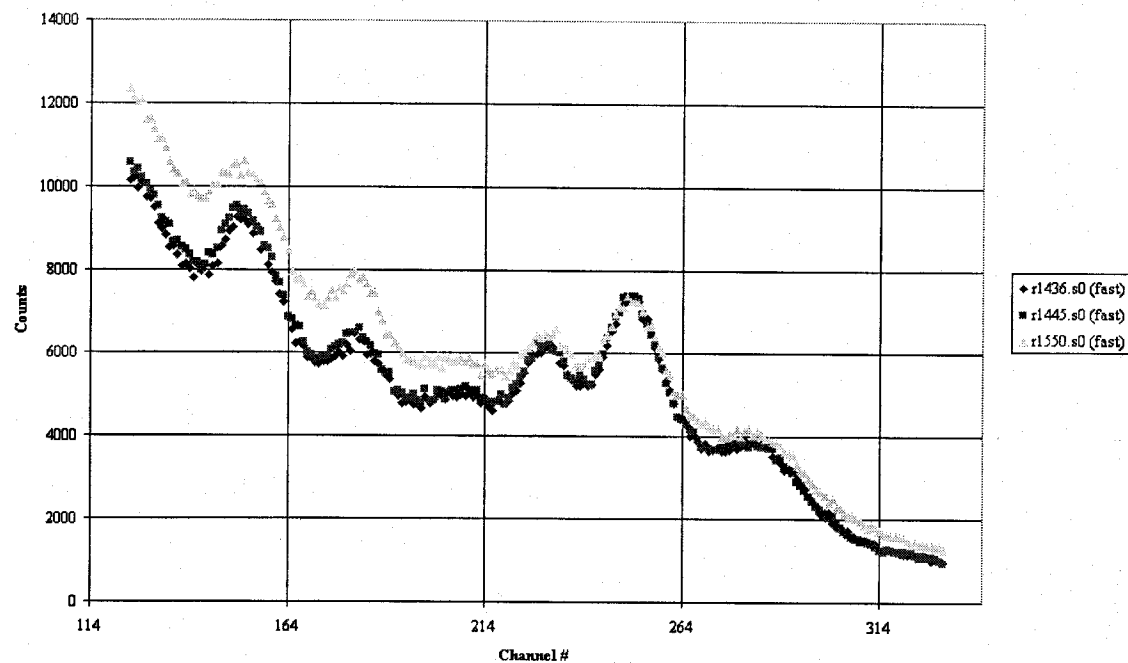


Figure 49. Spectra of a 90 mm (R1568) and a 122mm rocket (R1427).

Fast



Thermal

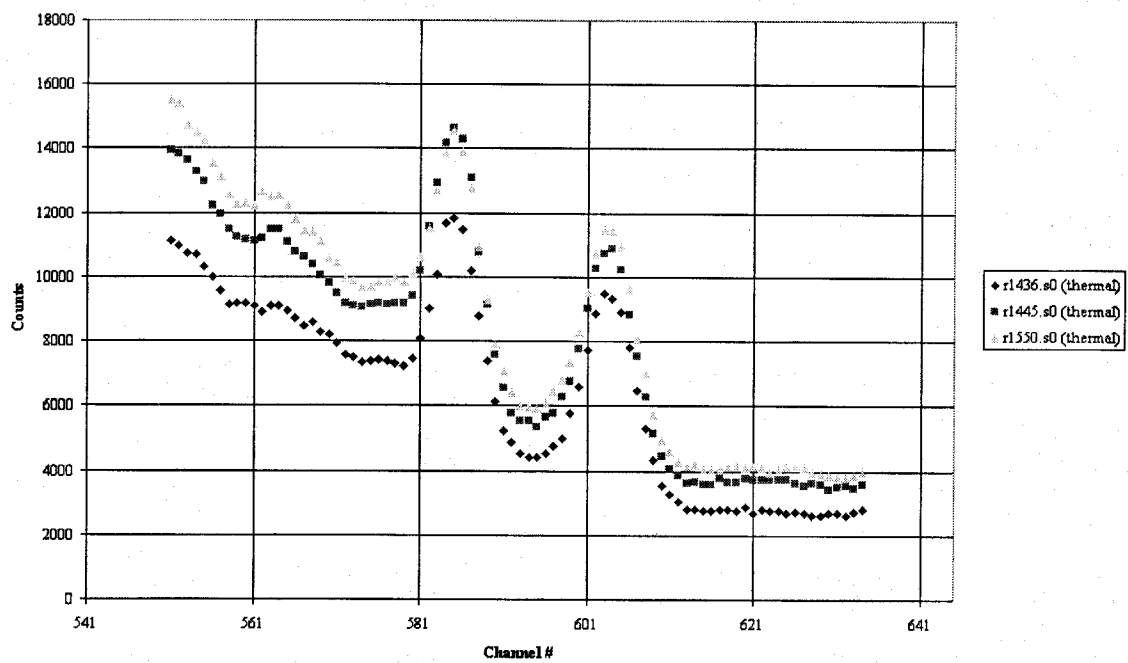
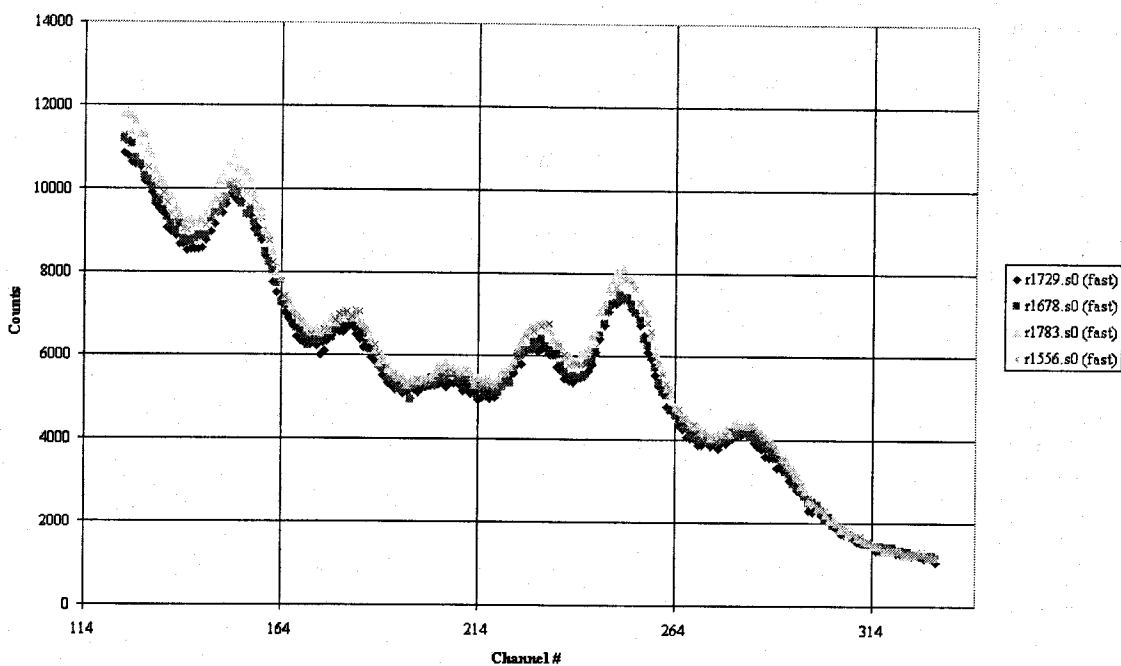


Figure 50. Spectra of 60 mm (R1436), 81mm (R1445), and 155mm (R1550) shells on soil.

Fast



Thermal

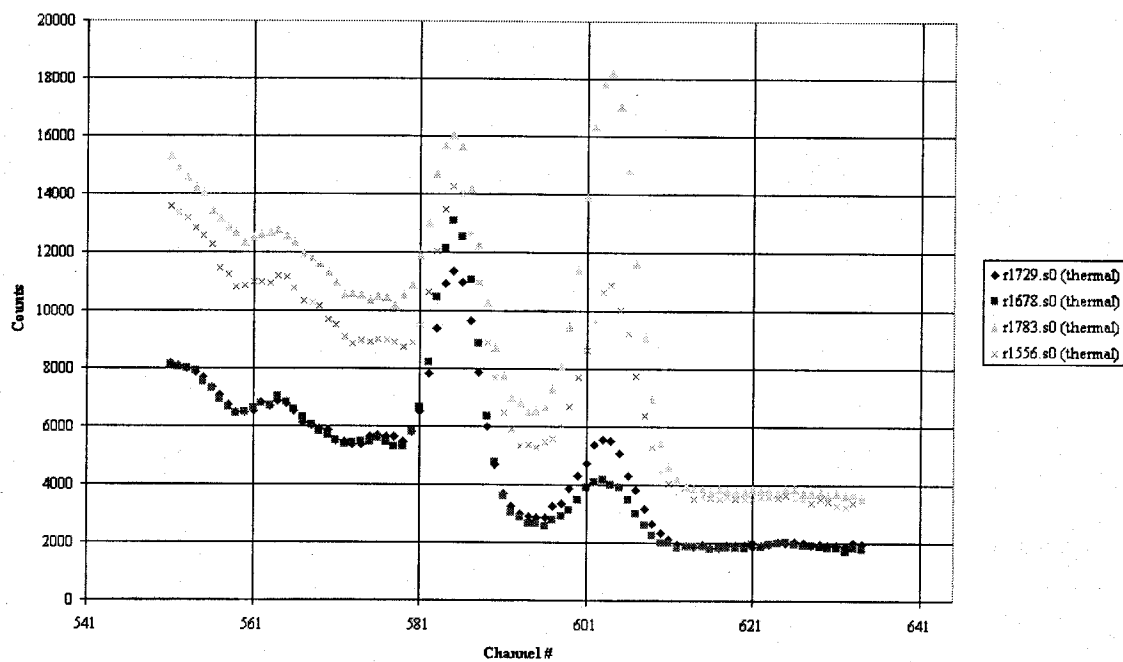
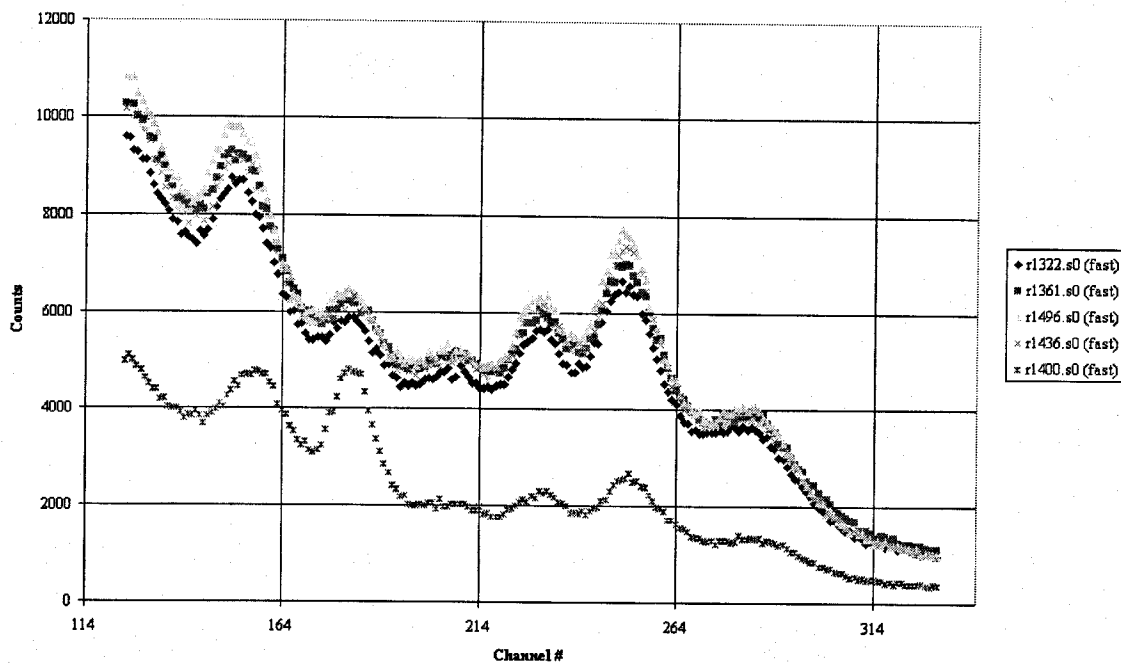


Figure 51. The Octol target on four media (R1729(sand) , R1676(gravel), R1783(wet soil), and R1556 (soil)).

Fast



Thermal

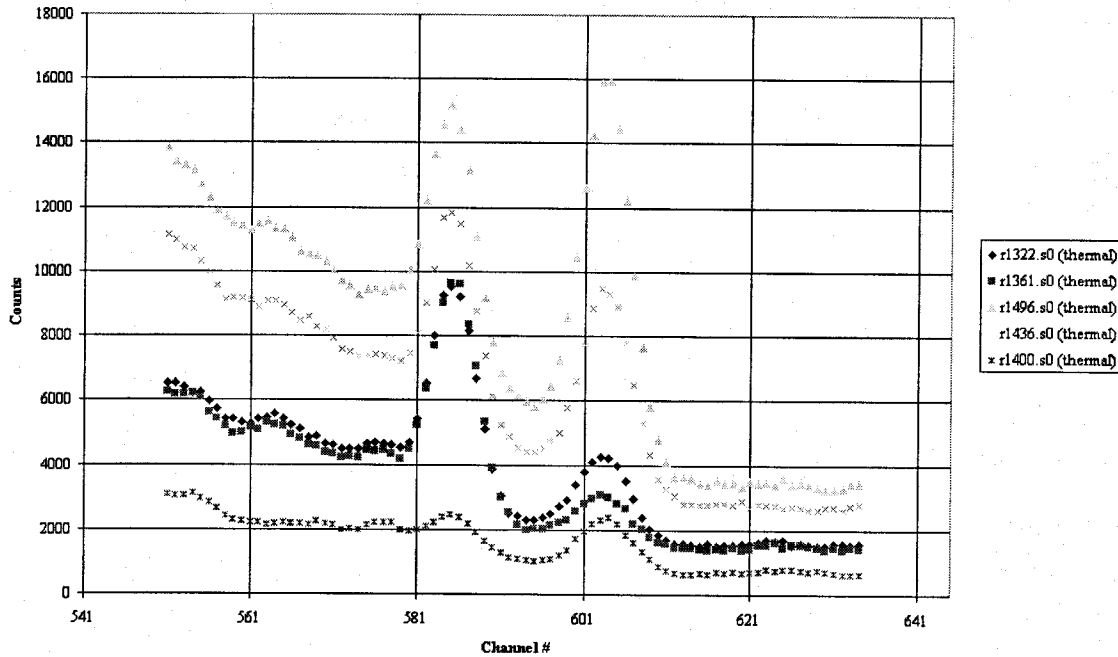
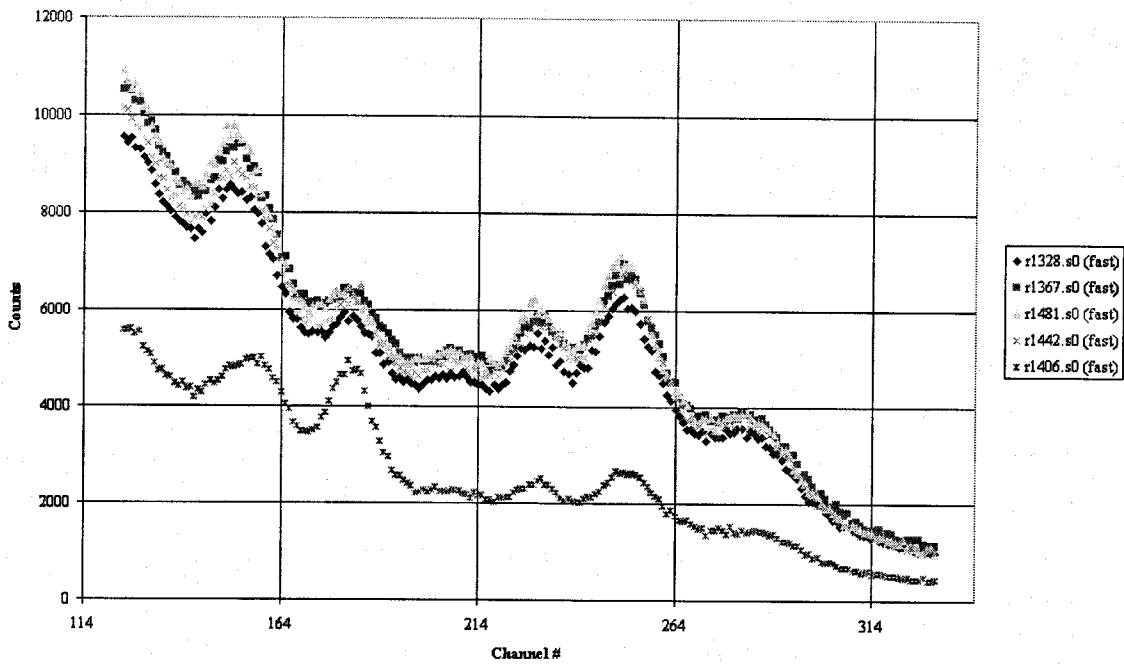


Figure 52. The 60 mm target on all media (R1322(sand), R1361(gravel), R1496(wetsoil), R1436(soil), and R1400 (table)).

Fast



Thermal

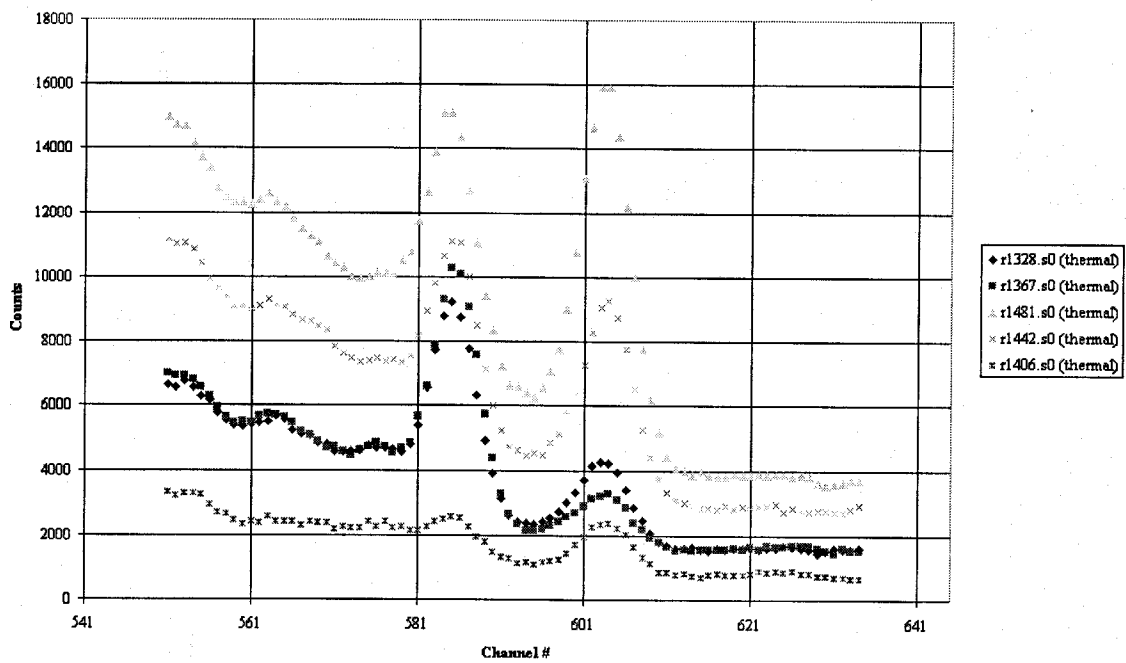
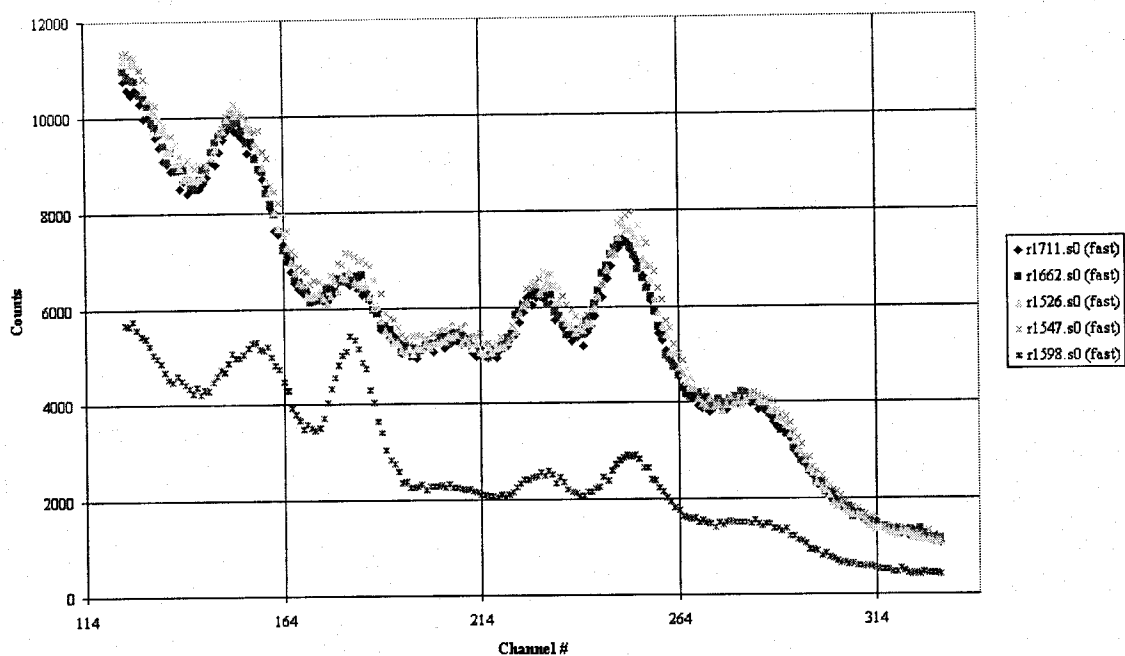


Figure 53. The 76 mm target on all media (R1328(sand), R1367(gravel), R1481(wet soil), R1442(soil), and R1406 (table)).

Fast



Thermal

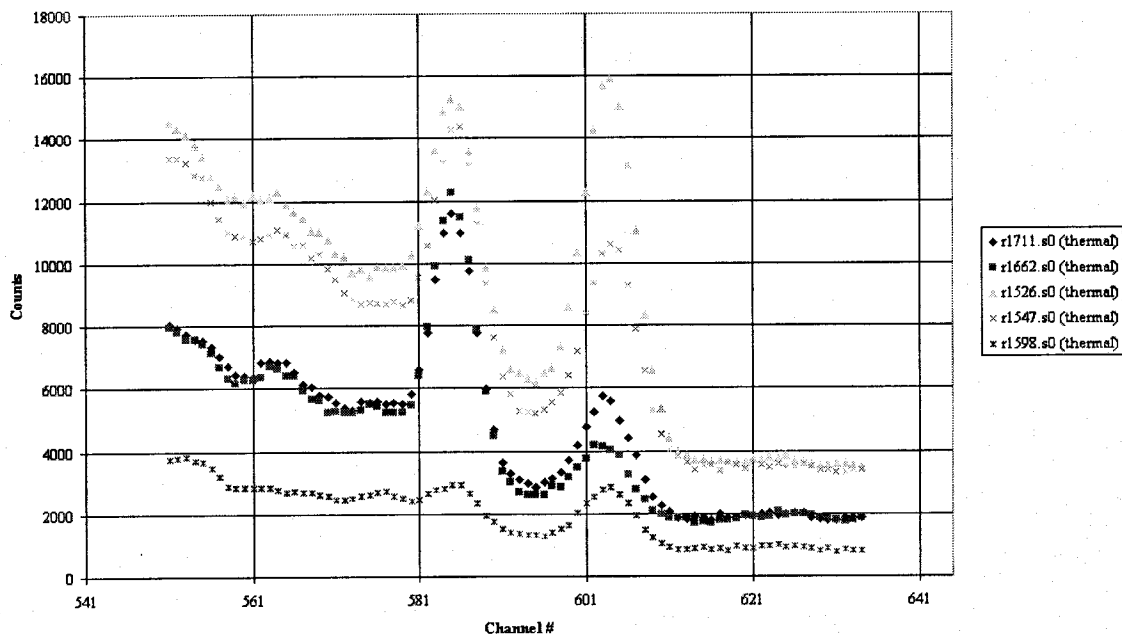


Figure 54. The smokeless powder target on all media (R1711(sand), R1662 (gravel), R1526 (wet soil), R1547(soil), and R1598(table)).

5.1.3 TEMPERATURE /HUMIDITY EFFECTS

When the PELAN's bismuth germanate (BGO) gamma-ray detector's temperature increases its light output decreases. In a practical sense, this decrease in light output effectively changes the gain of the amplification system. When the gain of the amplifier is changed, the energy calibration of the spectrum is also changed.

This is shown in Figure 55A, wherein the position of a particular gamma-ray from a radioactive source was tracked while the BGO is heated and cooled. The position of the gamma ray changes roughly 1.5% for every degree Celsius. This process is reversible i.e. cooling or heating the detector to its original temperature will return the peaks to their original position. A common method to compensate for this temperature-dependency is to utilize refrigerators to maintain a constant temperature on the crystal. For a portable system, this solution is not an option due to the increased bulk and weight.

The PELAN contains a small radioactive ^{137}Cs (0.2 uCi, an exempt quantity). When the "Start" or "Background" button is pushed, the PELAN first acquires a spectrum of this source before the neutron generator is started. It estimates the peak position and compares to a value kept in the "PELAN.ini" file. It calculates the relative movement of the peak and adjusts the amplifier to correct peak drift.

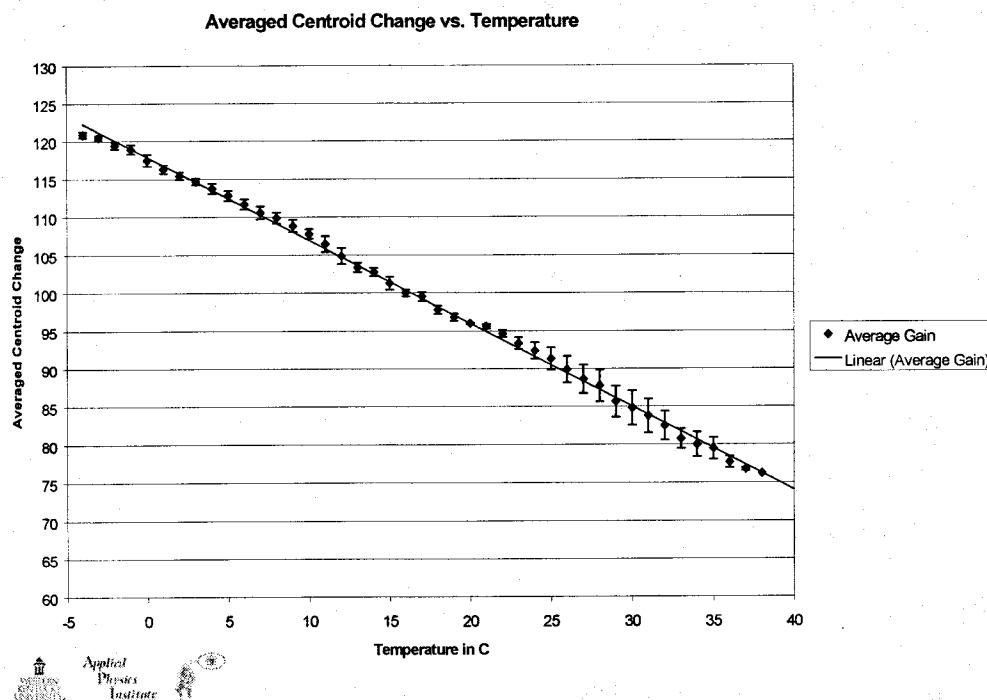


Figure 55A. Variation of gamma peak position as function of temperature for a BGO detector.

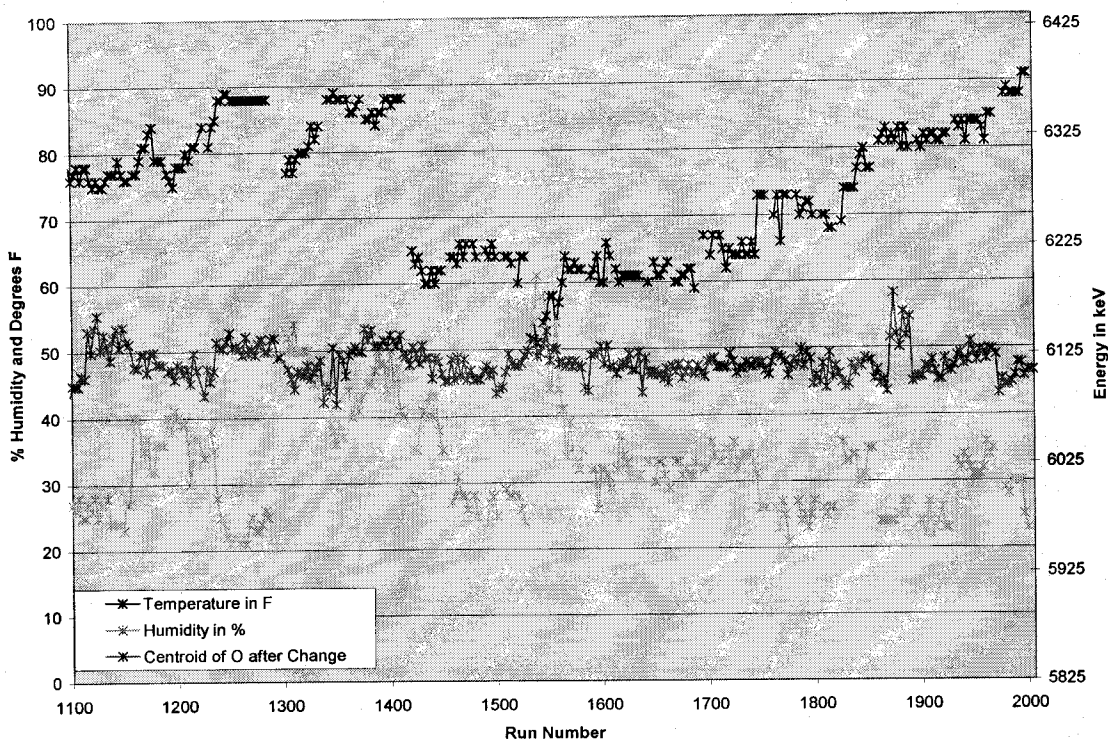


Figure 55B. Graphs of temperature, relative humidity, and change in energy position of the O gamma ray during the demonstration. Note: the left axis is both relativity humidity in % (lowermost plot) and degrees Farhenheit (uppermost plot).

The fact that the light output changes does not change the efficiency of the detector. It will, however, broaden peaks but the amount of broadening is small compared to the resolution of the detector.

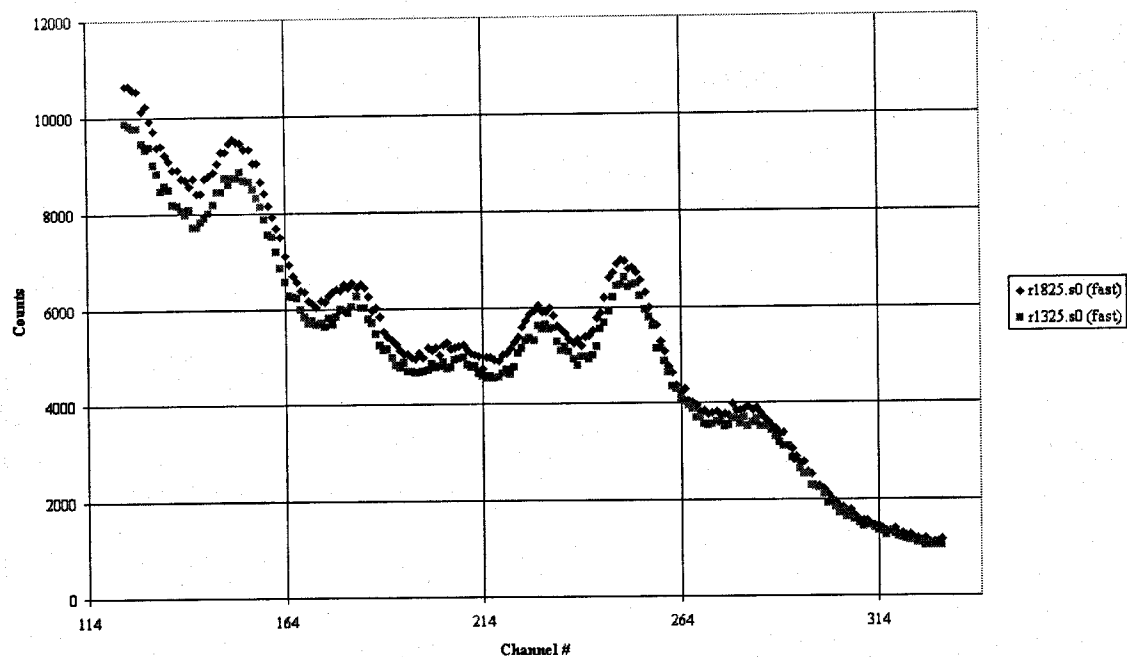
Figure 55B shows temperature readings ($^{\circ}\text{F}$) (uppermost curve) and relative humidity (%) during the demonstration. During the tests, the ambient temperature varied from 53°F to 93°F . Relative humidity varied between 22% to 63%. The energy of O gamma ray is also plotted on this graph. Without any correction, the energy should vary approximately 30% or nearly 2000 keV. As one can see, the variations in this energy are less than 1%! Thus, the automatic gain correction system seems to be working extremely well.

In Figures 56-58 are spectra taken at various temperatures and humidity. Figure 57 is most interesting because of the temperature extremes (nearly 15°C) and the change in humidity (nearly a factor of 3). In Figure 57, we see no apparent differences.

Figure 56 does show differences but we believe these to be from the environment. The signatures are consistent with an excess of water (high H and O contents) in one of the spectra. It cannot be from humidity seen the lower humidity spectrum is the one with the higher H and O contents. Figure 58 shows the same behavior.

Also note that in these three spectra, the peak width is constant at a given energy (see Figure 57 for best examples). These spectra have been corrected by the above-described process but there is no visible change in resolution.

Fast



Thermal

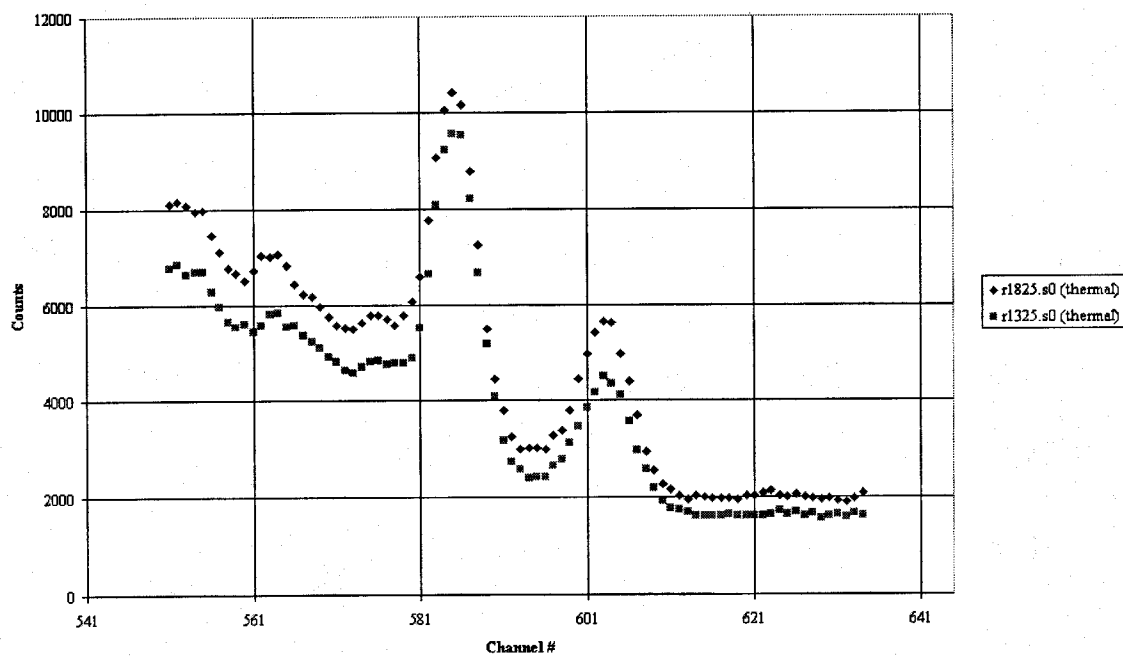
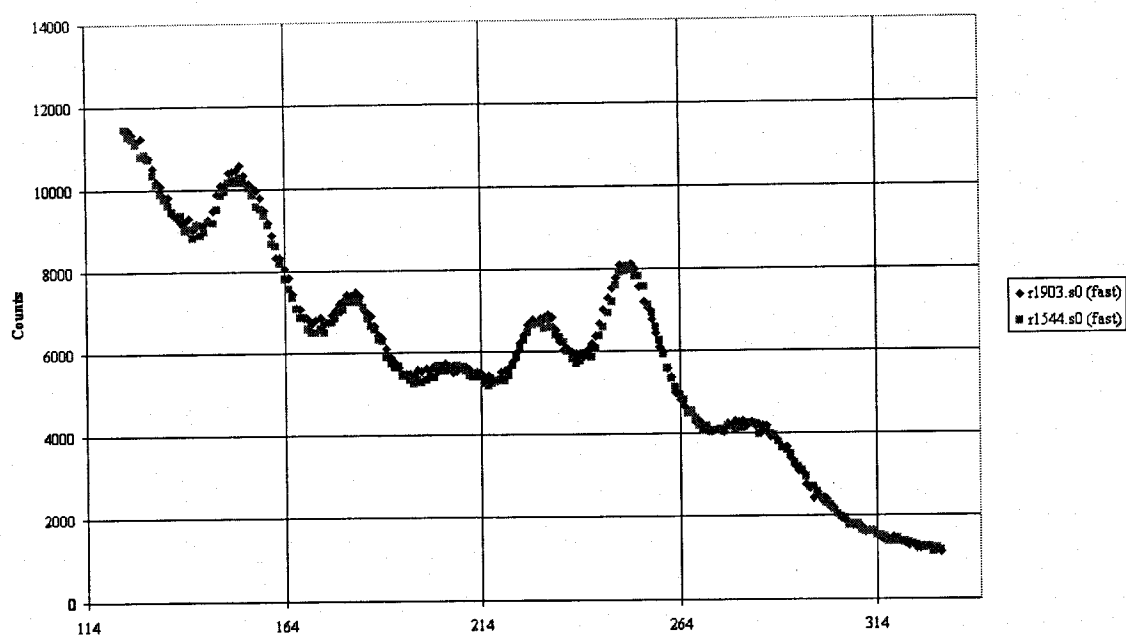


Figure 56. 76 mm shell with RDX, on sand at 69⁰ F, 36% humidity (R1825), and 81⁰ F, 48% humidity (R1325)

Fast



Thermal

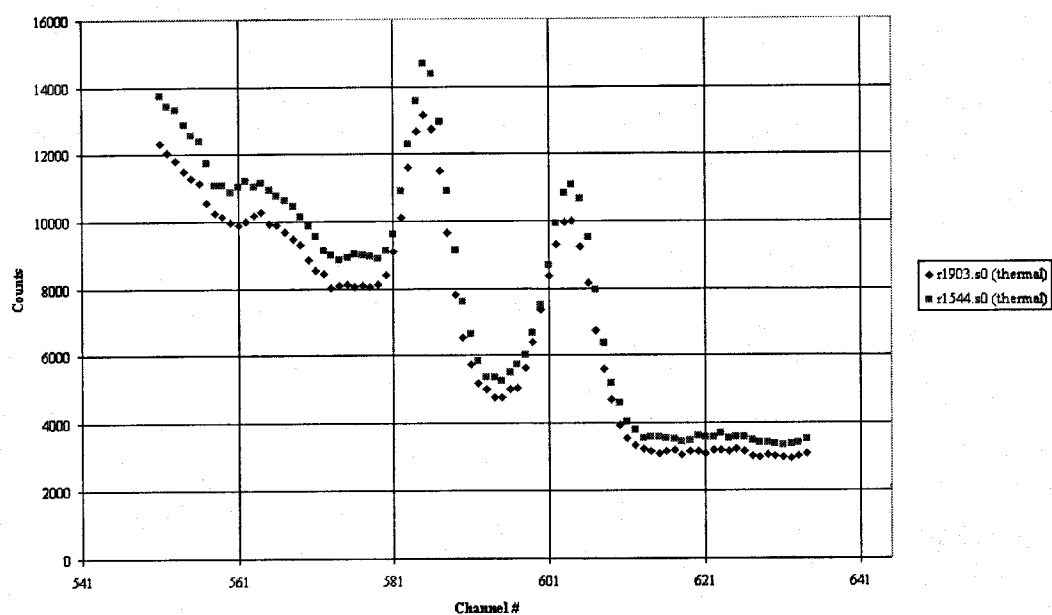
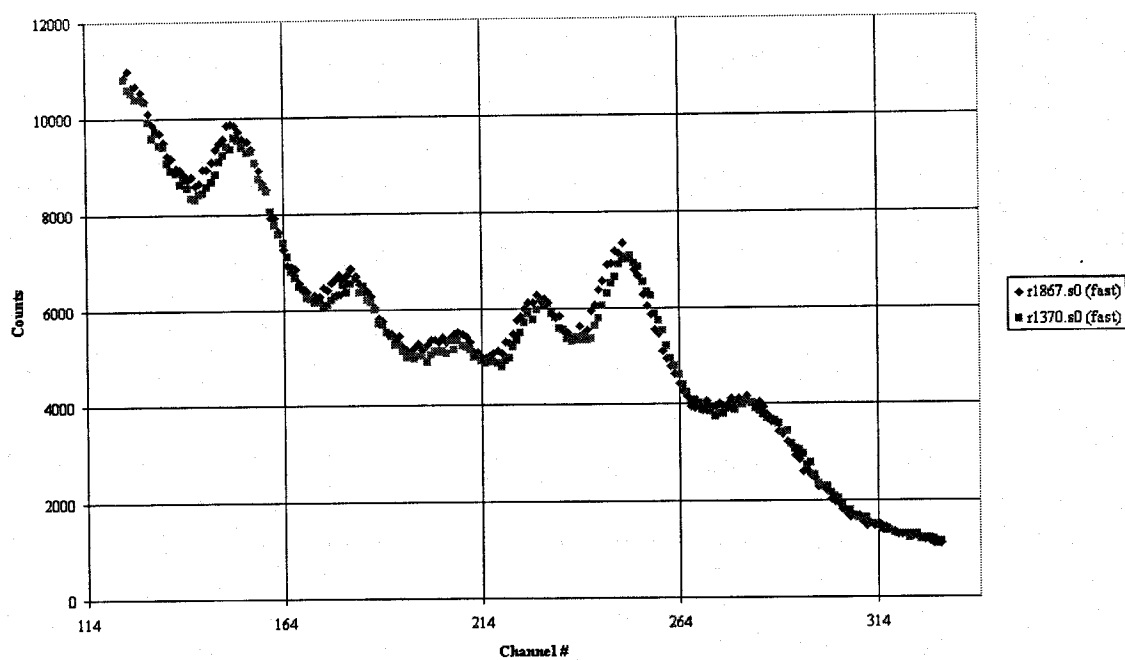


Figure 57. SEMTEX on soil at 82° F, 22% humidity (R1903), and 54° F, 58% humidity (R1544).

Fast



Thermal

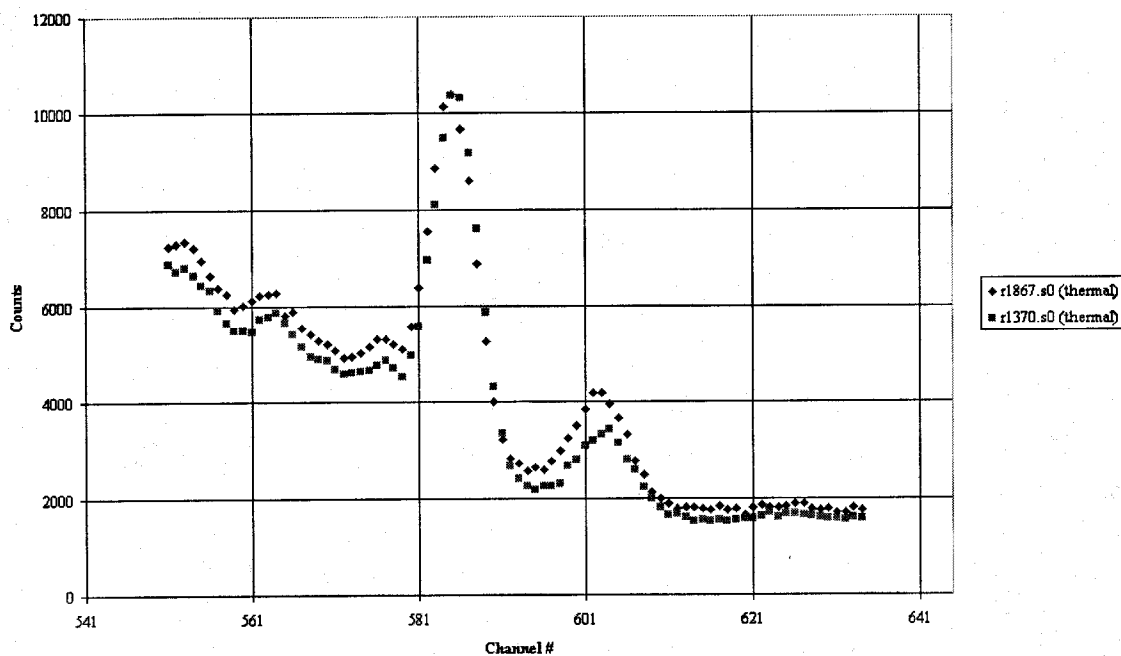


Figure 58. 81 mm on gravel at 83⁰ F, 24% humidity (R1867) and 87⁰F, 41% humidity (R1370).

5.1.4 LINEAR INDEPENDENCE OF SPECTRA

The scalar product (sometimes called “inner” or “dot” product) of two vectors is an excellent way to test the orthogonality or linear independence of two quantities. Recall

$\vec{a} \cdot \vec{b} = \|\vec{a}\| \|\vec{b}\| \cos \theta$ where $\|\vec{a}\|$ is the length of \vec{a} and $\|\vec{b}\|$ is the length of \vec{b} . Since

$\vec{a} \cdot \vec{b} = a_1 b_1 + a_2 b_2 + \dots + a_n b_n$, we can find the normalized scalar product of two spectra using the following equation:

$$\cos \theta = \frac{\sum_{i=1}^N a_i * b_i}{\left(\sum_{j=1}^N a_j^2 \right) \left(\sum_{j=1}^N b_j^2 \right)}$$

and if $\cos \theta = 0$, then the measurements are independent parameters. If $\cos \theta = 1$, then the samples are very similar and the performance will not change very much from sample to sample.

In Table 13, we show the scalar products (calculated over the fitting region of the fast spectrum i.e. channels 50 to 500) of various backgrounds taken at Indian Head, MD, as calculated from the above formula. The scalar products are nearly unity and thus implies that the backgrounds are again dominant and to a first approximation, nearly the same. This is in excellent agreement with the conclusions of the “Background Stability” section of this report.

Table 13. The scalar products of various spectra. See text for details

Surface	Shell (mm)	Run	b1020	b1022	b1038	b1008	b1080	b1064
Sand	155	b1020	1	0.9995	0.9997	0.9986	0.9988	0.9943
Sand	105	b1022	0.9995	1	0.9997	0.9990	0.9986	0.9916
Gravel	105	b1038	0.9997	0.9997	1	0.9990	0.9986	0.9924
Soil	105	b1008	0.9986	0.9990	0.9990	1	0.9994	0.9915
Wet Soil	105	b1080	0.9988	0.9986	0.9986	0.9994	1	0.9933
Table	105	b1064	0.9943	0.9916	0.9924	0.9915	0.9933	1

Recall Equation (1) from the “Methodology” section, The sample spectrum, S , can be represented by the equation:

$$S_i = k * B_i + \sum_{j=1}^n c_j * E_{i,j} \quad (1)$$

where B_i is the background spectrum at the i th channel and k is its coefficient, $E_{i,j}$ is the response of the j th element at the i th channel and c_j is its coefficient, and n is the total number of elements utilized to fit the spectrum. SPIDER employs a least-squares algorithm to fit Equation (1).

By computing the scalar products between the background spectrum (B_i) and the elemental responses (E_{ij}) for each element j , we can determine if there is any relationship or coupling between k and the elemental coefficients, c_j . Table 14 was calculated over the fast fitting region (from channels 50 to 500) for the three elements used in this fit (C, O, N). These data used in

this calculation were the 120mm on a sand surface (R1307) and its corresponding background, (b1308). Recall that B1308 is an interpolated background as described in the "Methodology" section. In Table 14, the closer the values are to 90° ($\cos\theta=1$), the less coupling between the two quantities. As we can see, there is a small amount of coupling but it is safe to say that c_j is nearly independent of k . As expected, O which is a major component of the sand has the strongest coupling and N, which was not present in the soil.

Table 14. Scalar products of the background with the elemental responses. See text for details.

Element	$\cos\theta$	θ
C	0.217	77°
O	0.301	72°
N	0.135	82°

In Figure 59A, the residuals for the fit of R1307 with B1307 are plotted. The spectrum is described by Poisson statistics and thus for a given channel, y_i , standard deviation, σ_{y_i} , is equal to $\sqrt{y_i}$. Thus, a spectrum of $\sqrt{y_i}$, represents the uncertainty (1σ) and the error (2σ) is represented by $2\sqrt{y_i}$. In Figure 59A, we have plotted both the 1σ and the 2σ spectra along with the residuals in order to determine the "goodness" of the fit.

There are two regions in which the residuals stray outside of 2σ : 1) one at the extreme of the fitting range at about channel 63 (1.575 MeV), and 2) at 4.430 MeV, the region of the C gamma ray (channel 180). The 1.575 MeV is believed to be a gamma ray from ^{209}Bi within the BGO detector. This gamma-ray depends on the amount of neutron scattering within the detector and thus depends on sample size. A response for this gamma ray can be utilized to decrease the size of the residuals but it is unlikely to have an impact on the final results.

The probable cause of the residual variations at 4.43 MeV is due to the fitting uncertainties associated with the deconvolution process. However, the residuals in this region are not as large as 1.575 MeV and certainly, they are within 3σ of the fit. Also, the more extreme residuals occur at the edges of the 4.430 MeV peak. This indicates that the peak may be "broadened" from the width in the response spectra. This change of shape may be due to high count rates in the data acquisition hardware or the under-correction of the interpolated background spectrum.

In Figure 59B, the residuals are compared with the elemental responses, E_{ij} , multiplied by their respective coefficients, c_j . If the residuals are larger than these modified elemental responses, then this indicates that the particular element is within the statistical noise. In the case of Figure 59B, only the N response is lower than the residuals, indicating that the N data may be questionable. The C and O responses are well above the residuals indicating a high confidence in these measurements.

Finally, for this fit, we can compare the scalar product of the residual spectrum with the contributions from the C, O, and N responses and the background spectrum. The scalar products are very close to zero indicating that these are not strongly coupled and that the residuals are a function of statistical fluctuations. In other words, the fit is considered "good".

Table 15. Scalar products of the residuals with the elemental responses. See text for details.

Element	$\cos\theta$	θ
Background	0.0083	89.5°
C	0.002	89.9°
O	0.003	89.8°
N	-0.0005	-90.02°

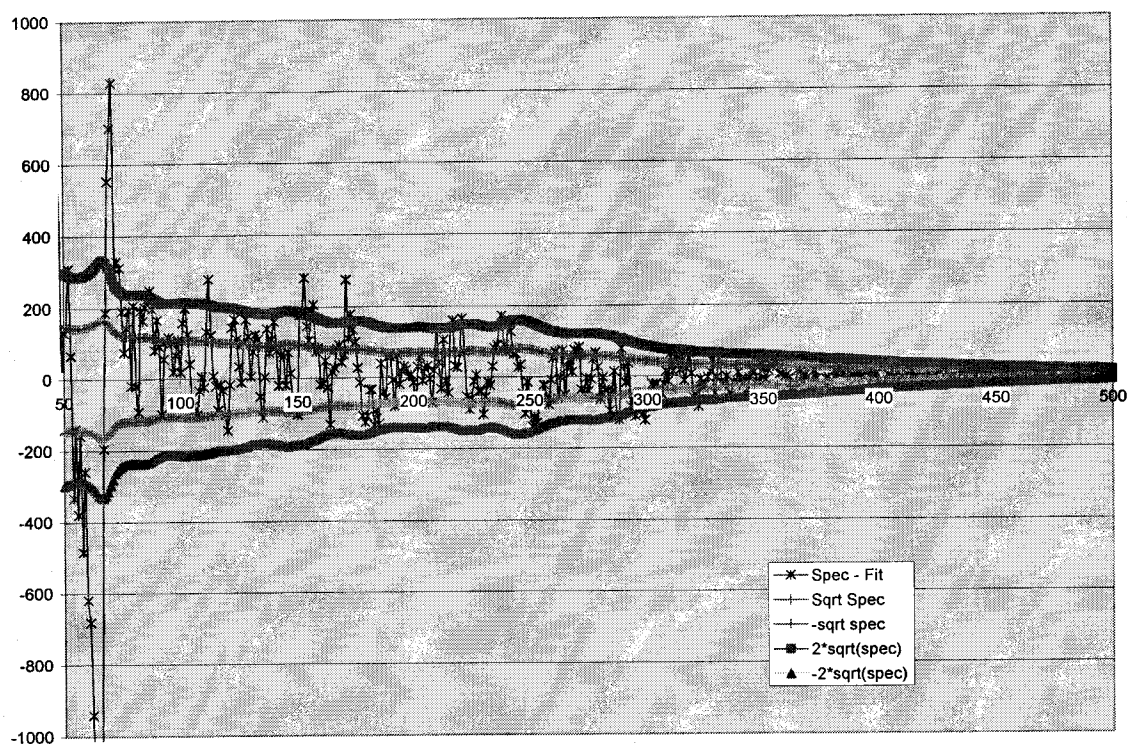


Figure 59A. The residuals of the fit for R1307 with B1308 are plotted (dark purple). The 1σ spectrum (green) and the 2σ (light purple) are plotted as confidence limits. See text for details.

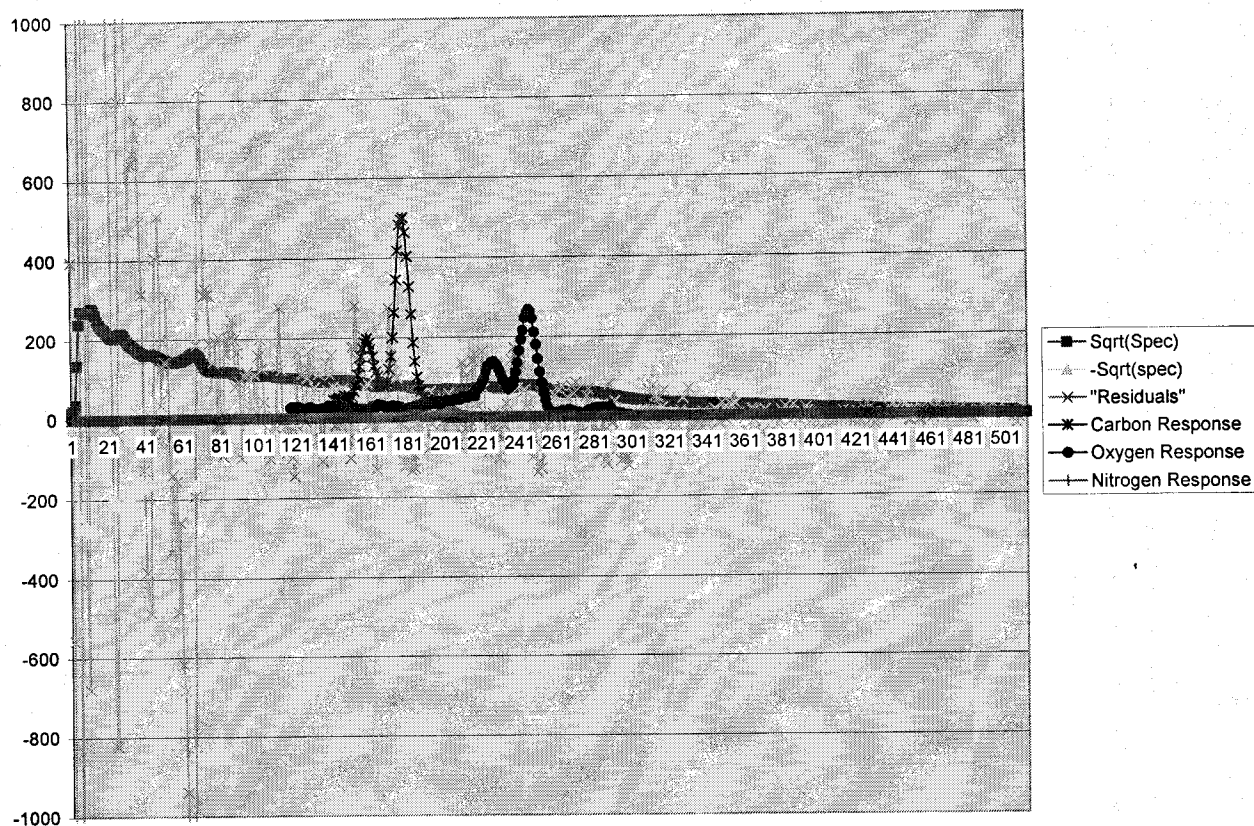


Figure 59B. The residuals (light blue), $\pm 1\sigma$ (purple and yellow), and the element responses multiplied by their respective coefficient: C (dark purple), O (brown), and N (green). See text for details.

Figures 60-62 show comparisons of the 81mm shell filled with plaster of Paris and TNT on three different media: sand (Fig. 60), gravel (Fig. 61), and wet soil (Fig. 62). Figures 60 and 62 show no visible differences. Figure 60 has a slightly higher H content for plaster of Paris than TNT.

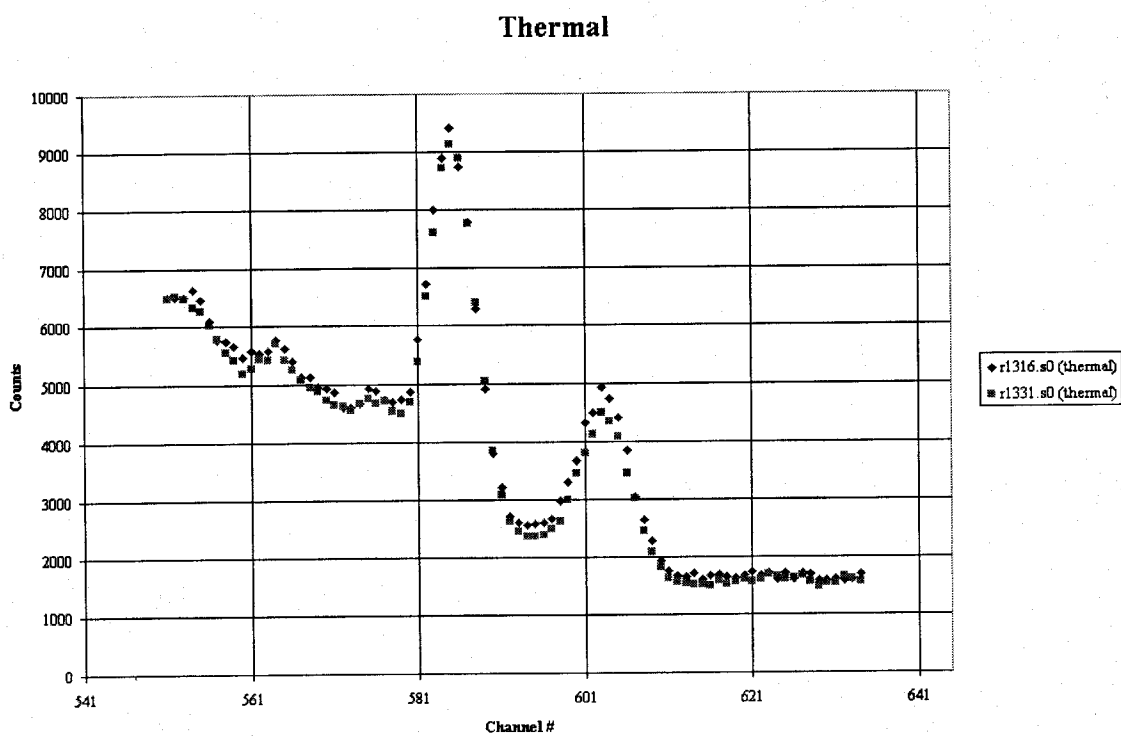
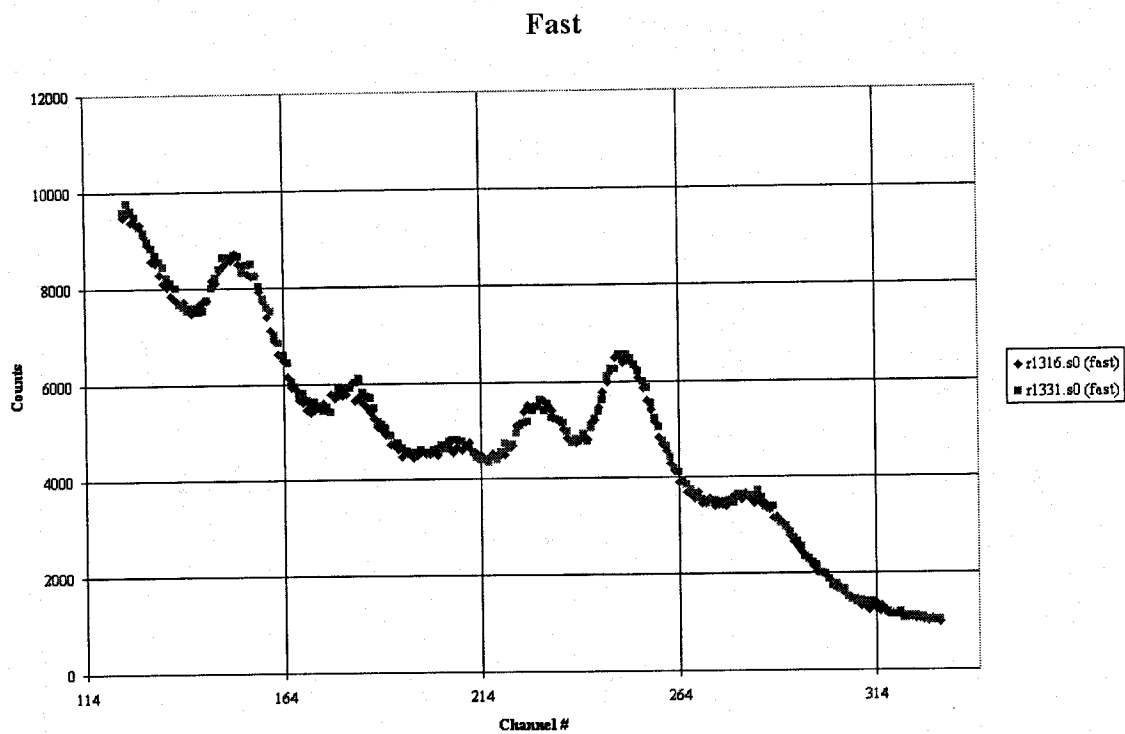


Figure 60. 81 mm POP (R1316) and TNT 81 mm (R1331) on sand.

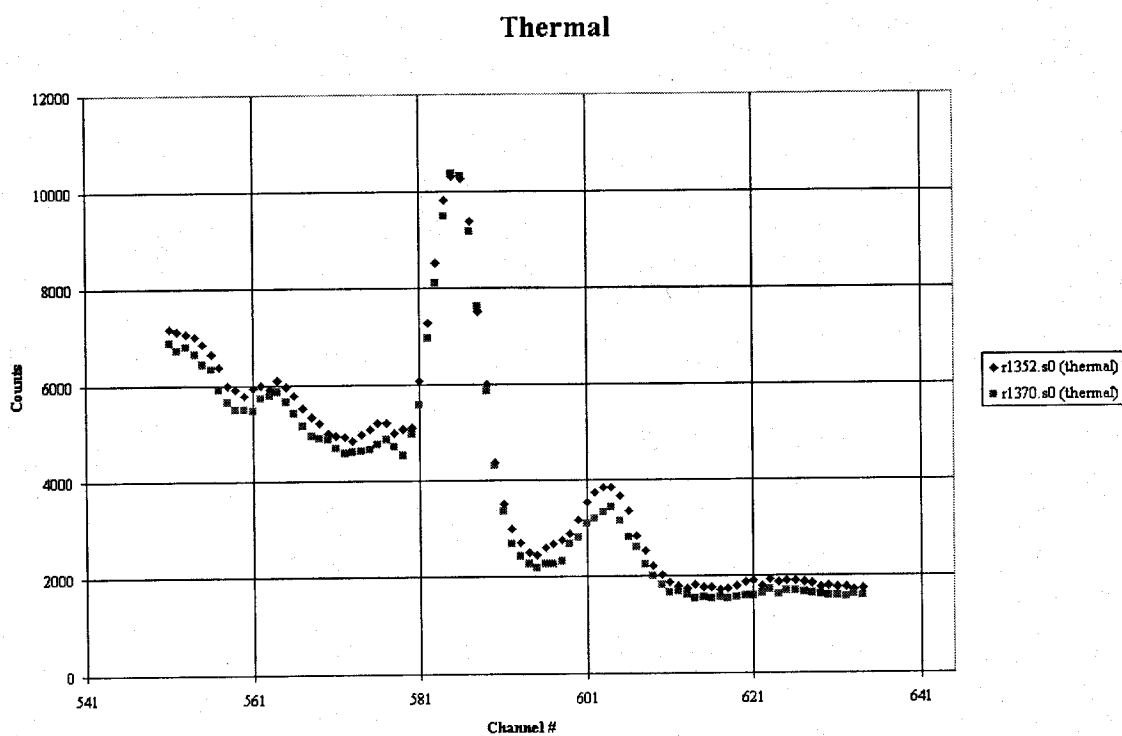
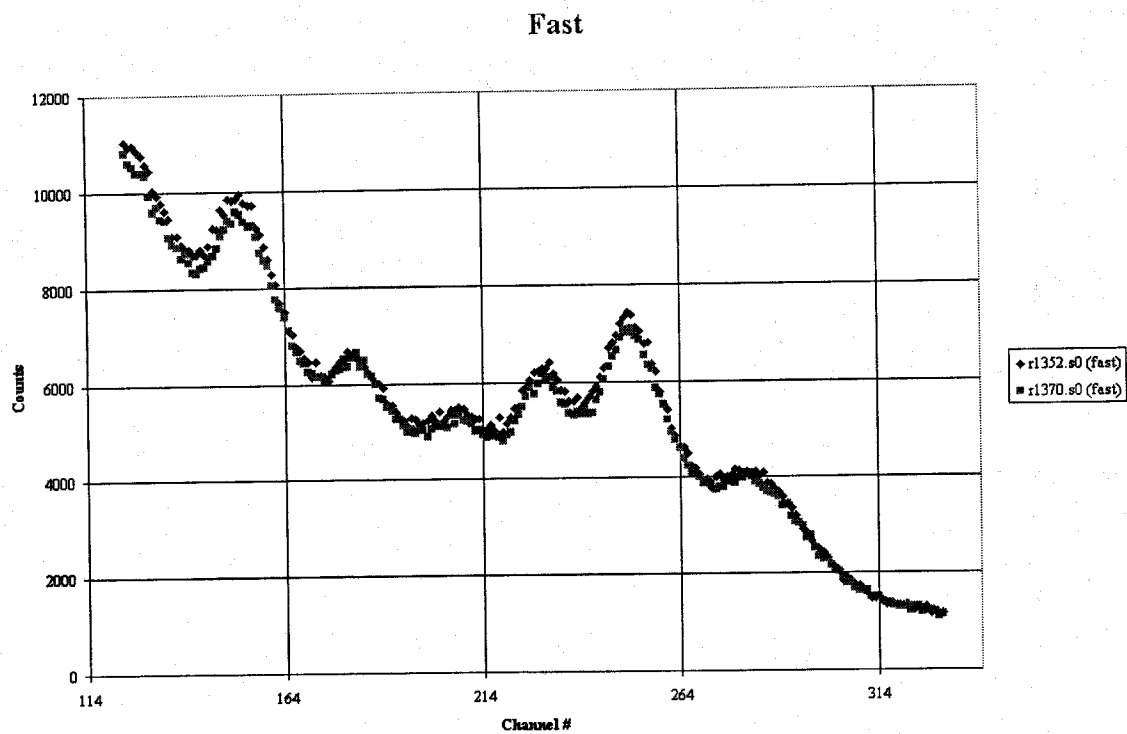
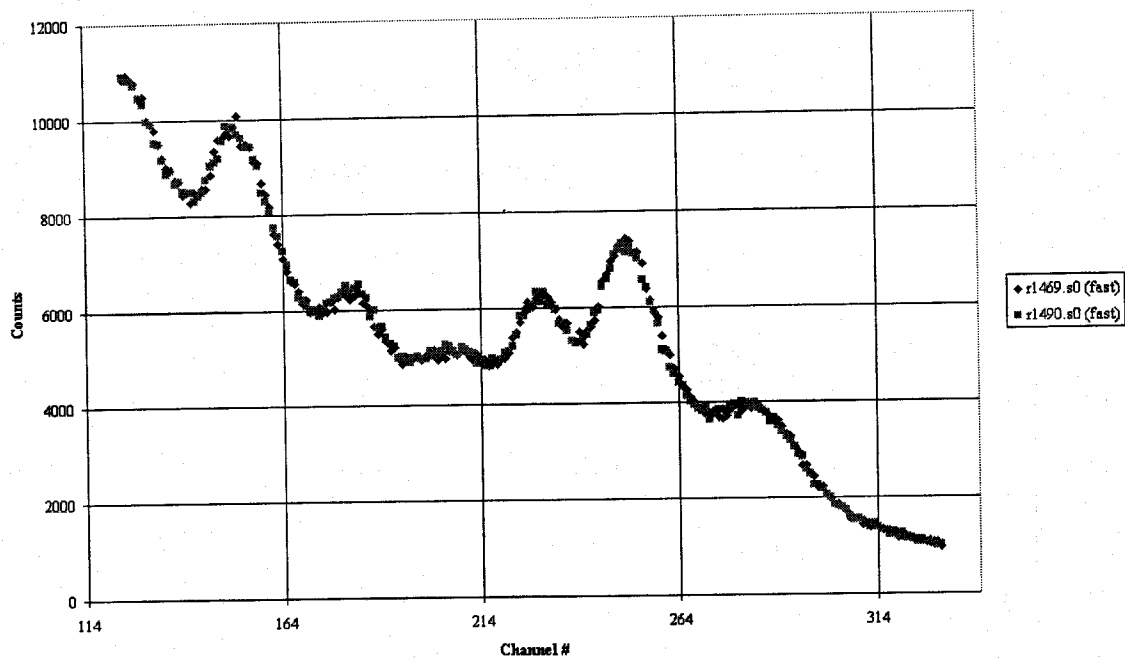


Figure 61. 81 mm POP (R1352) and TNT 81 mm (R1370) on gravel.

Fast



Thermal

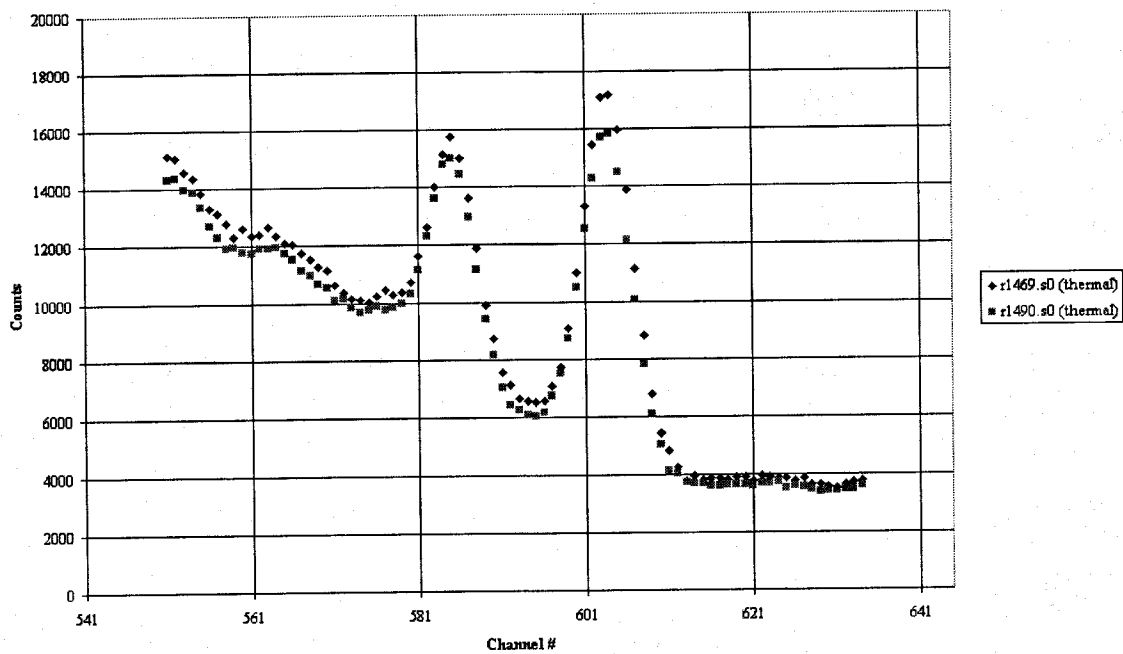


Figure 62. 81 mm POP (R1469) and TNT 81 mm (R1490) on wet soil.

5.1.5 COMPILED DATA

Table 16. Elemental composition (elements H, C, N, and O) used in the decision tree for all the shells on which data were taken either as part of the PELAN training set or as part of the unknowns.

Size (mm)	Fill	Surface	Run	Bkgd "Empty"	Bkgd "Fe"	C (cps)	H (cps)	N (cps)	O (cps)
2%	ANFO	GRAVE L	1666	1637	1640	3.2	13.8	6.2	10.8
2%	ANFO	SAND	1720	1690	1693	4.3	19.6	6.3	9.1
2%	ANFO	SOIL	1574	1529	1532	1.7	28	5.3	7.3
2%	ANFO	TABLE	1613	1583	1586	5.1	9.4	2.8	13
2%	ANFO	WETSO IL	1744	1756	1759	3.3	21.4	3.9	11.3
6%	ANFO	GRAVE L	1669	1637	1640	5.6	15.4	3.6	9.7
6%	ANFO	Gravel	1873	1855	1858	7.1	20.8	5.6	8.7
6%	ANFO	SAND	1720	1690	1693	6.6	23.3	5.1	8.3
6%	ANFO	SOIL	1577	1529	1532	3.3	28.3	3.6	7.1
6%	ANFO	TABLE	1616	1583	1586	4.6	12.5	3.4	13.4
6%	ANFO	WETSO IL	1747	1756	1759	4	22.3	4.6	11.1
6%	ANFO	Wetsoil	1942	1927	1930	9.81	35.55	6.73	8.58
15%	ANFO	GRAVE L	1688	1637	1640	9	26.9	4.7	11.9
15%	ANFO	SAND	1711	1690	1693	8.5	36.6	5.4	8.8
15%	ANFO	SOIL	1580	1529	1532	6.1	40.7	5.1	6.1
15%	ANFO	TABLE	1619	1583	1586	8.3	17.9	3.5	12.8
15%	ANFO	WETSO IL	1750	1756	1759	6.3	36.9	5.8	8.6
1	smokless	GRAVE L	1597	1637	1637	5.2	-5.3	-3.3	-8
1	smokless	SAND	1714	1690	1693	6.2	6.1	2.8	4.1
1	smokless	SOIL	1547	1529	1532	3.6	-2.2	2.1	4.9
1	smokless	TABLE	1589	1583	1586	10.7	0.5	0.2	5.3
1.8	semtex-1a	SAND	1696	1690	1693	5.7	3.3	2.1	4.5
1.8	semtex-1a	soil	1544	1529	1532	5.8	4.7	3	5.9
4.5	semtex-1a	SAND	1717	1690	1693	10.5	5.5	3.9	5.2
4.5	semtex-1a	TABLE	1595	1583	1586	15	5.1	1.8	9.6
60	BP	SAND	1304	1300	1302	0.8	-2.9	-1.1	-0.6
60	BP	TABLE	1394	1376	1379	-4.7	-0.4	0.2	-0.4
60	EMPTY	SOIL	1285	1157	1221	0.7	-15.2	-5.2	-7.1
60	EMPTY	SOIL	1288	1157	1221	0.7	-15.2	-5.2	-7.1

Size (mm)	Fill	Surface	Run	Bkgd "Empty"	Bkgd "Fe"	C (cps)	H (cps)	N (cps)	O (cps)
60	PLASTER	SAND	1807	1801	1804	1.7	0.1	0.8	-2.1
60	PLASTER	SOIL	1291	1157	1221	0.8	-16.3	-5.1	-7.8
60	POP	Gravel	1870	1855	1850	1.7	-0.4	0.6	-1
60	Pop	Table	1978	1972	1975	-2.54	0.05	0.99	-0.64
60	POP	WETSOIL	1499	1487	1484	1.5	2.8	0.7	0.7
60	RED	SAND	1810	1801	1804	1.4	-1.5	1.9	-1.9
60	RED	SOIL	1279	1157	1221	2	-10.7	-1.7	-4
60	TNT	GRAVEL	1361	1340	1337	2.5	3.5	0.7	4
60	TNT	Gravel	1861	1855	1858	3.6	0.6	0.7	-1
60	TNT	SAND	1322	1300	1302	1.9	-1.9	0	-2.1
60	TNT	SOIL	1436	1415	1418	-0.8	-2.5	-1.3	-1.6
60	TNT	Soil	1897	1891	1894	2.3	-1.2	0.4	-3.1
60	TNT	TABLE	1400	1376	1379	-1.6	4.3	1.1	-0.5
60	TNT	WETSOIL	1496	1487	1484	3.5	4.7	0	-0.3
60	TNT	WETSOIL	1508	1487	1484	2.4	1.1	0.7	-5
60	WAX	SAND	1687	1690	1693	2.1	0.5	-0.2	-0.5
60	WAX	SOIL	1300	1157	1221	1.6	-2.7	-3.8	-6.2
60	WAX	WETSOIL	1502	1487	1484	3.2	3.9	0	0
60	WAX	WETSOIL	1505	1487	1484	1.7	-0.3	0.3	0
76	RDX	GRAVEL	1364	1340	1337	5	5	2.5	4.9
76	RDX	SAND	1325	1300	1302	2.7	-0.8	1	0.3
76	RDX	SAND	1825	1819	1822	6	1.9	1.3	1.8
76	RDX	SOIL	1225	1157	1221	4	-1.5	-0.5	-1.3
76	RDX	SOIL	1228	1157	1221	4.1	-7.2	0	-1.1
76	RDX	SOIL	1231	1157	1221	4.4	-9	-0.7	-0.8
76	RDX	SOIL	1234	1157	1221	4.6	-4.3	-0.6	0
76	RDX	SOIL	1237	1157	1221	4.6	-9.3	-0.6	-1.7
76	RDX	SOIL	1240	1157	1221	4.8	-4.2	-0.6	-2
76	RDX	SOIL	1243	1157	1221	4.9	-5.7	-0.2	1
76	RDX	SOIL	1246	1157	1221	5	-3.8	-0.4	-2.2
76	RDX	SOIL	1306	1157	1221	2.9	1.9	-1.1	-0.3
76	RDX	SOIL	1309	1157	1221	3.8	-6.5	-0.6	-3.2
76	RDX	SOIL	1439	1415	1418	1.4	1.7	-1.4	-1.2
76	RDX	TABLE	1403	1376	1379	-2.7	0.2	2.7	1
76	RDX	WETSOIL	1478	1451	1454	5.4	-3.3	4.8	1.3
76	TNT	GRAVEL	1367	1340	1337	5.6	0.8	0	3.7
76	TNT	SAND	1328	1300	1302	4	-3.6	-1	-2.9

Size (mm)	Fill	Surface	Run	Bkgd "Empty"	Bkgd "Fe"	C (cps)	H (cps)	N (cps)	O (cps)
76	TNT	SOIL	1442	1415	1418	1.2	-10.6	-3.1	-5.8
76	TNT	Soil	1918	1891	1894	3.4	-0.6	-1.1	-1.6
76	TNT	TABLE	1406	1376	1379	-3.9	-1.2	0.6	-1.4
76	TNT	WETSO IL	1481	1451	1454	4.3	-13.8	2	-2.7
81	COMPB	TABLE	1409	1376	1379	1.6	-1.1	2.5	2.5
81	COMPB	Gravel	1867	1855	1858	9.5	3.5	3.6	1.5
81	COMPB	SAND	1331	1300	1302	4.8	-0.8	-0.1	0
81	COMPB	SOIL	1445	1415	1418	1.5	-17	-3	-0.6
81	COMPB	WETSO IL	1490	1487	1484	6	-5.6	2.4	0
81	EMPTY	SOIL	1288	1157	1221	0.8	-12.7	-3.2	-4.8
81	EMPTY	SOIL	1291	1157	1221	0.8	-12.7	-3.2	-4.8
81	PLASTE R	GRAVE L	1352	1340	1337	2.1	11.5	0.3	9.3
81	PLASTE R	SAND	1316	1300	1302	2.1	8.2	-1.7	-0.3
81	PLASTE R	SAND	1684	1690	1693	1	4.8	1	1.3
81	PLASTE R	SOIL	1191	1157	1189	3.1	6.5	-1.8	2.3
81	PLASTE R	SOIL	1194	1157	1189	2.1	-2.4	-2	1.1
81	PLASTE R	SOIL	1197	1157	1189	2.2	-3	-1.9	-0.8
81	PLASTE R	SOIL	1200	1157	1189	2.4	-4.9	-1.8	-0.6
81	PLASTE R	SOIL	1203	1157	1189	2.5	-3.4	-1	-0.8
81	PLASTE R	SOIL	1206	1157	1189	0.9	-4.6	-3.4	-0.2
81	PLASTE R	SOIL	1209	1157	1189	1	-4.5	-2.5	-0.2
81	PLASTE R	SOIL	1212	1157	1189	1.5	-4.1	-2	0.9
81	PLASTE R	SOIL	1215	1157	1189	2	-3.2	-1.3	0.3
81	PLASTE R	SOIL	1218	1157	1189	2	-1.7	-0.6	1.9
81	PLASTE R	SOIL	1303	1157	1221	1.1	-5.8	-5.3	-5.5
81	PLASTE R	SOIL	1430	1415	1418	-0.7	3.8	-0.2	-0.2
81	PLASTE R	TABLE	1391	1376	1379	-4.1	4.3	-0.8	5
81	POP	SAND	1846	1819	1822	1.5	7	-0.4	1.5
81	POP	WETSO IL	1469	1451	1454	2.8	3.8	0	1.6
81	POP	WETSO IL	1475	1451	1454	1.6	3.2	1	1.6
81	POP	Wetsoil	1957	1927	1930	5.95	3.81	0.92	1.13
81	SAND	SAND	1786	1801	1804	2.5	-3.7	-0.6	-3.1

Size (mm)	Fill	Surface	Run	Bkgd "Empty"	Bkgd "Fe"	C (cps)	H (cps)	N (cps)	O (cps)
81	Sand	SAND	1849	1819	1822	1	-1.9	0.3	-0.7
81	SAND	SOIL	1267	1157	1221	0.4	-11.2	-3	-3.7
81	SAND	Table	1999	1972	1975	-2.36	-2.6	-0.8	-0.28
81	Sand	Wetsoil	1960	1927	1930	6.81	-3.3	1.65	-0.03
81	TNT	SAND	1334	1300	1302	2.4	-2	0.2	-0.4
81	WAX	SAND	1690	1690	1693	5.4	7	-0.8	-3.7
81	WAX	SOIL	1270	1157	1221	3.8	0.5	-3.7	-5.4
82	COMPB	GRAVE L	1370	1340	1337	6.4	4.7	0	6.4
82	TNT	GRAVE L	1373	1340	1337	5.5	1.6	1.9	7.7
82	TNT	GRAVE L	1643	1637	1640	8.6	1.2	-0.5	0.3
82	TNT	SAND	1699	1690	1693	6	-2.3	0.7	-0.2
82	TNT	SAND	1828	1819	1822	6.8	1.5	1.9	1.9
82	TNT	SOIL	1448	1415	1418	-0.1	-14	-3	-0.6
82	TNT	SOIL	1535	1529	1532	3.1	-6.4	-0.3	-1
82	TNT	Soil	1900	1891	1894	5.1	-1.3	0.6	-1.7
82	TNT	TABLE	1412	1376	1379	-0.5	4.5	1.1	0.8
82	TNT	TABLE	1589	1583	1586	2.9	-2.6	0.2	1.7
82	TNT	WETSO IL	1493	1487	1484	4.6	-6.1	-0.2	-2.6
82	TNT	WETSO IL	1511	1487	1484	6	-5.5	2.1	-1.7
90	COMPB	WETSO IL	1514	1487	1484	6.5	3.1	3	-4.1
90	RDX	GRAVE L	1346	1340	1337	3.8	1.3	-0.2	-0.9
90	RDX	SAND	1310	1300	1302	3	1.7	0.6	1.5
90	RDX	SOIL	1424	1415	1418	3.7	1.3	-0.2	-2.6
90	RDX	TABLE	1385	1376	1379	-0.9	0.2	2.9	1.7
90	RDX	WETSO IL	1460	1451	1454	4.8	7.5	3.2	-1.5
90	RDX	Wetsoil	1936	1927	1930	9.43	1.52	4.07	-0.33
90	RED	SAND	1843	1819	1822	6.2	-3.4	-0.6	-3.1
90	RED	SOIL	1294	1157	1221	4.2	-13.4	-2.4	-7
90	RED	SOIL	1297	1157	1221	4.2	-13.4	-2.4	-7
90	Red	Table	1993	1972	1975	-3.37	-4.76	0.5	-2.05
90	RED	Wetsoil	1963	1927	1930	8.75	-12.9	0.91	-2.28
90	rocket 1.1lb60/40	GRAVE L	1667	1637	1640	18	2.6	3.7	4.2
90	rocket 1.1lb60/40	Gravel	1888	1855	1858	18.5	0.8	4.1	3.4

Size (mm)	Fill	Surface	Run	Bkgd "Empty"	Bkgd "Fe"	C (cps)	H (cps)	N (cps)	O (cps)
90	rocket 1.1lb60/40	SAND	1678	1690	1693	17.2	1.6	3	3.3
90	rocket 1.1lb 60/40	SOIL	1568	1529	1532	12.9	7.3	3.4	4
90	rocket 1.1lb60/40	TABLE	1583	1583	1586	12.1	3.5	2.6	9.2
90	rocket 1.1lb60/40	WETSOIL	1729	1756	1759	14.5	3	3	1.2
90	TNT/RDX	Wetsoil	1954	1927	1930	21.5	4.76	4.87	5.65
90	TX50	GRAVEL	1670	1637	1640	9.6	-1	1.9	1.5
90	TX50	SAND	1681	1690	1693	8.4	-1.1	1.7	0.1
90	TX50	SOIL	1538	1529	1532	4	-1	0.9	0.5
90	TX50	TABLE	1592	1583	1586	6.1	2.4	1.4	4.7
105	EMPTY	Wetsoil	1969	1927	1930	8.92	-2.66	2.62	-4.35
105	RED	Wetsoil	1966	1927	1930	9.86	2.59	2.24	-0.85
105	SAND	SAND	1789	1801	1804	0.9	-4.8	0.6	-1.4
105	SAND	SOIL	1282	1157	1221	-1.6	-8.4	-1.3	-2.7
105	SAND	Soil	1915	1891	1894	0.6	16	0.4	0.7
105	SAND	Table	1996	1972	1975	-7.92	6.26	1.08	4.26
105	WAX	GRAVEL	1355	1340	1337	8.2	23	-0.5	2.9
105	WAX	SAND	1319	1300	1302	4.7	18.2	-1.1	-3.1
105	WAX	SOIL	1159	1157	1189	4.4	13.9	-1.8	-3.6
105	WAX	SOIL	1162	1157	1189	5.3	11.6	0.1	-3.1
105	WAX	SOIL	1165	1157	1189	5	11	-1	-3.1
105	WAX	SOIL	1168	1157	1189	5.7	9.5	-0.2	-2.6
105	WAX	SOIL	1171	1157	1189	5.3	10.1	-1.5	-2.1
105	WAX	SOIL	1174	1157	1189	5.5	13.3	-1.9	-4
105	WAX	SOIL	1177	1157	1189	5.1	7.9	-0.5	-4
105	WAX	SOIL	1180	1157	1189	5.5	8.2	-3.5	-4.8
105	WAX	SOIL	1183	1157	1189	4.8	5.3	-0.3	-4.6
105	WAX	SOIL	1186	1157	1189	5.8	12.4	-1.2	-4.2
105	WAX	SOIL	1221	1157	1221	4.7	8	-1.8	-3.4
105	WAX	SOIL	1433	1415	1418	2.5	6.3	-2.6	-6.8
105	WAX	Soil	1906	1891	1894	6.5	24.5	-1.8	-4.1
105	WAX	TABLE	1397	1376	1379	-1.2	10.2	0.4	-1.3
105	WAX	TABLE	1586	1583	1586	7.3	5.3	-0.2	2.4
105	WAX	WETSOIL	1472	1451	1454	5.5	7.3	7.3	-4.4
105	WAX	Wetsoil	1948	1927	1930	10.3	4.48	-0.8	-3.45
120	TNT	GRAVE	1343	1340	1337	8.6	1.9	2.8	3.5

Size (mm)	Fill	Surface	Run	Bkgd "Empty"	Bkgd "Fe"	C (cps)	H (cps)	N (cps)	O (cps)
		L							
120	TNT	SAND	1307	1300	1302	11.3	0.7	2.3	4.1
120	TNT	SOIL	1421	1415	1418	7.8	-1.7	2.4	0.6
120	TNT	TABLE	1382	1376	1379	13.7	1.4	4.5	8.5
120	TNT	Wetsoil	1939	1927	1930	17.4	-3.51	7.54	3.9
122	COMPB	GRAVE L	1349	1340	1337	11.9	6.7	4.5	10.8
122	COMPB	SAND	1313	1300	1302	15.3	8.1	6.2	11
122	COMPB	SOIL	1427	1415	1418	11.1	11	3.3	4.8
122	COMPB	SOIL	1463	1451	1454	13.8	20.4	6.8	8.4
122	COMPB	TABLE	1388	1376	1379	13.5	5.8	6.5	14.5
122	COMPB	Table	1981	1972	1975	11.2	6.32	5.44	10.8
122	PROPEL.	WETSO IL	1466	1451	1454	26	18	6.8	18
155	13.2 TNT	SOIL	1550	1529	1532	18.8	5.4	4.9	5.5
155	EMPTY	SOIL	1312	1157	1221	-2.1	1.5	-2.1	-0.8
155	EMPTY	SOIL	1315	1157	1221	-2.1	1.5	-2.1	-0.8
155	RED	SAND	1852	1819	1822	14.7	55.1	-0.6	0.9
155	RED	SOIL	1318	1157	1221	7.5	33.5	1.7	5
155	RED	SOIL	1321	1157	1221	7.5	33.5	1.7	5
155	Red	Soil	1924	1891	1894	15.1	68.8	-0.7	2.5
155	TNT	GRAVE L	1673	1637	1640	20.5	8.4	3.5	7.7
155	TNT	SAND	1693	1690	1693	21.3	9	6.2	10
155	TNT	SAND	1831	1819	1822	18.2	3.6	4.7	6.8
155	TNT	TABLE	1604	1583	1586	29.4	-4	6.4	16.1
155	TNT	WETSO IL	1762	1756	1759	19.2	-4.8	7.9	5.2
155	WAX	Gravel	1864	1855	1858	14.1	102.9	1	-2.4
155	WAX	SOIL	1324	1157	1221	8.3	59.9	1.6	1.9
155	WAX	Wetsoil	1933	1927	1930	10.1	26.45	3.71	-2.9
AT Mine	TNT	Table	1990	1972	1975	33.4	10.42	5.47	9.94
AT Plastic mine	TNT	Gravel	1879	1855	1858	39.7	17.6	5.7	6.9
AT Steel mine	TNT	Gravel	1885	1855	1858	21.4	8	7.3	7.7
AT Steel mine	TNT	Wetsoil	1951	1927	1930	24	18.59	8.31	9.7
FFV028 steel mine	12.35 TNT	GRAVE L	1672	1637	1640	20	7.8	6.8	7.7
FFV028 steel mine	12.35 TNT	SAND	1723	1690	1693	21	10.7	6.8	7.3

Size (mm)	Fill	Surface	Run	Bkgd "Empty"	Bkgd "Fe"	C (cps)	H (cps)	N (cps)	O (cps)
FFV028 steel mine	12.35 TNT	SOIL	1571	1529	1532	16.1	18.1	5.9	7.5
FFV028 steel mine	12.35 TNT	TABLE	1610	1583	1586	14.9	6.3	7.1	12.9
FFV028 stl mine	12.35 TNT	WETSO IL	1741	1756	1759	18.2	-3.2	4.3	4.1
shape charge	0.9lbsOct ol	GRAVE L	1676	1637	1640	4.9	-1.6	2.9	4.7
shape charge	0.9lbsOct ol	SAND	1699	1690	1693	5.4	4.5	1.6	4.6
shape charge	0.9lbsOct ol	SOIL	1556	1529	1532	2.1	0.3	2.1	4.1
shape charge	0.9lbsOct ol	TABLE	1592	1583	1586	8.3	1.8	1.9	5
shape charge	0.9lbsOct ol	WETSO IL	1783	1777	1780	4.8	0.9	3.5	3
shape charge	6.1lbs pxb-108	SOIL	1553	1529	1532	18.4	3.3	5.5	7
shape charge	6.1lbs pxb-108	GRAVE L	1679	1637	1640	29.2	17.4	8.3	10.5
shape charge	6.1lbs pxb-108	SAND	1705	1690	1693	26.8	15.6	8.7	7.7
shape charge	6.1lbs pxb-108	TABLE	1595	1583	1586	24.3	-4.6	6.9	14.6
shape charge	6.1lbs pxb-108	WETSO IL	1765	1756	1759	21.5	-32.7	8.9	9.8
Shape Charge	Octal	Gravel	1876	1855	1858	5	1.3	3.3	4.1
Shape Charge	Octal	Table	1987	1972	1975	4.43	-0.21	2.38	3.86
Shape Charge	PBX-108	SAND	1834	1819	1822	30.2	15.9	9.5	8.6
Shape Charge	PBX-108	Wetsoil	1945	1927	1930	27.9	-28	6.3	0.99
Sheet explo	21lbPET N	GRAVE L	1685	1637	1640	36.3	39.8	5.4	19.4
Sheet explo	21lbPET N	SAND	1708	1690	1693	34.3	46.6	6.7	18.9
Sheet explo	21lbPET N	TABLE	1598	1583	1586	33.4	14.5	3.8	24.6
Sheet explo	21lbPET N	WETSO IL	1732	1756	1759	30.7	52	6.5	14.8
Sheet explo	21lbPET N	SOIL	1559	1529	1532	25	51.1	8	15.1
Sheet explo	PETN	Gravel	1882	1855	1858	36.1	41.1	6.2	18.4
Sheet	PETN	Soil	1921	1891	1894	32	53	6.9	14.4

Size (mm)	Fill	Surface	Run	Bkgd "Empty"	Bkgd "Fe"	C (cps)	H (cps)	N (cps)	O (cps)
explo									
TMRP 6	11.2lbTN T	WETSO IL	1735	1756	1759	34	33	5.8	5.2
TMRP-6	11.2lbTN T	GRAVE L	1675	1637	1640	38.7	13.4	6.1	9.3
TMRP-6	11.2lbTN T	SAND	1726	1690	1693	39.4	17.8	6.2	7.5
TMRP-6	11.2lbTN T	SOIL	1562	1529	1532	28.4	28.1	6.3	4.2
TMRP-6	11.2lbTN T	TABLE	1601	1583	1586	39.9	10.4	3.2	12.5
Val69 Mine	6lb CompB	GRAVE L	1682	1637	1640	9.7	0.1	1.1	3.6
Val69 Mine	6lb CompB	SAND	1702	1690	1693	8	2.1	1.2	2.5
Val69 Mine	6lb CompB	SOIL	1565	1529	1532	3.9	1.7	2.7	2.2
Val69 Mine	6lb CompB	TABLE	1607	1583	1586	10.5	1.8	2.1	4
Val69 Mine	6lb CompB	WETSO IL	1738	1756	1759	7.1	-1.8	2.3	-0.2
Val69 Mine	COMPB	SAND	1840	1819	1822	9.2	4.3	2.3	1.8
Val69 Mine	COMPB	Soil	1912	1891	1894	7.8	3.4	2.3	0.9
	semtex- 1a	Soil	1903	1891	1894	10.3	13	2.8	5.7
	semtex- 1a	Table	1984	1972	1975	10.2	4.13	1.4	7.54
	Smoke less	SAND	1837	1819	1822	7.1	2.3	3.7	5.9
	Smoke less	Soil	1909	1891	1894	5.7	5.2	2.9	3.3

5.1.6 RECEIVER OPERATOR CHARACTERISTIC CURVES

For those unfamiliar with ROC curves, a brief explanation is provided. False positive rate is plotted along the x-axis and true positive rate is plotted along the y-axis. A perfect curve should look similar to an asymptotic curve approaching one. The area under the curve is considered a measure of test accuracy i.e. the greater the area, the higher the accuracy. A curve which looks like a straight-line with a unity slope is undesirable.

Figure 63A shows the receiver operator characteristic (ROC) curve for the all the data collected during the demonstration. Elements H, C, O, and N are presented and their cut-offs or thresholds are varied between -15 to 100. The decision outcomes were “threat” or “no threat”.

In this figure (Fig. 63A), the area under the N curve is greatest implying that N is a key indicator of whether a threat exists. Surprisingly, O has the next highest area followed by C and then H. The curve for H since it nears a unity slope and thus, this shows that H content is not a good test to determine whether a threat is present. These curves provide a starting point for the decision tree.

We will examine whether the ROC curve presented in Figure 63A can be used to design a new decision tree in the next section.

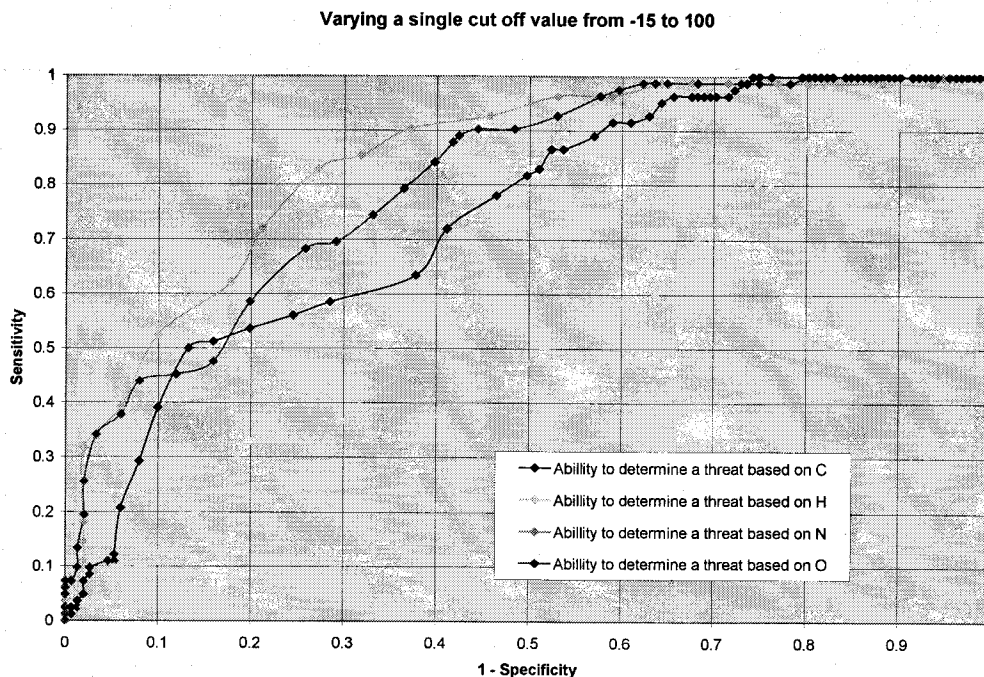


Figure 63A. ROC curve for elements H, C, O, and N as a function of cut-off value for all data. See text for details

5.1.6.1 ROCS for Ratios of Elements

The question arises whether ratios of elements should be used in the decision tree. In Figure 63B, we see that using the chemical elemental content, we can segregate between explosives and other materials.

In Figure 63C, we have created an ROC curve using the C content (cps), the O content (cps), and the C/O ratio. In Figure 63D, the ROC curve uses C, N, and the C/N ratio. The cutoffs or thresholds were varied between -50 to +100.

These figures both show that the ratio is no better than the data with which it is supplied. It is also interesting to note that the ROC curves of the products of elemental content (not shown) are very similar to the ratio.

Based on this should we use ratios in the decision trees? While the ROC curves for ratios may not be as good as the ROC curves for the individual elements, the ratios eliminate the problems caused by different sized objects (e.g. 1 lb of TNT and 10 lb of TNT should have the same C/N ratio). However, this advantage may be offset due to the distribution of data. For example, if while measuring water, a small amount of carbon, 0.5 cps, would create a small C/H ratio. The 0.5 cps is well within the bounds of a statistical zero (see Tables 4A through 4D for details). Unfortunately, we cannot draw any conclusions about the appropriateness of using ratios from the ROC curves.

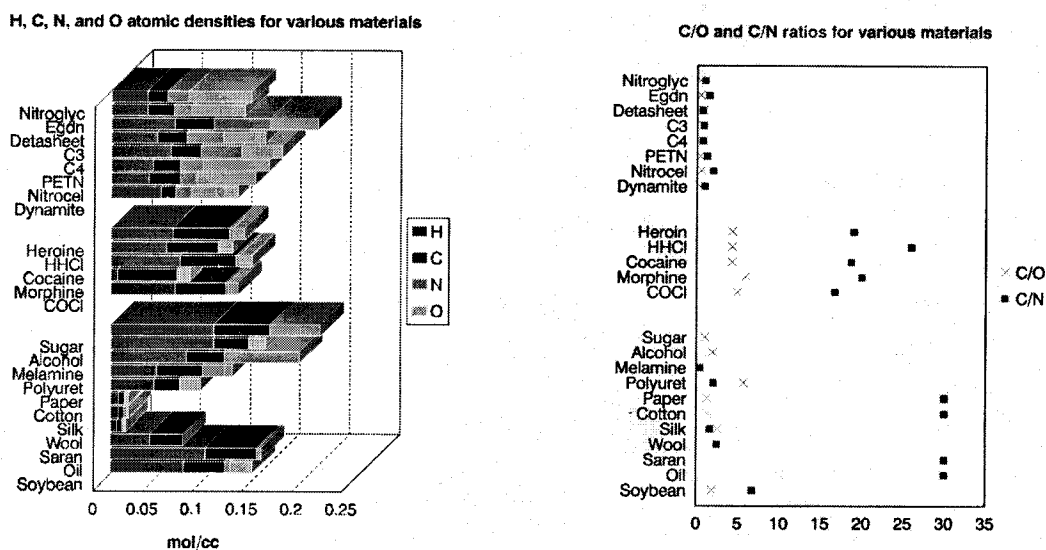


Figure 63B. The plot on the left shows atomic densities for explosive compounds, illicit drugs, and innocuous materials. The figure on the right shows how they can be segregated by using ratios of elements.

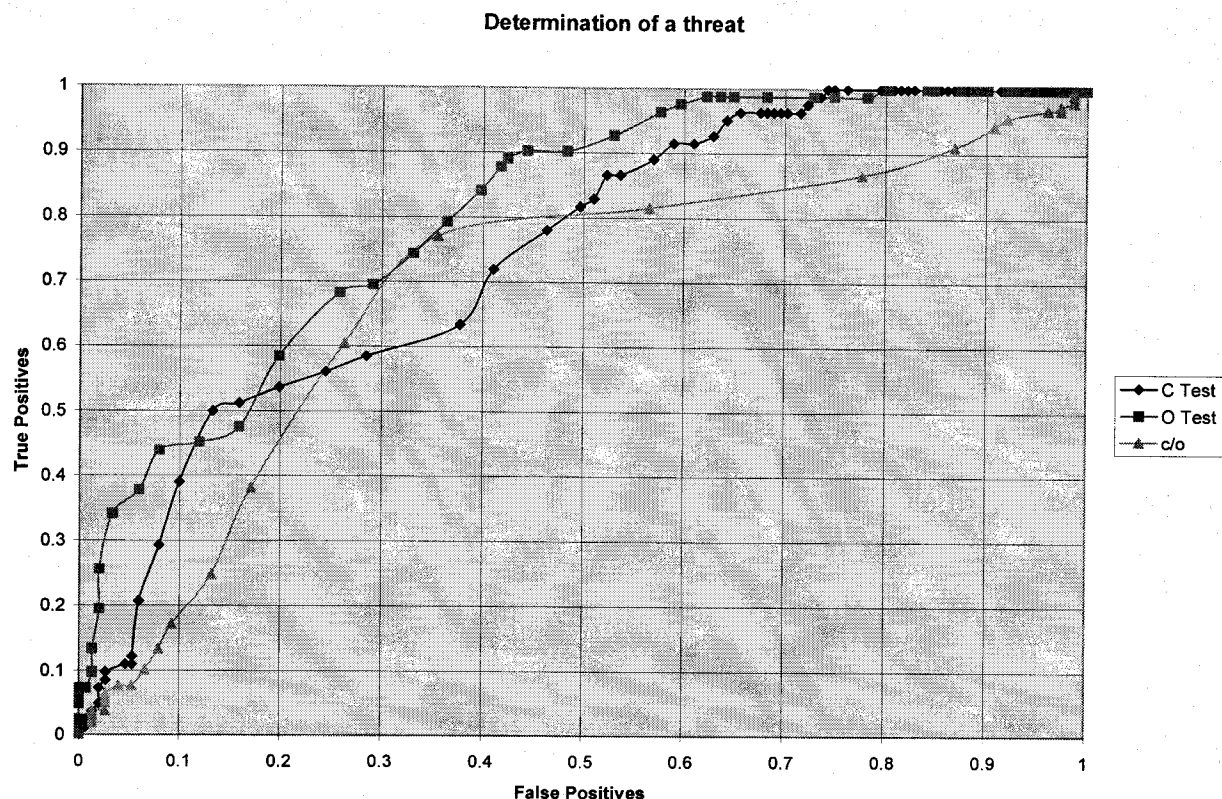


Figure 63C. ROC curves for C elemental content, O elemental content, and their ratio.

5.1.7 DECISION TREE

Runs #1300-1816 were taken with a variety of shells (with different fills) shape charges, sheet explosives, landmines, etc. . The purpose of these data were to assist in making a reliable decision tree. Subsequent to that, runs #1825-1999 were to be used as "blind tests" to check the reliability of the decision tree.

The time between the first group of runs and the second one, was not sufficient to create a reliable decision tree. Given the variety of fills, shells, explosives, etc., we opted to accumulate all the data and refrain from making decisions on the fill. Upon the return to API, after ascertaining that the date were correctly reduced while operating in an automatic mode at Indian Head, a decision tree was made, using H,C,O, and N and the elemental ratios C/H and C/N.

5.1.7.1 Building the First Decision Tree

The first step in building a decision-tree is to examine the repeated data and examine whether a pattern emerges. Tables 17A and 17B show the statistical analysis of the repeated spectra collected during this demonstration.

We now will examine the larger shell sizes (>105 mm). The large fill sizes in these shells give the strongest signals to analyze. On the table, both TNT and CompB have C/H > 1.

Examining the shells with sizes around 76mm, there is seems to be a correlation between the smaller amounts of H and the TNT. Since some of these amounts are less than 0, an artificial change (if $H < 0$ then $H = .001$) is made to simplify the conditions and further segregate the data.

Table 17B and Figure 63 both indicate a strong correlation between the N content and explosives. However, as discussed in Section 2.2, the more elements which can be used in a condition, the lower the probability of false alarms. Thus, the amount of N is deemed not sufficient and the ratio of C to N (C/N) is used to increase the selection criteria.

Table 17A. The average, standard deviation, maximum, and minimum for the C content (cps) and H content (cps) for the repeated spectra.

Number of Repeats	Size	Fill	Surface	C (cps)	St Dev (cps)	Max (cps)	Min (cps)	H (cps)	St Dev (cps)	Max (cps)	Min (cps)
2	60	TNT	GRAVEL	3.04	0.76	3.57	2.50	2.07	2.02	3.50	0.64
2	60	TNT	SOIL	0.74	2.18	2.28	-0.80	-1.87	0.89	-1.24	-2.50
2	60	TNT	WET SOIL	2.95	0.78	3.50	2.40	2.88	2.51	4.65	1.10
2	60	WAX	WET SOIL	2.45	1.06	3.20	1.70	1.80	2.97	3.90	-0.30
2	76	RDX	SAND	4.33	2.30	5.95	2.70	0.57	1.93	1.93	-0.80
11	76	RDX	SOIL	4.09	1.07	4.95	1.40	-4.35	3.81	1.91	-9.31
2	76	TNT	SOIL	2.30	1.56	3.40	1.20	-5.62	7.05	-0.63	- 10.60
3	81	PLASTE R	SAND	1.53	0.53	2.10	1.04	6.68	1.71	8.20	4.82
12	81	PLASTE R	SOIL	1.67	1.00	3.14	-0.70	-2.27	3.69	6.48	-5.84
3	81	PLASTE R	WETSOIL	3.45	2.25	5.95	1.60	3.60	0.35	3.81	3.20
2	81	SAND	SAND	1.73	1.07	2.48	0.97	-2.79	1.23	-1.92	-3.66
2	82	TNT	GRAVEL	7.06	2.21	8.62	5.50	1.39	0.30	1.60	1.17
2	82	TNT	SAND	6.39	0.56	6.78	5.99	-0.39	2.65	1.49	-2.26
3	82	TNT	SOIL	2.68	2.61	5.08	-0.10	-7.20	6.42	-1.25	- 14.00
2	82	TNT	TABLE	1.19	2.39	2.88	-0.50	0.97	4.99	4.50	-2.56
2	82	TNT	WETSOIL	5.30	0.99	6.00	4.60	-5.80	0.42	-5.50	-6.10
2	90	RDX	WETSOIL	7.12	3.27	9.43	4.80	4.51	4.23	7.50	1.52
2	90	TNT/RD X	GRAVEL	18.27	0.32	18.49	18.04	1.72	1.26	2.61	0.83
2	90	TNT/RD	WETSOIL	17.98	4.91	21.45	14.50	3.86	1.28	4.76	2.95

Number of Repeats	Size	Fill	Surface	C (cps)	St Dev (cps)	Max (cps)	Min (cps)	H (cps)	St Dev (cps)	Max (cps)	Min (cps)
		X									
2	105	SAND	SOIL	-0.50	1.48	0.55	-1.55	3.79	17.23	15.97	-8.39
13	105	WAX	SOIL	5.07	0.94	6.45	2.50	10.93	4.85	24.5	5.34
2	105	WAX	TABLE	3.04	5.99	7.27	-1.20	7.76	3.46	10.20	5.31
2	105	WAX	WETSOIL	7.92	3.42	10.33	5.50	5.89	1.99	7.30	4.48
2	122	COMPB	SOIL	12.45	1.91	13.80	11.10	15.70	6.65	20.40	11.00
2	122	COMPB	TABLE	12.33	1.65	13.50	11.16	6.06	0.37	6.32	5.80
2	155	RED	SOIL	11.28	5.36	15.07	7.49	51.14	24.95	68.78	33.49
2	155	TNT	SAND	19.77	2.21	21.33	18.20	6.27	3.83	8.98	3.56
2	6%	ANFO	GRAVEL	6.35	1.10	7.12	5.57	18.08	3.85	20.80	15.36
2	6%	ANFO	WETSOIL	6.89	4.13	9.81	3.97	28.91	9.40	35.55	22.26
2	Sheet explo	PETN	GRAVEL	36.15	0.14	36.25	36.05	40.47	0.91	41.11	39.82
2	Sheet explo	PETN	SOIL	28.53	4.93	32.01	25.04	52.08	1.32	53.01	51.14
2	Val69 Mine	COMPB	SAND	8.62	0.81	9.19	8.04	3.18	1.53	4.26	2.10
2	Val69 Mine	COMPB	SOIL	5.86	2.72	7.78	3.93	2.56	1.17	3.38	1.73

Table 17B. The average, standard deviation, maximum, and minimum for the N content (cps) and O content (cps) for the repeated spectra.

Number of Repeats	Size	Fill	Surface	N (cps)	St Dev (cps)	Max (cps)	Min (cps)	O (cps)	St Dev (cps)	Max (cps)	Min (cps)
2	60	TNT	GRAVEL	0.70	0.00	0.70	0.70	1.49	3.56	4.00	-1.03
2	60	TNT	SOIL	-0.47	1.18	0.37	-1.30	-2.33	1.03	-1.60	-3.06
2	60	TNT	WET SOIL	0.35	0.49	0.70	0.00	-2.65	3.32	-0.30	-5.00
2	60	WAX	WET SOIL	0.15	0.21	0.30	0.00	0.00	0.00	0.00	0.00
2	76	RDX	SAND	1.16	0.22	1.31	1.00	1.06	1.07	1.81	0.30
11	76	RDX	SOIL	-0.61	0.39	0.00	-1.40	-1.17	1.14	0.98	-3.15
2	76	TNT	SOIL	-2.09	1.43	-1.08	-3.10	-3.71	2.96	-1.62	-5.80
3	81	PLASTER	SAND	-0.38	1.33	0.95	-1.70	0.83	0.98	1.47	-0.30
12	81	PLASTER	SOIL	-1.99	1.35	-0.20	-5.31	-0.16	1.95	2.25	-5.46
3	81	PLASTER	WETSOIL	0.64	0.56	1.00	0.00	1.44	0.27	1.60	1.13
2	81	SAND	SAND	-0.17	0.62	0.27	-0.60	-1.91	1.70	-0.71	-3.11
2	82	TNT	GRAVEL	0.71	1.68	1.90	-0.48	4.01	5.23	7.70	0.31
2	82	TNT	SAND	1.26	0.85	1.86	0.66	0.86	1.42	1.86	-0.15
3	82	TNT	SOIL	-0.91	1.86	0.58	-3.00	-1.11	0.56	-0.60	-1.71
2	82	TNT	TABLE	0.64	0.66	1.10	0.17	1.26	0.64	1.71	0.80
2	82	TNT	WETSOIL	0.95	1.63	2.10	-0.20	-2.15	0.64	-1.70	-2.60
2	90	RDX	WETSOIL	3.64	0.62	4.07	3.20	-0.92	0.83	-0.33	-1.50
2	90	TNT/RDX	GRAVEL	3.90	0.34	4.14	3.66	3.78	0.57	4.18	3.37
2	90	TNT/RDX	WETSOIL	3.92	1.35	4.87	2.96	3.43	3.15	5.65	1.20
2	105	SAND	SOIL	-0.43	1.20	0.42	-1.27	-1.02	2.37	0.66	-2.69
13	105	WAX	SOIL	-1.38	1.02	0.12	-3.49	-3.87	1.16	-2.07	-6.80
2	105	WAX	TABLE	0.11	0.42	0.40	-0.19	0.53	2.59	2.36	-1.30
2	105	WAX	WETSOIL	3.27	5.71	7.30	-0.77	-3.93	0.67	-3.45	-4.40

Number of Repeats	Size	Fill	Surface	N (cps)	St Dev (cps)	Max (cps)	Min (cps)	O (cps)	St Dev (cps)	Max (cps)	Min (cps)
2	122	COMPB	SOIL	5.05	2.47	6.80	3.30	6.60	2.55	8.40	4.80
2	122	COMPB	TABLE	5.97	0.75	6.50	5.44	12.64	2.63	14.50	10.78
2	155	RED	SOIL	0.48	1.69	1.67	-0.72	3.73	1.74	4.96	2.50
2	155	TNT	SAND	5.46	1.09	6.23	4.69	8.37	2.26	9.97	6.77
2	6%	ANFO	GRAVEL	4.60	1.45	5.62	3.57	9.23	0.69	9.71	8.74
2	6%	ANFO	WETSOIL	5.66	1.52	6.73	4.58	9.85	1.79	11.11	8.58
2	Sheet explo	PETN	GRAVEL	5.80	0.56	6.19	5.40	18.86	0.71	19.36	18.35
2	Sheet explo	PETN	SOIL	7.47	0.76	8.01	6.93	14.75	0.52	15.11	14.38
2	Val69 Mine	COMPB	SAND	1.77	0.76	2.31	1.23	2.16	0.47	2.49	1.82
2	Val69 Mine	COMPB	SOIL	2.51	0.33	2.74	2.27	1.54	0.89	2.17	0.91

All of these factors went into the first decision tree for the shell data collected during the demonstration. Figure 64 shows the decision tree implemented for all the shell data.

Tables 18 and 19 show all the shell data in two segments: Table 18 includes all the data and the PELAN fill identification for shells between 155 mm and 76 mm inclusive. Table 19 has all the data and the PELAN fill identification for all 60 mm shells.

In both tables, some of the values have been manipulated to show their values in the decision tree process (e.g. all $H \leq 0$ have been set to $H=0.01$).

The highlighted rows mean:

- False positive PELAN identification
- False negative PELAN identification

where a false positive is a declaration of a hazard where none exists and false negative is declaration of a non-hazard where one exists.

In Table 18, using the highlighted blue line, we can divide the shells in two groups, namely the 155mm-90 mm shell group, and the 82 mm-76 mm shell group. The significance of this separation is due to the fact that prior to the Indian Head tests, the emphasis on the PELAN shell fill identification was concentrated to 105 mm and 90 mm shells. Therefore, the PELAN development was focused in that direction and not towards smaller shells. Based on the above grouping, Table 20 shows the percentage of false PELAN identification of the various fills.

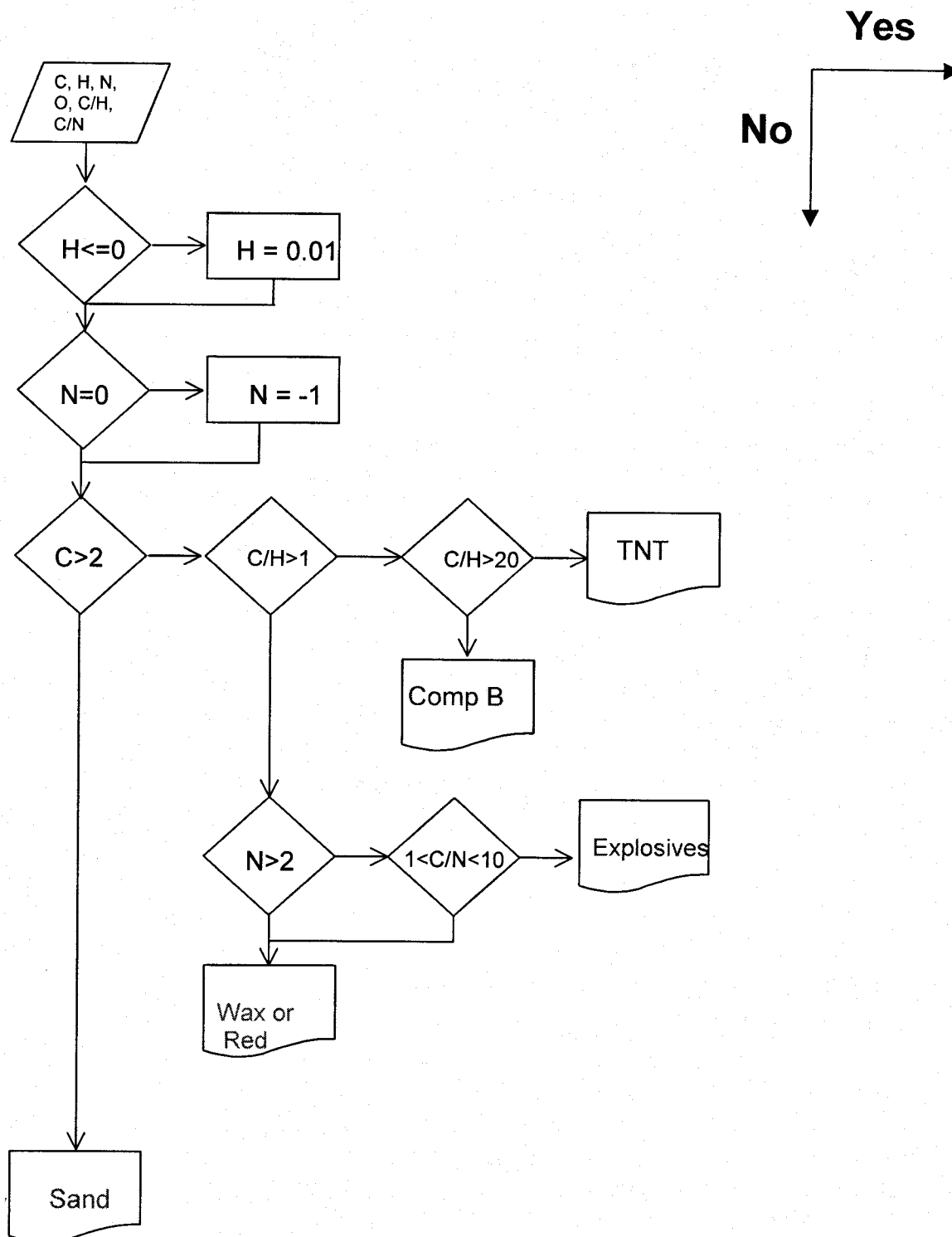


Figure 64. Decision tree for the shell data taken at NAVEODTECH.

Table 18. Data for shells from 155 mm to 76mm. Column 3 shows the actual fill of the shell, and the next-to-last column the PELAN identification. The last column indicates at which decision point the failure occurred.

Size (mm)	Amount of Fill	Fill	Surface	C (cps)	H (cps)	N (cps)	O (cps)	C/H	C/N	Decision Tree Result	Failure Mode
155	13.2 lbs	EMPTY	SOIL	-2.1	1.5	-2.1	-0.8	-1.40	0.98	Sand	
		RED	SOIL	7.5	33.5	1.7	5.0	0.22	4.49	Wax or Red	
		WAX	SOIL	8.3	59.9	1.6	1.9	0.14	5.20	Wax or Red	
		TNT	SOIL	18.8	5.4	4.9	5.5	3.51	3.86	CompB	
		TNT	TABLE	29.4	0.0	6.4	16.1	2941.00	4.62	TNT	
		TNT	GRAVEL	20.5	8.4	3.5	7.7	2.45	5.85	CompB	
		TNT	SAND	21.3	9.0	6.2	10.0	2.38	3.42	CompB	
		TNT	WETSOIL	19.2	0.0	7.9	5.2	1920.00	2.42	TNT	
		TNT	SAND	18.2	3.6	4.7	6.8	5.11	3.88	CompB	
		RED	SAND	14.7	55.1	-0.6	0.9	0.27	-24.05	Wax or Red	
		WAX	Gravel	14.1	102.9	1.0	-2.4	0.14	13.71	Wax or Red	
		RED	Soil	15.1	68.8	-0.7	2.5	0.22	-20.93	Wax or Red	
		WAX	Wetsoil	10.1	26.5	3.7	2.9	0.38	2.73	Explosives	
122	7.3 lbs	COMPB	SAND	15.3	8.1	6.2	11.0	1.89	2.47	CompB	
		COMPB	GRAVEL	11.9	6.7	4.5	10.8	1.78	2.64	CompB	
		COMPB	TABLE	13.5	5.8	6.5	14.5	2.33	2.08	CompB	
		COMPB	SOIL	11.1	11.0	3.3	4.8	1.01	3.36	CompB	
		COMPB	SOIL	13.8	20.4	6.8	8.4	0.68	2.03	Explosives	
		PROPEL.	WETSOIL	26.0	18.0	6.8	18.0	1.44	3.82	CompB	
		COMPB	Table	11.2	6.3	5.4	10.8	1.77	2.05	CompB	
120	2.7 lbs	TNT	SAND	11.3	0.7	2.3	4.1	16.14	4.91	CompB	
		TNT	GRAVEL	8.6	1.9	2.8	3.5	4.53	3.07	CompB	
		TNT	TABLE	13.7	1.4	4.5	8.5	9.79	3.04	CompB	
		TNT	SOIL	7.8	0.0	2.4	0.6	780.00	3.25	TNT	
		TNT	Wetsoil	17.4	0.0	7.5	3.9	1735.00	2.30	TNT	
105	2 lbs	WAX	SOIL	4.4	13.9	-1.8	-3.6	0.32	-2.45	Wax or Red	
		WAX	SOIL	5.3	11.6	0.1	-3.1	0.46	43.17	Wax or Red	
		WAX	SOIL	5.0	11.0	-1.0	-3.1	0.45	-4.83	Wax or Red	
		WAX	SOIL	5.7	9.5	-0.2	-2.6	0.60	-35.50	Wax or Red	
		WAX	SOIL	5.3	10.1	-1.5	-2.1	0.52	-3.47	Wax or Red	
		WAX	SOIL	5.5	13.3	-1.9	-4.0	0.42	-2.88	Wax or Red	
		WAX	SOIL	5.1	7.9	-0.5	-4.0	0.64	-9.79	Wax or Red	
		WAX	SOIL	5.5	8.2	-3.5	-4.8	0.67	-1.56	Wax or Red	

Size (mm)	Amount of Fill	Fill	Surface	C (cps)	H (cps)	N (cps)	O (cps)	C/H	C/N	Decision Tree Result	Failure Mode
		WAX	SOIL	4.8	5.3	-0.3	-4.6	0.89	-16.88	Wax or Red	
		WAX	SOIL	5.8	12.4	-1.2	-4.2	0.47	-4.83	Wax or Red	
		WAX	SOIL	4.7	8.0	-1.8	-3.4	0.59	-2.66	Wax or Red	
		SAND	SOIL	-1.6	0.0	-1.3	-2.7	-155.00	1.22	Sand	
		WAX	SAND	4.7	18.2	-1.1	-3.1	0.26	-4.27	Wax or Red	
		WAX	GRAVEL	8.2	23.0	-0.5	2.9	0.36	-16.40	Wax or Red	
		WAX	TABLE	-1.2	10.2	0.4	-1.3	-0.12	-3.00	Sand	
		WAX	SOIL	2.5	6.3	-2.6	-6.8	0.40	-0.96	Wax or Red	
		WAX	WETSOIL	5.5	7.3	7.3	-4.4	0.75	0.75	Wax or Red	
		WAX	TABLE	7.3	5.3	-0.2	2.4	1.37	-38.26	CompB	C/H>1
		SAND	SAND	0.9	0.0	0.6	-1.4	94.00	1.62	Sand	
		WAX	Soil	6.5	24.5	-1.8	-4.1	0.26	-3.66	Wax or Red	
		SAND	Soil	0.6	16.0	0.4	0.7	0.03	1.31	Sand	
		WAX	Wetsoil	10.3	4.5	-0.8	-3.5	2.31	-13.42	CompB	C/H>1
		RED	Wetsoil	9.9	2.6	2.2	-0.9	3.81	4.40	CompB	C/H>1
		EMPTY	Wetsoil	8.9	0.0	2.6	-4.4	892.00	3.40	TNT	C/H>1
		SAND	Table	-7.9	6.3	1.1	4.3	-1.27	-7.33	Sand	
90	1.6 lbs	TX50	SOIL	4.0	0.0	0.9	0.5	401.00	4.46	TNT	
		TX50	TABLE	6.1	2.4	1.4	4.7	2.50	4.24	CompB	
		TX50	GRAVEL	9.6	0.0	1.9	1.5	961.00	5.17	TNT	
		TX50	SAND	8.4	0.0	1.7	0.1	838.00	4.93	TNT	
		TNT/RDX	Wetsoil	21.5	4.8	4.9	5.7	4.51	4.40	CompB	
	1.1 lbs	rocket 1.1lb60/40	SOIL	12.9	7.3	3.4	4.0	1.77	3.84	CompB	
		rocket 1.1lb60/40	TABLE	12.1	3.5	2.6	9.2	3.48	4.74	CompB	
		rocket 1.1lb60/40	GRAVEL	18.0	2.6	3.7	4.2	6.91	4.93	CompB	
		rocket 1.1lb60/40	SAND	17.2	1.6	3.0	3.3	11.02	5.77	CompB	
		rocket 1.1lb60/40	WETSOIL	14.5	3.0	3.0	1.2	4.92	4.90	CompB	
		rocket 1.1lb60/40	Gravel	18.5	0.8	4.1	3.4	22.28	4.47	TNT	
		RED	SOIL	4.2	0.0	-2.4	-7.0	415.00	-1.71	TNT	C/H>1
		RED	SAND	6.2	0.0	-0.6	-3.1	621.00	-10.71	TNT	C/H>1
		RED	Wetsoil	8.8	0.0	0.9	-2.3	875.00	9.62	TNT	C/H>1
		Red	Table	-3.4	0.0	0.5	-2.1	-337.00	-6.74	Sand	
	1.8 lbs	RDX	SAND	3.0	1.7	0.6	1.5	1.76	5.00	CompB	
		RDX	GRAVEL	3.8	1.3	-0.2	-0.9	2.92	-19.00	CompB	
		RDX	TABLE	2.0	2.9	2.9	2.9	1.50	1.50	Sand	
		RDX	SOIL	3.7	1.3	-0.2	-2.6	2.85	-18.50	CompB	
		RDX	WETSOIL	4.8	7.5	3.2	-1.5	0.64	1.50	Explosives	

Size (mm)	Amount of Fill	Fill	Surface	C (cps)	H (cps)	N (cps)	O (cps)	C/H	C/N	Decision Tree Result	Failure Mode
		RDX	Wetsoil	9.4	1.5	4.1	-0.3	6.20	2.32	CompB	
		COMPB	WETSOIL	6.5	3.1	3.0	-4.1	2.10	2.17	CompB	
82	1.4 lbs	COMPB	GRAVEL	6.4	4.7	-1.0	6.4	1.36	-6.40	CompB	
		TNT	GRAVEL	5.5	1.6	1.9	7.7	3.44	2.89	CompB	
		TNT	TABLE	0.5	0.0	-3.0	-0.6	-10.00	0.03	Sand	C/H>1
		TNT	SOIL	-0.1	0.0	-3.0	-0.6	-10.00	0.03	Sand	C/H>1
		TNT	WETSOIL	4.6	0.0	-0.2	-2.6	460.00	-23.00	TNT	
		TNT	WETSOIL	6.0	0.0	2.1	-1.7	600.00	2.86	TNT	
		TNT	SOIL	3.1	0.0	-0.3	-1.0	307.00	-9.90	TNT	
		TNT	TABLE	2.9	0.0	0.2	1.7	288.00	16.94	TNT	
		TNT	GRAVEL	8.6	1.2	-0.5	0.3	7.37	-17.96	CompB	
		TNT	SAND	6.0	0.0	0.7	-0.2	599.00	9.08	TNT	
		TNT	SAND	6.8	1.5	1.9	1.9	4.55	3.65	CompB	
		TNT	SOIL	5.1	0.0	0.6	-1.7	508.00	8.76	TNT	
81	2 lbs	PLASTER	SOIL	3.1	6.5	-1.8	2.3	0.48	-1.79	Wax or Red	
		PLASTER	SOIL	2.1	0.0	-2.0	1.1	207.00	-1.02	TNT	C/H>1
		PLASTER	SOIL	2.2	0.0	-1.9	-0.8	220.00	-1.14	TNT	C/H>1
		PLASTER	SOIL	2.4	0.0	-1.8	-0.6	243.00	-1.34	TNT	C/H>1
		PLASTER	SOIL	2.5	0.0	-1.0	-0.8	247.00	-2.38	TNT	C/H>1
		PLASTER	SOIL	0.9	0.0	-3.4	-0.2	85.80	-0.25	Sand	
		PLASTER	SOIL	1.0	0.0	-2.5	-0.2	104.00	-0.41	Sand	
		PLASTER	SOIL	1.5	0.0	-2.0	0.9	150.00	-0.75	Sand	
		PLASTER	SOIL	2.0	0.0	-1.3	0.3	196.00	-1.51	Sand	
		PLASTER	SOIL	2.0	0.0	-0.6	1.9	198.00	-3.54	Sand	
		SAND	SOIL	0.4	0.0	-3.0	-3.7	43.40	-0.15	Sand	
		WAX	SOIL	3.8	0.5	-3.7	-5.4	7.57	-1.03	CompB	
		EMPTY	SOIL	0.8	0.0	-3.2	-4.8	76.00	-0.24	Sand	
		EMPTY	SOIL	0.8	0.0	-3.2	-4.8	76.00	-0.24	Sand	
		PLASTER	SOIL	1.1	0.0	-5.3	-5.5	111.00	-0.21	Sand	
		PLASTER	SAND	2.1	8.2	-1.7	-0.3	0.26	-1.24	Wax or Red	
		COMPB	SAND	4.8	0.0	-0.1	0.0	480.00	-48.00	TNT	
		TNT	SAND	2.4	0.0	0.2	-0.4	240.00	12.00	TNT	
		PLASTER	GRAVEL	2.1	11.5	0.3	9.3	0.18	7.00	Wax or Red	
		PLASTER	TABLE	-4.1	4.3	-0.8	5.0	-0.95	5.13	Sand	
		COMPB	TABLE	1.6	0.0	-2.5	-2.5	160.00	-0.64	Sand	
		PLASTER	SOIL	-0.7	3.8	-0.2	-0.2	-0.18	3.50	Sand	
		POP	WETSOIL	2.8	3.8	-1.0	1.6	0.74	-2.80	Wax or Red	
		POP	WETSOIL	1.6	3.2	1.0	1.6	0.50	1.60	Sand	
		COMPB	WETSOIL	6.0	0.0	2.4	0.0	600.00	2.50	TNT	
		PLASTER	SAND	1.0	4.8	1.0	1.3	0.22	1.09	Sand	
		WAX	SAND	5.4	7.0	-0.8	-3.7	0.77	-6.81	Wax or Red	
		SAND	SAND	2.5	0.0	-0.6	-3.1	248.00	-4.13	TNT	C/H>1
		POP	SAND	1.5	7.0	-0.4	1.5	0.21	-3.74	Sand	

Size (mm)	Amount of Fill	Fill	Surface	C (cps)	H (cps)	N (cps)	O (cps)	C/H	C/N	Decision Tree Result	Failure Mode
		Sand	SAND	1.0	0.0	0.3	-0.7	97.00	3.59	Sand	
		COMPB	Gravel	9.5	3.5	3.6	1.5	2.74	2.61	CompB	
		POP	Wetsoil	6.0	3.8	0.9	1.1	1.56	6.47	CompB	
		Sand	Wetsoil	6.8	0.0	1.7	0.0	681.00	4.13	TNT	C/H>1
		SAND	Table	-2.4	0.0	-0.8	-0.3	-236.00	3.06	Sand	
76	1.7 lbs	RDX	SOIL	4.0	0.0	-0.5	-1.3	403.00	-8.00	TNT	
		RDX	SOIL	4.1	0.0	0.0	-1.1	408.00	00	TNT	
		RDX	SOIL	4.4	0.0	-0.7	-0.8	437.00	-6.48	TNT	
		RDX	SOIL	4.6	0.0	-0.6	0.0	456.00	-7.72	TNT	
		RDX	SOIL	4.6	0.0	-0.6	-1.7	456.00	-7.20	TNT	
		RDX	SOIL	4.8	0.0	-0.6	-2.0	475.00	-8.39	TNT	
		RDX	SOIL	4.9	0.0	-0.2	1.0	486.00	-23.82	TNT	
		RDX	SOIL	5.0	0.0	-0.4	-2.2	495.00	-12.38	TNT	
		RDX	SOIL	2.9	1.9	-1.1	-0.3	1.54	-2.60	CompB	
		RDX	SOIL	3.8	0.0	-0.6	-3.2	382.00	-6.35	TNT	
		RDX	SAND	2.7	0.0	1.0	0.3	270.00	2.70	TNT	
		TNT	SAND	4.0	0.0	-1.0	-2.9	400.00	-4.00	TNT	
		RDX	GRAVEL	5.0	5.0	2.5	4.9	1.00	2.00	Explosives	
		TNT	GRAVEL	5.6	0.8	-1.0	3.7	7.00	-5.60	CompB	
		RDX	TABLE	-2.7	0.2	-2.7	-1.0	-13.50	-1.00	Sand	C<2
		TNT	TABLE	-3.9	0.0	0.6	-1.4	-390.00	-6.50	Sand	C<2
		RDX	SOIL	1.4	1.7	-1.4	-1.2	0.82	-1.00	Sand	C<2
		TNT	SOIL	1.2	0.0	-3.1	-5.8	120.00	0.39	Sand	C<2
		RDX	WETSOIL	5.4	0.0	4.8	1.3	540.00	1.13	TNT	
		TNT	WETSOIL	4.3	0.0	2.0	-2.7	430.00	2.15	TNT	
		RDX	SAND	6.0	1.9	1.3	1.8	3.08	4.54	CompB	
		TNT	Soil	3.4	0.0	-1.1	-1.6	340.00	-3.15	TNT	

Table 19 Data for the 60 mm shells. Column 3 shows the actual fill of the shell, and the next-to-last column the PELAN identification. The last column indicates at which decision point the failure occurred.

Size (mm)	Amount of Fill	Fill	Surface	C (cps)	H (cps)	N (cps)	O (cps)	C/H	C/N	Decision Tree Result	Failure Mode
60	0.9 lbs	RED	SOIL	2.0	0.0	-1.7	-4.0	196	-1.15	Sand	
		EMPTY	SOIL	0.7	0.0	-5.2	-7.1	65.50	-0.13	Sand	
		EMPTY	SOIL	0.7	0.0	-5.2	-7.1	65.50	-0.13	Sand	
		PLASTER	SOIL	0.8	0.0	-5.1	-7.8	81.90	-0.16	Sand	
		WAX	SOIL	1.6	0.0	-3.8	-6.2	156	-0.41	Sand	
		BP	SAND	0.8	0.0	-1.1	-0.6	78.00	-0.71	Sand	C<2
		TNT	SAND	1.9	0.0	-1.0	-2.1	190	-1.90	Sand	C<2
		TNT	GRAVEL	2.5	3.5	0.7	4.0	0.71	3.57	Wax or Red	N<2
		BP	TABLE	-4.7	0.0	0.2	-0.4	-470	-23.50	Sand	C<2
		TNT	TABLE	-1.6	4.3	1.1	-0.5	-0.37	-1.45	Sand	C<2
		TNT	SOIL	-0.8	0.0	-1.3	-1.6	-80.00	0.62	Sand	C<2

	TNT	WETSOIL	3.9	4.7	-1.0	-0.3	0.75	-3.50	Red	
	POP	WETSOIL	1.5	2.8	0.7	0.7	0.52	2.09	Sand	
	WAX	WETSOIL	3.2	3.9	-1.0	0.0	0.82	-3.20	Wax or Red	
	WAX	WETSOIL	1.7	-0.3	0.3	0.0	-5.67	5.67	Sand	
	TNT	WETSOIL	2.4	1.1	0.7	-5.0	2.18	3.43	CompB	
	WAX	SAND	2.1	0.5	-0.2	-0.5	4.40	-12.18	CompB	C/H>1
	PLASTER	SAND	1.7	0.1	0.8	-2.1	18.56	2.06	Sand	
	RED	SAND	1.4	-1.5	1.9	-1.9	-0.94	0.75	Sand	
	TNT	Gravel	3.6	0.6	0.7	-1.0	5.58	5.10	CompB	
	POP	Gravel	1.7	-0.4	0.6	-1.0	-4.49	2.81	Sand	
	TNT	Soil	2.3	-1.2	0.4	-3.1	-1.84	6.16	TNT	
	Pop	Table	-2.5	0.1	1.0	-0.6	-51	-2.57	Sand	

The false positive rate calculated in Table 20 utilizes the following formula:

$$\text{FalsePositiveRate} = \frac{\# \text{FalsePositives}}{\# \text{ofInertItemsEncountered}}$$

and the false negative rate:

$$\text{FalseNegativeRate} = \frac{\# \text{FalseNegatives}}{\# \text{ofExplosivesEncountered}}$$

Table 20. Collective results for decision tree in Figure 64.

Shell Size	Inert/Empty Shell Results			Explosive Shell Results		
	# Shells	# Incorrect Positive	% False Pos	# Shells	# Incorrect Negative	% False Neg
90-155	36	8	22	36	1	3
76-82	29	8	28	40	8	20
60	13	1	8	10	7	70
All	78	17	23	86	16	19

5.1.7.2 Analysis of Failures in First Decision Tree

The primary failure mode for false negatives is the low C count rate. For 13 out of 15 of the false negatives, $C < 2$. In the other two cases, $C > 2$ but its relatively high H content force $C/H < 1$. Since no or low N was measured, the second failure was in $N < 2$.

The primary failure mode (17 out of 18) for false positives was a very low or negative H count-rate. Since H is arbitrarily set to 0.01 if $H < 0$, this forces high C/H ratios. Once $C/H > 1$, then the only possible return value is an explosive. For completeness, a spurious N signal in a 155mm wax-filled shell forced a decision to "Explosives".

Making a more general statement about failures, we can say that they occur when the SPIDER analysis returns near-zero values. For example, the values returned in the four false negatives at 76mm are statistically zeroes or near-zero values.

In Figure 65, we have the ROC curves for the various stages of the decision tree shown in Figure 64. According to this diagram, the best decision points are the condition on C ($C > 2$), and the condition on N ($N > 2$). The curves for the C/H conditions are approximately the same. The most troubling curve is the C/N condition which seems to indicate an invalid test condition. Of the 164 test cases, only 5 survive to this condition. It may be that the decision tree would not suffer if this condition were relaxed or eliminated.

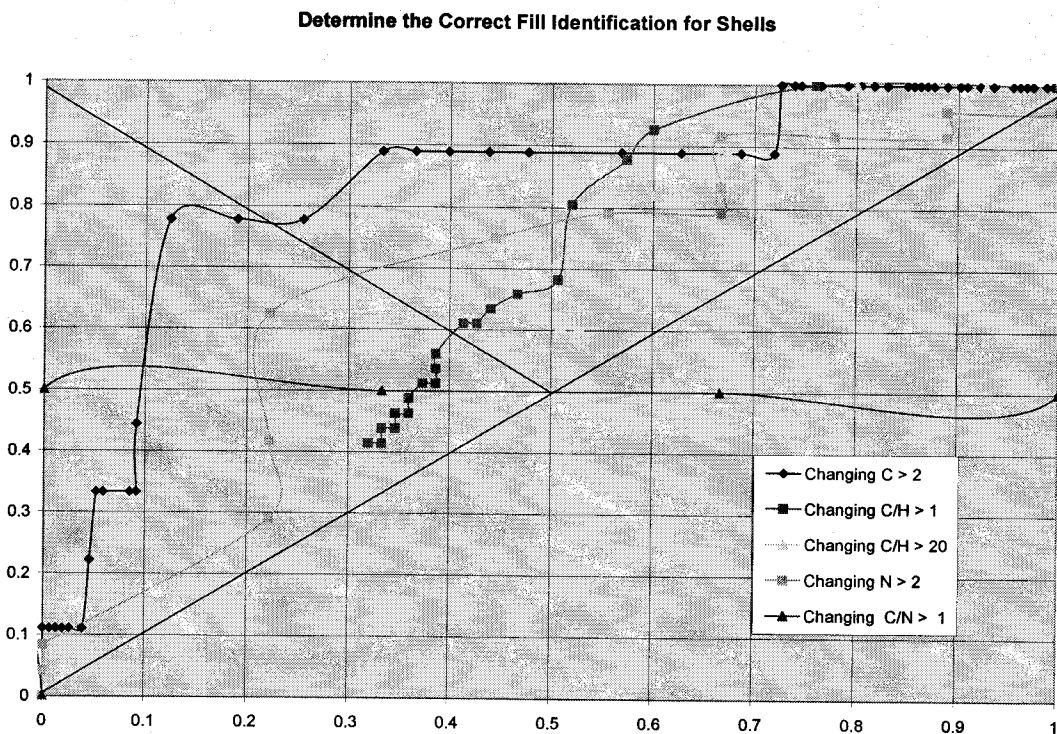


Figure 65. ROC curves for various decision tree points. The decision tree is shown in Figure 64. See text for details.

When re-examining the data during the completion of this report, we realized that segregating the data by shell-size had advantages in the decision-making process. A separate, nearly autonomous, decision-tree for each shell size could be made. An example is given in Figure 66 for 60mm shells. When this decision tree is applied to the 60 mm shell data in Table 19, a 38% false positive rate and 0% false negative rate is achieved. Based on this, we expect that we could improve the performance of the decision-making process by incorporating the size

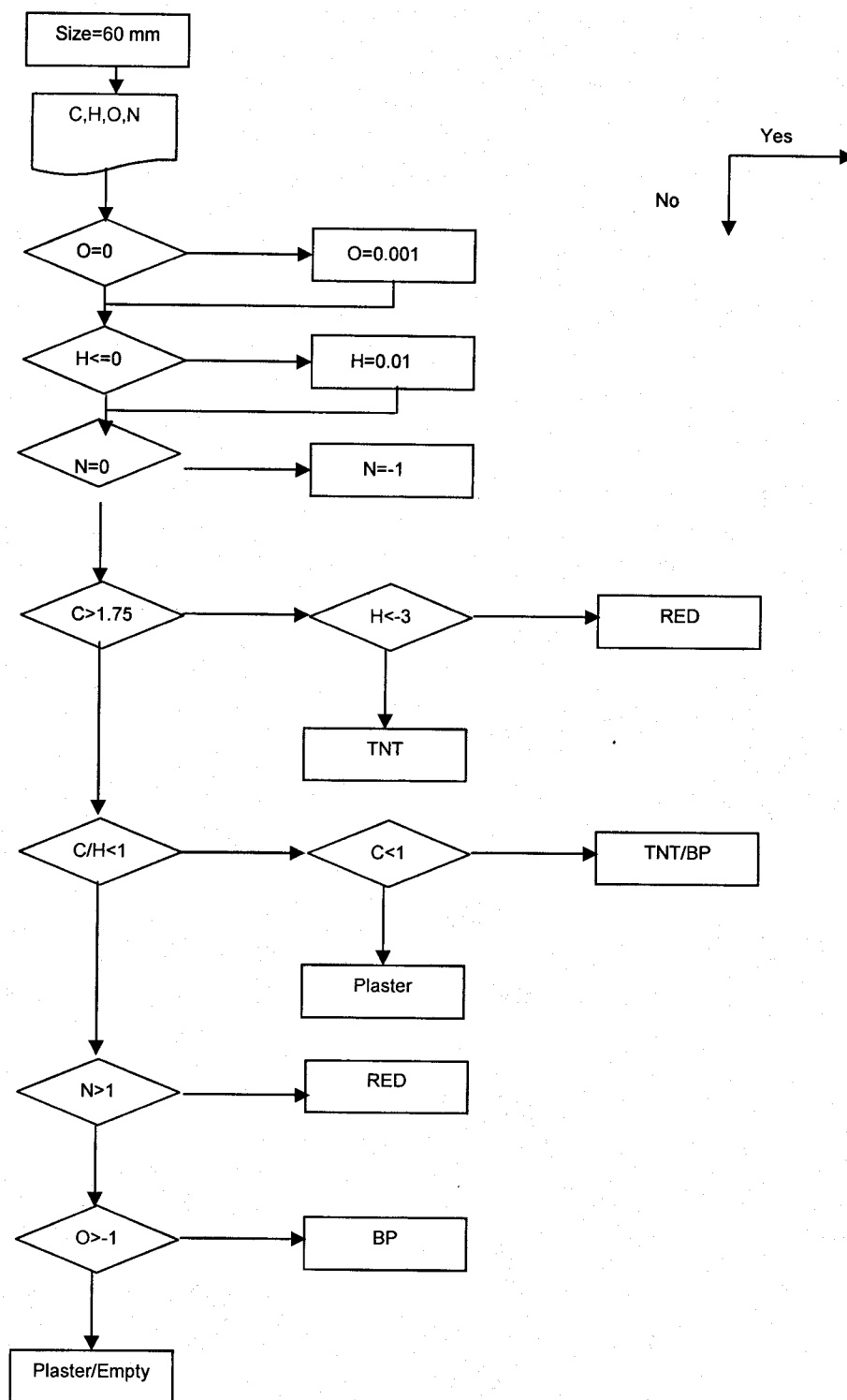


Figure 66. Decision tree for 60mm shells only.

5.1.7.3 Building the Second Decision Tree

Along with the testing of shells at Indian Head, several runs were also taken using explosives that are not used as shell fill. These explosives included SEMTEX, ANFO, Sheet explosive, shape charges, smokeless powder, as well as landmines. To include these runs in a PELAN decision tree, the shell decision tree shown in Fig. 64 was modified as shown in Figure 67. The modification was primarily in the N content, to allow the identification of ANFO. Table 21 is a compilation of all the data taken at Indian Head, with all forms of explosives. The wrong PELAN identification are highlighted as before, namely green for False Positive, and red for False Negative.

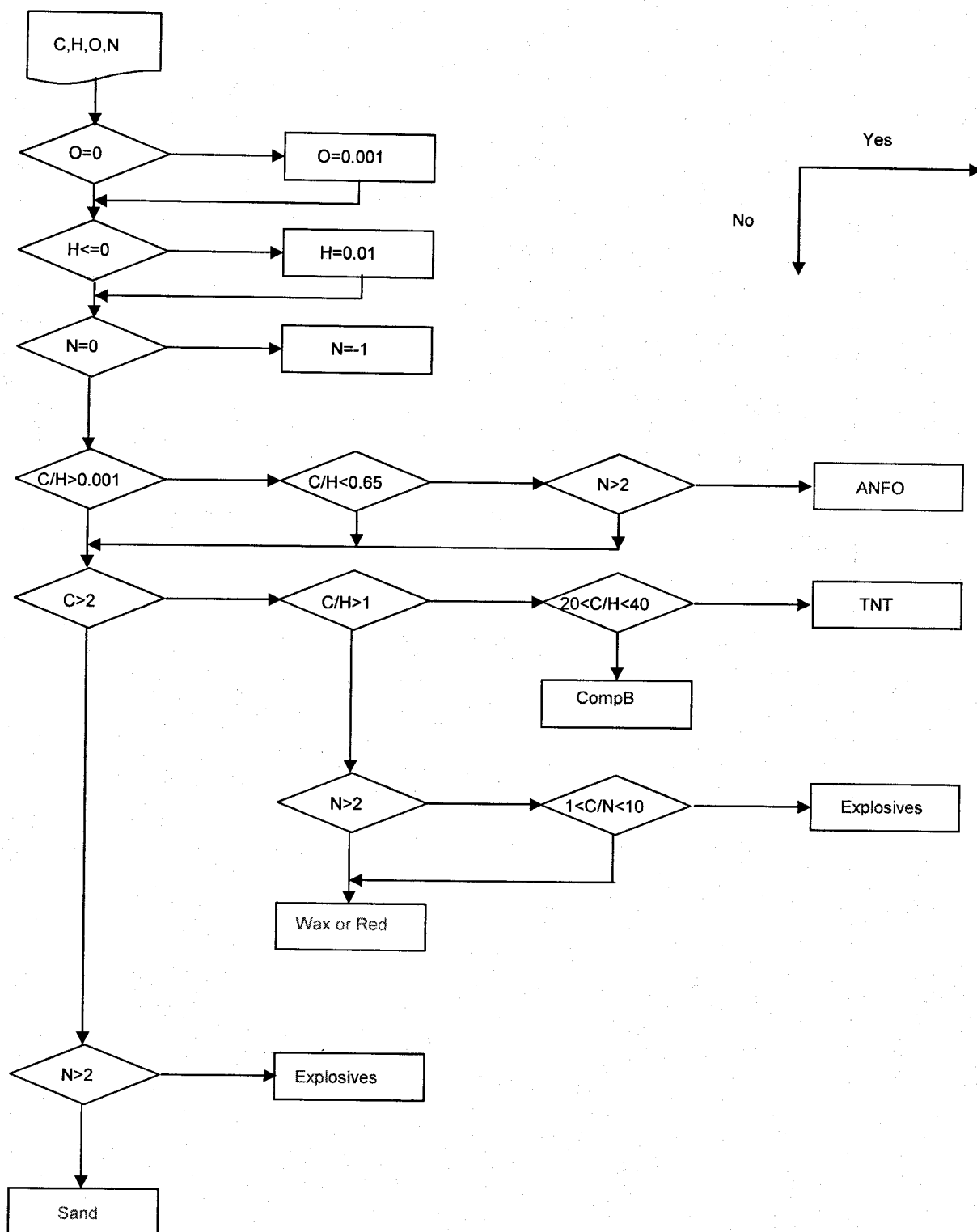


Figure 67. Decision tree for all the data taken at NAVEODTECH.

Table 21. Data for all explosives and inerts examined with PELAN, sorted by size and fill material.

Run	Size	Fill	Surface	C	H	N	O	C/H	C/N	O/N	Decision Tree Results	Failure Mode
1556	shp chrg	0.9lbsOctol	SOIL	2.1	0.3	2.1	4.1	6.1	1.0	1.9	CompB	
1619	shp chrg	0.9lbsOctol	TABLE	8.3	1.8	1.9	5.0	4.5	4.5	2.7	CompB	
1678	shp chrg	0.9lbsOctol	GRAVEL	4.9	-1.6	2.9	4.7	-3.1	1.7	1.6	CompB	
1729	shp chrg	0.9lbsOctol	SAND	5.4	4.5	1.6	4.6	1.2	3.5	3.0	CompB	
1783	shp chrg	0.9lbsOctol	WETSOIL	4.8	0.9	3.5	3.0	5.3	1.3	0.8	CompB	
1571	FFV02 8 stl mine	12.35 TNT	SOIL	16.1	18.1	5.9	7.5	0.9	2.7	1.3	Explosives	
1634	FFV02 8 stl mine	12.35 TNT	TABLE	14.9	6.3	7.1	12.9	2.4	2.1	1.8	CompB	
1655	FFV02 8 stl mine	12.35 TNT	GRAVEL	20.0	7.8	6.8	7.7	2.6	2.9	1.1	CompB	
1744	FFV02 8 stl mine	12.35 TNT	SAND	21.0	10.7	6.8	7.3	2.0	3.1	1.1	CompB	
1798	FFV02 8 stl mine	12.35 TNT	WETSOIL	18.2	-3.2	4.3	4.1	-5.6	4.2	1.0	CompB	
1559	Sheetex pl	21lbPETN	SOIL	25.0	51.1	8.0	15.1	0.5	3.1	1.9	ANFO	
1622	Sheetex pl	21lbPETN	TABLE	33.4	14.5	3.8	24.6	2.3	8.9	6.5	CompB	
1681	Sheetex pl	21lbPETN	GRAVEL	36.3	39.8	5.4	19.4	0.9	6.7	3.6	Explosives	
1732	Sheetex pl	21lbPETN	SAND	34.3	46.6	6.7	18.9	0.7	5.1	2.8	Explosives	
1786	Sheetex pl	21lbPETN	WETSOIL	30.7	52.0	6.5	14.8	0.6	4.7	2.3	ANFO	
1553	shp chrg	6.1lbs pxb-108	SOIL	18.4	3.3	5.5	7.0	5.6	3.4	1.3	CompB	
1616	shp chrg	6.1lbs pxb-108	TABLE	24.3	-4.6	6.9	14.6	-5.3	3.5	2.1	CompB	
1675	shp chrg	6.1lbs pxb-108	GRAVEL	29.2	17.4	8.3	10.5	1.7	3.5	1.3	CompB	
1726	shp chrg	6.1lbs pxb-108	SAND	26.8	15.6	8.7	7.7	1.7	3.1	0.9	CompB	
1774	shp chrg	6.1lbs pxb-108	WETSOIL	21.5	-32.7	8.9	9.8	-0.7	2.4	1.1	CompB	
1565	Val69 Mine	6lb CompB	SOIL	3.9	1.7	2.7	2.2	2.3	1.4	0.8	CompB	
1628	Val69 Mine	6lb CompB	TABLE	10.5	1.8	2.1	4.0	5.8	5.0	1.9	CompB	
1687	Val69 Mine	6lb CompB	GRAVEL	9.7	0.1	1.1	3.6	161.7	9.2	3.5	CompB	
1738	Val69 Mine	6lb CompB	SAND	8.0	2.1	1.2	2.5	3.8	6.5	2.0	CompB	
1792	Val69	6lb CompB	WETSOIL	7.1	-1.8	2.3	-0.2	-3.9	3.1	-0.1	CompB	

Run	Size	Fill	Surface	C	H	N	O	C/H	C/N	O/N	Decision Tree Results	Failure Mode
	Mine											
1840	Val69 Mine	COMPB	SAND	9.2	4.3	2.3	1.8	2.2	4.0	0.8	CompB	
1912	Val69 Mine	COMPB	Soil	7.8	3.4	2.3	0.9	2.3	3.4	0.4	CompB	
1876	Shape Charge	Octal	Gravel	5.0	1.3	3.3	4.1	3.8	1.5	1.3	CompB	
1987	Shape Charge	Octal	Table	4.43	-0.21	2.38	3.86	-21.1	1.9	1.6	CompB	
1834	Shape Charge	PBX-108	SAND	30.2	15.9	9.5	8.6	1.9	3.2	0.9	CompB	
1945	Shape Charge	PBX-108	Wetsoil	27.87	-27.99	6.3	0.99	-1.0	4.4	0.2	CompB	
1882	Sheetex pl	PETN	Gravel	36.1	41.1	6.2	18.4	0.9	5.8	3.0	Explosives	
1921	Sheetex pl	PETN	SOil	32.0	53.0	6.9	14.4	0.6	4.6	2.1	ANFO	
1903		semtex-1a	Soil	10.3	13.0	2.8	5.7	0.8	3.6	2.0	Explosives	
1984		semtex-1a	Table	10.16	4.13	1.4	7.54	2.5	7.3	5.4	CompB	
1837		smokless	SAND	7.1	2.3	3.7	5.9	3.2	1.9	1.6	CompB	
1909		smokless	Soil	5.7	5.2	2.9	3.3	1.1	2.0	1.1	CompB	
1879	AT Plastic mine	TNT	Gravel	39.7	17.6	5.7	6.9	2.3	7.0	1.2	CompB	
1885	AT Steel mine	TNT	Gravel	21.4	8.0	7.3	7.7	2.7	2.9	1.0	CompB	
1951	AT Steel mine	TNT	Wetsoil	23.98	18.59	8.31	9.7	1.3	2.9	1.2	CompB	
1990	AT Mine	TNT	Table	33.42	10.42	5.47	9.94	3.2	6.1	1.8	CompB	
1562	TMRP-6	11.2lbTNT	SOIL	28.4	28.1	6.3	4.2	1.0	4.5	0.7	CompB	
1625	TMRP-6	11.2lbTNT	TABLE	39.9	10.4	3.2	12.5	3.9	12.3	3.8	CompB	
1684	TMRP-6	11.2lbTNT	GRAVEL	38.7	13.4	6.1	9.3	2.9	6.4	1.5	CompB	
1735	TMRP-6	11.2lbTNT	SAND	39.4	17.8	6.2	7.5	2.2	6.3	1.2	CompB	
1789	TMRP-6	11.2lbTNT	WETSOIL	34.0	33.0	5.8	5.2	1.0	5.9	0.9	CompB	
1574	2wt%	ANFO	SOIL	1.7	28.0	5.3	7.3	0.1	0.3	1.4	ANFO	
1604	2wt%	ANFO	TABLE	5.1	9.4	2.8	13.0	0.5	1.8	4.6	ANFO	
1666	2wt%	ANFO	GRAVEL	3.2	13.8	6.2	10.8	0.2	0.5	1.8	ANFO	
1717	2wt%	ANFO	SAND	4.3	19.6	6.3	9.1	0.2	0.7	1.4	ANFO	
1765	2wt%	ANFO	WETSOIL	3.3	21.4	3.9	11.3	0.2	0.9	2.9	ANFO	
1577	2wt%	ANFO	SOIL	3.3	28.3	3.6	7.1	0.1	0.9	2.0	ANFO	
1607	6wt%	ANFO	TABLE	4.6	12.5	3.4	13.4	0.4	1.4	4.0	ANFO	
1669	6wt%	ANFO	GRAVEL	5.6	15.4	3.6	9.7	0.4	1.6	2.7	ANFO	
1720	6wt%	ANFO	SAND	6.6	23.3	5.1	8.3	0.3	1.3	1.6	ANFO	
1768	6wt%	ANFO	WETSOIL	4.0	22.3	4.6	11.1	0.2	0.9	2.4	ANFO	
1873	6wt%	ANFO	Gravel	7.1	20.8	5.6	8.7	0.3	1.3	1.6	ANFO	
1942	6wt%	ANFO	Wetsoil	9.81	35.55	6.73	8.58	0.3	1.5	1.3	ANFO	
1580	15wt%	ANFO	SOIL	6.1	40.7	5.1	6.1	0.1	1.2	1.2	ANFO	

Run	Size	Fill	Surface	C	H	N	O	C/H	C/N	O/N	Decision Tree Results	Failure Mode
1613	15wt%	ANFO	TABLE	8.3	17.9	3.5	12.8	0.5	2.4	3.7	ANFO	
1672	15wt%	ANFO	GRAVEL	9.0	26.9	4.7	11.9	0.3	1.9	2.5	ANFO	
1723	15wt%	ANFO	SAND	8.5	36.6	5.4	8.8	0.2	1.6	1.6	ANFO	
1771	15wt%	ANFO	WETSOIL	6.3	36.9	5.8	8.6	0.2	1.1	1.5	ANFO	
1547	1	smokeless	SOIL	3.6	-2.2	2.1	4.9	-1.6	1.7	2.3	CompB	
1598	1	smokeless	TABLE	10.7	0.5	0.2	5.3	19.8	48.7	24.2	CompB	
1662	1	smokeless	GRAVEL	5.2	-5.3	-3.3	-8.0	-1.0	-1.6	2.5	CompB	
1711	1	smokeless	SAND	6.2	6.1	2.8	4.1	1.0	2.2	1.5	CompB	
1544	1.8	semtex-1a	soil	5.8	4.7	3.0	5.9	1.2	1.9	1.9	CompB	
1708	1.8	semtex-1a	SAND	5.7	3.3	2.1	4.5	1.7	2.7	2.2	CompB	
1595	4.5	semtex-1a	TABLE	15.0	5.1	1.8	9.6	2.9	8.3	5.3	CompB	
1705	4.5	semtex-1a	SAND	10.5	5.5	3.9	5.2	1.9	2.7	1.3	CompB	
1304	60	EMPTY	SAND	0.7	-15.2	-5.2	-7.1	0.0	-0.1	1.4	Sand	
1331	60	EMPTY	SOIL	0.7	-15.2	-5.2	-7.1	0.0	-0.1	1.4	Sand	
1273	60	PLASTER	SOIL	0.8	-16.3	-5.1	-7.8	-0.1	-0.2	1.5	Sand	
1807	60	PLASTER	SAND	1.7	0.1	0.8	-2.1	18.6	2.1	-2.6	Sand	
1499	60	POP	WETSOIL	1.5	2.8	0.7	0.7	0.5	2.1	1.0	Sand	
1870	60	POP	Gravel	1.7	-0.4	0.6	-1.0	-4.5	2.8	-1.6	Sand	
1978	60	Pop	Table	-2.54	0.05	0.99	-0.64	-50.8	-2.6	-0.6	Sand	
1319	60	RED	SOIL	2.0	-10.7	-1.7	-4.0	-0.2	-1.1	2.3	Sand	
1810	60	RED	SAND	1.4	-1.5	1.9	-1.9	-0.9	0.8	-1.0	Sand	
1361	60	TNT	GRAVEL	2.5	1.5	0.7	4.0	0.7	3.6	5.7	Wax or Red	N<2
1400	60	TNT	TABLE	-1.6	4.3	1.1	-0.5	-0.4	-1.5	-0.5	Sand	C<2
1436	60	TNT	SOIL	-0.8	-2.5	-1.3	-1.6	0.3	0.6	1.2	Sand	C<2
1496	60	TNT	WETSOIL	3.5	4.7	0.0	-0.3	0.8	-	-	Wax or Red	N<2
1508	60	TNT	WETSOIL	2.4	1.1	0.7	-5.0	2.2	3.4	-7.1	CompB	
1861	60	TNT	Gravel	3.6	0.6	0.7	-1.0	5.6	5.1	-1.5	CompB	
1897	60	TNT	Soil	2.3	-1.2	0.4	-3.1	-1.8	6.2	-8.3	CompB	
1502	60	WAX	WETSOIL	3.2	3.9	0.0	0.0	0.8	-	-	Wax or Red	
1505	60	WAX	WETSOIL	1.7	-0.3	0.3	0.0	-5.7	5.7	0.0	Sand	
1613	60	WAX	SOIL	1.6	-2.7	-3.8	-6.2	-0.6	-0.4	1.6	Sand	
1225	76	RDX	SOIL	4.0	-1.5	-0.5	-1.3	-2.7	-8.0	2.5	CompB	
1228	76	RDX	SOIL	4.8	-7.2	0.0	-1.1	-0.7	4800.0	-1140.0	CompB	
1228	76	RDX	SOIL	4.8	-4.2	-0.6	-2.0	-1.1	-8.4	3.6	CompB	
1231	76	RDX	SOIL	4.4	-9.0	-0.7	-0.8	-0.5	-6.5	1.2	CompB	
1237	76	RDX	SOIL	2.9	1.9	-1.1	-0.3	1.5	-2.6	0.3	CompB	
1240	76	RDX	SOIL	4.9	-5.7	-0.2	1.0	-0.9	-23.8	-4.8	CompB	
1243	76	RDX	SOIL	5.0	-3.8	-0.4	-2.2	-1.3	-12.4	5.6	CompB	
1246	76	RDX	SOIL	4.6	-4.3	-0.6	0.0	-1.1	-7.7	0.0	CompB	
1249	76	RDX	SOIL	4.6	-9.3	-0.6	-1.7	-0.5	-7.2	2.6	CompB	
1252	76	RDX	SOIL	3.8	-6.5	-0.6	-3.2	-0.6	-6.3	5.2	CompB	
1325	76	RDX	SAND	2.7	-0.8	1.0	0.3	-3.4	2.7	0.3	CompB	
1364	76	RDX	GRAVEL	5.0	5.0	2.5	4.9	1.0	2.0	2.0	Explosives	

Run	Size	Fill	Surface	C	H	N	O	C/H	C/N	O/N	Decision Tree Results	Failure Mode
1403	76	RDX	TABLE	-2.7	0.2	2.7	1.0	-13.5	-1.0	0.4	Explosives	
1478	76	RDX	WETSOIL	5.4	-3.3	4.8	1.3	-1.6	1.1	0.3	CompB	
1825	76	RDX	SAND	6.0	1.9	1.3	1.8	3.1	4.5	1.4	CompB	
1328	76	TNT	SAND	4.0	-3.6	-1.0	-2.9	-1.1	-4.0	2.9	CompB	
1367	76	TNT	GRAVEL	5.6	0.8	0.0	3.7	7.0	-	-	CompB	
1481	76	TNT	WETSOIL	4.3	-13.8	2.0	-2.7	-0.3	2.2	-1.4	CompB	
1918	76	TNT	Soil	3.4	-0.6	-1.1	-1.6	-5.4	-3.1	1.5	CompB	
1409	81	COMPB	TABLE	1.6	-1.1	2.5	2.5	-1.5	0.6	1.0	Explosives	
1331	81	COMPB	SAND	4.8	-0.8	-0.1	0.0	-6.0	-48.0	0.0	CompB	
1490	81	COMPB	WETSOIL	6.0	-5.6	2.4	0.0	-1.1	2.5	0.0	CompB	
1867	81	COMPB	Gravel	9.5	3.5	3.6	1.5	2.7	2.6	0.4	CompB	
1328	81	EMPTY	SOIL	0.8	-12.7	-3.2	-4.8	-0.1	-0.2	1.5	Sand	
1191	81	PLASTER	SOIL	3.1	6.5	-1.8	2.3	0.5	-1.8	-1.3	Wax or Red	
1197	81	PLASTER	SOIL	2.0	-1.7	-0.6	1.9	-1.2	-3.5	-3.4	Sand	
1200	81	PLASTER	SOIL	1.5	-4.1	-2.0	0.9	-0.4	-0.8	-0.4	Sand	
1203	81	PLASTER	SOIL	2.0	-3.2	-1.3	0.3	-0.6	-1.5	-0.2	Sand	
1206	81	PLASTER	SOIL	2.4	-4.9	-1.8	-0.6	-0.5	-1.3	0.3	CompB	C/H>1
1209	81	PLASTER	SOIL	1.0	-4.5	-2.5	-0.2	-0.2	-0.4	0.1	Sand	
1212	81	PLASTER	SOIL	0.9	-4.6	-3.4	-0.2	-0.2	-0.3	0.0	Sand	
1215	81	PLASTER	SOIL	2.5	-3.1	-1.0	-0.8	-0.7	-1.1	0.3	CompB	C/H>1
1218	81	PLASTER	SOIL	2.2	-3.0	-1.9	-0.8	-0.7	-1.1	0.4	CompB	C/H>1
1276	81	PLASTER	SOIL	1.1	-5.8	-5.3	-5.5	-0.2	-0.2	1.0	Sand	
1316	81	PLASTER	SAND	2.1	8.2	-1.7	-0.3	0.3	-1.2	0.2	Wax or Red	
1352	81	PLASTER	GRAVEL	2.1	11.5	0.3	9.3	0.2	7.0	31.0	Wax or Red	
1391	81	PLASTER	TABLE	-4.1	4.3	-0.8	5.0	-1.0	5.1	-6.3	Sand	
1430	81	PLASTER	SOIL	-0.7	3.8	-0.2	-0.2	-0.2	3.5	1.0	Sand	
1750	81	PLASTER	SAND	1.0	4.8	1.0	1.3	0.2	1.1	1.4	Sand	
1469	81	POP	WETSOIL	2.8	3.8	0.0	1.6	0.7	-	-	Wax or Red	
1475	81	POP	WETSOIL	1.6	3.2	1.0	1.6	0.5	1.6	1.6	Sand	
1846	81	POP	SAND	1.5	7.0	-0.4	1.5	0.2	-3.7	-3.8	Sand	
1957	81	POP	Wetsoil	5.95	3.81	0.92	1.13	1.6	6.5	1.2	CompB	C/H>1
1267	81	SAND	SOIL	0.4	-11.2	-3.0	-3.7	0.0	-0.1	1.2	Sand	
1813	81	SAND	SAND	2.5	-3.7	-0.6	-3.1	-0.7	-4.1	5.2	CompB	C/H>1
1849	81	Sand	SAND	1.0	-1.9	0.3	-0.7	-0.5	3.6	-2.6	Sand	
1960	81	Sand	Wetsoil	6.81	-3.3	1.65	-0.03	-2.1	4.1	0.0	CompB	C/H>1
1999	81	SAND	Table	-2.36	-2.6	-0.77	-0.28	0.9	3.1	0.4	Sand	
1334	81	TNT	SAND	2.4	-2.0	0.2	-0.4	-1.2	12.0	-2.0	CompB	
1753	81	WAX	SOIL	5.4	7.0	-0.8	-3.7	0.8	-6.8	4.6	Wax or Red	
1370	82	COMPB	GRAVEL	6.4	4.7	0.0	6.4	1.4	-	-	CompB	

Run	Size	Fill	Surface	C	H	N	O	C/H	C/N	O/N	Decision Tree Results	Failure Mode
1373	82	TNT	GRAVEL	5.5	1.6	1.9	7.7	3.4	2.9	4.1	CompB	
1412	82	TNT	TABLE	2.9	-2.6	0.2	1.7	-1.1	16.9	10.1	CompB	
1418	82	TNT	SOIL	4.6	-6.1	-0.2	-2.6	-0.8	-23.0	13.0	CompB	
1493	82	TNT	WETSOIL	6.0	-5.5	2.1	-1.7	-1.1	2.9	-0.8	CompB	
1511	82	TNT	WETSOIL	3.1	-6.4	-0.3	-1.0	-0.5	-9.9	3.3	CompB	
1535	82	TNT	SOIL	2.9	-2.6	0.2	1.7	-1.1	16.9	10.1	CompB	
1589	82	TNT	TABLE	8.6	1.2	-0.5	0.3	7.4	-18.0	-0.6	CompB	
1643	82	TNT	GRAVEL	6.0	-2.3	0.7	-0.2	-2.7	9.1	-0.2	CompB	
1699	82	TNT	SAND	6.8	1.5	1.9	1.9	4.6	3.6	1.0	CompB	
1828	82	TNT	SAND	5.1	-1.3	0.6	-1.7	-4.1	8.8	-2.9	CompB	
1900	82	TNT	Soil	6.5	3.1	3.0	-4.1	2.1	2.2	-1.4	CompB	
1514	90	COMPB	WETSOIL	3.0	1.7	0.6	1.5	1.8	5.0	2.5	CompB	
1310	90	RDX	SAND	3.8	1.3	-0.2	-0.9	2.9	-19.0	4.5	CompB	
1346	90	RDX	GRAVEL	-0.9	0.2	2.9	1.7	-4.5	-0.3	0.6	Explosives	
1385	90	RDX	TABLE	3.7	1.3	-0.2	-2.6	2.8	-18.5	13.0	CompB	
1424	90	RDX	SOIL	4.8	7.5	3.2	-1.5	0.6	1.5	-0.5	Explosives	
1460	90	RDX	WETSOIL	9.43	1.52	4.07	-0.33	6.2	2.3	-0.1	CompB	
1936	90	RDX	Wetsoil	4.2	-13.4	-2.4	-7.0	-0.3	-1.7	2.9	CompB	C/H>1
1322	90	RED	SOIL	6.2	-3.4	-0.6	-3.1	-1.8	-10.7	5.3	CompB	
1843	90	RED	SAND	12.9	7.3	3.4	4.0	1.8	3.8	1.2	CompB	
1963	90	RED	Wetsoil	12.1	3.5	2.6	9.2	3.5	4.7	3.6	CompB	C/H>1
1993	90	Red	Table	-3.37	-4.76	0.5	-2.05	0.7	-6.7	-4.1	Sand	
1568	90	rocket 1.1lb60/40	SOIL	12.9	7.3	3.4	4.0	1.8	3.8	1.2	CompB	
1631	90	rocket 1.1lb60/40	TABLE	12.1	3.5	2.6	9.2	3.5	4.7	3.6	CompB	
1652	90	rocket 1.1lb60/40	GRAVEL	18.0	2.6	3.7	4.2	6.9	4.9	1.1	CompB	
1741	90	rocket 1.1lb60/40	SAND	17.2	1.6	3.0	3.3	11.0	5.8	1.1	CompB	
1795	90	rocket 1.1lb60/40	WETSOIL	14.5	3.0	3.0	1.2	4.9	4.9	0.4	CompB	
1888	90	rocket 1.1lb60/40	Gravel	18.5	0.8	4.1	3.4	22.3	4.5	0.8	TNT	
1954	90	TNT/RDX	Wetsoil	21.45	4.76	4.87	5.65	4.5	4.4	1.2	CompB	
1538	90	TX50	SOIL	4.0	-1.0	0.9	0.5	-3.9	4.5	0.5	CompB	
1592	90	TX50	TABLE	6.1	2.4	1.4	4.7	2.5	4.2	3.3	CompB	
1646	90	TX50	GRAVEL	9.6	-1.0	1.9	1.5	-9.3	5.2	0.8	CompB	
1702	90	TX50	SAND	8.4	-1.1	1.7	0.1	-7.9	4.9	0.0	CompB	
1969	105	EMPTY	Wetsoil	8.92	-2.66	2.62	-4.35	-3.4	3.3	-4.7	CompB	C/H>1
1966	105	RED	Wetsoil	9.86	2.59	2.24	-0.85	3.8	4.4	-0.4	CompB	C/H>1
1270	105	SAND	SOIL	-1.6	-8.4	-1.3	-2.7	0.2	1.2	2.1	Sand	
1816	105	SAND	SAND	0.9	-4.8	0.6	-1.4	-0.2	1.6	-2.5	Sand	
1915	105	SAND	Soil	0.6	16.0	0.4	0.7	0.0	1.3	1.6	Sand	
1996	105	SAND	Table	-7.92	6.26	1.08	4.26	-1.3	-7.3	3.9	Sand	
1159	105	WAX	SOIL	4.4	13.9	-1.8	-3.6	0.3	-2.4	2.0	Wax or Red	
1162	105	WAX	SOIL	5.3	11.6	0.1	-3.1	0.5	43.2	-25.4	Wax or Red	
1165	105	WAX	SOIL	5.0	11.0	-1.0	-3.1	0.5	-4.8	3.0	Wax or Red	

Run	Size	Fill	Surface	C	H	N	O	C/H	C/N	O/N	Decision Tree Results	Failure Mode
1168	105	WAX	SOIL	5.7	9.5	-0.2	-2.6	0.6	-35.5	16.3	Wax or Red	
1171	105	WAX	SOIL	5.3	10.1	-1.5	-2.1	0.5	-3.5	1.4	Wax or Red	
1174	105	WAX	SOIL	5.5	13.3	-1.9	-4.0	0.4	-2.9	2.1	Wax or Red	
1177	105	WAX	SOIL	5.1	7.9	-0.5	-4.0	0.6	-9.8	7.6	Wax or Red	
1180	105	WAX	SOIL	5.5	8.2	-3.5	-4.8	0.7	-1.6	1.4	Wax or Red	
1183	105	WAX	SOIL	4.8	5.3	-0.3	-4.6	0.9	-16.9	16.3	Wax or Red	
1186	105	WAX	SOIL	5.8	12.4	-1.2	-4.2	0.5	-4.8	3.5	Wax or Red	
1261	105	WAX	SOIL	4.7	8.0	-1.8	-3.4	0.6	-2.7	1.9	Wax or Red	
1319	105	WAX	SAND	4.7	18.2	-1.1	-3.1	0.3	-4.3	2.8	Wax or Red	
1355	105	WAX	GRAVEL	8.2	23.0	-0.5	2.9	0.4	-16.4	-5.8	Wax or Red	
1397	105	WAX	TABLE	-1.2	10.2	0.4	-1.3	-0.1	-3.0	-3.3	Sand	
1433	105	WAX	SOIL	2.5	6.3	-2.6	-6.8	0.4	-1.0	2.6	Wax or Red	
1472	105	WAX	WETSOIL	5.5	7.3	7.3	-4.4	0.8	0.8	-0.6	Wax or Red	
1610	105	WAX	TABLE	7.4	5.3	-0.2	-2.1	0.3	-3.8	2.3	CompB	
1906	105	WAX	Soil	6.5	24.5	-1.8	-4.1	0.3	-3.7	2.3	Wax or Red	
1948	105	WAX	WETSOIL	10.3	1.5	1.5	1.5	1.5	1.5	1.5	CompB	
1307	120	TNT	SAND	11.3	0.7	2.3	4.1	16.1	4.9	1.8	CompB	
1343	120	TNT	GRAVEL	8.6	1.9	2.8	3.5	4.5	3.1	1.3	CompB	
1382	120	TNT	TABLE	13.7	1.4	4.5	8.5	9.8	3.0	1.9	CompB	
1421	120	TNT	SOIL	7.8	-1.7	2.4	0.6	-4.6	3.3	0.3	CompB	
1939	120	TNT	Wetsoil	17.35	-3.51	7.54	3.9	-4.9	2.3	0.5	CompB	
1313	122	COMPB	SAND	15.3	8.1	6.2	11.0	1.9	2.5	1.8	CompB	
1349	122	COMPB	GRAVEL	11.9	6.7	4.5	10.8	1.8	2.6	2.4	CompB	
1388	122	COMPB	TABLE	13.5	5.8	6.5	14.5	2.3	2.1	2.2	CompB	
1427	122	COMPB	SOIL	11.1	11.0	3.3	4.8	1.0	3.4	1.5	CompB	
1463	122	COMPB	SOIL	13.8	20.4	6.8	8.4	0.7	2.0	1.2	Explosives	
1981	122	COMPB	Table	11.16	6.32	5.44	10.78	1.8	2.1	2.0	CompB	
1466	122	PROPEL.	WETSOIL	26.0	18.0	6.8	18.0	1.4	3.8	2.6	CompB	
1550	155	13.2 TNT	SOIL	18.8	5.4	4.9	5.5	3.5	3.9	1.1	CompB	
1334	155	EMPTY	SOIL	-2.1	1.5	-2.1	-0.8	-1.4	1.0	0.4	Sand	
1325	155	RED	SOIL	7.5	33.5	1.7	5.0	0.2	4.5	3.0	Wax or Red	
1852	155	RED	SAND	14.7	55.1	-0.6	0.9	0.3	-24.0	-1.5	Wax or Red	
1924	155	RED	Soil	15.1	68.8	-0.7	2.5	0.2	-20.9	-3.5	Wax or Red	
1601	155	TNT	TABLE	29.4	-4.0	6.4	16.1	-7.4	4.6	2.5	CompB	
1649	155	TNT	GRAVEL	20.5	8.4	3.5	7.7	2.4	5.9	2.2	CompB	
1714	155	TNT	SAND	21.3	9.0	6.2	10.0	2.4	3.4	1.6	CompB	
1762	155	TNT	WETSOIL	19.2	-4.8	7.9	5.2	-4.0	2.4	0.7	CompB	
1831	155	TNT	SAND	18.2	3.6	4.7	6.8	5.1	3.9	1.4	CompB	

Run	Size	Fill	Surface	C	H	N	O	C/H	C/N	O/N	Decision Tree Results	Failure Mode
1264	155	WAX	SOIL	8.3	59.9	1.6	1.9	0.1	5.2	1.2	Wax or Red	
1864	155	WAX	Gravel	14.1	102.9	1.0	-2.4	0.1	13.7	-2.3	Wax or Red	
1933	155	WAX	Wetsoil	10.11	26.45	3.71	-2.9	0.4	2.7	-0.8	Explosives	

5.2 Data Assessment

Over two weeks in May 2002, an extensive amount of data was taken with a PELAN III at NAVEOCTECH/Indian Head, MD. In order to further investigate the stability of the background, supplemental background data were taken at WKU. The results of this investigation resulted to the following conclusions:

- The scalar products between various background spectrum indicate that there is a strong coupling between backgrounds i.e. that the backgrounds are very similar. Thus, performance should not change much from background to background.
- The coefficient of the background is nearly orthogonal to the elemental responses multiplied by their respective coefficients. This indicates that there is very little inter-dependence between the various coefficients and that the spectrum is being properly fitted.
- The environment plays a key role in the uncertainty in the measurement. For example, an environment with a high H content tends to have a high measurement uncertainty. This is due to the effective subtraction which takes place in the SPIDER program. Simply put: if one subtracts two large numbers with independent errors, the difference may be smaller than the propagated error.
- For sand, gravel and the table, the backgrounds are relatively stable and may be taken once per day. It is even advisable to take only one background at a given location to minimize Si activation.
- For the soil at Indian Head (which is presumed to be clay), we found that the soil to hold moisture and release it slowly. Thus, the thermal spectrum will change from day to day (particularly after precipitation). For ten-repeated runs at WKU, we did not see any changes in the soil. Due to its intrinsic high H content, the WKU soil and the Indian Head soil had higher uncertainties for the reasons stated in the first bullet.
- The repeatability of the data (data precision), was found to depend on the quantity of each element in a given explosive, the amount of the explosive itself, and the environment wherein the explosive is measured.
- The ROC curves of elemental ratios are no better than the ROC curves of the elemental contents which comprise them.
- The decision tree used for the identification of the shell fill shows that PELAN has a 19% false negative rate overall and a 22% false positive rate. The false negative rate becomes 3% for shells 90 mm and above. These larger shells have a 22% false positive rate.
- The decision tree can be improved by the addition of a condition on size. In this manner, each size shell will have its own decision tree which may improve its false negative and false positive rates. For example, the false negative rate for 60 mm shells decreases from 70% to 0% when a 60mm-shell-specific decision tree is applied.

One key question is how much data should be taken for a particular shell/environment. Unfortunately, there is no clear cut answer to this. The best answer is that sufficient data should be taken until a normal distribution can be fitted to the individual elemental content with a low chi-squared. For certain shells, such as the 60mm, a large number of shells must be measured to acquire a normal distribution due to the low mass of the explosive, the signal to noise ratio, etc. For the 155mm shell during the reproducibility tests, the normal distribution was reached after a few trials.

Another question is whether more data acquisition time would improve the measurement. In the table below, we show the results for two 60 mm shells with TNT on gravel. We have added these together and then fitted them with SPIDER.

Run	Fill	Size	Surface	C (cps)	O (cps)	N (cps)	H (cps)
1861	TNT	60	Gravel	3.6	-1	0.7	0.6
1361	TNT	60	Gravel	2.5	4	0.7	3.5
1861+1361	TNT	60	Gravel	3.81	1.24	0.29	1.8

In this case, there is no evidence that doubling the time of acquisition will increase the intensity of the measurement. When doubling the measurement time for the spectrum, the measurement time of the background must be doubled. Since the SNR is roughly constant, there seems to be no gain by increasing the acquisition time beyond what is necessary to have sufficient statistics for analysis.

We believe that the above extensive data bears well towards the validation of PELAN as a potentially useful tool for the identification of explosives.

5.3 Technology Comparison

Although PELAN is the "next generation" of neutron-based measurement devices, the data presented within this report is too limited to provide a full comparison at this time

6. Cost Assessment

6.1 Cost Reporting

To help ESTCP develop and validate the expected operational costs of the PELAN system, we provide a table of all relevant costs associated with initial capital investments and operational and maintenance costs. These costs are summarized in Table 5-1 whose format is based on that recommended in the Federal Remediation Technologies Roundtable format found in Guide to Documenting and Managing Cost and Performance Information for Remediation Projects (Revised Version), EPA 542-B-98-007, October 1998. (www.frtr.gov)

The costs in Table 22 are based on an expected lifetime of 5 years for the PELAN system. The major maintenance cost is that for a replacement neutron tube whose lifetime is guaranteed to 300 hours by the vendor, but, in practice, has typically operated for up to 900 hours. For the labor estimates, we assume that the UXO shell has already been excavated for other standard inspection procedures so costs associated with the excavation have not been included here. For the labor inspection, we assume that one person is required to operate the system and that four (4) UXO shells can be inspected in the field per hour, 8 hours a day, 40 hours a week for 5 years. This amounts to a total of 41,600 UXO shells inspected in 5 years. Vacation time, holidays and other leave time have not been included in this estimation. Throughput depends on the nature of the operations. The PELAN system is capable of quite high throughput with rates as short as one or two minutes for set-up and a 5-minute analysis cycle. In practice the limitations will likely be the operational conditions and not the system itself.

Table 22. Costs for Inspection of UXO Specific to PELAN Technology

Type of Cost	Technology	Cost for Calculating		Year 2	Year 3	Year 4	Year 5
		Unit Cost (\$)	Year 1				
1. Capital							
Mobilization / demobilization	0		0				
Planning and preparation							
Material license fee, radiation safety plan	1,000		1,000				
Site work	0		0				
Equipment and appurences							
PELAN unit	100,000		100,000				
Transport cart	10,000		10,000				
Storage containers (2)	1,000		1,000				

Type of Cost	Technology	Cost for Calculating					
	Cost (\$)	Unit Cost(\$)	Year 1	Year 2	Year 3	Year 4	Year 5
Radiation monitors	15,000		15,000				
Indirect costs	5,000		5,000				
TOTAL	131,000		131,000				
Startup and testing							
Operational training	2,000		2,000				
Other	0		0				
Total capital costs		134,000	134,000				
2. Operation and Maintenance							
Labor							
Labor, operation support, staff labor	520,000						
Materials							
Neutron tube replacement	10,750						
Rechargeable battery (5)	500						
Utilities and Fuel	0						
Equipment ownership, rental or lease	0						
Performance testing and analysis	5,000						
Other							
Radiation badges and reporting	1,000						
Total operation and maintenance costs		537,250	107,450	107,450	107,450	107,450	107,450
3. Other Technology-Specific Costs							
Compliance testing and analysis	0						
Soil, sludge, and debris evac, coll, control	0						
Disposal of residues	0						
4. Other project costs	0						
Total technology cost	671,250		241,450	107,450	107,450	107,450	107,450
Total cost for calculating unit cost		671,250					

Type of Cost	Technology	Cost for Calculating					
	Cost (\$)	Unit Cost(\$)	Year 1	Year 2	Year 3	Year 4	Year 5
Quantity examined	41,600	UXO pieces examined over 5 year period					
Calculated unit cost	\$16.14	per UXO piece					

6.2 Cost Analysis

The following information is provided as preparation for presenting the cost analysis that is required in the ESTCP final report and the ESTCP cost and performance report.

• Cost Comparison

The baseline alternative technology is currently to excavate the UXO shell and, unless external markings can be used to identify the contents, to assume the worst case, that is, that the UXO shell contains explosives or chemical agents. If no information can reliably identify the contents, the UXO shell is blown in place. The PELAN technology would be used to reliably identify the UXO fill allowing for the most efficient means to remove the UXO.

• Cost Basis

The cost basis is summarized in Section 6.1 and used to estimate the operation and maintenance costs shown in Table 22.

• Cost Drivers

The cost drivers are the initial capital investment in a PELAN system and the operational labor for inspection of the UXO. These cost estimates are shown in Table 22.

• Life Cycle Costs

We estimate that the operation life of a PELAN system is 6 years based on our experience with several PELAN prototype units used for other applications. The costs for the life cycle of the PELAN unit are summarized in Table 22. As noted in Section 6.1, for the operational costs, we assume a throughput rate of 4 UXO shells per hour, 40 hours per week, 2080 hours per year, for a total of 41,600 UXO inspections. No significant facility costs are assumed because the unit need only be stored in a secured area. The user will need to obtain a radiation materials license to receive, store, and use PELAN; these costs are included in Table 22. The greatest maintenance cost is replacing the neutron tube after every 900 hours of use; Table 22 includes the cost of one additional tube over the 5 year life cycle.

7. Regulatory Issues

7.1 Environmental Checklist

- NRC Form 241 (prior to shipment of PELAN)

7.2 Other Regulatory Issues

Not applicable.

7.3 End-User Issues

During the demonstration, several end users were shown the PELAN. These end-users included officers from Naval Intelligence and Radiation Safety personnel from the Norfolk Naval Base. They were shown how the PELAN can be carried as two separate units and how to operate the instrument.

8. Technology Implementation

8.1 DoD Need

It is difficult to estimate the DoD need for a device such as PELAN. We believe that a single PELAN should be available to every environmental restoration site. The final unit cost will be a factor in how many total units will be deemed "necessary".

8.2 Transition

Commercialization of the PELAN will be performed by Science Applications International Corporation. They have purchased the manufacturing license for this product. In the next year, SAIC plans to build at least two commercial prototype unit.

The next step for the PELAN is to take more data and strength its decision-making algorithms. In particular, we must focus on the shell sizes smaller than 90 mm. PELAN has been designed for the 105 mm -size shell, however, based on our survey, we must examine ways to increase the signal-to-noise ratio in the spectra.

9. Lessons Learned

1. PELAN can be operated for 8 hour shifts.
2. Movement of shells from magazine to target to magazine takes approximately 10 minutes. In a demonstration such as this, one can only expect about 4 interrogations per hour rather than 7.
3. The moisture content of soils with high clay content can change rapidly. For clay soils in the future, the background must be examined every 4 hours.
4. Local weather and other projects can interfere with tight schedules. Plan for at least 1 lost day per every 10 working days.
5. The largest source of statistical uncertainty appears to be background measurement. Uncertainties for elements are greatest when there is a significant amount of that element in the background.
6. Increasing the data collection times does not lead to greater accuracy.
7. While ROC curves are useful in analyzing the total performance of a particular decision tree, they are difficult to use when building a decision tree.

8. Greater use of shell size segregation should be made. For example, the false negative rate for 60 mm shells decreases from 70% to 0% when a 60mm-shell-specific decision tree is applied.
9. A specific elemental content for a given shell/environment should be repeated until the data approximates a normal distribution function. For larger shells, this may be a few times. However, it may be require a very large data set to achieve this distribution with the smaller shells.

10. References

- 1 J. Putnam, "UXO Site Remediation Technology", *4th Int'l Symp. on Technology and the Mine Problem*, Monterey CA, March 2000.
- 2 G. Vourvopoulos, *Chemistry and Industry*, 18 April 1994, p. 297-300.
- 3 H. D. Scot, C. Stoller, B. A. Roscoe, R. E. Plasek, and R. Adolph, A New Compensated Through-Tubing Carbon/Oxygen Tool for Use in Flowing Wells in *Trans. Of the SPWLA 32nd Annual Logging Symposium*, Midland TX, June 1991, paper MM.
- 4 A. T. Kirchner, IAE Coal Research 40, London, UK, Sept. 1991.
- 5 L. Dep, M. Belbot, G. Vourvopoulos, and S. Sudar, *J. of Radioanal. and Nucl. Chem.*, Vol. 234, Nos. 1-2 (1998) 107-112.
- 6 Symposium on Explosive Detection Technology, S. Khan, Ed., Atlantic City, NJ, 1991.
- 7 D. R. Brown and T. Gozani, *NIM B 99*, 1995, p. 753-756.
- 8 G. Vourvopoulos, and J. Thornton, A Transportable, Neutron-Based Contraband Detection System in *Proc. of Counterdrug Law Enforcement: Applied Technology for Improved Operational Effectiveness*, Nashua, NH, p.2-39, 1995.
- 9 G. Vourvopoulos, F. J. Schultz, and J. Kehayias, A Pulsed Fast/Thermal Neutron Interrogation System in *Symp. on Explosive Detection Technology*, Ed. S. Khan, FAA Technical Center, Atlantic City, 1991, p.27.
- 10 P. C. Womble, F. J. Schultz, and G. Vourvopoulos, *NIM B 99*, 1995, p. 757.
- 11 G. Vourvopoulos, L. Dep, S. Sudar, P. C. Womble, and F. J. Schultz, Neutron-Generator Based On-Line Coal Analysis: A Progress Report in *Proc. 8th Int'l Conf. On Coal Science*, Eds. J.A. Pajares and J.M.D. Tascon, Elsevier Science B. V., Oviedo, Spain, 1995.

Appendix A. Points of Contact

Name	Phone	Email
Phillip Womble	270 781 3859	<u>Womble@wku.edu</u>
Anne Andrews	703-696-3826	<u>Anne.Andrews@osd.mil</u>
Denice Forsht	301 744 6850 ext 303	<u>Forsht@eodpoe2.navsea.navy.mil</u>
Scott Steward	301 744-6850 ext 292	<u>Steward@eodpoe2.navsea.navy.mil</u>
Chris O'Donnel	301 744-6849 ext 262	<u>ODONNEL@EODPOE2.NAVSEA.NAVY.MIL</u>
Jeffrey Marqusee	703-696-2117	<u>Jeffrey.marqusee@osd.mil</u>
Jeffrey Fairbanks	703-736-4514	<u>Jef@hgt.com</u>
Hien Dinh	301-744-6850 ext. 267	<u>DINH@eodpoe2.navsea.navy.mil</u>

Appendix B – Data Archiving and Demonstration Plan

The demonstration data is being sent to the ESTCP program office along with this report. The data is to be saved on read/writable CD-ROM. The raw spectra, the elemental content, and the test descriptions will be available.

Copies of the demonstration plan and the data may be obtained from Dr. Phillip C. Womble at Western Kentucky University or Dr. Anne Andrews of ESTCP. Drs. Andrews and Womble have copies of the approved demonstration plan.

Copies of the photographs from the demonstration may be obtained from Dr. Womble or Ms. Denice Forsht of NAVEODTECH.